Year : 2014

Evolutionary Games on Weighted and Spatial Networks

Buesser Pierre

UNIL | Université de Lausanne

FACULTÉ DES HAUTES ÉTUDES COMMERCIALES
DÉPARTEMENT DE SYSTÈMES D'INFORMATION

Evolutionary Games on Weighted and Spatial Networks

THÈSE DE DOCTORAT

présentée à la

Faculté des Hautes Etudes Commerciales
de l'Université de Lausanne

pour l'obtention du grade de
Docteur en Systèmes d'Information

par

Pierre Buesser

Directeur de thèse
Prof. Marco Tomassini

Jury

Prof. Francisco Santos, expert externe
Prof. Ángel Sánchez, expert externe
Prof. Benoît Garbinato, expert interne
Prof. Alessandro Villa, président

LAUSANNE
2014

IMPRIMATUR
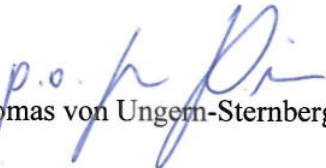
Sans se prononcer sur les opinions de l'auteur, la Faculté des Hautes Etudes Commerciales de l'Université de Lausanne autorise l'impression de la thèse de Monsieur Pierre BUESSER, licencié en Physique de l'Ecole Polytechnique Fédérale de Lausanne, titulaire d'un diplôme de master en Physique de l'Ecole Polytechnique Fédérale de Lausanne, en vue de l'obtention du grade de docteur en Systèmes d'Information.

La thèse est intitulée :

EVOLUTIONARY GAMES ON WEIGHTED AND SPATIAL NETWORKS

Lausanne, le 12 janvier 2015

Le doyen

Thomas von Ungern-Sternberg

Jury

Professor Marco Tomassini
Professor at the Faculty of Business and Economics of the University of Lausanne.
Thesis supervisor.

Professor Ángel Sánchez
Professor and Vice Chair for Research at the Departamento de Matemáticas of Universidad Carlos III de Madrid.
External expert.

Professor Francisco Santos
Assistant Professor at the Department of Computer Science and Engineering of Instituto Superior Técnico (IST), University of Lisbon.
External expert.

Professor Benoît Garbinato
Professor at the Faculty of Business and Economics of the University of Lausanne.
Internal expert.

Professor Alessandro Villa
Professor at the Faculty of Business and Economics of the University of Lausanne.
President of the Jury.

Université de Lausanne
Faculté des Hautes Etudes Commerciales

Doctorat en Systèmes d'Information

Par la présente, je certifie avoir examiné la thèse de doctorat de

Pierre BUESSER

Sa thèse remplit les exigences liées à un travail de doctorat.
Toutes les révisions que les membres du jury et le-la soussigné-e ont
demandées durant le colloque de thèse ont été prises en considération et
reçoivent ici mon approbation.

Signature : _____ Date : __28/12/2014__

Prof. Marco TOMASSINI
Directeur de thèse

Université de Lausanne
Faculté des Hautes Etudes Commerciales

Doctorat en Systèmes d'Information

Par la présente, je certifie avoir examiné la thèse de doctorat de

Pierre BUESSER

Sa thèse remplit les exigences liées à un travail de doctorat.
Toutes les révisions que les membres du jury et le-la soussigné-e ont
demandées durant le colloque de thèse ont été prises en considération et
reçoivent ici mon approbation

Signature :   Date : 19/12/2014

Prof. Angel SANCHEZ
Membre externe du jury

Université de Lausanne
Faculté des Hautes Etudes Commerciales

Doctorat en Systèmes d'Information

Par la présente, je certifie avoir examiné la thèse de doctorat de

Pierre BUESSER

Sa thèse remplit les exigences liées à un travail de doctorat.
Toutes les révisions que les membres du jury et le-la soussigné-e ont
demandées durant le colloque de thèse ont été prises en considération et
reçoivent ici mon approbation

Signature : _____ Date : 22/12/2014

Prof. Francisco SANTOS

Membre externe du jury

Université de Lausanne
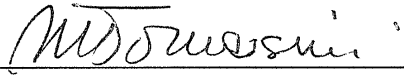Faculté des Hautes Etudes Commerciales

Doctorat en Systèmes d'Information

Par la présente, je certifie avoir examiné la thèse de doctorat de

Pierre BUESSER

Sa thèse remplit les exigences liées à un travail de doctorat.
Toutes les révisions que les membres du jury et le-la soussigné-e ont
demandées durant le colloque de thèse ont été prises en considération et
reçoivent ici mon approbation

Signature : _____ Date : 19.12.2014

Prof. Benoît GARBINATO
Membre interne du jury

Abstract

In game theory the fitness of an agent is not fixed but depends on the other agents choices. In the standard interpretation of game theory the game is played only once and the agents know all the details of the games. Evolutionary game theory was an adaptation of game theory in the context of biology brought by Maynard Smith and George R. Price in 1973. In evolutionary game theory, the game is played many times. It deals with large populations and studies the dynamic of the strategy frequencies in the population. Generally the population has been considered such that each player has the possibility to interact with each other player with the same probability. This approach leads to the replicator equation introduced by Taylor and Jonker in 1978. Social networks have been studied since the pioneering work of Milgram in 1967. The most simple network models are the random one and the regular spatial lattice, however the analysis of social networks has shown that these networks display other features such as scale-free degree (number of neighbors) distribution, high clustering, short average path length, community structure etc. Two well-studied models of complex networks are the scale-free and Watts-Strogatz small-world ones. The scale-free model takes into account this specific degree distribution which can be more realistic than more basic ones. The Barabási-Albert model (1999) is a well-known example of scale-free model where the scale-free distribution is obtained naturally by the process of preferential attachment. Watts-Strogatz networks possess both a short average path length and a high clustering coefficient, two features often observed in real networks. Following these developments, several studies have extended evolutionary game theory to these complex network models. For example, Santos et al. found that scale-free degree distributions are highly favorable to cooperation. In this thesis work, we tried to extend the state of the art of the research in various directions. Weighted networks are networks where weights are assigned to the links between the agents, which take into account the importance of the relations between an agent and his neighbors. In the same line several other extensions of evolutionary game theory have been explored, such as dynamical networks. Migration of the players in space is another example. In this type of models, the positions of the players evolve such that the agents move randomly or toward the places where they earn the largest payoff. In this thesis we focus on weighted networks, spatial networks models, and spatial migration of the agents. Concerning the game, this work investigates for the most part cooperation. This involves two-player games where the players A and B can choose between two strategies C and D, where C stand for coopera-

tion and D for defection. Choosing C will benefit both players only if the other adopts the same strategy, choosing D benefits the player only if the other chooses C and it does not benefit the other player. If both players choose D they end up with a low payoff. We first study the evolution of cooperation on weighted networks and on spatial networks. In a second part we study the evolution of cooperation when the players can migrate in space in order to improve their payoff. In this context we study also a different type of game, where a player can choose a strategy among three strategies dominating each other cyclically, and study how diversity of strategies can be maintained through the spatial shapes of the patterns formed. Our findings are the following. Concerning weighted networks, some real weight distribution and some weight distribution obtained from network formation models do not affect strongly cooperation. However, it seems that attributing the weights according to some types of degree-weight correlations on an underlying Barabási-Albert network has a strong effect on cooperation. Using correlation functions where the variable is the product of the degrees of the end nodes of the edge, we find an increase of cooperation for some parameter range. However, when the correlation depends on the difference of the degrees we can explore assortative and disassortative weights, and we find that for disassortative weights, as opposed to assortative or neutral weights, high levels of cooperation can be reached. We show that it is possible to derive unweighted networks topologies from these weighted networks that give rise to similar levels of cooperation. In a second part, using spatial networks, we study the effect of spatial scale-free networks, and show that cooperation is only slightly changed in these types of models with respect to classical scale-free models. However exploring other hierarchical topologies which are embedded in space, we show that they lead to particularly high levels of cooperation. In this part we also notice some interesting effects due to the strategy update type. In a third part, exploring migration, we find that when the agents tend to imitate their neighbors more randomly while they migrate opportunistically to the best places, cooperation spreads in the population, even for the games which are very detrimental for cooperation. We study also the patterns obtained with opportunistic migration when the strategies of the agents are fixed, we find that for some games the agents tends to adopt a directional motion and that for large interaction radii mobile clusters forms. In the same line we study three-strategy cyclic games coevolving with opportunistic migration. We find that while the imitation update becomes more random the size of the cyclical patterns goes through a peak where it tends to diverge before decreasing again. While the parameter tuning the random imitation rate is changed and the peak is crossed the order in which the different cyclical strategies follow each other is reversed.

Acknowledgements

Contents

Chapter 1

Introduction

1.1 Introduction and Motivation

Game Theory is an extension of decision theory, an "interactive decision theory", where an agent's optimal action depends on expectations on the actions of other agents [20]. Game theory has successfully been applied in diverse fields such as evolutionary biology, economy, and social science in general. A game is defined by a set of players, a set of strategies, the informations available to each player and the players' payoffs for each configuration of the strategies. Classical game theory aims at finding the equilibrium states of the population implied by the rational choices of the players such that no players can profit by changing their strategy. In classical game theory a dynamical process is not necessary since the players try to optimize their payoff knowing that the other players will also try to optimize their payoffs. While in classical game theory the assumption of rationality is very strong, it is relaxed in evolutionary game theory where the payoffs, and not a complex choice, directly dictates which strategies will thrive. In a biological context, the organisms which are more fit will tend to produce more offspring. In a sociological context, the most successful players will be imitated more often.

Evolutionary games have been traditionally studied in the context of well-mixed and very large populations. (see e.g. [15, 41]). However, starting with the work of Nowak and May [25], and especially in the last few years, more complex population structures have been brought to the focus of research. Indeed, social interactions can be more precisely represented as networks of contacts in which nodes represent agents and links stand for their relationships [24]. Most of the results in the context of networks, owing to the difficulty of analytically solving non mean-field models, come from numerical simulations, but there are also some theoretical results. In game theory, games can be seen as metaphors for human interactions and social dilemmas. In this work we focus on different types of games, describing the interaction of two players when two or three strategies are available. The population evolves as a result of the application, by each player, of some strategy update rule. Both players update rules and players population structure influence the final outcome.

We focus mainly on the issue of cooperation, although we will also deal with cyclic games. We model cooperation by two-strategy games. It is a model for the dilemma faced by the individual when he has to choose between the benefit of the group (cooperation) or

his own benefit at the expense of the group (defection). The problem with the second choice is that if all the players adopt it, no one can profit from cooperative individuals. The main issue is to understand how cooperation can thrive when individuals are selfish. Different mechanisms may lead to cooperation such as network topology, adaptive networks and migration among others. Because cooperation is so fundamental in society, we first discuss its main features, as observed in many laboratory and field experiments.

1.2 Cooperation in Society and Experiments

Cooperation appears when members of a group act for the benefit of the whole group. It is observed in both human and animal societies. For example social insects such as ants share tasks, unite against predators and construct huge nests where they can store food and breed. Some other example of cooperation among animals are cooperative grooming, respecting proximity-based territory, supporting injured individuals, cooperating for hunting, alarm calling.

Human is a very cooperative species. It can be observed in families, bands, industry, information systems, markets, political and military organizations, states, laws, firms, insurances, schools, universities, etc.

Cooperation among humans is characterized by the possibility to communicate efficiently. The language makes it possible to create rules and laws, and to construct cooperative projects. Another characteristic of human cooperation is that it can extend to complete strangers rather than being limited to genetically related individuals and members of a group. Human cooperation has also been observed in cases where agents cannot expect any reward for it.

Although the results of this thesis are theoretical, it is interesting to first review how people behave in some real experiments. Thus, in the following we present some experiments with real people and real money which can be found in [6] in more details.

In the *ultimatum game* a subject A is given a sum of money. Then he can offer a part of this amount to a subject B. The player B knows the initial amount of money given to player A and can accept or reject the offer. If B accepts it, both players receive the money according to the offer, if B rejects it both players receive nothing. The game is *one-shot*, which means that it is played only one time. If the players are selfish and want to maximize their profit in this experiment the player B should accept any positive amount of money, thus player A should give the minimum possible positive amount and the receiver should accept it. However the results of this experiment show that players of type A tend to give significant amount of money such as 50% of the initial amount, and players of type B tend to refuse offers below 25%. Thus players of type B do not only maximize their payoff but also refuse propositions even if that cannot improve their payoff in future rounds of this game. The fact that player's of type A propose large amounts of money might be due to the fact that they expect a large acceptance threshold and want to maximize their profit or that they take their decision for any other reason. Finally players of type B were asked why they refused offers, expressed anger, and wanted to punish other player's greed. Thus this shows that players also take decisions according to their feelings rather than

just for maximizing their payoffs. The result is that they punish the defectors and reward the cooperators.

Another game is the one-shot *prisoner's dilemma*. In that game the two players, *A* an *B*, can chose to cooperate or defect by respectively paying a cost *c* or nothing, knowing that if he cooperates, the other player receives a benefit *b*, and nothing otherwise. Therefore mutual cooperation maximizes the sum of the player's payoff, but one of the two players can earn more at the expense of the other by defecting while the latter cooperates. In [19], experimenters run the game in three different ways with monetary payoff. In the first one players play the standard game where players don't know their partner choice. In the second one, the player has the choice to cooperate or not after he has been informed that the first player has cooperated. In the third treatment the first player is also told that the second player will be informed about his choice before playing. The results showed that 38% of the players cooperated in the standard game, 62% cooperated in the second case and 59% cooperated in the third case. This experiment shows that the majority of players do not cooperate in the standard case. In the second and third cases however, a large part of the players cooperates, even if the second player would earn a better payoff by defecting. Again, these results shows that player's choices are a mixing of selfishness and motives that do not depend from the actual payoff but could be due to internalized norms, feelings such as pleasure to reward, self-esteem, guilt and anger. It is interesting to remark that in the second and third case the choice of the second player amounts to the same as a simple imitation of the first player.

Another game where this reciprocation can be observed is the *gift exchange game*. For this game a group of players was divided in *employers* and *employees*. An employer hires an employee with a wage w and the employee exert an effort e with $0 \leq w \leq 100$ and $0.1 \leq e \leq 1$, the payoff of the employer is $100e - w$ and the payoff of the employee is $u = w - c(e)$, where $c(e)$ is an increasing function with increasing slope ($c', c'' > 0$). The game was repeated with different partners such that each interaction is one-shot and the payoffs where paid with real money at end. If an employee wants to maximizes his profits he has to choose the minimum effort, and if the employer presume that the employee is selfish he will give the minimal wage. However the experiment shows that employees reward good wages with larger efforts and that employers proposed also larger payoffs. It appears that the employees could earn more by exerting the minimal effort. On the other hand employers could be selfish and predict the behavior of the employees. Thus, in order to determine if the employers are purely selfish, the employers were also given the possibility to punish and reward employees at a cost in a second experiment. A purely selfish employer would never punish or reward an employee. However the employers punished 68% of the time the employees that did not fulfill their contract, rewarded 70% of the time those that over fulfilled their contract and 44% of the time those that respected it exactly. Therefore both employers and employees tend to reciprocate the choice of the other rather than just maximizing their profit.

In another experiment, a *public goods game* was implemented and repeated for ten rounds. At the beginning of a round, each player receives one dollar and can choose to put in a public account or to keep it. For each dollar that he gives to the public account, $ 0.5 is added to the final payoff of each player. Finally, each player receives its payoff at the end of the ten rounds. The maximal payoff is obtained when all the players contribute $1

to the public account in each round. However, a selfish player will not contribute since contributing costs more if the choices of the others remain fixed. However it is observed that players tend to contribute half their private account in the first round and then it decays to nearly zero. This decay could be interpreted as a learning process where the players are prudent at the beginning but then understand how to maximize their payoff by not contributing. But if the game is played inside several groups and that at the end of a series of rounds the groups a reformed, the players tend also to put half of their account in the first round of the next session. One interpretation is that they start by cooperating, but then try to punish the defectors by not participating. This idea is supported by another experiment where the players first play in random groups, but then they can rank the other players according to their preferences to play with them, then the game is repeated but the players are assigned to groups according to their ranks, such that the players with the best ranks play with similar players. For the random groups the average rate of contribution was 38%. With the assortative groups the average rate of contribution is 70% on the whole. The groups with the higher rankings had a rate of 90% while the groups with the lower rankings had an average rate of 45%, which is higher than in the random groups.

The *third party punishment game* [8] shows another aspect of human reciprocity. In this game two players A and B play a dictator game : A receives an amount (100 tokens) of money and decides how to share it with B. B is just a passive player. In the third party punishment game a third player C receive a amount of money (50 tokens) and observes the transfer from A to B. Then C can assign punishment to A at a cost of 1 token for 3 tokens of punishment. As a result the players of type C only punished the A players who gave less than 50 tokens, the less they gave the more they were punished. Thus the C players punished the greedy A players at a cost even if the A players defected with respect to B players and not C. This shows that players tend to reciprocate the strategy even if they are not involved directly in the interaction. These experiments show that humans like to reward cooperators and punish defectors even if this doesn't lead to a higher payoff. Agents feel pleasure or satisfaction when rewarding cooperators and punishing defectors. Thus, with respect to cooperation, reciprocating other agents strategies seems to be a common behavior among humans.

But how this behavior may have come to spread among humans? An explanation is that it is transmitted by culture and genetic code. Feelings of self-esteem, anger toward defectors, shame and culpability could be transmitted in the genes and in the culture. If the groups in which the agents cooperate the most are the most successful, the related culture and genes will spread better than the other, a complete development of this idea can be found in [6]. Note that this idea of comparing cultural and biological evolution is not new and dates back to William James (1880) and Julian Huxley (1955).

After this necessarily brief glimpse on the origins and the effects of cooperation in society, we now turn to a description of the structure and the objectives of the present thesis.

1.3 Previous Work and Objectives

This thesis is composed of three parts. First we will study evolutionary game theory when the population is represented by weighted complex networks. In a second part population will be represented by spatial unweighted networks. In the third part the population will evolve on a spatial lattice and the agents will be able to adapt their position in order to increase their payoff.

Regarding game theory on networks with static agents, most of the previous work has dealt with unweighted graphs. This is understandable as a logical first step, since attributing reliable weights to relationships in social networks is not a simple matter because the relationship is often multi-faceted and implies psychological and sociological features that are difficult to define and measure, such as friendship, empathy, and common beliefs. In spite of these difficulties, including the strength of agents' ties would be a step toward more realistic models. In this thesis we propose to use both empirical and theoretical weight distributions on standard unweighted social network models in order to understand the influence of weighted networks on evolutionary games.

Networks in which there is an underlying spatial structure are also very important and have attracted attention (see [5] for an excellent recent review). In evolutionary games regular graphs such as one- and two-dimensional lattices have been used early on to provide a local structure to the population of interacting agents [2, 25]. One of the objectives of this thesis will be to extend the ideas and methods of evolutionary game theory to fixed unweighted spatial networks that go beyond discrete two-dimensional lattices and are more realistic.

In the majority of real situations both in biology and in human societies, actors have the possibility to move around in space. In the last decade there have been several new studies of the influence of mobility on the behavior of various games in spatial environments representing essentially two strands of research: one in which the movement of agents is seen as a random walk, and a second one in which the agents try to find a position that maximizes their fitness. Of course, intermediate situations may also exist. In this thesis we mainly use a type of opportunistic migration which consists in randomly trying several free positions in space within a given migration radius and in moving to the most profitable one. We show that success-driven migration notably changes the dynamical evolution of the population, and leads to very high levels of cooperation. Particularly when we increase the number of random imitations compared to the number of payoff dependent imitations.

In the last part, always in the context of opportunistic migration, we study a three strategy cyclic game. In this game three strategies S_1, S_2, S_3 are available. The strategies form a cycle such that when a strategy is adopted, the payoff earned while the other adopts the next strategy in the cycle is higher than the payoff obtained against the same strategy or the former one in the cycle. This type of game is not only of theoretical interest since it is partly responsible for the biodiversity on Earth, and has been actually observed in several biological situations such as the dynamic behavior of side-blotched lizards populations [35], coral reef invertebrates [17], and competition among different bacteria strands [18] among others. Cyclic behavior has also been found in studies of the public goods game type when players, besides being able to choose between cooperating or defecting behavior, also have

the choice of not taking part in the game (so-called "loner" strategy) [10]. Interestingly, this oscillating behavior was actually observed in an experiment with human subjects by D. Semman et al. [34].

In a spatial setting such as two-dimensional grids or, more generally, on relational networks, several results have been obtained. Szabó and Hauert [37] and Szabó and Vukov [39] studied the Prisoner's Dilemma on two-dimensional grids with three strategies: cooperate, defect, and loners and observed that the three strategies survive in a cyclic dominance way akin to the rock-paper-scissors (RPS) game. A similar phenomenon manifests itself on random graphs but with different characteristics. In [38] Szabó et al. investigated the behavior of the RPS game on regular small-world networks. In more recent work A. Szolnoki and coworkers have further studied the evolutionary Prisoner's Dilemma on spatial grids and random graphs showing that with a third tit-for-tat strategy the system can show a variety of interesting behaviors including stationary and oscillatory states [40].

Our objectives in this thesis, in the context of cooperation, are the following :

1. Understand how cooperation can thrive.
2. Explore the effect of weights for different types of degree-weight correlations and other weighted network models.
3. Find unweighted network topologies which foster cooperation.
4. Explore cooperation on spatial networks.
5. Explore different strategy update rules.
6. The effect of migrating to better places on the strategies evolution.
7. Which kind of spatial patterns are formed by migration only, i.e. when players keep a fixed strategy.
8. Variation of the imitation noise, i.e. players imitate their neighbors randomly rather than according to the payoffs.

In the context of cyclic games, we explore the effect of the following points on the diversity of strategies and the size of the spatial patterns :

1. The effect of migrating to better places.
2. Variation of the imitation noise.

1.4 Game Theory

1.4.1 Definitions

In order to make this thesis self-contained as far as possible, in this section we define the basic notions of game theory and give some general results. A game consist of a set of m players $1, 2, \ldots, m$ and for each player i a set of N_i available strategies S_i, and the payoffs Π_i attributed to each player for each strategy choice of all the players. When the set of available strategies is the same for all the players it will be denoted simply as S. A strategy can be interpreted as a specification of the moves a player will make in the game and the payoff is the outcome of the strategy choice given the choices of the other players.

A **mixed strategy** s for a player i is a probability distribution over the N_i strategies available to that player, with coefficients $p_1, .., p_N$. Since $p_i \geq 0$ and $\sum p_i = 1$, the set of all strategies available to player i can be represented as a simplex

$$\Delta_i = \{\mathbf{s} = (p_1, ..., p_{N_i}) \in \mathbb{R}^{N_i} : p_j \geq 0 \ and \ \sum_{j=1}^{N_i} p_j = 1\} \tag{1.1}$$

We will call it Δ when the set of strategies available is the same for all players. Note that the pure strategies are the unit vectors e_j.

Let S_i be the set of all possible strategies available to player i, a *strategy profile* in pure or mixed strategies is a m-tuple $\sigma = (s_1, ..., s_m)$ such that $s_1 \in S_1, ..., s_m \in S_m$ for pure strategies or $s_1 \in \Delta_1, ..., s_m \in \Delta_m$ for mixed strategies . The set of all strategy profiles is called Ψ.

In game theory, there are two standard representations of games, namely the normal form and the extensive form. The extensive form of a game represents a possible sequence of player's choices as a tree as in Figure 1.1. In that case the order of play is clear, player P_1 has the choice between strategy A_1 and A_2 and then player P_2 has the choice between strategy B_1 and B_2 if player P_1 has chosen A_1 and B_3, B_4 in the opposite case. The payoffs can be represented as the leafs of the tree, in Fig. 1.1 the first term of the bracket is the first player's payoff and the following term is the second player's payoff. It is also possible to specify the information available to a player about the previous choices of players, for example in fig. 1.1, player 2 can be unaware of the choice of player 1, and is represented by a dashed line between the two nodes labeled 2.

Unlike extensive forms, normal forms are not represented as a sequence of actions but
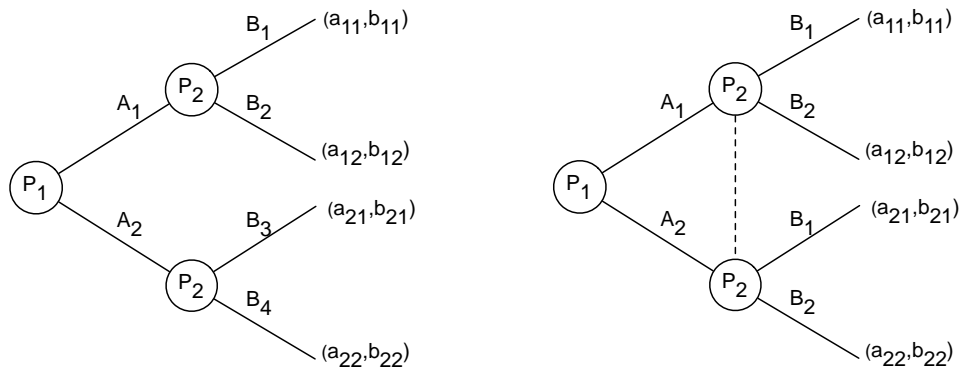
Fig. 1.1 An extensive form representation with complete information (left image), and partial information (right image)

represent the game by way of a payoff function which assign a payoff to a player as a function of the strategies chosen by the m players. In that case the temporal sequence of the game is not taken into account and everything happens as if all players played simultaneously. Formally, a payoff function is a function $\Pi : S_1 \times S_2 \times ... \times S_m \to \mathbb{R}$, which

Π_A, Π_B	B_1	B_2	$\ldots$	B_m
A_1	a_{11}, b_{11}	a_{12}, b_{12}	$\ldots$	a_{1m}, b_{1m}
A_2	a_{21}, b_{21}	a_{22}, b_{22}	$\ldots$	a_{2m}, b_{2m}
$\vdots$	$\vdots$	$\vdots$	$\ddots$	$\vdots$
A_n	a_{n1}, b_{n1}	a_{n2}, b_{n2}	$\ldots$	a_{nm}, b_{nm}

Table 1.1 A normal form representation.

is specified for each player. For a 2-player game, the payoff function can be represented as a payoff bi-matrix as can be seen in Table 1.1 where the first (second) entry in the bracket is the payoff of player $A(B)$. We call M_A the matrix containing the payoffs earned by player A, and M_B the matrix containing the payoffs of player B. Here the payoff matrix entries correspond to pure strategy choices, in order to take into account mixed strategies, the payoff of player i against player j is given by $\mathbf{s}_i \cdot M_i \mathbf{s}_j$ where $\mathbf{s}_k$ is the mixed strategy profile of player k. In order to facilitate the notation we will note (s, σ_{-i}) a strategy profile in which player i plays strategy s and the other players follow the strategy profile σ_{-i}. The payoff of a player i adopting strategy s_i when the other players adopt their strategies according to strategy profile σ will be noted $\Pi_i(s_i, \sigma_{-i})$.

A two-player game is said to be *symmetric* if the set of strategies for player 1 and player 2 is the same and the payoff bi-matrix is such that $M_1 = M_2^\top = M$, i.e. the transpose of one matrix is equal to the other and is called M. In other words the payoff of player 1 if 1 adopts strategy s and player 2 adopts strategy t is equal to the payoff of player 2 when player 2 adopts strategy s and player 1 adopts strategy t. This type of games are used when all the players are identical.

If the payoff bi-matrix of a two-player game is such that the sum of the players payoffs is always null, i.e $M_1 = -M_2 = M$ the game is called a *zero-sum game*. For this class of games the *Minimax theorem* stipulate that there exists a value v such that

$$v = \max_{\mathbf{p}} \min_{\mathbf{q}} \Pi(\mathbf{p}, \mathbf{q}) = \min_{\mathbf{q}} \max_{\mathbf{p}} \Pi(\mathbf{p}, \mathbf{q}) = \max_{\mathbf{q}} \min_{\mathbf{p}} \Pi(\mathbf{q}, \mathbf{p}) \qquad (1.2)$$

where $\Pi(\mathbf{p}, \mathbf{q}) = \mathbf{p} \cdot V \mathbf{q}$. Which is equivalent to

$$v = \max_{\mathbf{p}} \min_{\mathbf{q}} \Pi(\mathbf{p}, \mathbf{q}) = \max_{\mathbf{q}} \min_{\mathbf{p}} \Pi(\mathbf{q}, \mathbf{p}) \qquad (1.3)$$

by definition of the payoff matrix M. In other words there always exists a mixed strategy which is optimal for both player.

The strategy t_i of player i is said to *strictly dominate* the strategy s_i if $\Pi_i(t_i, \sigma_{-i}) > \Pi_i(s_i, \sigma_{-i})$ for all $\sigma \in \Psi$. In order to find the "solution" of a game it is possible to first simplify the game by iteratively eliminating the strictly dominated strategies. Indeed a basic postulate of rationality in game is to consider that rational players never play strictly dominated strategies. Thus the strictly dominated strategies can be eliminated from the game. When a strictly dominated strategy is eliminated some remaining strategies can be strictly dominated in the new game. Therefore the strictly dominated strategies can be removed iteratively until no more strictly dominated strategy exists in the game. It is

possible to show that the set of remaining strategies is independent of the details of the elimination procedure ([7]). In some case, as in the famous prisoner's dilemma game, only one strategy profile survives the elimination procedure and is therefore the solution of the game under perfect rationality. However it is more common that more than one strategy remain after the iterative elimination of strictly dominated strategies. Furthermore, for a player, the process of eliminating recursively his strategies and to know which strategies the other players will eliminate requires a strong rationality.

Nash Equilibrium. Another more general way of modeling solutions and equilibria of a game is the concept of Nash equilibrium [22]. A strategy profile σ is a Nash equilibrium (NE) if no player can benefit by changing strategy while the other players keep theirs unchanged. More formally a strategy profile $\sigma^* = (s_1^*, \ldots, s_m^*)$ is a *Nash equilibrium*, iff

$$\forall i, \forall s_i \neq s_i^* : \qquad \Pi_i(s_i^*, \sigma_{-i}^*) \geq \Pi_i(s_i, \sigma_{-i}^*). \tag{1.4}$$

If the inequality is strict, σ^* is called a *strict Nash equilibrium*. A *best response* for a player is the best strategy choice given the choices of the other players. A Nash equilibria can be defined in terms of *best response* as a strategy profile where each agent's strategy choice s_i^* is a best response to the other player's strategies.

A very important theorem in classical game theory is *Nash's theorem* [21]. This theorem asserts that for all finite normal-form games there exists at least one Nash equilibrium in pure or mixed strategies.

A *symmetrical Nash equilibrium* is a NE where all the agents play the same strategy.

By definition a Nash equilibrium is stable against single unilateral changes concerning only one player. However it is possible that some players change their strategies at the same time and that it increases the payoffs of some other players without decreasing the payoff of any player. In that case the initial Nash equilibrium is called *inefficient*. In the opposite case the NE is called *Pareto efficient*. These concepts can be used to refine the concept of Nash equilibrium and determine what is the final outcome of a game. It is interesting to note that in the Prisoner's Dilemma game there is only one Nash equilibrium but this equilibrium is not Pareto-efficient. Therefore there exist a state which maximize the total payoff of the players and it is not the Nash equilibrium.

A very useful result in classical game theory is the invariance of the dominance and best response relations, and the set of Nash equilibria under *positive affine transformations* of the players payoff function. More formally, let G and G^* be two games. For each player i, positive real number a_i and real number b_i such that $\Pi_i(\sigma)^* = a_i \Pi_i(\sigma) + b_i$ for all strategy profile σ, the set of Nash equilibria is invariant, as well as the dominance and best response relations.

Moreover if a constant b_i is added to the payoff of player i only for a fixed strategy profile σ_{-i} of the other players, Nash equilibria and dominance as well as best response relations are unchanged.

For a two player game with payoff bi-matrix (M_1, M_2) the first transformation is the affine transformation, $M_i^* = a_i M_i + b_i$ for $i \in 1, 2$, and the second transformation amounts to adding the constant b_1 to one column of M_1, or b_2 to one raw of M_2. These transformations allow to simplify the payoff matrix and analyze it instead of the original one.

Another consideration that can help to find the Nash equilibria is that a NE cannot be

strictly dominated, therefore it is possible to first iteratively eliminate all the strictly dominated strategies.

Finally, in order to derive the Nash equilibria in mixed strategies, we compute the mixed strategy profile with the condition that, given a player, the expected payoffs for each strategy choices are equal. If this condition is fulfilled the player has no incentive to change its mixed strategy since the payoffs would be the same. This system of equations, together with the normalization of the probabilities constraint, has the Nash equilibria as solution.

1.4.2 Games

In this section we analyze two-player, two-strategy symmetric games. Such a game is defined by a matrix

$$\begin{pmatrix} a & b \\ c & d \end{pmatrix}$$

By the invariance property we can reduce the matrix to

$$\begin{pmatrix} a_1 & 0 \\ 0 & a_2 \end{pmatrix}$$

With this matrix it is possible to show that these games can be classified according to the following types [36]:

1. *Coordination class*: $a > c$, $d > b$ or $a_1 > 0$, $a_2 > 0$. Two strict Nash equilibrium in pure strategy, and one non-strict NE in mixed strategies:

   - $s^* = t^* = 1$
   - $s^* = t^* = 0$
   - $s^* = t^* = v$

   All NE are symmetric, i.e. $s^* = t^*$.

2. *Anti-coordination class*: $a < c$, $d < b$ or $a_1 < 0$, $a_2 < 0$. Two strict Nash equilibrium in pure strategy, and one non-strict NE in mixed strategies:

   - $s^* = 1, t^* = 0$
   - $s^* = 0, t^* = 1$
   - $s^* = t^* = v$

   The first two NE are asymmetric, and the third is symmetric.

3. *Strict dominance class [41]*: $(a - c)(d - b) \leq 0$ or $a_1 a_2 < 0$. One pure strategy strictly dominates the other and there is only one symmetric pure strategy strict Nash equilibrium:

   - $s^* = 1, t^* = 1$ or $s^* = 0, t^* = 0$

   In the following paragraphs we analyze five well-known games that will be heavily used in this thesis. The first four are classical two-person, two-strategy, symmetric games,

namely the Prisoner's Dilemma (PD), the Hawk-Dove Game (HD), the Stag Hunt (SH), and the Harmony game (H). These games are traditionally defined by the following generic payoff bi-matrix:

$$
\begin{array}{cc}
 & \begin{array}{cc} C & \quad D \end{array} \\
\begin{array}{c} C \\ D \end{array} & \begin{pmatrix} R,R & S,T \\ T,S & P,P \end{pmatrix}
\end{array}
\tag{1.5}
$$

The set of strategies is $\Lambda = \{C, D\}$, where C stands for "cooperation" and D means "defection". In the payoff matrix R stands for the *reward* the two players receive if they both cooperate, P is the *punishment* if they both defect, and T is the *temptation*, i.e. the payoff that a player receives if he defects while the other cooperates and gets the *sucker's payoff* S. In general we have $R > P$, since mutual cooperation should be more profitable than mutual defection.

The Prisoner's Dilemma. For this game, the payoff values are ordered such that $T > R > P > S$. Defection is always the best rational individual choice, so that (D, D) is the unique strict Nash Equilibrium (NE). This game belongs to the strict dominance [41] class of games as defined above. The interest of this game is that the strategy profile $\sigma = (C, C)$ in which both players profit equally is unstable, since cooperation is strictly dominated by defection. Therefore both players adopt defection; thus $\sigma^* = (D, D)$ is the NE, but this Nash equilibrium is inefficient since changing the strategies of the players to (C, C) increases the payoffs of both players. The prisoner's dilemma is ubiquitous in society and economics. Some examples are competing companies on market selling the same products and battling for the marketplace, arms race between superpowers, climate change, etc. The prisoner's dilemma is easily extended to more than two players, in such a game the payoff depends on the interaction between N persons. For example the payoff can be $b - c$ ($b > c > 0$) for the cooperators and b for the defectors if more than n persons cooperate and 0 otherwise.

The Hawk-Dove. In the HD game, the order of P and S is reversed, yielding $T > R > S > P$. This game is characterized by the high temptation to defect and the low punishment, thus mutual defection leads to the lowest payoff. When both players cooperate they have a strong incentive to play D, therefore one of the players will adopt defection which is better for that player and worse for the other. On the other hand, if the strategy profile is (D, D), it is more profitable for both players that one of them chooses cooperation. Finally the solution will be that one player cooperates while the other defects. (C, D) and (D, C) are the NE of the game in pure strategies, and there is a third equilibrium in mixed strategies. This game is in the anti-coordination class and no strategy is strictly dominated. The strategy profiles (D, C) and (C, D) are Pareto-efficient. The mixed Nash-equilibria can be computed by equating the expected payoffs of the strategies C and D for any of the symmetrical players and using the normalization of the probabilities leading to $\sigma^* = ((P - S)/(R + P - S - T), (R - T)/(R + P - S - T))$.

The Stag Hunt. In this game, the ordering is $R > T > P > S$, which means that mutual cooperation (C, C) is the best outcome, Pareto-efficient, and a NE. The second NE, where both players defect is less efficient but also less risky. The tension is represented by the fact that the socially preferable coordinated equilibrium (C, C) might be missed for "fear" that the other player will play D instead. There is a third mixed strategy Nash equilibrium given by $\sigma^* = ((P - S)/(R + P - S - T), (R - T)/(R + P - S - T))$ as in the HD, but it is an unstable fixed point.

Harmony. Finally, in the H game $R > S > T > P$ or $R > T > S > P$. In this case C strongly dominates D and the trivial unique NE is (C, C).

The last game is a cyclic two-player three-strategy game.

Rock-Paper-Scissors. In the Rock-Paper-Scissors (RPS) game the three states cyclically dominate each other. The game can be modeled by the following matrix:

$$
\begin{array}{c}
 \\
S1 \\
S2 \\
S3
\end{array}
\begin{array}{ccc}
S1 & S2 & S3 \\
\left(\begin{array}{ccc}
a & b_2 & -b_1 \\
-b_1 & a & b_2 \\
b_2 & -b_1 & a
\end{array}\right)
\end{array}
\tag{1.6}
$$

where b_1 and b_2 are positive. By invariance under affine transformations we can subtract a to the payoff matrix and reduce the game to the case $a = 0$. There is no Nash equilibrium in pure strategy since when player 1 starts for example with strategy S_3 player 2 adopts strategy S_2, but then 1 is better off with strategy S_1, and the process continues cyclically. On the other hand there is a Nash equilibrium in mixed strategies given by $\sigma^* = (1/3, 1/3, 1/3)\ \forall a, b_1, b_2$.

1.5 Evolutionary Game Theory

Evolutionary game theory is the theory of the dynamic adaptation and learning in repeated games played with bounded rationality. In this section we restrict to *population games*. Population games are defined by an underlying two-player game and some strategy update rule, with the assumption that the population is large and that the players are identical, and thus the game is symmetrical too. In this type of game mixed strategies can be interpreted as the frequencies of players adopting each strategy in the population.

1.5.0.1 Evolutionarily Stable Strategies

An evolutionarily stable strategy (ESS) is a strategy which cannot be invaded by another strategy in the sense that its payoff is higher than the payoff of the invader if the frequency of the invader in the population is small enough. Formally, if $\Pi(s, t)$ represents the payoff

of strategy s against strategy t, a strategy s is an ESS if for all $t \in \Delta$ with $t \neq s$, the inequality

$$\Pi(s, (1-\epsilon)s + \epsilon t) > \Pi(t, (1-\epsilon)s + \epsilon t)$$

holds for all $\epsilon > 0$ that are sufficiently small.

It is possible to split the formal definition of evolutionary stability into two conditions such that one of them implies that the strategy is a symmetric Nash equilibrium and the other one is a stability condition:

1. Nash equilibrium : $\Pi(s,s) \geq \Pi(t,s)$
2. Stability condition : $\Pi(s,t) > \Pi(t,t)$

for all $t \neq s$. Note that a strict Nash equilibrium, i.e. $\Pi(s,s) > \Pi(t,s) \forall t \neq s$, is an ESS, therefore the second condition is only needed if $\exists\, t$ such that $\Pi(s,s) = \Pi(t,s)$.

It is now possible to analyze further the games of section 1.4.2 with the concept of ESS. Indeed, for games in the coordination class such as the Stag-Hunt, the two Nash equilibria in pure strategies are ESS since they are strict NE. However the mixed strategy equilibrium s is not evolutionarily stable since each pure strategy earns more against itself than s earns against the pure strategy.

For the games in the anti-coordination class such as the Hawk-Dove, it is possible to show that the mixed strategy Nash equilibria s is evolutionary stable. Note that the pure strategy Nash equilibria have different strategies for the two players therefore the ESS definition cannot be applied.

Finally for games in the strict dominance class such as the prisoner's dilemma, the Nash equilibrium is strict and symmetric and therefore it is an ESS.

For the RPS game the unique Nash equilibrium $s = (1/3, 1/3, 1/3)$ is not strict as can be checked with the Nash equilibrium condition. However the stability condition applied to s implies that s is evolutionarily stable when $b_2 > b_1$ and not evolutionarily stable otherwise. For $b_2 = b_1$, $\Pi(s,t) = \Pi(t,t)$ for all $t \neq s$. A discussion of a class of RPS games with an equivalent parameter space can be found in [41].

1.5.0.2 The Replicator Equations

The replicator equations allow to analyze Nash equilibria and evolutionary stability from the point of view of large and well-mixed population with differential equations. Generally it is not possible to obtain an exact solution since the equations are non-linear, but instead the rest points are analyzed in terms of stability. Let's $s_1, \ldots, s_N$ be the strategies available to the players; the replicator equations describe the temporal evolution of the players strategy frequencies $x_1, \ldots, x_N$. As in the mixed strategy case, the frequencies sum up to one and are positive numbers.

Let Θ_i be a measure of evolutionary success of a strategy i. Then a player adopting strategy i should leave an offspring with a probability proportional Θ_i, and therefore the derivative $\dot{x}_i$ of the frequency of strategy i is proportional to $x_i \Theta_i$. Taking $\Theta_i = $ (fitness of $E_i - $ average fitness) as a measure of evolutionary success we obtain the replicator equations:

$$\dot{x}_i = x_i(F_i((x)) - \bar{F}(\mathbf{x})) \qquad i = 1, \dots, N, \qquad (1.7)$$

where F_i is the fitness function of strategy i and $\bar{F}$ is the average fitness over all the strategies. In order to simplify the analysis, the payoff function F is often assumed to depend linearly upon the strategies frequency. Therefore the replicator equations can be rewritten as

$$\dot{x}_i = x_i((M\mathbf{x})_i - \mathbf{x} \cdot M\mathbf{x}) \qquad i = 1, \dots, N, \qquad (1.8)$$

where M is a two players N strategies payoff matrix. In the context of human societies strategies spreads through imitations rather than births. Therefore it is interesting to note that these equations are also valid for a population where an agent i imitates a randomly chosen other player j with probability proportional to the difference between the payoffs $\Delta_{ji} = \Pi_j - \Pi_i$ if Δ_{ji} is positive, and a null probability if Δ_{ji} is negative, [13, 14, 36]. Furthermore, the rest points of equations 1.8, i.e the points $\mathbf{x}$ for which $\mathbf{x}(t) = \mathbf{x}$ for all t, are given by the following conditions

$$(M\mathbf{x})_1 = \dots = (M\mathbf{x})_N,$$
$$x_1 + \dots + x_N = 1.$$

Note that the simplex Δ is an invariant of equations 1.8.
In the framework of the replicator equations a point $\mathbf{x}^*$ is a *Nash equilibrium* if

$$\mathbf{x} \cdot M\mathbf{x}^* \leq \mathbf{x}^* \cdot M\mathbf{x}^* \qquad (1.9)$$

for all $\mathbf{x} \in \Delta$, and an *evolutionarily stable state* if

$$\mathbf{x}^* \cdot M\mathbf{x} > \mathbf{x} \cdot M\mathbf{x} \qquad (1.10)$$

for all $\mathbf{x} \neq \mathbf{x}^*$ in a neighborhood of $\mathbf{x}^*$. In less formal terms $\mathbf{x}^*$ is evolutionarily stable if after a sufficiently small deviation from $\mathbf{x}^*$ the population return to it. In order to briefly summarize theoretical results we need also some definitions of stability for differential equations.
If for all points x close enough to an equilibrium point x_e the temporal orbits stay near x_e forever, then x_e is *Lyapunov stable*. If the orbits converge to x_e, then x_e is *asymptotically stable*. If x_e is Lyapunov stable and all points x which are not on a border of Δ converge to x_e then x_e is called *globally stable*. The definition does not include the borders since the boundary faces of Δ are invariants.
The ω-*limit* of a point $\mathbf{x}$ is the set of accumulation points of $\mathbf{x}(t)$, for $t \to \infty$:

$$\omega(\mathbf{x}) = \{\mathbf{y} \in \mathbb{R}^n : \mathbf{x}(t_k) \to \mathbf{y} \quad \text{for some sequence} \quad t_k \to +\infty\} \qquad (1.11)$$

The following general results describe Nash equilibria and evolutionary stability from the point of view of the replicator equations [15, 16, 36].

1. If $\mathbf{x}^* \in \Delta$ is a Nash equilibrium of the game described by the payoff matrix M, then $\mathbf{x}^*$ is a rest point.
2. If $\mathbf{x}^*$ is a strict Nash equilibrium, then it is asymptotically stable.
3. If $\mathbf{x}^*$ is the ω-limit of an orbit $\mathbf{x}(t)$ in the interior of Δ, then $\mathbf{x}^*$ is a Nash equilibrium.

4. If $\mathbf{x}^*$ is Lyapunov stable, then it is a Nash equilibrium.

Additionally, every interior rest point is a Nash Equilibrium and all the corners of the simplex are rest points. These results show that the relation between Nash equilibria and the replicator equations is not trivial.
Concerning the evolutionary stability we have the following results [15, 16, 36]

1. If $\mathbf{x}^*$ is an evolutionarily stable state for the game and payoff matrix M, then it is an asymptotically stable rest point.
2. If $\mathbf{x}^*$ is an interior evolutionarily stable state, then it is a global attractor.

Furthermore for two strategies symmetrical games, a rest point is asymptotically stable if and only if the corresponding mixed strategy is evolutionary stable ([41]).
Here also, the replicator equations 1.8 are invariant under positive affine transformations of the payoff except for a change in the timescale as can be checked. And they are invariant under the addition of constants to the columns of the payoff matrix.

1.5.0.3 Two-Player Symmetric Games

In this section we analyze two-player symmetric games with the replicator dynamics following [41]. Since the replicator dynamics equations 1.8 are invariant under addition of constants to the columns the following payoff matrix can be used again:

$$\left(\begin{array}{cc} a_1 & 0 \\ 0 & a_2 \end{array} \right).$$

Therefore the replicator dynamics for frequency of players adopting the first strategy is

$$\dot{x}_1 = x_1 x_2 (a_1 x_1 - a_2 x_2), \tag{1.12}$$

with $x_1 + x_2 = 1$. Letting $\dot{x}_1 = 0$ and analyzing the term $a_1 x_1 - a_2 x_2$ when neither a_1 nor a_2 is null we obtain easily the same three categories as in section 1.4.2,

1. *Coordination class [41]*: $a_1 > 0$, $a_2 > 0$. The growth of rate of x_1 changes sign at the mixed strategy equilibrium $x_1 = \lambda = a_2/(a_1 + a_2)$. x_1 decreases when $x_1 < \lambda$, and x_1 increases when $x_1 > \lambda$. Therefore the NE $x_1 = \lambda$ is unstable and the population converges to one of the pure strategy states as can be observed in fig. 1.2 first image.
2. *Anti-coordination class [41]*: $a_1 < 0$, $a_2 < 0$. Here also the growth of rate of x_1 changes sign at the mixed strategy equilibrium $x_1 = \lambda$. However x_1 increases when $x_1 < \lambda$, and x_1 decreases when $x_1 > \lambda$. Therefore the NE $x_1 = \lambda$ is stable and the population converges to the mixed strategy Nash equilibrium, see fig. 1.2 second image.
3. *Strict dominance class [41]*: $a_1 a_2 < 0$. If $a_1 > 0$ and $a_2 < 0$, x_1 alway increases, otherwise it always decreases. Therefore the population converges either to strategy 1 or to strategy 2 for any initial value. See fig. 1.2 third image where the case $a_1 > 0$, $a_2 < 0$ is depicted.
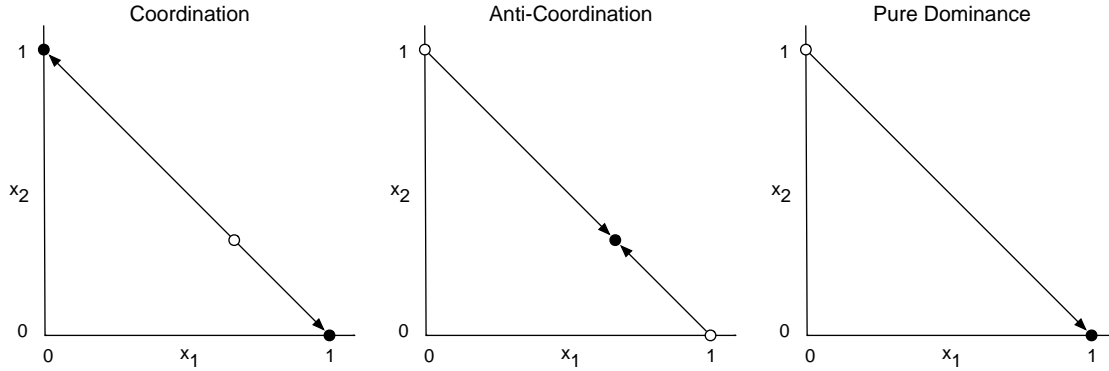
Fig. 1.2 Orbits of the replicator dynamic in Δ for the three classes of 2-players games. Open circles represent unstable fixed points. First image: the population converges to either strategy 1 or 2 depending on the initial condition (Coordination class). Second image: the population converges to the mixed Nash equilibrium (Anti-coordination class). Third image: the population converges to either strategy 1 or 2 depending on the payoff values for any initial conditions (Strict dominance class), here only the case where the population converges to strategy 1 is displayed

These results can be applied to the social dilemmas discussed in section 1.4.2. For example in the PD game case, which is in the strict dominance class, the population converges to defection for any initial value.

1.5.0.4 Rock-Paper-Scissors

For the **_RPS_** game there exists an unique rest point $\mathbf{x}^*$ in the interior of Δ, which is also the unique Nash equilibrium. An interesting theorem which holds for the matrix M represented in Eq. 1.6 for $a = 0$, in the general case where the parameters b_1 and b_2 can be different in each line,[15, 16].
The following conditions are equivalent for the RPS game given by the matrix M for $a = 0$.

1. *$\boldsymbol{x}^*$ is asymptotically stable,*
2. *$\boldsymbol{x}^*$ is globally stable,*
3. *det $M > 0$,*
4. *$\boldsymbol{x}^* \cdot M\boldsymbol{x}^* > 0$.*

In particular, the third condition is equivalent to $b_2 > b_1$ in the case where b_1 and b_2 are the same numbers in all lines. When this condition is fulfilled all points in the interior of Δ converge to $\mathbf{x}^*$. Let $x(t) = (x_1, x_2, x_3)$ be an orbit in Δ, then it is possible to show that the product $x_1 x_2 x_3$ increases for $b_1 > b_2$, decreases for $b_1 < b_2$ and is constant for $b_1 = b_2$. This shows that the orbits drift away from the rest point, converge to the rest point, are cycles defined by $x_1 x_2 x_3 = const$, respectively, [41]. As the orbits converge to the borders they visit the neighborhood of all corners cyclically and stay more time in each corners.
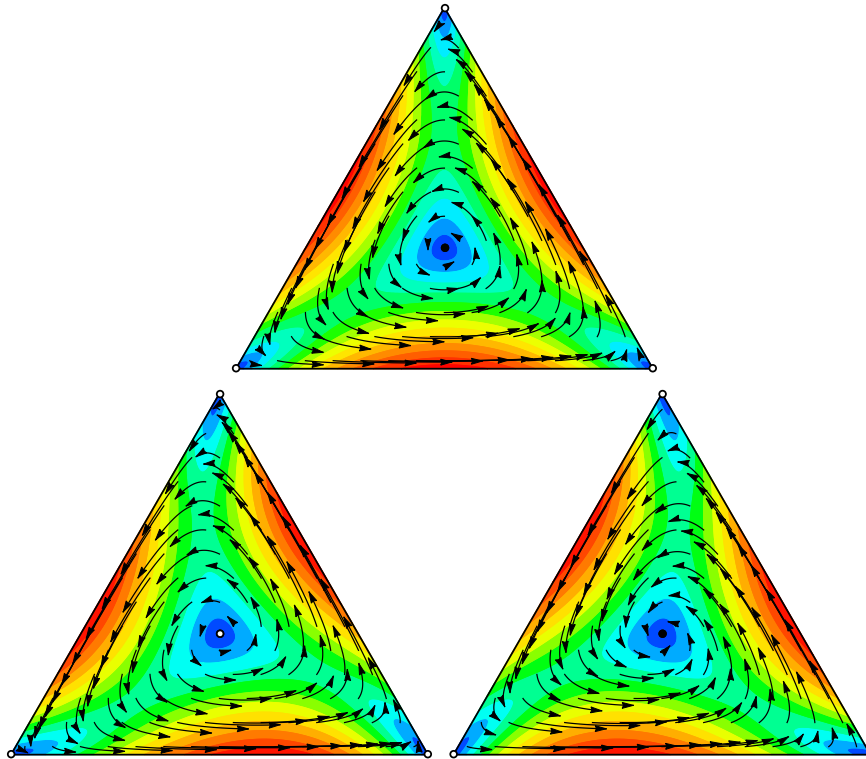
Fig. 1.3 Orbits of the replicator dynamic in Δ for RPS game with $b_1 = 1$ and $b_2 = 0.55$. The length of the arrows and the colors indicate speed. Top image: $b_1 = 1, b_2 = 1$, the orbits are closed orbits around the rest point; Left image: $b_1 = 1.5, b_2 = 0.5$, the orbits drift apart from the rest point; Right image: $b_1 = 0.5, b_2 = 1.5$, the orbits converge to the rest point; Image made by the game dynamic simulation program "Dynamo", [3]

This can be observed in Fig. 1.3 where the three cases are depicted.

1.6 Networks

A network captures the connectivity structure of a system. It includes the detailed information about the relations between the agents. Since the connectivity structure affects the dynamic, networks are important tools.

A network is a collection of points joined together by lines. In order to describe a network we use the concepts of *graph theory*. Network theory deals with real data sets such as the world wide web or social networks.

1.6.1 Definitions

A graph is generally thought as a representation of a set of objects connected by links. The objects are called *vertices* and labeled by a number and the links are called *edges* and are noted (i, j), where i and j are the labels of the two vertices connected. A graph is noted $G = (E, V)$ where E is the set of edges of G and V is the set of vertices. A *path* is a sequence of edges $(a_1, a_2), (a_2, a_3), \ldots, (a_{n-1}, a_n)$. A subgraph $G' = (E', V')$ is a graph such that E' is included in E, and V' is included in V. An *induced subgraph G'* of G is a subgraph of G in which $e = (i, j) \in E'$ *iff* $e \in E$ and $i, j \in V'$. In other words, E' contains all the edges in E which run between any two vertices in V'. A *component G'* is an induced subgraph of G in which there is a path between all pair of vertices in V' and there is no path in G between vertices i and j if $i \in V'$ and $j \notin V'$.
A graph is *directed* if the edges are directed, if all edges are symmetric the graph is said to be *undirected*.
A neighbor of a vertex i is any other vertex j adjacent to i. The set of neighbors of i is denoted by V_i. The *degree k_i* of a vertex i is the number of vertices in V_i. A vertex with high degree compared to other vertices is called a *hub*.
The *degree distribution* of G is the probability p_k to chose randomly a vertex with degree k, and the *degree sequence* is the set of degrees $k_1, \ldots, k_n$ for all vertices. The *cumulated degree distribution* is the probability P_k to chose randomly a vertex with degree $k' \geq k$

$$P_k = \sum_{k'=k}^{\infty} p_{k'}. \tag{1.13}$$

The advantage of cumulated degree distribution is that it is less noisy. For degree distribution of the form $p_k = Ck^{-\alpha}$ for $k \geq k_{min}$ for some k_{min} the cumulated degree distribution is also a power law but with coefficient $\alpha - 1$.

$$P_k = C \sum_{k'=k}^{\infty} p_{k'} \simeq C \int_k^{\infty} k'^{-\alpha} \, \mathrm{d}k' \tag{1.14}$$

$$= \frac{C}{\alpha - 1} k^{-(\alpha-1)} \tag{1.15}$$

Power-law degree distributions can be detected with logarithmic xy-axes since they appear approximatively as straight lines.
The distance between nodes is difficult to define since networks are often not embedded in a spatial layout. The *geodesic distance* between two vertices is the length of the shortest path separating these vertices (the smallest number of edges separating them).
The *clustering coefficient* measures the ratio of triangles (three vertices fully connected) over the number of connected triples (a triangle with a missing edge). There are two different definitions for the clustering coefficient, one global and one local. The global one is the number of triangles divided by the number of connected triples in the whole network

$$C = \frac{\text{number of triangles} \times 3}{\text{number of connected triples}} \tag{1.16}$$

where the number of triangles is multiplied by 3 since each triangle corresponds to 3 connected triples. It can also be seen as the number of paths of length 2 which are closed

divided by the number of paths of length two. Therefore C is also a measure of *transitivity* in the network. The clustering coefficient measures the density of triangles in a network, but it is possible to measure the densities of other *motifs* in the network. Note also that social networks have a larger clustering coefficient than other type of networks, [24]. One reason might be that people meet often in groups where the agents tends to be all connected.

Another definition for the clustering coefficient uses the notion of *local clustering coefficient*. The local clustering coefficient of a vertex i is defined as the number of pairs of neighbors of i that are connected divided by the total number of pairs of neighbors of i. Then in order to obtain a global clustering coefficient we average this quantity over all the vertices. Note that this clustering coefficient is not exactly equivalent to the first one.

A *bipartite network* $G(V, E)$ is a graph where the vertices can be partitioned into two disjoint sets $V_1 \cup V_2 = V$, $V_1 \cap V_2 = \emptyset$, such that there are no edges $e = (i, j)$ between vertices belonging to the same set:

$$\{(i, j) : i \in V_1, j \in V_2\}, \ \forall e \in E.$$

A weighted network is also noted $G(V, E)$ where V is the set of vertices and E is the set of weighted edges. The weight of an edge (i, j) is noted w_{ij}. The strength $s(i)$ of a vertex i is defined as $s(i) = \sum_{j \in V_i} w_{ij}$, and $p(s)$, $p(w)$ denote respectively the *strength* and *weight* distributions. The *adjacency matrix* A_{ij} of a network is a matrix which entries are the directed weights of the edges between the nodes i and j. If the graph is unweighted the entries are 0 or 1, and if it is undirected, $A_{ij} = A_{ji}$.

1.6.2 Assortativity by characteristic and degree

In this section we introduce the *assortativity coefficient*, following [24]. Let us consider that each vertex has a characteristic given by a scalar value, such as the degree, and call x_i the characteristic of vertex i. Then let (x_i, x_j) be a pair of values for the vertices at the end of an edge (i, j): we can define the assortativity as the covariance of these values over the edges

$$cov(x_i, x_j) = \frac{\sum_{ij} A_{ij}(x_j - \mu)(x_i - \mu)}{\sum_{ij} A_{ij}} \tag{1.17}$$

where $\mu = \frac{\sum_{ij} A_{ij} x_i}{A_{ij}}$ is the mean of x_i over the edges and A_{ij} is the adjacency matrix. After some calculations, we obtain

$$cov(x_i, x_j) = \frac{1}{2m} \sum_{ij} \left(A_{ij} - \frac{k_i k_j}{2m} \right) x_i x_j. \tag{1.18}$$

Where m is the number of edges. In order to obtain the *coefficient of assortativity* we normalize this covariance in order that it takes the value 1 in the case where each characteristic is placed on the network such that a vertex i is only connected to vertices j

such that $x_i = x_j$. Note that such a configuration for a given set of vertices with given characteristics is often not possible. If $x_i = x_j$ for all pair of neighbors (i, j), the previous equation can be rewritten as :

$$cov(x_i, x_j) = \frac{1}{2m} \sum_{ij} \left(A_{ij} x_i^2 - \frac{k_i k_j}{2m} x_i x_j \right) = \frac{1}{2m} \sum_{ij} \left(k_i \delta_{ij} - \frac{k_i k_j}{2m} \right) x_i x_j. \tag{1.19}$$

And the normalized *assortativity coefficient* is

$$r = \frac{\sum_{ij} \left(A_{ij} - \frac{k_i k_j}{2m} \right) x_i x_j}{\sum_{ij} \left(k_i \delta_{ij} - \frac{k_i k_j}{2m} \right) x_i x_j}. \tag{1.20}$$

where δ_{ij} is the Kronecker coefficient. This measure takes the value 1 in a perfectly assortative configuration, -1 in a perfectly disassortative configuration and 0 when the values of at the end of the edges are uncorrelated. A case of particular interest is the assortative mixing by degrees, where the $x_i = k_i$ are the degrees of the vertices. After replacing the x_i by the k_i in equation 1.20 we obtain

$$r = \frac{S_1 S_e - S_2^2}{S_1 S_3 - S_2^2} \tag{1.21}$$

where $S_e = \sum_{ij} A_{ij} k_i k_j$, $S_p = \sum_i k_i^p$, for $p = 1, 2, 3$.
In this work we will refer to this value as the *assortativity coefficient*. In real networks the assortativity coefficient is generally positive for the social networks such as for example in scientific coauthorship and negative in other types of networks such as information or technological networks.
It is interesting to note that in [24], the authors also give another kind of assortativity coefficient Q called *modularity* in the case where the characteristics c_i are enumerative types, i.e discrete types. In that case the modularity is computed by taking the total number of edges that run between vertices of the same type divided by the total number of edges m

$$Q = \frac{1}{2m} \sum_{ij} A_{ij} \delta(c_i, c_j). \tag{1.22}$$

Then in order that the modularity be null in the case where the edges are randomly assigned to pairs of vertices in the network, the value of the modularity in that latter case is subtracted

$$Q = \frac{1}{2m} \sum_{ij} \left(A_{ij} - \frac{k_i k_j}{2m} \right) \delta(c_i, c_j). \tag{1.23}$$

The modularity is strictly smaller than 1 and positive if there are more edges between vertices of the same type than in the random case.
In the previous measure the average was made over the edges. However, if the modularity describe the assortativity as viewed from the vertices, it is more convenient to take the average over the latter. In that case, enumerative assortativity can be obtained by taking the frequency of neighbors of a vertex i that have the same characteristic as i and averaging over all the vertices.

$$Q = \sum_i \frac{1}{k_i} \sum_j A_{ij} \delta(c_i, c_j). \tag{1.24}$$

If we measure the assortativity on a fixed network, we can subtract the value of Q in the case where the characteristics are randomly assigned over the network. In that way the neutral case has the same network topology as the network on which assortativity is measured. By subtracting the latter neutral case we obtain that

$$Q = \sum_i \frac{1}{k_i} \sum_j A_{ij} (\delta(c_i, c_j) - C). \tag{1.25}$$

where $C = \sum_c p(c)^2$ and $p(c)$ is the frequency of the characteristic c, i.e the probability to find this characteristic on a vertex after random assignement.

1.6.3 Network Topologies

In this section we define some important standard graph topologies and present undirected network models.

1.6.3.1 Regular Networks

A *regular network* is a network where all vertices have the same number of neighbors. A *complete graph G* is a graph where all the vertices are connected to each other.
Spatial lattices are the simplest type of spatial network. In a spatial lattice the vertices are embedded in euclidean space on a grid. For simplicity the grid is often a square grid. Then the edges are attributed to each pair of vertices whose distance is smaller than a constant d_{max}. Such a lattice can be appreciated in Fig. 4.4 first image. The problem with spatial lattices are the borders. In order to overcome this problem periodic boundary conditions are used. This amounts to folding the spatial plane to form a torus as can be seen in Fig. 4.4 second image. In this way the degrees of vertices are homogeneous.

1.6.3.2 Random Networks

A *random graph* is a graph in which some parameters are randomly chosen. A simple form of random graph $G(n, m)$ is a graph where the number of vertices is fixed to n and the number of edges to m. The edges are randomly assigned to pairs of vertices. However this type of network is difficult to handle mathematically. A more easy to handle model is the Erdos-Rényi random graphs noted $G(n, p)$ [24, 28]. In this model we have also n vertices but an edge exists between any pair of vertices with probability p. Many properties of this type of network can be calculated analytically; here we give some results, more detailed information can be found in [24]. An example of a random graph of size $n = 100$ is depicted in Fig. 1.5 left image. The mean degree of a random graph is $c = \langle k \rangle = (n - 1)p$. The
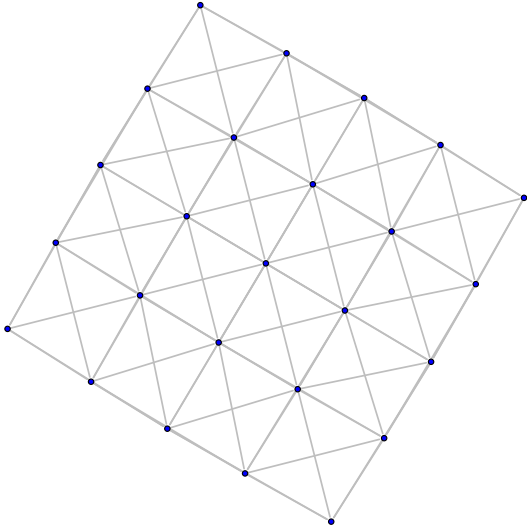
Fig. 1.4 Left image : Regular lattice of side 4 with connections to the 8 nearest neighbors. Right image : Periodical border conditions of the plane.

degree distribution can be computed as follows. The probability to be connected to k chosen vertices and not to the other $n - 1 - k$ vertices is $p^k (1 - p)^{n-1-k}$ and there are $\binom{n-1}{k}$ ways to chose k vertices among $n - 1$. Thus the degree distribution is

$$p_k \; = \; \binom{n-1}{k} p^k (1 - p)^{n-1-k}, \tag{1.26}$$

which is a binomial distribution. In the limit of large n and small p such that $np = const$, it is possible to show that this distribution becomes a Poisson distribution

$$p_k \; = e^{-c} \frac{c^k}{k!}, \tag{1.27}$$

where c is the mean degree, see [24]. This degree distribution can be seen in figure 1.5 right image, where the axis are logarithmic.

The clustering coefficient is the probability that two neighbors of a vertex are neighbors, this probability is independent of the other edges and is $p = c/(n - 1)$. Therefore

$$C \; = \frac{c}{n - 1}. \tag{1.28}$$

This quantity is vanishing for $n \to \infty$ with a fixed mean degree.

An interesting feature of random graph is the appearance of a *giant component*, i.e. a connected component containing an exponential number of nodes with respect to the other components, when the mean degree c is larger than 1. It is possible to derive an equation for the size of the giant component S, [24]:

$$S = 1 - e^{-cS}. \tag{1.29}$$
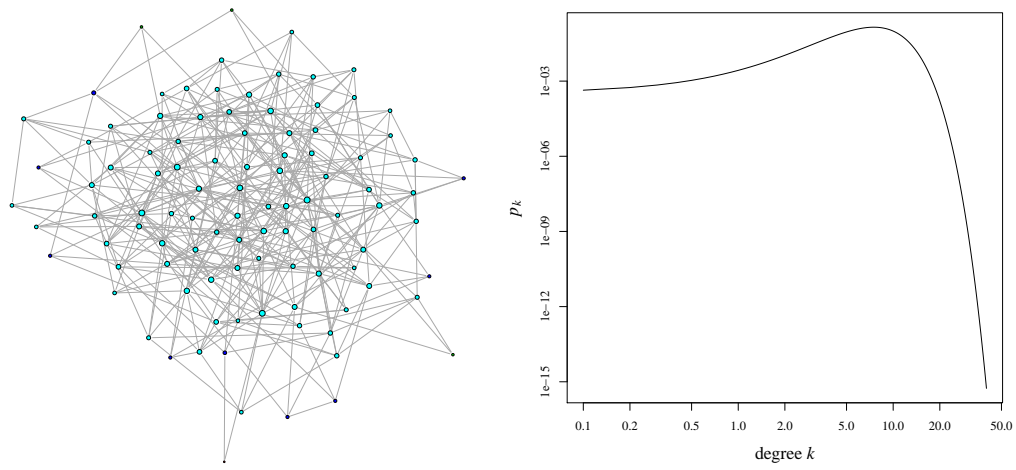
Fig. 1.5 Left image : a random graph of size 100. Right image : Degree distribution of a random graph with $c = 8$ in the limit of large n. The axis scale is logarithmic.
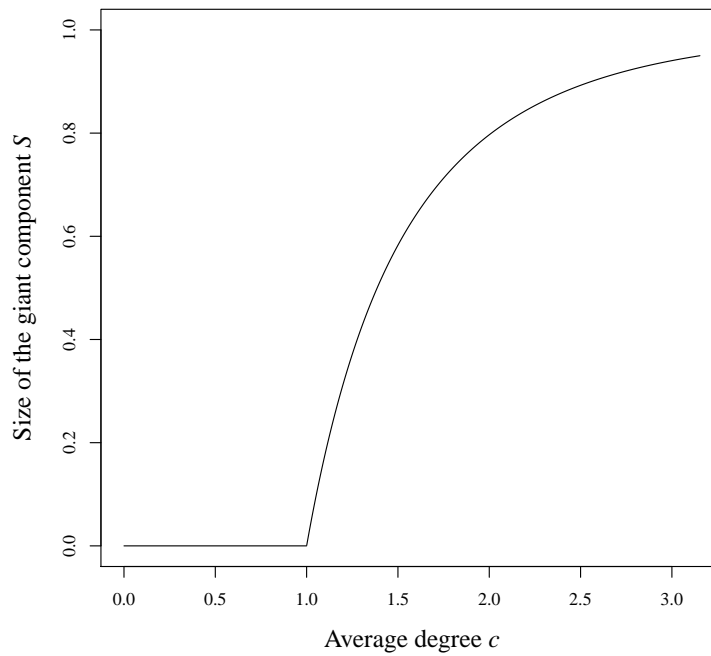
Fig. 1.6 Size of the largest component as a function of the average degree c.

However this equation has no simple solution, but it is possible to plot c as a function of S and then revert the axes. Figure 1.6 displays the size of the giant component as a function of the average degree by using equation 1.29 for $c > 1$.

1.6.3.3 The Configuration Model

The configuration model is a generalization of random graphs to arbitrary degree distributions. In this section we follow mainly Newman's book [24]. In order to construct an instance of the configuration model we need a given degree sequence $\{k_1, k_2, \ldots, k_n\}$, which can be drawn from the degree distribution p_k. Note also that the sum of the degrees has to be even. Then each vertex i with degree k_i is attributed k_i stubs of edge. Finally to form the network the stubs are connected randomly to form complete edges. Self-edges and multi-edges, i.e. several edges that connect the same pair of vertices, might be formed, but the expected number of self-edges and multi-edges is constant as a function of n, therefore the frequency of such edges vanishes for large networks. In the construction self-edges can be erased and multi-edges reduced to simple edges. The clustering coefficient can be computed and is given by

$$C = \frac{1}{n} \frac{[\langle k^2 \rangle - \langle k \rangle]^2}{\langle k \rangle^3}. \tag{1.30}$$

It is also possible to compute the condition for the existence of the giant component as

$$\langle k^2 \rangle - 2\langle k \rangle > 0. \tag{1.31}$$

Using the formalism of generating functions it is possible to obtain an equation for the size of the giant component, however we do not show it here. An interesting special case are the *power-low* degree distributions defined by

$$p_k = \begin{cases} 0 & \text{for } k = 0 \\ k^{-\alpha}/\zeta(\alpha) & \text{for } k \geq 1 \end{cases} \tag{1.32}$$

where $\zeta(\alpha) = \sum_{k=1}^{\infty} k^{-\alpha}$ is the Riemann zeta function. In that case equation 1.31 leads to the following result. The network has a giant component only if $\alpha < 3.4788$. Furthermore, if $\alpha < 2$, the giant component fils the entire network. Concerning the clustering coefficient, it is shown in [23] that

$$C \sim n^{-\beta}, \quad \beta = \frac{3\alpha - 7}{\alpha - 1}, \tag{1.33}$$

which implies that if $\alpha > 7/3$, then $C \to 0$ as $n \to \infty$, at $\alpha = 7/3$, C is constant as a function of n and for $\alpha < 7/3$, C increases with increasing n.

1.6.3.4 Small-World Model.

An important property of real networks is that the shortest path between most of the vertices is small even for very large networks, and is named the *small-world* effect. Watts
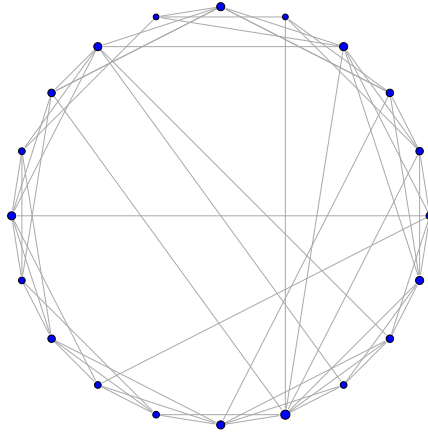
Fig. 1.7 A Watts-Strogatz small-world model for $c = 3$, $p = 0.05$ and $n = 20$.

and Strogatz proposed a model where a high clustering coefficient and the small-world effect can be obtained in the same network. The small-world model is a combination of a spatial network with high clustering coefficient, as a ring network, and a random network with small average shortest path length between vertices. The construction algorithm starts with a ring network where a vertex is connected to all vertices at a distance smaller or equal to c in terms of spatial hops on the ring, with $c > 1$ in order to obtain triangles. Then all the edges are visited and are removed with fixed probability p, and replaced by an edge between two randomly chosen vertices. Thus for $p = 0$ the network is a ring with high clustering, and for $p = 1$ the network is a random graph with a short average distances between vertices. In between, as p increases from 0 the average path length decreases faster than the clustering coefficient, showing that the two properties are compatible.

1.6.3.5 Preferential Attachment.

The concept of cumulative advantage was first studied by Yule and Willis in 1925 in the context of biology, and by Price in 1976 in the context of citation networks [29]. In the context of networks, the model was rediscovered in 1999 by Barabási and Albert [1] and called *preferential attachment*. The interest of this kind of models is that the generated networks possess a power-law degree distribution. Indeed a number of real networks have a degree distribution that obey approximatively a power-law degree distribution. In this section we present the model of Barabási-Albert (BA network). In order to construct a BA network we start with an initial connected network of m_0 nodes. New nodes are added to the network one by one and connected to $m < m_0$ existing nodes with a probability that is proportional to the degree of the existing nodes. Formally the probability to connect to node i is $k_i / \sum_j k_j$. In the limit of large k the generated network has a degree distribution proportional to k^{-3}, thus the BA model generates a degree distribution with a power-law tail with $\alpha = 3$. This result can be derived analytically. The left image of Fig. 1.8 depicts a
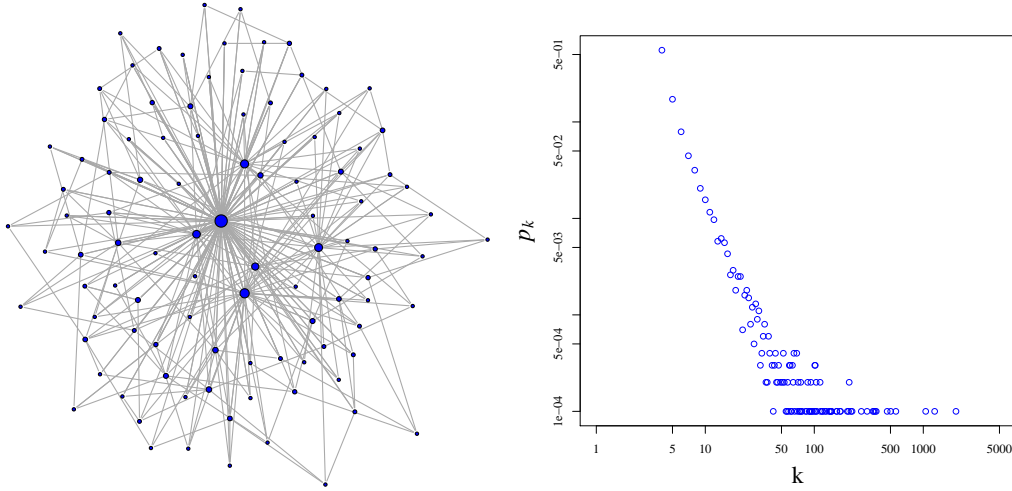
Fig. 1.8 Left image : a Barabási-Albert graph of size 100. Right image : Degree distribution of a Barabási-Albert graph with $n = 10000$ and $\langle k \rangle \simeq 8$, $(m = 4)$. The axis scale is logarithmic.

BA network of size 100 with $m = 4$, which corresponds to $\langle k \rangle = 8$. The right image shows the degree distribution for a similar network of size $n = 10000$ with logarithmic x and y axes. The approximately straight line degree distribution of this network can be observed. It is interesting to compare this image with the random network Poisson distribution. In the BA case the distribution decreases slowly as k increases since some vertices with very high degrees exist. Note that the mean degree is equal to $2 \times m$ and therefore it is a constant as a function of n.

1.6.3.6 Spatial Networks.

There are several types of spatial networks, a good review can be found in [5]. Here we present briefly some basic models. The simplest spatial random graphs is the *random geometrical graph* (RGG) model. In this model vertices are distributed randomly in the euclidean space and are connected to all other vertices that lie at a spatial distance smaller than R. The degree distribution can be calculated as follows. For simplicity we restrict to the homogeneous distribution of vertices on a 2-D plane of side 1, thus the probability $q(R)$ that a vertex i is in the neighborhood of another vertex j is the area of the neighborhood of radius R divided by the total area which is 1 by definition, or more formally $q(R) = \pi R^2$. Therefore the degree distribution is the binomial distribution

$$p_k = \binom{n-1}{k} q^k (1-q)^{n-1-k} \tag{1.34}$$

As in the RG case it can be reduced to a Poisson distribution in the limit $n \to \infty$ while the mean degree $c = \langle k \rangle = n\pi R^2$ remains fixed.

$$p_k \ = e^{-c}\frac{c^k}{k!}, \tag{1.35}$$

Contrary to the random graph, the average clustering coefficient is high due to spatial constraints and can also be calculated as $C = 0.58650$ for the 2D case.

An interesting class of spatial networks are those with a scale-free distribution. In [32], the authors proposed a model to construct such a network. In this model the vertices are placed on the sites of a d-dimensional euclidean lattice of size R with periodic boundary conditions and are assigned a random degree k from a scale-free distribution. Then each node is connected to the k nearest neighbors. However it might be impossible to make the connection to some of them, since they can already have reached their assigned degree. In addition, In this model, the connections can be formed only up to a distance given by $r(k) = Ak^{1/d}$, where A is a given constant.

1.6.3.7 Weighted Network Models

There are few models of weighted networks. One way to construct a weighted network is to start with an unweighted topology, such as a BA network and add the weights as a function of the unweighted topology. The simplest topological feature to take into account is the degree. To take weight-degree correlations into account, one possible approach is to assume that $w_{ij} \propto (k_i \, k_j)^\alpha$ for some small exponent α. Such an empirical correlation has indeed been detected for the world-wide airport network [4] with $\alpha \approx 1.5$, and similar behavior, perhaps with different values of the exponent, seems to be likely in all kind of transportation networks in which there are fluxes that must respect local conservation [27]. However, social networks are different in this respect; there aren't any obvious quantities that could constrain the relationship between link weights and number of contacts. For example, both [4] and [26, 27] found that $\langle w_{ij} \rangle$ is uncorrelated with $k_i \times k_j$ for mobile phone call nets as well as for a coauthorship network.
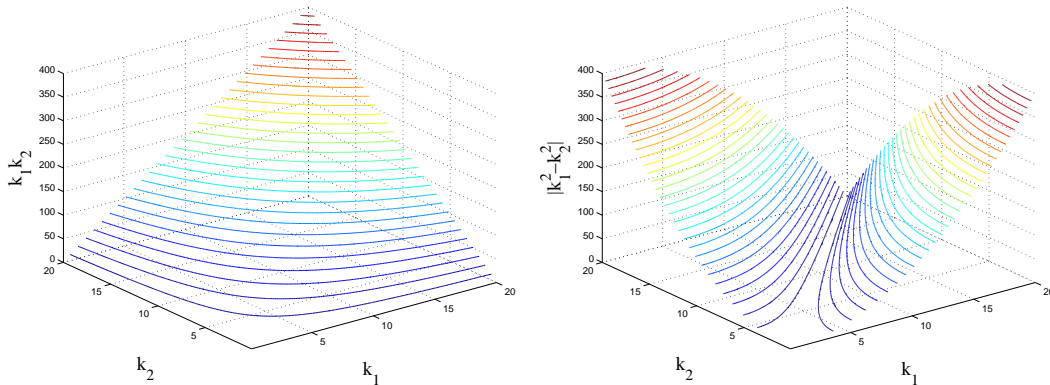
Fig. 1.9 Contour line plot of $k_i k_j$ (left) and $|k_i^2 - k_j^2|$ (right).
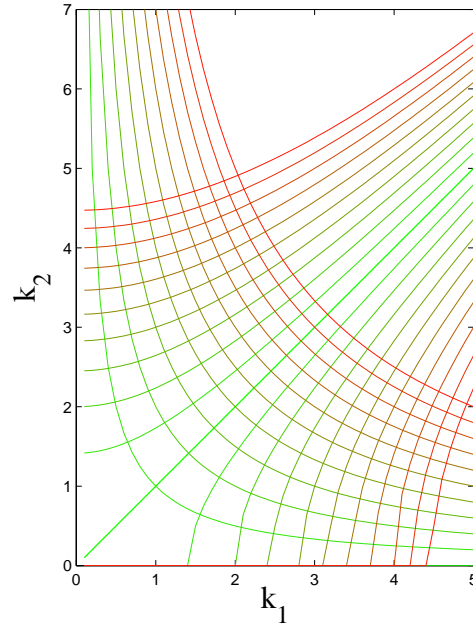
Fig. 1.10 The perpendicular curves defined by $k_i k_j = const$ and $|k_i^2 - k_j^2| = const$.

In the degree-weight correlation above the coordinate $k_i k_j$ is the joint contribution; a complementary view would be to use the difference between k_i and k_j which amounts to a local degree comparison. Thus, as there is no correlation between the form $k_i k_j$ and real weights, one can take its perpendicular field $|k_i^2 - k_j^2|$ in the degree-weight correlation. In other words, in the space spanned by the parameter (k_i, k_j), the mean weight values over the curves $k_i k_j = const$ are constant when the product $k_i k_j$ changes. Thus in order to find a new degree-weight correlation we propose to average over the perpendicular field $|k_i^2 - k_j^2| = const$, since the variable $|k_i^2 - k_j^2|$ takes into account correlations along the perpendicular direction. The two functions $k_i k_j$ and $|k_i^2 - k_j^2|$ can be seen in Figs. 1.9 and the fields defined by $k_i k_j = const$ and $|k_i^2 - k_j^2| = const$ in fig.1.9. Finally we use the following degree-weight correlation

$$w_{ij} \propto (|k_i^2 - k_j^2| + 1)^\gamma \tag{1.36}$$

Where the exponent γ allows to explore the weight-degree correlation from a more disassortative case ($\gamma > 0$) to an assortative case ($\gamma < 0$), passing through the unweighted case ($\gamma = 0$). A strictly positive constant is added to the difference of square degrees to avoid division by 0 for negative γ (more details can be found in chapter 3 where these weighted networks are used in the context of evolutionary games).

Another type of weighted models are models where multi-edges are naturally created in the construction algorithm and can be interpreted as weights. Here we present the team assembly model by Guimerà et al. [9] which is a bipartite model that is used in chapter 2 of the present thesis. The bipartite network includes two distinct set of vertices V_1 and

V_2, V_1 represents teams and V_2 represent members of teams. In order to obtain a weighted network from this bipartite graph, after it has been built, the teams are discarded and members are connected proportionally to the number of teams in which they are both members.

In this growing model, teams are formed sequentially taking their members either from a set of newcomers or a set of incumbents. The model starts at time zero with an endless pool of newcomers. Once they are selected for a team, newcomers becomes incumbents. Each time step t, a new team is formed and added to the network. The team consists of m agents. With a probability p, the agent is drawn from the pool of incumbents and with probability $1-p$ from the pool of newcomers. If the new agent is an incumbent and there is already another incumbent in the team, the new agent is selected with probability q from the set of collaborators of a randomly selected incumbent in the team. With probability $1-q$, it is randomly selected from the set of all incumbents.

1.7 Games on Networks

The behavior of evolutionary games is strongly affected by the underlying social structure; here the theory of networks gives the theoretical background to study games on these structures. The mean-field approximation given by the replicator dynamics is valid on two different graph topologies in the limit $n \to \infty$. The first one is the complete graph where all players are connected. The second topology is a dynamic one where players choose randomly a new set of neighbors at each time step.

In general game theory on complex networks is studied by means of simulations. In fact, the outcome is often very difficult to obtain with analytical tools. Here we present our game theoretical simulation methods.

In the bulk of this thesis we investigate the four classical two-person, two-strategy, symmetric games, namely the Prisoner's Dilemma (PD), the Hawk-Dove Game (HD), the Stag Hunt (ST), and the Harmony game (H) as defined in section 1.4.2. We use the following payoff matrix M where C stands for cooperation and D for defection.

$$
\begin{array}{cc}
 & \begin{array}{cc} C & D \end{array} \\
\begin{array}{c} C \\ D \end{array} & \begin{pmatrix} R & S \\ T & P \end{pmatrix}
\end{array}
\tag{1.37}
$$

In order to study the usual standard parameter space [31, 33], we restrict the payoff values in the following way: $R = 1$, $P = 0$, $-1 \leq S \leq 1$, and $0 \leq T \leq 2$. The parameter space with variable S and T, called *ST-Plane*, is shown in Fig. 1.11.

We will also investigate the rock-paper-scissors game, defined in 1.4.2, and use the payoff matrix 1.6 with $a = 0$, where the strategies are labelled S_1, S_2, S_3. In order to restrict the parameter space we take $b_1, b_2 \in [0, 2]$. With this setting the regions above the diagonal and under the diagonal of the plane corresponding to parameters b_1, b_2 correspond respectively to the cases $b_1 > b_2$ and $b_1 < b_2$ discussed in section 1.5.0.3.

The simulation of a game proceeds as follows: the players are initially assigned a random strategy at the beginning, each strategy has the same probability to be chosen. Then,
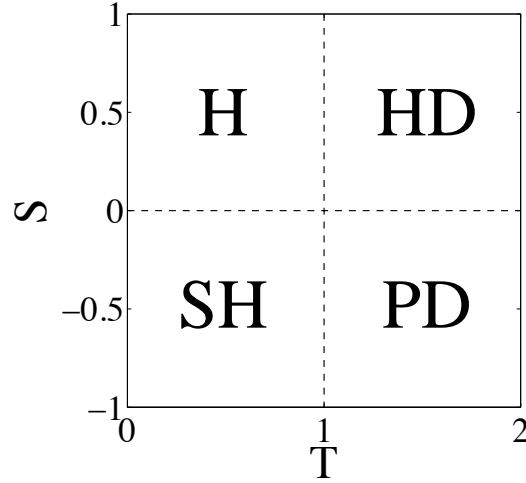
Fig. 1.11 H, SH, HD and PD games as a function of the game parameters S and T.

the players can update their strategies either synchronously or asynchronously. In the synchronous update the n players play at the same time and the new payoffs are calculated only after all players have updated their strategies. On the other hand, in the asynchronous case, players are randomly chosen one by one and their payoffs are computed at each time, and not after the n players have been chosen. In both cases we call the time interval needed for n players to update their strategies a *time step*. In this thesis we mainly use the asynchronous update since it seems to us the less constrained one, although synchronous dynamics is used in chapter 2. After the players have been assigned a random strategy we let the system evolve until the population has reached a stable or quasi-stable state, at which point we take our measures.

1.7.1 Update Rules

In this section we specify how individual's payoffs are computed and how agents decide to revise their current strategy. On complex networks the agents interact with their first neighbors as defined by the topology. On spatial lattices the agents interact with all the neighbors inside a disk of radius R_G. Let $\sigma_i(t)$ be a vector giving the strategy profile of player i at time t and let M be the payoff matrix of the game. The cumulated payoff collected by i at time step t is

$$\Pi_i(t) = \sum_{j \in V_i} \sigma_i(t) \, M \, \sigma_j^\top(t). \tag{1.38}$$

where the neighborhood V_i of i was defined in section 1.6.1. Rather than summing the two-players game payoffs with each neighbors, the total payoff could be computed with non-linear rules. In this work we restrict to the linear case except for the mean-payoff which is the same quantity divided by the degree k_i. In the weighted network case, the

pairwise payoffs $M_{ij} = \sigma_i \ M \ \sigma_j^T$ are multiplied by the weights w_{ij} of the corresponding links before computing the accumulated payoff earned by i. This takes into account the relative importance of the relationship as represented by its weight.

Several strategy update rules are customary in evolutionary game theory. First we describe three well known imitative update rules.

The *local fitness-proportional* or *replicator* rule is stochastic and gives rise to replicator dynamics in a well mixed population [11, 12]. Player i's strategy σ_i is updated by randomly drawing another player j from the neighborhood V_i, and replacing σ_i by σ_j with probability:

$$p(\sigma_i \to \sigma_j) = \begin{cases} (\Pi_j - \Pi_i)/K & \text{if } \Pi_j > \Pi_i \\ 0 & \text{if } \Pi_j \leq \Pi_i \end{cases} \tag{1.39}$$

where $\Pi_j - \Pi_i$ is the difference of the payoffs earned by j and i respectively. $K = \max(k_i, k_j)[max\{R, S, T, P\} - min\{R, S, T, P\}]$ ensures proper normalization of the probability $p(\sigma_i \to \sigma_j)$. This normalization increases the frequency of imitations between nodes with smaller degree.

A more flexible update rule without the problem of normalization is the *Fermi* rule. Here the randomly chosen player i is given the opportunity to imitate a randomly chosen neighbor j with probability :

$$p(\sigma_i \to \sigma_j) = \frac{1}{1 + exp(-\beta(\Pi_j - \Pi_i))} \tag{1.40}$$

where β is a constant corresponding to the inverse temperature of the system, i.e. high temperature implies that imitation is random to a large extent and depends little on the payoffs. Thus when $\beta \to 0$ the probability of imitating j tends to a constant value 0.5 and when $\beta \to \infty$ the rule becomes deterministic: i imitates j if $(\Pi_j - \Pi_i) > 0$, otherwise it doesn't. For $\beta \in [1.0, 10.0]$ the rule leads approximatively to similar results as the *local fitness-proportional* one.

Another imitative strategy update protocol is to switch to the strategy of the neighbor that has scored best in the last time step. In contrast with the previous one, this rule is deterministic. This *imitation of the best* (IB) policy can be described in the following way: the strategy $s_i(t)$ of individual i at time step t will be

$$s_i(t) = s_j(t-1), \tag{1.41}$$

where

$$j \in \{V_i \cup i\} \ s.t. \ \Pi_j = \max\{\Pi_k(t-1)\}, \ \forall k \in \{V_i \cup i\}. \tag{1.42}$$

That is, individual i will adopt the strategy of the player with the highest payoff among its neighbors including itself. If there is a tie, the winner individual is chosen uniformly at random.

The next update rule is a randomized version of the imitation of the best, we will call it *IBR*. This rule is also an alternative to the replicator rule since it does not have the problem of normalization. Here player i chooses and imitates a neighbor j with probability given by formula 1.39, where K is now such that $\sum_{j \in V_i} p_{ij} = 1$.

The last rule is called *best response*. This rule stipulates that the agents adopt the strategy that gives them the highest payoff given the neighbors' strategies at the previous time step. This rule is different from the other since the players do not imitate their neighbors. The above model rules are common and almost standard in numerical simulation work, which has the advantage that the mathematics is simpler and results can be compared with previous work such as, for instance, [31, 33]. However, it is far from clear whether these rules are representative of the ways in which human players actually take their strategic decisions, as has been shown by many laboratory experiments. In these experiments it seems that learning and heuristics play an important role. Moreover, players are inhomogeneous in their behavior while our stereotyped automata all behave in the same way and never change or adapt.
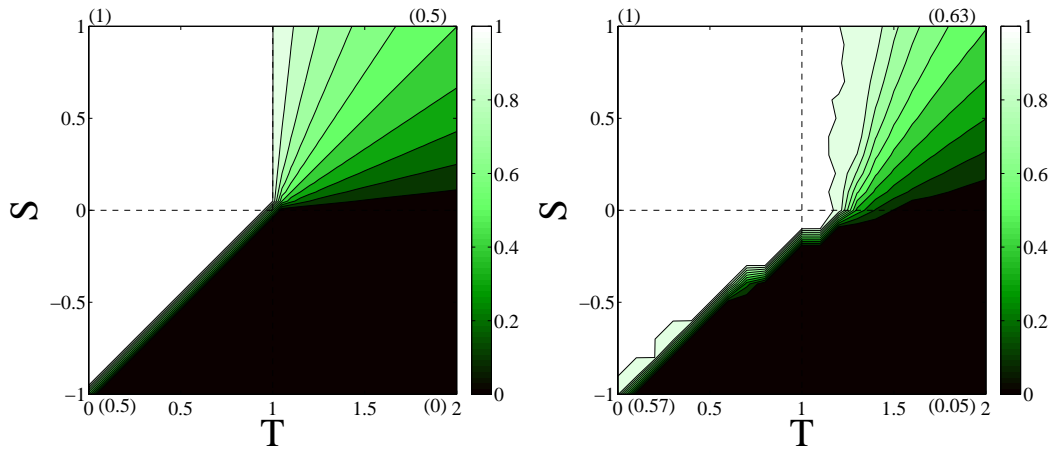
Fig. 1.12 Replicator dynamics stable states with 50% cooperators and defectors initially. Lighter tones stand for more cooperation. Values in parentheses next to each quadrant indicate average cooperation in the corresponding game space. Left image : well mixed population or complete graph. Right image : random graph with $n = 10000$, p $= 8/(n-1)$ and $\langle k \rangle = 8$.

1.7.2 The Effect of Topology on Two Strategy Games

A good review on the effect of topology on evolutionary games is found in [31]. Authors study the ST-plane with the replicator rule, the IB rule (called unconditional imitation), the Fermi rule and the best response rule, and different topologies such as regular lattices, Erdos-Rényi random graphs and Barabási-Albert graphs. In Figs. 1.12 and 1.13 we show the steady states obtained in the ST-plane with the replicator dynamics on several topologies. In Figs. 1.12 cooperation on random graph is compared to the well-mixed case. It can be observed that the levels of cooperation are slightly better with random graph for all the games. In Figs. 1.13 cooperation on a Barabási-Albert graph and a regular lattice are displayed, the levels of cooperation are higher in the SH games for the regular lattice,
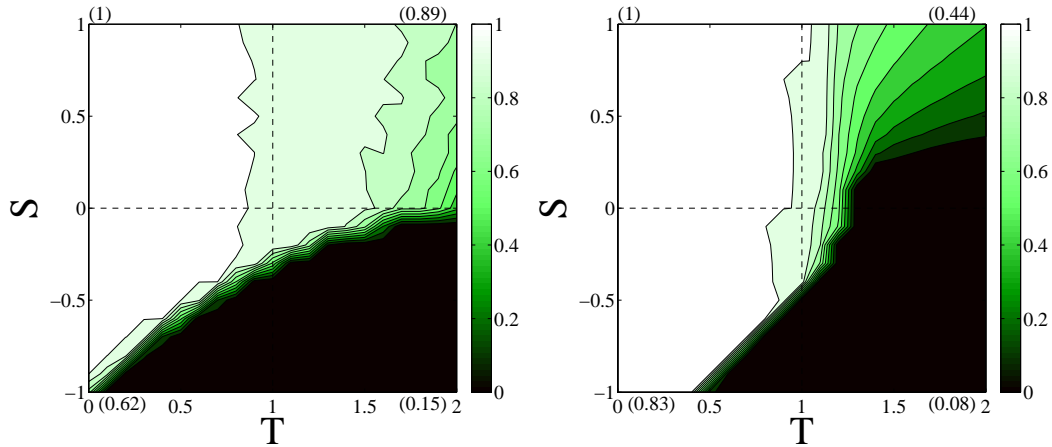
Fig. 1.13 Replicator dynamics stable states. Left image : Barabási-Albert graph with $n = 10000$ and $\langle k \rangle = 8$. Right image : regular lattice with $n = 10000$ and $\langle k \rangle = 8$. The initial frequency of cooperators and defectors is 50%. Values in parentheses next to each quadrant indicate average cooperation in the corresponding game space.

while they are larger in the HD games for the BA model. In the Barabási-Albert graph the dynamic is influenced by the inhomogeneous degree distribution. Vertices with a higher degree compared to most of their neighbors receive larger payoff since they cumulate the payoffs over all their neighbors. For this reason they are imitated by their neighbors with smaller degrees. In this context defectors tend to turn their neighbors to defectors and finally earn a small payoff compared to cooperators with large hubs. This might explain the large levels of cooperation for the games where all the payoffs are positive. In a regular lattice the cooperators can form spatial clusters where they interact mostly with other cooperators.

1.7.3 The Effect of Space on Cyclic Games

In a well mixed population the RPS games can be divided into two classes, the games where the mixed-strategy equilibrium repels the orbits (type 1) and the games where the mixed-strategy equilibrium is an attractor (type 2). Thus for games of type 1, if the population is finite, the players adopt all the same strategy at equilibrium. However on a spatial lattice, games of type 1 leads to the formation of finite size regions or spiral patterns where players adopt the same strategy. For Games of type 2, the strategies tend to coexist and it can be observed in the spatial case that the patterns tends to be very small. We display some examples in figure 1.14 for two different interaction radii and two different games representing the two types, type 2 is represented in the first column and type 1 in the second. It can be observed for games of both type that for larger R_g the transition between one type of game and the other is less smooth with respect to the case where the interaction radius is small. Therefore the general effect of space and locality is to
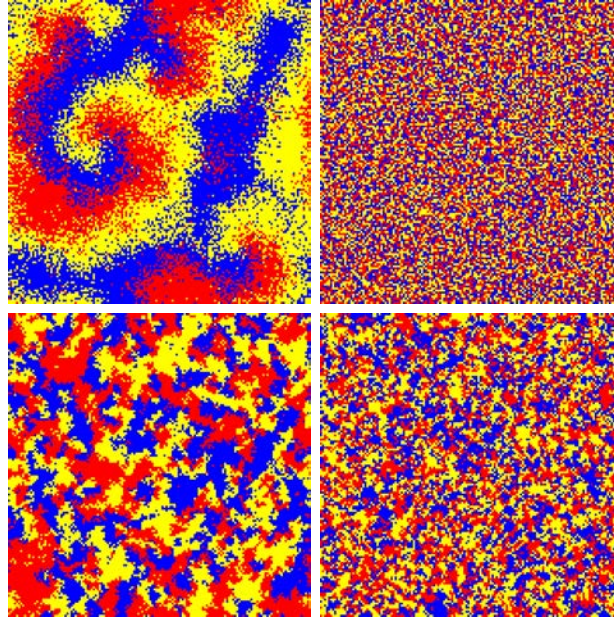
Fig. 1.14 Typical screen shots of the RPS game with the Fermi rule and $\beta = 10$. First row : $R_g = 5$. Second row : $R_g = 1.5$. First column : $b_1 = 1.5$, $b_2 = 0.5$. Second column : $b_1 = 0.5$, $b_2 = 1.5$. The lattice size is $L = 150$.

stabilize the patterns and prevent extinction. Since the system is bounded, it is interesting to study the size of the patterns when different parameters, such as the mobility [30], are changed.

1.8 The Chapters to Follow

In this section we present briefly the content of each of the chapters to follow. In all the chapters, except in the last, we investigate standard two-person, two-strategy evolutionary games. In the last chapter we investigate standard three-strategy cyclic games. In the first two chapters the games are simulated on weighed static networks derived from unweighted graph topologies such as random and scale-free ones. We assign weights randomly or according to some theoretical weight-degree correlations. In addition, weighted graph derived from bipartite networks model and real bipartite networks are used in chapter 2.

Chapter 2, The Influence of Tie Strength on Evolutionary Games on Networks: An Empirical Investigation. In the absence of any reliable model for generating weighted social networks, we attribute weights to links in a few ways supported by empirical data. In the baseline case the weights are attributed randomly to edges and drawn from a uniform distribution in $[0, 1]$ or a power-law distribution. The results of the extensive simulation work shows that taking the tie strength into account does not change in a radical manner the long-run steady-state behavior of the studied games. Then we

assign weights according to the particular weight-degree correlation $(k_i k_j)^\alpha$ observed on transportation networks but that does not seem to be common in social networks. In that case we observed a non negligible increase of cooperation for alpha between 0 and 1.5. The next weighted model is obtained from the team assembly model, a bipartite model formation, here the weighted and unweighted models give almost the same results. Besides model networks, we also included a real-life case drawn from a coauthorship network. In this case, taking the weights into account only changes the results slightly with respect to the raw unweighted graph, although to draw more reliable conclusions on real social networks many more cases should be studied as these weighted networks become available.

Chapter 3, Supercooperation in Evolutionary Games on Correlated Weighted Networks. In this chapter we use $(|k_i^2 - k_j^2|+1)^\gamma$ as degree-weight correlation on Barabási-Albert and random scale-free unweighted graphs. Unlike the degree-weight correlation of the previous chapter this correlation is a function of the difference of the degrees and therefore it can be tuned between assortative and disassortative. Our numerical simulation results show that for $\gamma > 0$, the weights lead to unprecedented levels of cooperation in the whole games' phase space, well above those found for the corresponding unweighted complex networks. We provide intuitive explanations for this favorable behavior by transforming the weighted networks into unweighted ones with particular topological properties. The resulting structures help to understand why cooperation can thrive and also give ideas as to how such supercooperative networks might be built. In particular we describe a small cooperative model composed of low and high degree vertices with a specific connectivity structure.

Chapter 4, Evolution of Cooperation on Spatially Embedded Networks. In this chapter we study the game dynamics on networks embedded in a Euclidean two-dimensional space with different kinds of degree distributions such as regular, random, and scale-free ones. Using several imitative microscopic dynamics, we study the evolution of global cooperation on the above network classes and on specific cooperative topologies such as Apollonian networks and a spatial version of the supercooperative networks described in the previous chapter. Spatial scale-free networks are good for cooperation but cooperation is notably higher on Apollonian and spatial supercooperative networks. Both classes of networks enhance average cooperation in all games with respect to standard random geometric graphs and regular grids.

In the following chapters we study the coevolution of the games with the migration of agents on the spatial layout. In order to update their positions the players can move randomly or test several places around them and move to the most profitable one. The space is represented by a discrete grid except in chapter 5 where space is continuous.

Chapter 5, Random Diffusion and Cooperation in Continuous Two-Dimensional Space. The goal of this chapter is to investigate whether cooperation can evolve and be stable when agents can move randomly in continuous space. When the agents all have the same constant velocity cooperation may evolve if the agents update their strategies imitating the most successful neighbor. If a fitness difference proportional is used instead,

cooperation does not improve with respect to the static random geometric graph case. When viscosity effects set-in and agent velocity becomes a quickly decreasing function of the average number of neighbors they have, one observes the formation of a dimorphic population composed by monomorphic stable clusters of cooperators or defectors in the Prisoner's Dilemma. However, cooperation does not spread in the population as in the constant velocity case.

Chapter 6, Spatial Organization of Cooperation with Contingent Agent Migration. Studying the effect of cooperation on discrete grids with the imitation of the best update rule, we show that cooperation may thrive for small interaction radius. We compare the results obtained with opportunistic migration and random migration. We observe that cooperation levels are larger in the opportunistic migration case. Then we show that the difference between the two cases is even larger for smaller player densities. This is due to the fact that in the random case, the density is homogeneous and therefore the degree of players is smaller and they tend to interact in pairs, instead of interacting with larger numbers of players. Indeed, by definition of the payoff matrix, an interactions between two players is highly profitable for defector compared to the well-mixed case. Finally we investigate the case where the rate of strategy update is high compared to the rate of migration update. We observe that for low sucker payoffs, cooperation cannot thrive, and that this might be due to an increase of the agents mobility preventing cooperator clusters to be stable. Finally we set the rate of strategy update to zero in order to study the effects of the mobility of agents alone. We observe that in the low sucker payoff region, mobility increases, explaining the loss of cooperation observed. Additionally, for high interaction radii, this type of games leads to the formation of dynamical patterns having a definite direction of motion. These clusters are composed of a group of cooperators followed by a swarm of defectors. On the other hand, when S is large, players end up blocked into stationary clusters.

Chapter 7, Opportunistic Migration in Spatial Evolutionary Games. In the same line as in the previous chapter, using the imitation of the best rule for strategy revision, it is shown that agents do not need to spend to much effort in order to search a new position for cooperation to evolve. When the stochastic Fermi strategy update is used, and that agents migrate opportunistically, cooperation cannot evolve in the Prisoner's Dilemma if the imitation is deterministic. However, when imitation becomes more random, fully or partially cooperative states are reached in all games for all migration radii tested and for short to intermediate interaction radii. Indeed, in the case where players imitate randomly chosen neighbors, only the spatial configuration of the players dictates which strategy will thrive.

Chapter 8, The Role of Opportunistic Migration in Cyclic Games. We study cyclic evolutionary games in a spatial diluted grid environment in which agents strategically interact according to the Fermi rule, but can also migrate opportunistically as in previous chapters. We investigate the size of the patterns formed as a function of the game and imitation noise. We find that opportunistic migration can reverse the cyclic prevalence between the strategies when the imitation noise is large enough compared to the

payoff-driven imitation. At the transition the average size of the patterns diverges. We try to explain this inversion of cyclicity by configuration analysis and a simple calculation.

References

[1] R. Albert A.-L. Barabási. Emergence of scaling in random networks. *Science*, 286:509–512, 1999.

[2] R. Axelrod. *The Evolution of Cooperation.* Basic Books, Inc., New-York, 1984.

[3] F. Franchetti B. Sandholm, E. Dokumaci. Dynamo: Diagrams for evolutionary game dynamics. *http://www.ssc.wisc.edu/ whs/dynamo*, 2012.

[4] A. Barrat, M. Barthélemy, R. Pastor-Satorras, and A. Vespignani. The architecture of weighted complex networks. *Proc. Natl. Acad. Sci.*, 101(11):3747–3752, 2004.

[5] M. Barthélemy. Spatial networks. *Physics Reports*, 499:1–101, 2011.

[6] S. Bowles and H. Gintis. *A Cooperative Species.* Princeton University Press, Princeton and Oxford, 2011.

[7] J. Tirole D. Fudenberg. *Game Theory.* The MIT Press, Cambridge, 1991.

[8] E. Fehr and U. Fischbacher. Third-party punishment and social norms. *Evolution and Human Behavior*, 25:63–87, 2004.

[9] Roger Guimerà, Brian Uzzi, Jarrett Spiro, and Luís A. Nunes Amaral. Team assembly mechanisms determine collaboration network structure and team performance. *Science*, 308(5722):697–702, 2005.

[10] C. Hauert, S. DeMonte, J. Hofbauer, and K. Sigmund. Volunteering as Red Queen mechanism for cooperation in public goods games. *Science*, 296:1129–1132, 2002.

[11] C. Hauert and M. Doebeli. Spatial structure often inhibits the evolution of cooperation in the snowdrift game. *Nature*, 428:643–646, April 2004.

[12] D. Helbing. Interrelations between stochastic equations for systems with pair interactions. *Physica A*, 181:29–52, 1992.

[13] D. Helbing. A stochastic behavioral model and a 'microscopic' foundation of evolutionary game theory. *Theor. Decis.*, 40:149–179, 1996.

[14] D. Helbing. Microscopic foundation of stochastic game dynamical equations. *Vienna Circle Institute Yearbook*, 5:211–224, 1998.

[15] J. Hofbauer and K. Sigmund. *Evolutionary Games and Population Dynamics.* Cambridge, N. Y., 1998.

[16] K. Sigmund J. Hofbauer. Evolutionary game dynamics. *Bulletin of the American Mathematical Society*, 40:479–519, 2003.

[17] J. B. C. Jackson and L. Buss. Allelopathy and spatial competition among coral reef invertebrates. *Proc. Natl. Acad. Sci.*, 72:5160–5163, 1975.

[18] B. Kerr, M. A. Riley, M. W. Feldman, and B. J. M. Bohannan. Local dispersal promotes biodiversity in a real-life game of rock-paper-scissors. *Nature*, 418:171–174, 2002.

[19] T. Kiyonari, S. Tanida, and T. Yamagishi. Social exchange and reciprocity: confusion or a heuristic? *Evolution and Human Behavior*, 21:411–427, 2000.

[20] R. B. Myerson. *Game Theory.* Harvard University Press, Cambridge, MA, 1991.

[21] J. Nash. Equilibrium points in n-person games. *PNAS*, 36:48–49, 1950.

[22] J. Nash. *Non-cooperative games.* Ph.D. dissertation, Princeton University, 1950.

[23] M. E. J. Newman. The structure and function of complex networks. *SIAM Review*, 45:167–256, 2003.

[24] M. E. J. Newman. *Networks: An Introduction.* Oxford University Press, Oxford, UK, 2010.

[25] M. A. Nowak and R. M. May. Evolutionary games and spatial chaos. *Nature*, 359:826–829, October 1992.

[26] J.-P. Onnela, J. Saramäki, J. Hyvönen, G. Szabó, M. Argollo de Menezes, K. Kaski, A.-L. Barabási, and J. Kertész. Analysis of a large-scale weighted network of one-to-one human communication. *New Journal of Physics*, 9:179, 2007.

[27] J.-P. Onnela, J. Saramäki, J. Hyvönen, G. Szabó, D. Lazer, K. Kaski, J. Kertész, and A.-L. Barabási. The architecture of weighted complex networks. *Proc. Natl. Acad. Sci.*, 101(11):3747–3752, 2004.

[28] E. Rényi P. Erdos. On random graphs. *Publicationes Mathematicae*, 6:290–297, 1959.

[29] D.S. Price. A general theory of bibliometric and other cumulative advantage processes. *J. Amer. Soc. Inform. Sci.*, 27:292–306, 1976.

[30] T. Reichenbach, M. Mobilia, and E. Frey. Mobility promotes and jeopardizes biodiversity in rock-paper-scissors games. *Nature*, 448:1046–1049, 2007.

[31] C. P. Roca, J. A. Cuesta, and A. Sánchez. Evolutionary game theory: temporal and spatial effects beyond replicator dynamics. *Physics of Life Reviews*, 6:208–249, 2009.

[32] A. F. Rozenfeld, R. Cohen, D. Ben-Avraham, and S. Havlin. Scale-free networks on lattices. *Phys. Rev. Lett.*, 89:218701, 2002.

[33] F. C. Santos, J. M. Pacheco, and T. Lenaerts. Evolutionary dynamics of social dilemmas in structured heterogeneous populations. *Proc. Natl. Acad. Sci. USA*, 103:3490–3494, 2006.

[34] D. Semman, H-J. Krambeck, and M. Milinski. Volunteering leads to rock-paper-scissors dynamics in a public goods game. *Nature*, 425:390–393, 2003.

[35] B. Sinervo and C. M. Lively. The rock-scissors-paper game and the evolution of alternative male strategies. *Nature*, 380:240–243, 1996.

[36] G. Szabó and G. Fáth. Evolutionary games on graphs. *Physics Reports*, 446:97–216, 2007.

[37] G. Szabó and C. Hauert. Evolutionary prisoner's dilemma game with voluntary participation. *Phys. Rev. E*, 66:062903, 2002.

[38] G. Szabó, A. Szolnoki, and R. Izsák. Rock-scissors-paper game on regular small-world networks. *J. Phys. A: Math. Gen.*, 37:2599–2609, 2004.

[39] G. Szabó and J. Vukov. Cooperation for volunteering and partially random partnership. *Phys. Rev. E*, 69:036107, 2004.

[40] A. Szolnoki, M. Perc, and G. Szabó. Phase diagrams for three-strategy evolutionary prisoner's dilemma games on regular graphs. *Phys. Rev. E*, 80:056104, 2010.

[41] J. W. Weibull. *Evolutionary Game Theory.* MIT Press, Boston, MA, 1995.

Part I
Cooperation on Static Graphs

Chapter 2

The Influence of Tie Strength on Evolutionary Games on Networks: An Empirical Investigation

Abstract Extending previous work on unweighted networks, we present here a systematic numerical investigation of standard evolutionary games on weighted networks. In the absence of any reliable model for generating weighted social networks, we attribute weights to links in a few ways supported by empirical data ranging from totally uncorrelated to weighted bipartite networks. The results of the extensive simulation work on standard complex network models shows that, except in a case that does not seem to be common in social networks, taking the tie strength into account does not change in a radical manner the long-run steady-state behavior of the studied games. Besides model networks, we also included a real-life case drawn from a coauthorship network. In this case also, taking the weights into account only changes the results slightly with respect to the raw unweighted graph, although to draw more reliable conclusions on real social networks many more cases should be studied as these weighted networks become available.

2.1 Introduction

The importance of the population structure on evolutionary game theory has been fully realized in recent years. In fact, the customary infinite well-mixed populations used in the theory have the appeal of simplicity and lend themselves to exact mathematical analysis [19] but network science has clearly shown that fully mixed populations are only an approximation, sometimes a bad one, to the actual interactions among agents. These social interactions can instead be more precisely represented as graphs in which nodes represent agents and links stand for their relationships [9]. In the last few years evolutionary games on networks have been thoroughly investigated and many results are available. Most of them come from numerical simulations, but there are also some theoretical results, mainly on degree-homogeneous graphs. It would be impossible to cite all the works in this fast-developing field but good recent reviews can be found in [12, 14, 16].

The bulk of the work on evolutionary games on complex networks so far has dealt with unweighted graphs, so that the intensity of the relationships has not been taken into account in general. This is right as a first step and allows one to ignore the interplay between

topology and structure, but a further step toward more realism consists in including the strength of a relationship. Indeed, there are only few works in which the role of link weights in evolutionary game dynamics have been considered [4, 18]. However, such investigations have been rather limited in character and there is not, as far as we know, any systematic treatment dealing with this potentially important aspect of games on networks. In the present work we present such a study of the behavior of paradigmatic evolutionary games on weighted networks.

Attributing weights to links in technological networks such as computer networks, power grids, or airline route networks, is relatively easy. For example, data packets for a computer network, and number of flights, passengers, or seats for airlines are quantities that make sense and can be defined and measured easily and without ambiguity. Contrastingly, attributing weights to relationships in social networks is not a simple matter because the relationship is often multi-faceted and relying on psychological and sociological features that are difficult to define and measure, such as friendship, empathy, and common beliefs. Nevertheless, there are some social networks for which at least a proxy for the intensity of a relationship can be defined and accurately measured. This is the case, for instance, for e-mail networks, phone calls networks, and coauthorship networks among others [8, 10, 11]. Other examples come from the field of animal networks in which animals can be marked or recognized in some way and repeated co-occurences of animals adds to the weight of their relationship [3].

For the sake of definiteness, we shall assume in the following that suitable weights can be attributed to the network edges and, since we shall explore several possible ways of performing the assignment, our work will be primarily based on standard model networks in order to try to unravel the interplay and the correlation between the purely topological aspect of the relationships and their intensity for the chosen games. Nevertheless, to connect our work to real-life nets, we shall also consider a known collaboration network. Moreover, to avoid having to deal with further degrees of freedom, we use fixed networks, i.e. networks in which neither the number of nodes nor the number of links is subject to change over time. Likewise, there is no rewiring of existing links among the network nodes. Co-evolutionary models can be more realistic (see e.g. [12, 13, 15, 20]) but in this work we are especially interested in singling out the effect of link weights in static networks, which is a satisfactory approximation if the network dynamics is slowly fluctuating. The present investigation is based on extensive numerical simulations.

The article is organized as follows. In the next section we briefly introduce the main games used and their parameter space, as well as the evolutionary rules for strategy update. In Sect. 2.3 we provide justifications for a number of ways of attributing weights to network links and we numerically study evolutionary games behavior using typical model networks and several link weight distributions. Finally, we discuss the results and give our conclusions in Sect. 2.4.

2.2 Evolutionary Games on Networks

2.2.1 The Standard Games

We study the four standard two-person, two-strategy, symmetric games, namely the Prisoner's Dilemma (PD), the Hawk-Dove (HD), the Stag Hunt (ST), and the Harmony game (H). We briefly summarize the main features of these games here for completeness; more detailed accounts can be found elsewhere [17, 19]. The games have the generic payoff bi-matrix of Table 2.1. In this matrix, R stands for the *reward* the two players receive if they

	C	D
C	(R,R)	(S,T)
D	(T,S)	(P,P)

Table 2.1 Generic payoff bi-matrix for the two-person, two-strategies symmetric games discussed in the text.

both cooperate (C), P is the *punishment* for bilateral defection (D), and T is the *temptation*, i.e. the payoff that a player receives if she defects while the other cooperates. In this case, the cooperator gets the *sucker's payoff S*. In order to study the standard parameter space, we restrict the payoff values in the following way: $R = 1$, $P = 0$, $-1 < S < 1$, and $0 < T < 2$. In the resulting TS-plane, each game corresponds to a different quadrant depending on the ordering of the payoffs.

For the PD, the payoff values are ordered such that $T > R > P > S$. Defection is always the best rational individual choice, so that (D, D) is the unique Nash Equilibrium (NE) and also the only Evolutionarily Stable Strategy (ESS) [19]. Mutual cooperation would be socially preferable but C is strongly dominated by D.

In the Hawk-Dove game, the order of P and S is reversed, yielding $T > R > S > P$. Thus, in the SD when both players defect they each get the lowest payoff. (C, D) and (D, C) are NE of the game in pure strategies. There is a third equilibrium in mixed strategies where strategy D is played with probability p, and strategy C with probability $1 - p$, where p depends on the actual payoff values. The only ESS of the game is the mixed strategy, while the two pure NE are not ESSs [19]. Players have a strong incentive to play D, which is harmful for both parties if the outcome produced happens to be (D, D).

In the Stag Hunt, the ordering is $R > T > P > S$, which means that mutual cooperation (C, C) is the best outcome, Pareto-superior, and a NE. The second NE, where both players defect is less efficient but also less risky. The dilemma is represented by the fact that the socially preferable coordinated equilibrium (C, C) might be missed for "fear" that the other player will play D instead. The third mixed-strategy NE in the game is evolutionary unstable and not an ESS [19].

Finally, in the Harmony game $R > S > P > T$. In this case C strongly dominates D and the trivial unique NE is (C, C). The game is non-conflictual by definition and does not cause any dilemma: we include it just to complete the quadrants of the parameter space.

2.2.2 Population Structure and Dynamics

We represent the population of players by an undirected weighted graph $G(V, E)$, where the set of vertices V represents the individuals, and the set of weighted edges E represents their symmetric interactions. The weight of an edge $e \in E$ will be denoted by w_e or by w_{ij}, by using the edge end points i and j and the weights w_e are normalized in $[0, 1]$. The population size N is the cardinality of V. A neighbor of an agent i is any other agent j adjacent to i. The set of neighbors of i is denoted by V_i. The cardinality of this set is the degree k_i of vertex $i \in V$; $p(k)$ denotes the degree distribution of the graph, i.e. the probability that an arbitrarily chosen node has degree k. The average degree of the network is given by $\langle k \rangle = \sum_k k\, p(k)$. For the weighted aspects of the network $p(w_e)$ represents the link weight distribution, and $p(s)$ denotes the *strength* distribution, where the strength $s(i)$ of a vertex i is defined as $s(i) = \sum_{j \in V_i} w_{ij}$, i.e. the sum of the weights of the links incident in i [2].

For the evolutionary dynamics, we must next define the decision rule by which individuals update their strategy and the timing of the dynamical process. There are several possible strategy update rules that can be used [14, 16] . The results are not very much qualitatively dependent on the specific rule type, although there are quantitative differences between them [14]. For the sake of simplicity, we use two rules that are sufficiently different so as to represent typical diverse behavior: *imitation of the best* and *local replicator dynamics*. These updating rules will be explained below.

Let $\sigma_i \in \{C, D\}$ be the current strategy of player i and let us call M the payoff matrix of the game. The quantity

$$\Pi_i(t) = \sum_{j \in V_i} \sigma_i(t)\, M\, \sigma_j^T(t)$$

is the accumulated payoff collected by player i at time step t. Since we work with weighted networks, the pairwise payoffs $M_{ij} = \sigma_i\, M\, \sigma_j^T$ are multiplied by the weights w_{ij} of the corresponding links before computing the accumulated payoff earned by i. This takes into account the relative importance of the relationship as represented by its weight.

Another possibility is to use the normalized weight w_{ij} as a probability of interaction of agents i and j, i.e. i and j will play with probability w_{ij} as in [18]. Here we use the former choice but some numerical experiments have shown that the results do not differ qualitatively by using the latter instead.

In imitation of the best, the strategy $\sigma_i(t)$ of individual i at time step t will be

$$\sigma_i(t) = \sigma_j(t - 1),$$

where

$$j \in \{V_i \cup i\}\ s.t.\ \Pi_j = \max\{\Pi_k(t-1)\},\ \forall k \in \{V_i \cup i\}.$$

That is, individual i will adopt the strategy of the player with the highest payoff among its neighbors including itself. If there is a tie, the winner individual is chosen uniformly at random, but otherwise the rule is deterministic.

The local replicator dynamics rule is stochastic and it is consistent with the original mean-field evolutionary game theory equations [6]. Here it has been slightly modified to take into account the weighted nature of the network. Player i's strategy σ_i is updated

by drawing another player j from the neighborhood V_i with a probability proportional to w_{ij}, and replacing σ_i by σ_j with probability

$$p(\sigma_i \to \sigma_j) = (\Pi_j - \Pi_i)/K,$$

if $\Pi_j > \Pi_i$, and keeping the same strategy if $\Pi_j \leq \Pi_i$. $K = \max(s_i, s_j)[(\max(1, T) - \min(0, S)]$, with s_i and s_j being the strenghts of nodes i and j respectively, ensures proper normalization of the probability $p(\sigma_i \to \sigma_j)$.

Finally, if we define $C(t) = (\sigma_1(t), \ldots, \sigma_N(t))$ as being the configuration or state of the population at time t, then the simulation advances synchronously according to the symbolic global evolution rule F:

$$C(t + 1) = F(C(t)).$$

In other words, all the individuals in the network play the game once with all their respective neighbors, accumulate their payoffs, and decide their strategy for the next time step according to the above rules. The evolution could also be fully or partially asynchronous. In partially asynchronous dynamics a fraction f of the population is simultaneously updated in each time step [13]. In fully asynchronous update an individual is chosen at random, she plays the game once with her neighbors, and she updates her strategy accordingly. Then the payoff of all individuals is set to zero and another individual is drawn uniformly at random in the whole population at the next time step. In several studies, following an enquiry by [7], it has been shown that asynchronous evolution doesn't change the main qualitative aspects of the dynamics of games on networks (for example, see [6, 13, 14]). Thus, here we use synchronous dynamics.

2.2.3 Simulation Parameters

All simulations were performed for a networked population size of $N = 2000$ and mean degree $\langle k \rangle = 8$ unless otherwise stated. The initial density of cooperators is 0.5, uniformly distributed over the vertices of the networks. Given that our main goal here is to compare weighted and unweighted networks with respect to evolutionary games, in the interest of simplicity, we do not explore unbalanced initial conditions. Each value in the phase space reported in the following figures is the average of 50 independent runs. Each run has been performed on a fresh realization of the corresponding graph. To detect steady states[1] of the dynamics we first let the system evolve for a transient period of $5000 \times N$ time steps. After a quasi-equilibrium state is reached past the transient, averages are calculated during $500 \times N$ additional time steps. A steady state has always been reached in all simulations performed within the prescribed amount of time, for most of them well before the limit. The state space explored is defined by $R = 1$, $P = 0$, $-1 < S < 1$, and $0 < T < 2$ and the T and S axes have been sampled at intervals of 0.1.

---

[1] True equilibrium states in the sense of dynamical systems stability are not guaranteed to be reached by the simulated dynamics. For this reason we prefer to use the terms steady states or quasi-equilibrium states which are states that have little or no fluctuation over an extended period of time.

2.3 Games on Weighted Networks

In the last decade the structure of hundreds of medium to large networks have been investigated thanks to readily available electronic data [9]. However, the large majority of these graphs were of the unweighted type. The reasons are that, as hinted at in the introduction, apart from technological or economic networks such as trade networks, in the realm of social nets it is often difficult to associate sensible weights to an edge representing some kind of relationship between two agents. However, there are some published studies that can be used as a starting point to estimate suitable forms for the weights, given that some very different hypothesis have been voiced in the literature. One extreme position, called the *dyadic hypothesis* [11] is to argue that the weight of a particular tie does not depend on the network structure around the two concerned agents but only on the nature of their relationship. In this view, tie strengths are completely uncorrelated with topological features such as node degree and clustering coefficient. In two detailed studies of large social networks, the first being a scientific coauthorship network [1] and the second a mobile call [10] network, it has been empirically shown that this is not the case. Although the non-correlation hypothesis does not seem to be a likely one in social networks, it is still useful as a benchmark: a kind of null model against which to test some more realistic assumptions. In our first simulation model we thus assume that weights are attributed to links without correlation with the topology. In order to get rid of topological effects and to observe the effect of the link strength only on the dynamics, we first model the games on regular random graphs in which each node has the same degree but links are otherwise randomly distributed. Random graphs are the closest network approximation to a mean-field well mixed population, ideally represented by a complete network and, in the limit of very large population sizes, the standard results of evolutionary game theory should hold [14, 19] at least approximately.

Figure 2.1 depicts the average cooperation levels on regular random graphs of degree $k = 8$ and $N = 2000$ nodes at steady state, when the weights are assigned at random according to a uniform distribution in $[0, 1]$ distributed uniformly at random among the available links.

Left images correspond to imitate the best update rule while the right ones corresponds to local replicator dynamics. Unsurprisingly, the results are almost identical with those obtained on the same family of graphs but using unweighted networks (bottom row images). This result is also fully coherent with the cooperation levels found in [14] for unweighted Erdös-Rényi random graphs with the same $\langle k \rangle$. Clearly, when weights are assigned uniformly at random there is an implicit averaging over the whole set of edges when calculating payoffs and the inclusion of weights does not not change the qualitative results. In passing, we note the remarkable level of cooperation reached in the SH game with the imitate the best strategy update rule, a phenomenon already observed in [14].

To investigate whether degree inhomogeneity changes the picture, we have also simulated the same games on Barabási-Albert (BA) scale-free graphs of the same size and $\langle k \rangle = 8$. The results, shown in Fig. 2.2 (top row) are again very similar to the unweighted cases (bottom row), and there is full agreement with the results of Roca et al. [14]. One is thus led to the conclusion that, when weights are distributed uniformly at random among
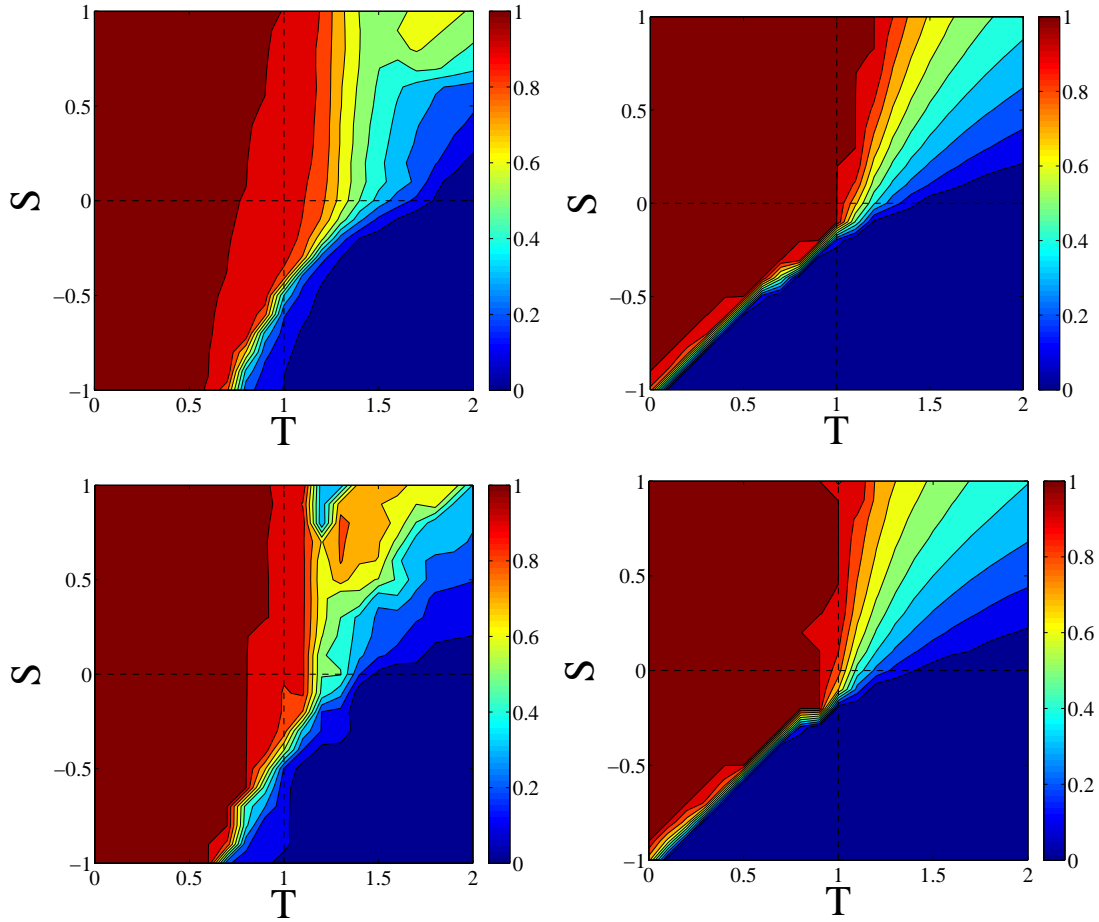
Fig. 2.1 Average degree of cooperation at steady state for regular random graphs with $\langle k \rangle = 8$. Left column : imitation of the best. Right column: replicator dynamics. Top row: link weights uniformly and independently distributed. Bottom row: unweighted regular random graphs. Network sizes $N = 2000$. Each grid point value is the average over 50 independent runs. Blue means more defection.

the edges there is almost no difference with the unweighted case for both update rules. This in turn shows that when weights are totally uncorrelated with the topological aspects of the network, such as degree or clustering coefficient, their influence is negligible.

Indeed, even when the weight distribution is a long-tailed one such as a power-law $p(w_e) \propto w_e^{-\gamma}$, the results are very similar, as shown in Fig. 2.3, where the value of the exponent γ is 2. The reasons seem intuitively clear: since there are few strong links, hubs with many connections will get only a few of those, which will change the picture very little with respect to the unweighted case. Likewise, the few strong links that will exist among poorly connected vertices, because of the low degree of the end points, will not be able to influence a sizable portion of the network. Only statistical outliers could change
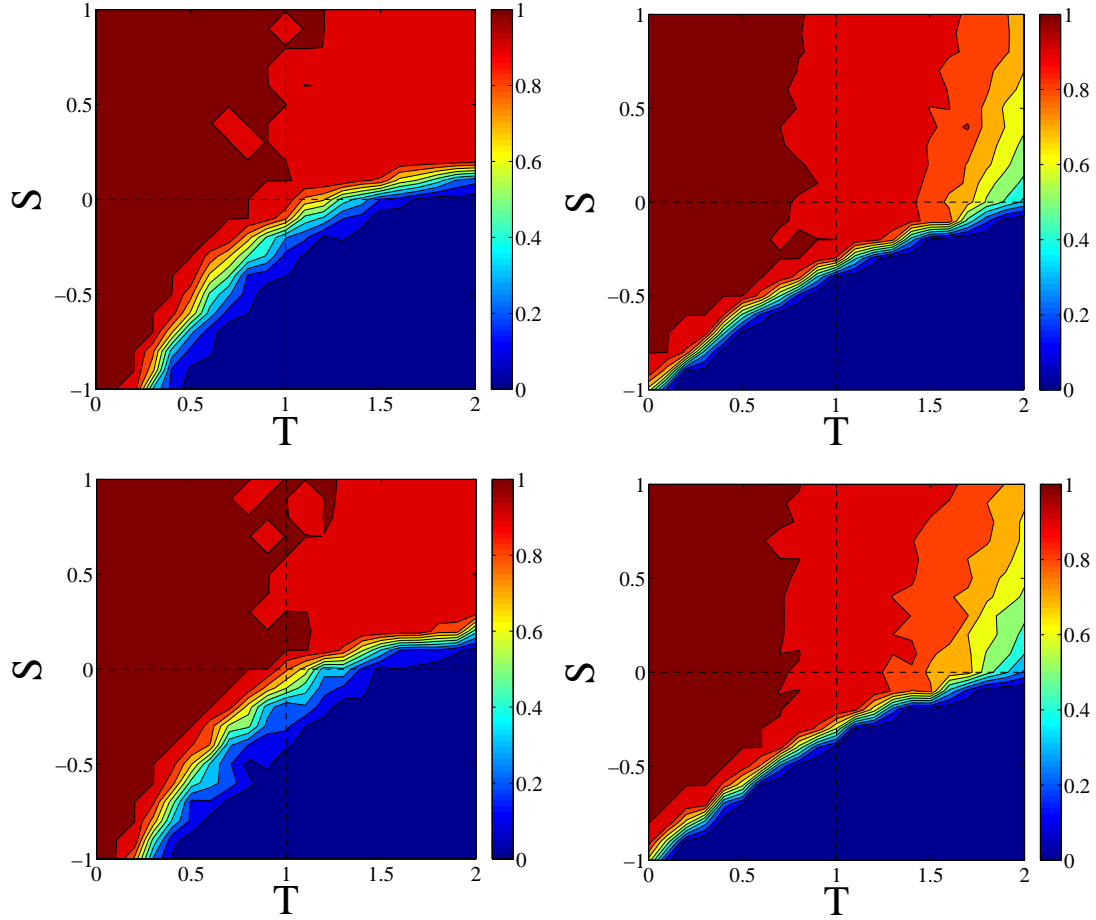
Fig. 2.2 Average degree of cooperation at steady state for BA scale-free networks with $\langle k \rangle = 8$. Left images: imitation of the best. Right images: replicator dynamics. Top row: link weights drawn from a uniform distribution. Bottom row: unweighted BA scale-free networks. Network sizes $N = 2000$. Each grid point value is the average over 50 independent runs. Blue stands for more defection.

this significantly but, over many graph realizations, the fluctuations will be smoothed and only mean values will matter.

The inescapable conclusion is the following: if one assumes the dyadic hypothesis for setting the edge weights, owing to system averaging, there is almost no effect on cooperation. But we have already remarked that empirical research to date indicates that edge weights and topological properties are related. To take weight-degree correlations into account one possible approach is to assume that $w_{ij} \propto (k_i \, k_j)^{\alpha}$ for some small exponent α. Such an empirical correlation has indeed been detected for the world-wide airport network [1] with $\alpha \approx 1.5$, and similar behavior, perhaps with different values of the exponent, seems to be likely in all kind of transportation networks in which there are fluxes that must respect local conservation [11]. However, social networks are different in this respect, they are much more local and there aren't any obvious quantities that could constrain the relationship
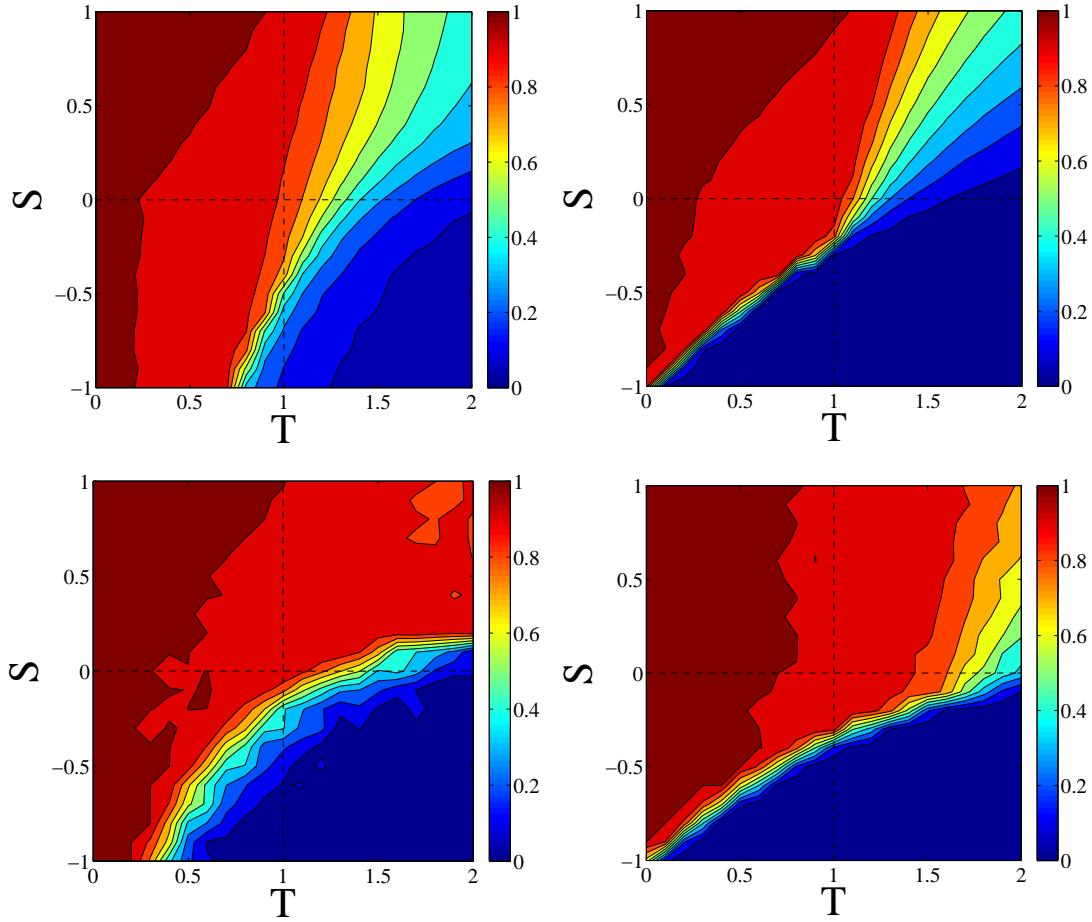
Fig. 2.3 Average degree of cooperation at steady state when link weights are distributed according to an inverse power-law with an exponent of 2. Left column: imitate the best. Right column: replicator dynamics. Top row: regular random graphs; bottom row: BA scale-free graphs. $N = 2000$, averages over 50 runs.

between link weights and number of contacts. For example, both [1] and [10, 11] found that $\langle w_{ij} \rangle$ is uncorrelated with $k_i \times k_j$ for mobile phone call nets as well as for a coauthorship network.

In [4] Du et al. have tried to account for the effect of link weights on the PD on Barabási-Albert scale-free graphs with the Fermi function [16]:

$$p(\sigma_i \rightarrow \sigma_j) = \frac{1}{1 + \exp(-\beta(\Pi_j - \Pi_i))},$$

as a strategy update rule with $\beta = 10$. This setting gives results very similar to our replicator rule in unweighted networks, as it has been clearly shown in [14]. The payoff was rescaled using the corresponding link weight as explained in Sect. 2.2.2. They assumed the above degree product form for the weights, studying the evolutionary behavior of the PD

for several negative and positive values of the exponent α. However, their simulations only covered a tiny part of the game phase space due to their use of the so-called "reduced" PD game in which $R = 1$ and $S = P = 0$, which makes T the only free parameter and corresponds to the straight line at the frontier between the PD and the SD games. Although, as remarked above, this form of degree-weight correlation is not supported by empirical data in social networks, for the sake of completeness we performed simulations for the whole four games phase space. The results for replicator dynamics are shown in Fig. 2.4 where we report the average cooperation values for values of α between -3 and 3 starting with $\alpha = -3$ in the leftmost top row picture; α then increases from left to right and takes positive values starting from the second picture in the bottom row. The last top row image and the first bottom raw image correspond to the case $\alpha = 0$, i.e. the unweighted networks. From these images it appears that cooperation seems to increase around $\alpha = 1$ but it is difficult to really see it. In order to better quantify the effect, in Fig. 3.1 we plot the average cooperation values for each game as a function of α. Now it becomes clear that, taking the average over the whole game phase space, in the three non-trivial games there is a "plateau" of cooperation between $\alpha = 0.5$ and $\alpha = 1$ approximately (of course the HG case is only shown for completeness). For values lower than 0 and beyond 1.5 the trend is toward a lower, almost constant level of cooperation. This is confirmed by the values obtained for $\alpha = -10$ and $\alpha = 10$ which are shown for reference as small traits on each curve on the left and the right of the figure respectively. Du et al. [4] found a big increase in cooperation for large negative values of α and for α close to -1 while they found a deep minimum of cooperation around $\alpha = -1.5$. This, however, only applies to the region of the space represented by the segment at the frontier between the PD and SD games. Our results show that this non-monotonic behavior is not observed when the entire phase space is taken into account.
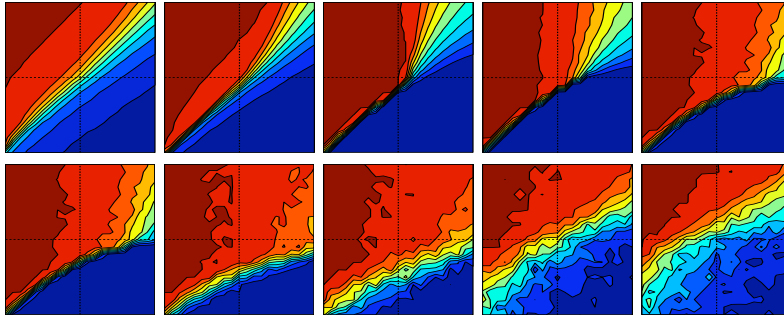

Fig. 2.4 Average cooperation at steady state using replicator dynamics on BA networks of size $N = 2000$ and $\langle k \rangle = 8$ as a function of the parameter α (see text). Top row images, from left to right $\alpha = -3, -2, -1, -0.5, 0$. Bottom row, from left to right $\alpha = 0, 0.5, 1, 2, 3$. The initial density of cooperators is 0.5 in all cases. Averages over 50 runs.
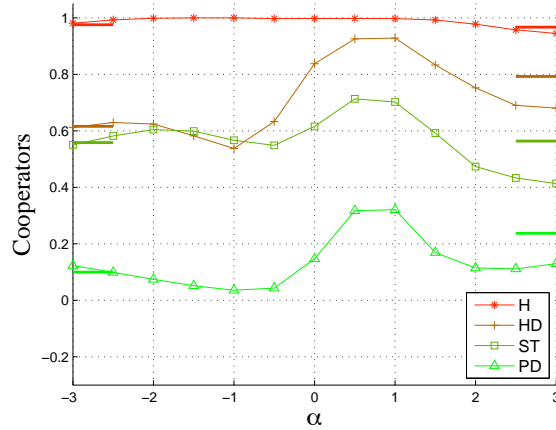
Fig. 2.5 The points show, for each game, the average amount of cooperation at steady state in the whole game's phase space as a function of α. Lines are just a guide for the eye.

2.3.1 Weighted Networks from Bipartite Graphs

We have seen above that there can be a generally positive influence on cooperative strategies in weighted networks when the link weights are proportional to the products of the endpoints degrees with an exponent between 0.5 and 1. However, the few available empirical studies exclude the presence of such a correlation in typical social networks [1, 10, 11]. But many social networks are of the *affiliation* type, meaning the participation of a set of actors in a set of groups or interest centers. Each set is represented by the vertices of a graph and there is a link $X - G$ between two elements of the sets when an actor X participates to group G. In this model there can be no links between vertices belonging to the same set. Such a situation can be described by using *bipartite graphs*. Although social networks such as friendship or mutual communication nets are not of this kind, there are many significant examples of bipartite graphs in society such as scientist coauthoring an article, directors belonging to the same board, people that have bought the same book in Amazon, actors starring in the same movie, and so on [9].

A graph $G(V, E)$ in which $V = \{v_1, \ldots, v_N\}$ is the set of vertices or nodes, and $E = \{e_1, \ldots, e_M\}$ is the set of edges or links, is said to be bipartite when the vertices can be partitioned into two disjoint sets $V_1 \cup V_2$, $V_1 \cap V_2 = \emptyset$, such that there are no edges $e = \{u, v\}$ between vertices belonging to different sets:

$$\{\{u, v\} : u \in V_1, v \in V_2\}, \ \forall e \in E.$$

The *incidence matrix* B of a bipartite network with, say, l groups and m actors is an $l \times m$ rectangular matrix such that the generic matrix element B_{ij} is 1 if actor j belongs to group i and 0 otherwise [9].

From the bipartite graph, it is an easy matter to obtain two derived graphs which are called *projections*. One can construct a graph in which two actors are connected if they adhere to the same group, or we can also build the projection in which two groups are

connected if they share a common actor. The two projections capture the essence of the relationships we are looking for but they do not account for the "weight" of a relationship. Indeed, it is sensible to say that it is not the same whether two people sit together on a single board or on several, or whether an article has only two coauthors or ten. In some sense, their degree of interaction should be higher in the former case. To account for this, the projection can be weighted; for example, for the actors projection, an edge, i.e. a pair of connected actors, will have a weight equal to the number of common groups. The weighted projection can be obtained from the incidence matrix B as follows [9]:

$$P = B^T B, \quad \text{where} \quad P_{ij} = \sum_{k=1}^{l} B_{ik}^T B_{kj} \tag{2.1}$$

where B^T is the transpose of B, and l is the number of groups. The elements P_{ij} of the $m \times m$ matrix P are the weights, i.e. the number of common groups shared by the actors i and j, whereas the diagonal elements P_{ii} are the number of groups to which actor i belongs. This provides us with a "natural" way of attributing ways to the links of the projection graph and thus can in principle be used to gauge the behavior of the standard games on the resulting weighted networks.

Among several existing models of bipartite graphs, we choose the team assembly model by Guimerà et al. [5]. In this growing model, teams are formed sequentially taking their members both from a set of newcomers and a set of incumbents. Teams correspond to top nodes, newcomers to new bottom nodes and incumbents to existing bottom nodes. The model starts at time zero with an endless pool of newcomers. Once they are selected for a team, newcomers become incumbents. Each time step t, a new team is formed and added to the network. The team consists of m agents. With a probability p, the agent is drawn from the pool of incumbents and with probability $1 - p$ from the pool of newcomers. If the new agent is an incumbent and there is already another incumbent in the team, the new agent is selected with probability q from the set of collaborators of a randomly selected incumbent in the team. With probability $1 - q$, it is randomly selected from the set of all incumbents.

For our graphs, we used values of $p = 0.6$, $q = 0.9$ (both empirically justified [5]) and $m = 4$. In order to generate graphs with exactly $N = 1000$ agents, we repeated the procedure described before for a number M of teams equal to $\lfloor n/m(1-p) \rfloor$ and kept only those graphs with exactly $N = 1000$ agents.

Once the graphs are constructed, we let the game dynamics develop as previously explained. The results are depicted in Fig. 2.6 for the unweighted case, and in Fig. 2.7 for the weighted graphs both for replicator dynamics and imitate the best strategy update rules. It appears that the level of cooperation is very similar for weighted and unweighted networks in both cases, with the only difference that, in the weighted case, the transition region between cooperation and defection becomes less crisp. This can be due to the fact that weights act as a form of noise in the evaluation of payoffs, which gives more fluctuations in the transition region. However, the bottom line is that, once more, the effect of the link strength on cooperation is rather small. One interesting observation is that the amount of cooperation on these graphs, weighted or unweighted, is high, of the order of what has been found for unweighted BA scale-free networks [14]. The reason is simple: due
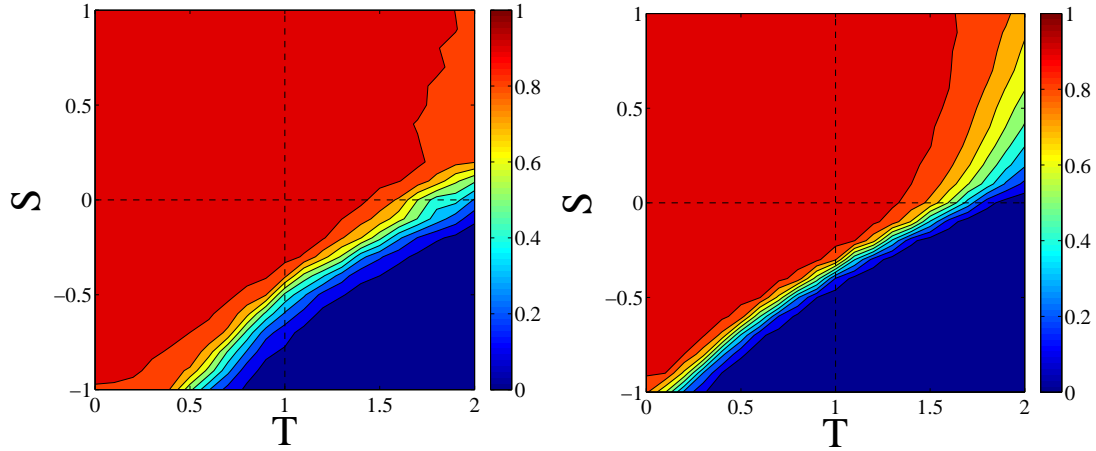
Fig. 2.6 Average cooperation in unweighted assembly model graphs. Left image: imitation of the best. Right image: replicator dynamics. Size of graphs is $N = 1000$. Each grid point is the average of 50 independent runs.
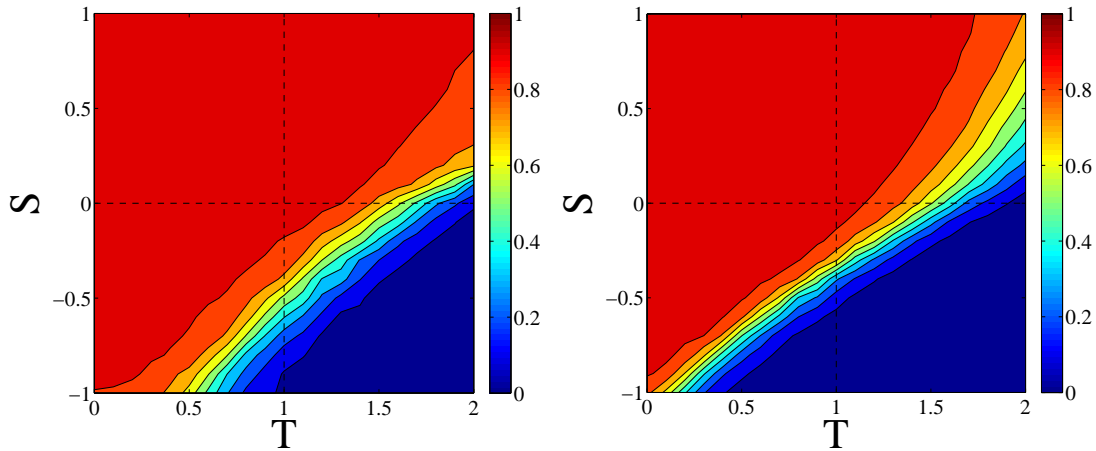
Fig. 2.7 Average cooperation in weighted assembly model graphs. Left image: imitation of the best. Right image: replicator dynamics. Size of graphs is $N = 1000$. Each grid point is the average of 50 independent runs.

to the way in which the graphs are built [5], their degree distribution turns out to be very close to scale-free (results not shown here). It is thus obvious that the games' behavior should be very similar. This in turn also shows once again that the purely topological aspects of the networks are more important than the weights in determining the steady states of the games.

As a further example of a weighted graph resulting from a bipartite interaction, we consider the network of scientists belonging to the Econophysics community [2]. This net-

---

[2] Kindly provided by Zhang Peng, personal communication.
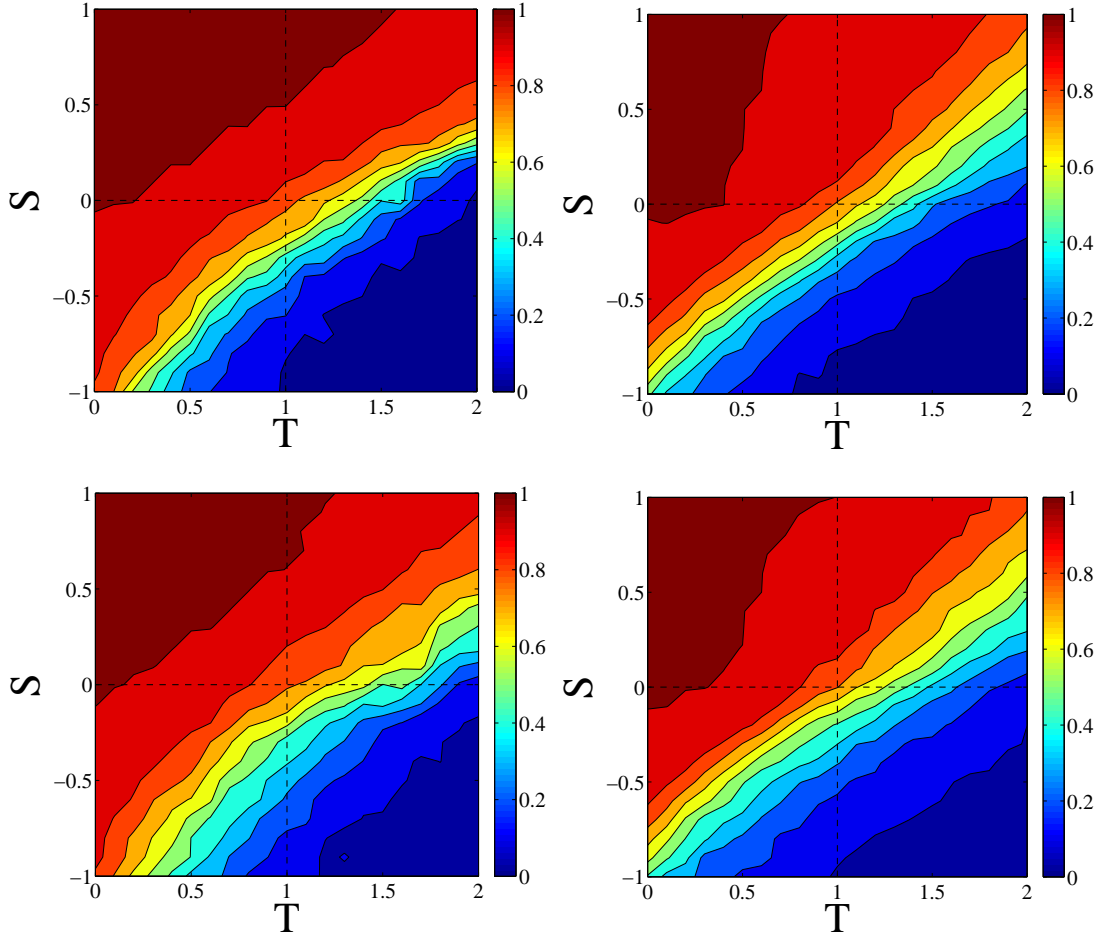
Fig. 2.8 Average degree of cooperation at steady state on the collaboration network of econo-physicists. Left column: imitate the best. Right column: replicator dynamics. Top row: standard weighting scheme; bottom row: corrected weighting scheme (see text). Averages over 50 independent runs.

work has a size $N = 738$ and 1866 edges, wich gives $\langle k \rangle \simeq 5.06$. In this network two nodes (authors) are connected if they have coauthored at least one scientific article. Link weights are assigned in two ways; the first corresponds to Eq. 2.1 in which the weight corresponds simply to the number of common papers, suitably normalized; in the second scheme, this row weight is corrected for a factor that accounts for the number of coauthors of a given paper, on the grounds that the larger the number of authors a paper has, the lesser the likelihood that the authors know each other equally well. Thus the weight of the link between two coauthors i and j is given by $w_{ij} = \sum_k \delta_i^k \delta_j^k / (n_k - 1)$ [8], where δ_j^k is 1 if author i was a coauthor of paper k and 0 otherwise, and n_k is the number of coauthors of paper k (single author papers are excluded).
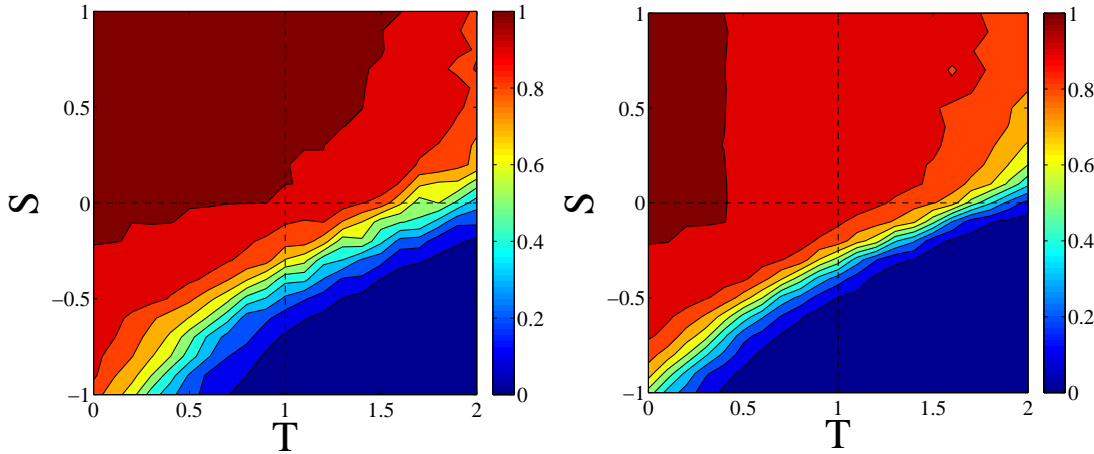
Fig. 2.9 Average degree of cooperation at steady state on the unweighted collaboration network of econophysicists. Left column: imitate the best. Right column: replicator dynamics. Averages over 50 independent runs.

Figure 2.8 shows the results for the two weighting schemes described above for imitation of the best update (left figures) and local replicator dynamics update (right figures). It is apparent that results are qualitatively very similar. We can compare these results with those obtained in the unweighted graphs (Fig. 2.9). The behavior is similar but, on the whole, the degree of cooperation in the three non-trivial games is slightly lower for the weighted versions of this social network. Although no general conclusions can be drawn from this single instance, it can be said that, at least in this case, taking into account the strengths of ties does not help cooperation. Whether or not this is a more general phenomenon in social networks would require a much more complete investigation using real networks coming from different types of social interactions. Unfortunately, reliable weighted network data are still few.

Table 2.2 summarizes the average cooperation levels reached in the various network types studied in this section, both weighted and unweighted, for the three non-trivial games PD, SG, and SH.

2.4 Discussion and Conclusions

The focus of this paper is on the influence of the weighted nature of social interaction networks on evolutionary games played on those networks, an issue that has been somewhat neglected until now. The first major question was: how do weighted edges affect the results of standard evolutionary games on complex networks? Owing to the lack of generally accepted theoretical models of the formation and structure of weighted social networks, we tried to answer the question by using numerical simulation and several methods for assigning weights to links. Three different roads were tried: in the first, weights

Table 2.2 Average cooperation at steady state in weighted and unweighted networks derived from bipartite graphs. 'ib' and 'rd' stand for 'imitate the best' and 'replicator dynamics' update rules respectively. PD, SG, and SH design the Prisoners Dilemma, Snowdrift, and Stag Hunt games respectively.

	PD, ib	PD, rd	SG, ib	SG, rd	SH, ib	SH, rd
Guimerà weighted	0.232	0.141	0.883	0.797	0.815	0.668
Guimerà unweighted	0.246	0.137	0.895	0.811	0 .807	0.650
Econophysicists, standard weights	0.164	0.147	0.845	0.746	0.673	0.585
Econophysicists, corrected weights	0.203	0.171	0.828	0.754	0.701	0.582
Econophysicists, unweighted	0.221	0.157	0.933	0.875	0.704	0.611

were assigned to edges according to some probability distribution independently of the underlying network topology. This means that the intensity of a binary relationship does not depend on the environment of the corresponding link and goes under the name of dyadic hypothesis in social networks. In the second empirical model, the weight of a link is correlated in some way with the degrees of the end points. Finally, in the third model, we started from bipartite affiliation graphs and generated weighted graphs using the model proposed in [5] and a real collaboration graph.

The results obtained using the first uncorrelated model clearly show that the influence of weights on the games is almost negligible. Furthermore, in this case topology and weights do not interact, as shown by the results on scale-free networks. Even in the case where the network is topologically inhomogeneous, and the weights are distributed according to a power-law, there is little difference with the unweighted case.

However, available empirical data on large networks suggest that topology and degree can be correlated to some extent. Assuming the link/weight correlation found in [1] for air flights between airports and used in [4] for the evolutionary PD on BA scale-free networks, which postulates that weights w_{ij} are proportional to $(k_i k_j)^\alpha$, we have numerically studied the full phase space of the standard games for several positive and negative exponent α values thus extending the work of [4] which was limited to a very small region of the game configuration space. For values of α larger than 0 and smaller than 1.5 approximately, there is indeed a non-negligible increase of the average cooperation for all the non-trivial games. However, it must be said that recent empirical research on typical social networks does not support such a weight dependence [1, 10, 11].

The third model comes from the realization that many social networks are of the affiliation type, which can be represented by bipartite graphs. We have thus studied model weighted networks built according to the method of [5]. On these graphs, the average results in terms of cooperation are very good but this appears to be due to the scale-free nature of the resulting networks and not to the weighted aspects, since weighted and unweighted networks give almost the same results. Finally, we examined the case of an actual coauthorship network, a projection of the bipatite graph formed by authors on the one hand, and the papers they have written together on the other. Our results show that weights are even slightly detrimental for cooperation for this particular network, although the main features remain similar with respect to the unweighted case. This last investiga-

tion was performed to illustrate the study with a real-life case but the results cannot be generalized in the absence of a sufficient amount of statistics on several social networks. In this respect, we mention that in previous work, Voelkl and Kasper studied the donor game, an analogous of the PD, using a number of networks representing weighted interactions in primate groups [18]. Using a fitness proportional update rule, they found that the fixation probability of cooperation in the groups was larger on the average with respect to a baseline well mixed population of the same size. The networks were very small and degree-inhomogeneous in many cases. Indeed, the authors refrained from attributing the results to the weighted nature of their networks; instead, they mainly invoked topological reasons and concluded that those, rather than the weights, were the more important contribution to network reciprocity. Although they did not examine the unweighted networks, in the light of the results presented here, it is likely that their explanation is essentially correct for this particular case.

Summing up all the previous considerations, a general conclusion can be drawn, taking into account the fact that our numerical simulation study cannot be considered exhaustive, but it has certainly been extensive. The conclusion is that, for well known model network classes, the weighted aspect of links does not seem to have a large influence on evolutionary games played on networks, the topological aspects being more important. It appears that weights essentially act as a source of noise on the payoff values. Thus, studying the unweighted versions of networks would seem to suffice for evolutionary games, at least in the case of standard model graphs. Of course, our conclusion does not apply to other domains. For example, link weights certainly play a very important role in diffusion and fragmentation processes on networks. Nevertheless, a thorough study of evolutionary games on reliably weighted actual social networks is still lacking. The single actual network that was studied here and the report [18] are insufficient, in our opinion, to draw any reliable conclusions. Our future work will be directed towards a better understanding of evolutionary games on real weighted networks, including dynamical ones, and the relationships with their topological features.

References

[1] A. Barrat, M. Barthélemy, R. Pastor-Satorras, and A. Vespignani. The architecture of weighted complex networks. *Proc. Natl. Acad. Sci.*, 101(11):3747–3752, 2004.

[2] M. Barthélemy, A. Barrat, R. Pastor-Satorras, and A. Vespignani. Characterization and modeling of weighted networks. *Physica A*, 346:34–43, 2005.

[3] D. P. Croft, R. James, and J. Krause. *Exploring Animal Social Networks*. Princeton, N.J., 2008.

[4] W.B. Du, H. R. Zheng, and M.B. Hu. Evolutionary prisoner's dilemma on weighted scale-free networks. *Physica A*, 387:3796–3800, 2008.

[5] Roger Guimerà, Brian Uzzi, Jarrett Spiro, and Luís A. Nunes Amaral. Team assembly mechanisms determine collaboration network structure and team performance. *Science*, 308(5722):697–702, 2005.

[6] C. Hauert and M. Doebeli. Spatial structure often inhibits the evolution of cooperation in the snowdrift game. *Nature*, 428:643–646, April 2004.

[7] B. A. Huberman and N. S. Glance. Evolutionary games and computer simulations. *Proc. Natl. Acad. Sci.*, 90:7716–7718, August 1993.

[8] M. E. J. Newman. Scientific collaboration networks. II. shortest paths, weighted networks, and centrality. *Phys. Rev. E*, 64:016132, 2001.

[9] M. E. J. Newman. *Networks: An Introduction.* Oxford University Press, Oxford, UK, 2010.

[10] J.-P. Onnela, J. Saramäki, J. Hyvönen, G. Szabó, M. Argollo de Menezes, K. Kaski, A.-L. Barabási, and J. Kertész. Analysis of a large-scale weighted network of one-to-one human communication. *New Journal of Physics*, 9:179, 2007.

[11] J.-P. Onnela, J. Saramäki, J. Hyvönen, G. Szabó, D. Lazer, K. Kaski, J. Kertész, and A.-L. Barabási. The architecture of weighted complex networks. *Proc. Natl. Acad. Sci.*, 101(11):3747–3752, 2004.

[12] M. Perc and A. Szolnoki. Coevolutionary games - A mini review. *Biosystems*, 99:109–125, 2010.

[13] E. Pestelacci, M. Tomassini, and L. Luthi. Evolution of cooperation and coordination in a dynamically networked society. *J. Biol. Theory*, 3(2):139–153, 2008.

[14] C. P. Roca, J. A. Cuesta, and A. Sánchez. Evolutionary game theory: temporal and spatial effects beyond replicator dynamics. *Physics of Life Reviews*, 6:208–249, 2009.

[15] F. C. Santos, J. M. Pacheco, and T. Lenaerts. Cooperation prevails when individuals adjust their social ties. *PLoS Comp. Biol.*, 2:1284–1291, 2006.

[16] G. Szabó and G. Fáth. Evolutionary games on graphs. *Physics Reports*, 446:97–216, 2007.

[17] F. Vega-Redondo. *Economics and the Theory of Games.* Cambridge University Press, Cambridge, UK, 2003.

[18] B. Voelkl and C. Kasper. Social structure of primate interaction networks facilitates the emergence of cooperation. *Biol. Lett.*, 5:462–464, 2009.

[19] J. W. Weibull. *Evolutionary Game Theory.* MIT Press, Boston, MA, 1995.

[20] M. G. Zimmermann and V. M. Eguíluz. Cooperation, social networks, and the emergence of leadership in a prisoner's dilemma with adaptive local interactions. *Phys. Rev. E*, 72:056118, 2005.

Chapter 3

Supercooperation in Evolutionary Games on Correlated Weighted Networks

Abstract In this work we study the behavior of classical two-person, two-strategies evolutionary games on a class of weighted networks derived from Barabási-Albert and random scale-free unweighted graphs. Using customary imitative dynamics, our numerical simulation results show that the presence of link weights that are correlated in a particular manner with the degree of the link endpoints, leads to unprecedented levels of cooperation in the whole games' phase space, well above those found for the corresponding unweighted complex networks. We provide intuitive explanations for this favorable behavior by transforming the weighted networks into unweighted ones with particular topological properties. The resulting structures help to understand why cooperation can thrive and also give ideas as to how such supercooperative networks might be built.

3.1 Introduction

Game theory has proved useful in a number of settings in biology, economy, and social science in general. Evolutionary game theory in particular is well suited to the study of strategic interactions in animal and human populations and has been a very useful mathematical tool for dealing with these kind of situations. Evolutionary games have been traditionally studied in the context of well-mixed and very large populations (see e.g. [8, 25]). However, starting with the work of Nowak and May [12], and especially in the last few years, population structures with local interactions have been brought to the focus of research. Indeed, it is a fact of life that social interactions can be more precisely represented as networks of contacts in which nodes represent agents and links stand for their relationships [11]. The corresponding literature has already grown to a point that makes it difficult to be exhaustive; however, good recent reviews can be found in [15, 19, 23]. Most of the new results, owing to the difficulty of analytically solving non mean-field models, come from numerical simulations, but there are also some theoretical results, mainly on degree-homogeneous graphs. On the other hand, most of the work so far has dealt with unweighted graphs. This is understandable as a logical first step, since attributing reliable weights to relationships in social networks is not a simple matter because the relationship is often multi-faceted and implies psychological and sociological features that are difficult to define and measure, such as friendship, empathy, and common

beliefs. In spite of these difficulties, including the strength of agents' ties would be a step toward more realistic models. In fact, sometimes at least a proxy for the intensity of a relationship can be defined and accurately measured. This is the case for e-mail networks, phone calls networks, and coauthorship networks among others. For example, in an extensive study of mobile phone calls network [14], the authors used the number of calls between two given agents and the calls' duration to capture at least part of the underlying more complex social interaction. The same can be done in coauthorship networks in which the strength of a tie can be related to the number of common papers written by the two authors [10].
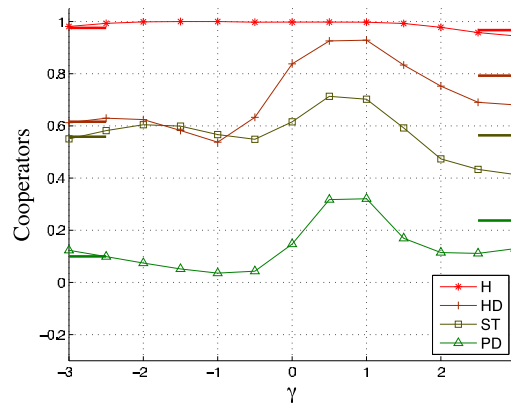
Fig. 3.1 (Color online) The points show, for each game, the average fraction of cooperation at steady state in the whole game's phase space as a function of γ, $-3 \leq \gamma \leq 3$ in Barabási–Albert networks. The weight-degree correlation is $w_{ij} = (k_i k_j)^\gamma$ and the strategy update rule is replicator dynamics. Each point is the average of 50 independent runs; continuous curves are just a guide for the eye. Small lines on the right and left borders indicate the cooperation level for $\gamma = \pm 10$.

Little work has been done on evolutionary games on weighted networks to date. Two recent contributions are [5, 24]. We have recently offered a rather systematic analysis of standard evolutionary games on several network types using some common weight distributions with no correlations with the underlying network topology features such as node degree and local clustering [4]. The results in all cases studied in [4] are that the evolutionary game dynamics are little affected by the presence of weights, that is, the graph topology, together with the game class and the strategy update rules seem to be the main factors dictating strategy evolution in the population. This is a reassuring result to the extent to which it allows us to almost ignore the weights and focus on the structural aspect only. However, the previous results, as said above, were obtained with standard weight distribution functions and ignoring possible correlations with other topological features. Thus, it is still possible that some particular weight assignment that takes these factors into account could make the dynamics to behave in a more radically different way. Indeed, in [5], Du et al. have investigated the Prisoner's Dilemma on Barabási–Albert scale-free graphs with a particular form of two-body correlation between the link weights and the

$$
\begin{array}{c|cc}
 & C & D \\
\hline
C & R, R & S, T \\
D & T, S & P, P
\end{array}
$$

Table 3.1 Generic payoff bi-matrix for the two-person, two-strategies symmetric games discussed in the text.

degrees of the link endpoints, finding an increase of cooperation under some conditions with respect to the unweighted case. We shall discuss and extend their results in Sect. 3.3. In the present paper we have studied another form of degree-weight correlation that is more likely to occur in social networks and gives unprecedented amounts of cooperation promotion on scale-free networks. In the following we first give a brief description of the games used and of the population dynamics; then we present and discuss our results.

3.2 Evolutionary Games on Networks

3.2.1 The Games Studied

We investigate four classical two-person, two-strategy, symmetric games, namely the Prisoner's Dilemma (PD), the Hawk-Dove Game (HD), the Stag Hunt (ST), and the Harmony game (H). We briefly summarize the main features of these games here for completeness; more detailed accounts can be found elsewhere [25]. The games have the generic payoff bi-matrix of Table 3.1.

The set of strategies is $\Lambda = \{C, D\}$, where C stands for "cooperation" and D means "defection". In the payoff matrix R stands for the *reward* the two players receive if they both cooperate, P is the *punishment* if they both defect, and T is the *temptation*, i.e. the payoff that a player receives if he defects while the other cooperates getting the *sucker's payoff* S. In order to study the standard parameter space, we restrict the payoff values in the following way: $R = 1$, $P = 0$, $-1 \leq S \leq 1$, and $0 \leq T \leq 2$. In the resulting TS-plane, each game corresponds to a different quadrant depending on the ordering of the payoffs.

For the PD, the payoff values are ordered such that $T > R > P > S$. Defection is always the best rational individual choice, so that (D, D) is the unique Nash Equilibrium (NE) and also the only fixed point of the replicator dynamics [25]. Mutual cooperation would be socially preferable but C is strongly dominated by D.

In the HD game, the order of P and S is reversed, yielding $T > R > S > P$. Thus, in the HD when both players defect they each get the lowest payoff. Players have a strong incentive to play D, which is harmful for both parties if the outcome produced happens to be (D, D). (C, D) and (D, C) are NE of the game in pure strategies. There is a third equilibrium in mixed strategies which is the only dynamically stable equilibrium [25].

In the ST game, the ordering is $R > T > P > S$, which means that mutual cooperation (C, C) is the best outcome, Pareto-superior, and a NE. The second NE, where both players defect is less efficient but also less risky. The tension is represented by the fact that the socially preferable coordinated equilibrium (C, C) might be missed for "fear" that the other

player will play D instead. The third mixed-strategy NE in the game is evolutionarily unstable [25].

Finally, in the H game $R > S > T > P$ or $R > T > S > P$. In this case C strongly dominates D and the trivial unique NE is (C, C). The game is non-conflictual by definition and does not cause any dilemma, it is mentioned to complete the quadrants of the parameter space.

With these conventions, in the figures that follow, the PD space is the lower right quadrant; the ST is the lower left quadrant, and the HD is in the upper right one. Harmony is represented by the upper left quadrant.
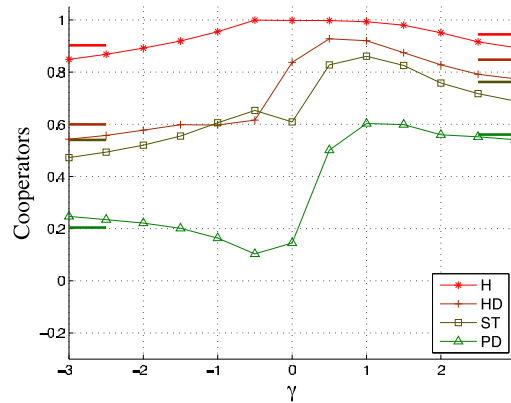
Fig. 3.2 (Color online) The points show, for each game, the average fraction of cooperation at steady state in the whole game's phase space as a function of γ, with weight-degree correlations $w_{ij} = (|k_i^2 - k_j^2| + 1)^\gamma$ in weighted Barabási–Albert networks. The strategy update rule is replicator dynamics. Averages over 50 independent runs.

3.2.2 Population Structure

The population of players is a connected, weighted, undirected graph $G(V, E)$, where the set of vertices V represents the agents, while the set of edges E represents their symmetric interactions. The population size N is the cardinality of V. The set of neighbors of an agent i is defined as: $V_i = \{j \in V \mid dist(i, j) = 1\}$, and its cardinality is the degree k_i of vertex $i \in V$. The average degree of the network is called $\langle k \rangle$. Given two arbitrary nodes $k, l \in V$, the weight of the link $\{kl\}$ is called w_{kl}.

For the network topology we use the classical Barabási–Albert (BA) [1] networks which are grown incrementally starting with a clique of m_0 nodes and adding a new node with $m \leq m_0$ edges at each time step. The probability that a new node will be connected to node i depends on the current degree k_i of the latter: the larger k_i the higher the connection probability. The model evolves into a stationary network with power-law probability distribution for the vertex degree $P(k) \sim k^{-\alpha}$, with $\alpha \sim 3$. For the simulations, we started
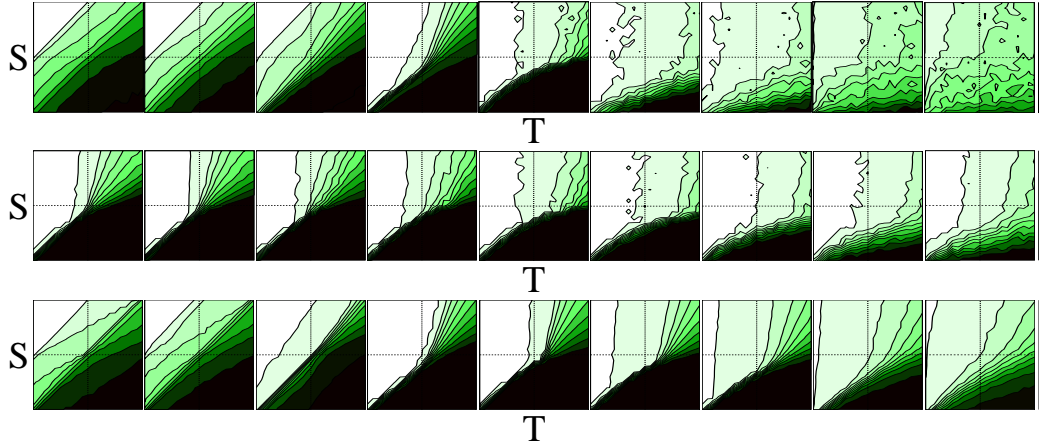
Fig. 3.3 (Color online) Average cooperation over 50 runs at steady state on networks of size $N = 2000$ and $\langle k \rangle = 8$ as a function of the parameter γ (see text). For all lines of images, $\gamma = -3, -2, -1, -0.5, 0, 0.5, 1, 2, 3$ from left to right. The initial density of cooperators is 0.5 in all cases. In all images the x-axis corresponds to $0 \leq T \leq 2$, and the y-axis represents the interval $-1 \leq S \leq 1$. Dark tones mean more defection; the color bar on the right goes from 0 cooperation to full cooperation at the top. Upper line: weighted BA graph; Middle line: weighted BA graph, with unweighted payoffs (see text); Bottom line: weighted Erdös-Rényi random graphs.
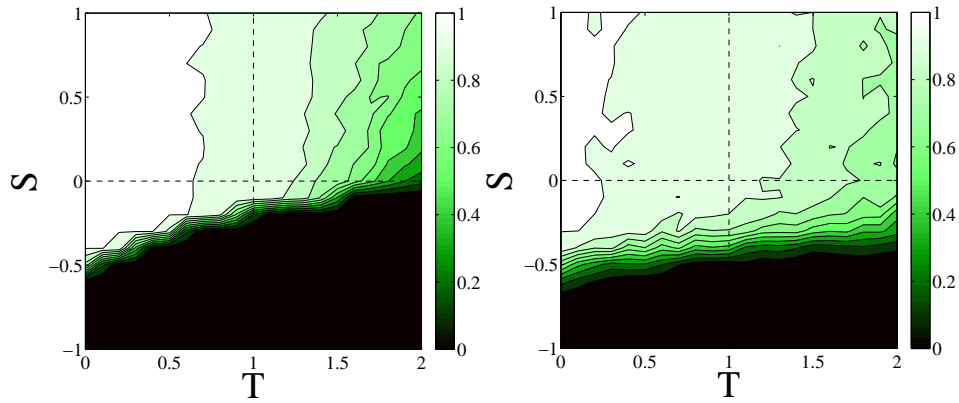
Fig. 3.4 (Color online) Average cooperation over 50 runs in Barabási–Albert networks for $\gamma = 0.0$ on the left and $\gamma = 1.0$ on the right. The initial cooperation is 0.3 and strategy update is by replicator dynamics.

with a clique of $m_0 = 9$ nodes and, at each time step, the new incoming node has $m = 4$ links. In addition, we also used standard Erdös-Rényi random graphs [3] and scale-free random graphs [9], as explained in Sect. 8.3.
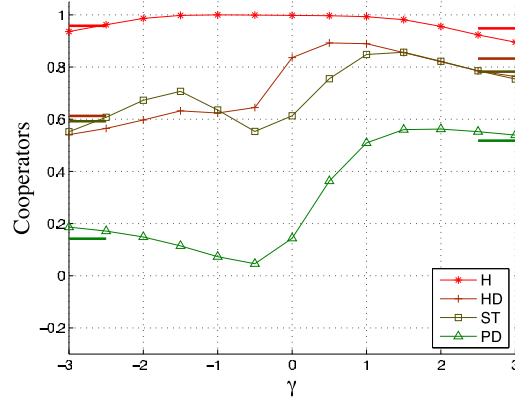
Fig. 3.5 (Color online) The points show, for each game, the average fraction of cooperation in Barabási–Albert networks at steady state in the whole game's phase space as a function of γ for the rule $(|k_i - k_j| + 1)^\gamma$ using replicator dynamics.

3.2.3 Payoff Calculation and Strategy Update Rules
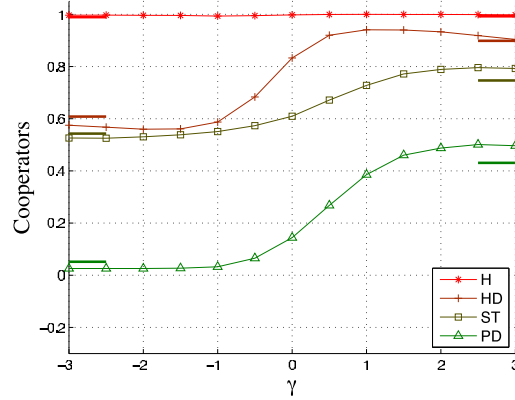
Fig. 3.6 (Color online) Average cooperation levels for the replicator dynamics in Barabási–Albert networks when payoff is computed according to the unweighted network (see text).

We need to specify how individual's payoffs are computed and how agents decide to revise their present strategy, taking into account that only local interactions are permitted. Let $\sigma_i \in \{C, D\}$ be the current strategy of player i and let us call M the payoff matrix of the game. The quantity

$$\Pi_i(t) = \sum_{j \in V_i} \sigma_i(t) \, M \, \sigma_j^T(t) \tag{3.1}$$

is the cumulated payoff collected by player i at time step t. Since we work with weighted networks, the pairwise payoffs $M_{ij} = \sigma_i \, M \, \sigma_j^T$ are multiplied by the weights w_{ij} of the corresponding links before computing the accumulated payoff M_{ij}' earned by i. This takes into account the relative importance or frequency of the relationship as represented by its weight. Thus, the modified cumulated payoff of node i at time t is $\widehat{\Pi}_i = \sum_{j \in v_i} M_{ij}'$. However, if the weights are seen simply as an expression of trust, the payoff is computed with the unweighted network and the weights affect only the strategy update rule, because, as the frequency of the relationship is held constant, the additional trust only influences which neighbor the player wants to imitate.

Several strategy update rules are customary in evolutionary game theory. Here we shall describe two imitative update protocols that have been used in our simulations.
The *local fitness-proportional* rule is stochastic and gives rise to replicator dynamics [7]. Player i's strategy σ_i is updated by drawing another player j from the neighborhood V_i with probability proportional to the weight w_{ij} of the link, and replacing σ_i by σ_j with probability:

$$p(\sigma_i \to \sigma_j) = (\widehat{\Pi}_j - \widehat{\Pi}_i)/K,$$

If $\widehat{\Pi}_j > \widehat{\Pi}_i$, and keeping the same strategy if $\widehat{\Pi}_j \leq \widehat{\Pi}_i$, where $\widehat{\Pi}_j - \widehat{\Pi}_i$ is the difference of payoffs earned by j and i respectively. $K = \max(s_i, s_j)[(\max(1, T) - \min(0, S)]$ ensures proper normalization of the probability $p(\sigma_i \to \sigma_j)$, in which s_i and s_j are the strenghts of nodes i and j respectively, the strength of a node being the sum of the weights of the edges emanating from this node.
The second strategy update rule is the *Fermi rule* [23]:

$$p(\sigma_i \to \sigma_j) = \frac{1}{1 + \exp(-\beta(\widehat{\Pi}_j - \widehat{\Pi}_i))}.$$

This gives the probability that player i switches from strategy σ_i to σ_j, where j is a neighbor of i chosen with probability proportional to the weight w_{ij} of the link between them. The parameter β gives the amount of noise: a low β corresponds to high probability of error and, conversely, high β means low error rates.

3.2.4 Simulation Parameters

The networks used in all simulations are of size $N = 2000$ with mean degree $\langle k \rangle = 8$. The TS-plane has been sampled with a grid step of 0.1 and each value in the phase space reported in the figures is the average of 50 independent runs, using a fresh graph realization for each run.

The evolution proceeds by first initializing the players at the nodes of the network with one of the two strategies at random such that each strategy has a fraction of approximately 1/2. Other proportions have also been used. Agents in the population are given opportunities to revise their strategies all at the same time (synchronous updating). We have also checked that asynchronous sequential update gives similar results. We let the system evolve for a period of 4000 time steps, after any transient behavior has died out,
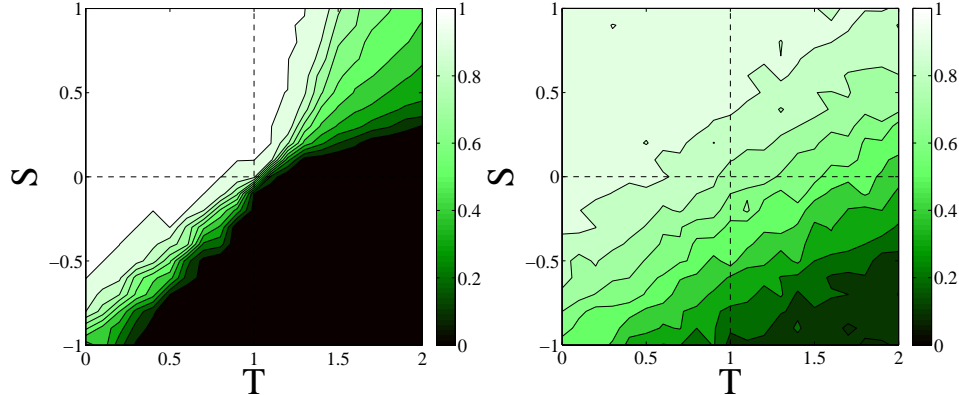
Fig. 3.7 (Color online) Average cooperation in Barabási–Albert networks over 50 runs for $\gamma = 0$ on the left and average cooperation over 200 runs for $\gamma = 1$ after 12000 synchronous time steps on the right. Both cases belong to the diffusion approximation, that is Fermi rule with $\beta = 0.01$.

and we take average cooperation values. At this point the system has reached a steady state in which there is little or no fluctuation.

3.3 Degree-Weight Correlations

In a recent work Du et al. [5], based on observed degree-weight correlations in transportation networks [2], assumed that $w_{ij} \propto (k_i k_j)^\gamma$ for some small exponent γ, where w_{ij} is the weight of edge $\{ij\}$, and k_i, k_j are the degrees of its end points. The authors used Barabási-Albert model graphs which are, among the standard model complex networks, those that are more conducive to cooperation [21, 22]. Although they only presented results for the points in the phase space belonging to the frontier segment between the PD and HD games (so-called "weak" PD game), here we provide the full average results for each game's parameter space as a function of the exponent γ in Fig. 3.1 using replicator dynamics. The complete numerical results for the whole phase space are to be found in [4].

For $\gamma \geq 0$, there is indeed a small but non-negligible increase in cooperation around $\gamma = 0.0$ to 0.5. However, the problem is that the assumed degree-weight correlation is typical of transportation networks but has not been observed in social networks [2, 13, 14]. The reason could be that while in transportation networks there are fluxes that must respect local conservation [14], social networks have a more local nature. In the degree-weight correlation above the coordinate $k_i k_j$ is the joint contribution; a complementary view would be to use the difference between k_i and k_j which amounts to a local degree comparison. Thus, as there is no correlation between the form $k_i k_j$ and real weights, we take its perpendicular counterpart $|k_i^2 - k_j^2|$ in the degree-weight correlation, which contains the same information as the absolute value of the difference of degrees. Taking these considerations into account we have:

$$w_{ij} \propto (|k_i^2 - k_j^2| + 1)^{\gamma} \tag{3.2}$$

The exponent γ allows us to explore the weight-degree correlation from a more disassortative case ($\gamma > 0$) to an assortative case ($\gamma < 0$), passing through the unweighted case ($\gamma = 0$). We added a strictly positive constant to the difference of square degrees to avoid division by 0 for negative γ.

It is important to point out that we do not mean to imply that this kind of correlation is present in actual social networks as we do not have the empirical data analysis needed to show that this is the case. Indeed, to our knowledge, there are not enough publicly available reliable data on weighted social networks to test it out empirically. As a consequence, our results will refer to model weighted networks, not to real ones, but this has been the case for most studies of evolutionary games on unweighted networks as well ([19, 21, 22, 23] and references therein).
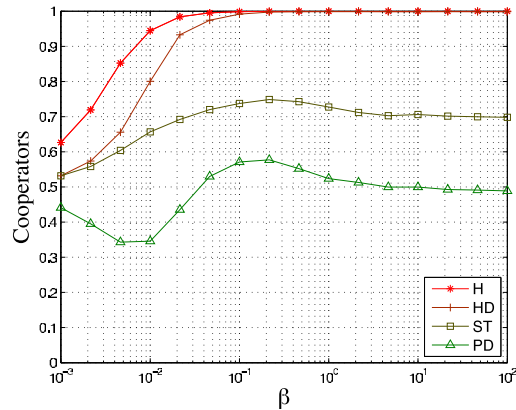
Fig. 3.8 (Color online) Average cooperation in all games on Barabási–Albert networks over 100 runs for $\gamma = 1$ after 4000 synchronous time steps with the Fermi rule as a function of β.

3.4 Results

The average cooperation figures for BA networks, in which weights are set according to the degree-weight correlation described by Eq. 3.2, are shown in Fig. 3.2 as a function of the exponent γ. The strategy update rule is replicator dynamics. The increase in cooperation is notable in the positive γ range, especially in the hardest PD game, well beyond what is found in unweighted BA networks, as can be seen in Figs. 3.3 by comparing the 5th image in the top panel, which corresponds to an unweighted network ($\gamma = 0$), with the next images in the same panel. Moreover, it is seen that the HD and ST games also benefit in this range. Taking into account that BA scale-free networks have been found to be among the most effective to date in terms of amplifying cooperation, these findings seems to be very interesting. In Fig. 3.3 it can be seen that, in contrast to the positive γ case, for negative

γ there is no cooperation gain whatsoever. A qualitative explanation of this result is the following. When $\gamma < 0$, Eq. 3.2 attributes small weights to links between nodes that have widely different degrees. Because of the way in which weights are used to choose neighbors and to compute payoffs in the game dynamics, this in turn will prevent hubs from playing their role in propagating cooperation. The situation for $\gamma = -0.5$ becomes qualitatively similar to that of a random graph in which the degree distribution is more homogeneous, and it is well known that random graphs are not conducive to cooperation [19]. When γ decreases further and approaches -3, in practice the network becomes more and more segmented into small components that have very weak links between them.
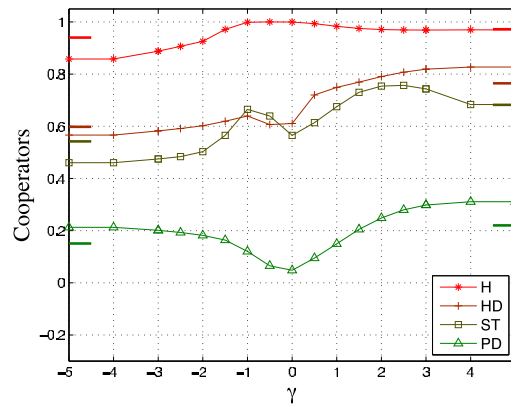
Fig. 3.9 (Color online) The points show, for each game, the average fraction of cooperation at steady state in the whole game's phase space as a function of γ for Erdös-Rényi random graphs. Strategy update is by replicator dynamics and the points are averages over 50 independent runs.

As expected, the initial conditions influence final cooperation frequencies. As an example, we display the phase space at steady state starting from 30 percent cooperation in Fig. 3.4 for $\gamma = 0$ and 1. The average cooperation is less, especially for the SH and PD games; however, cooperation levels are still significantly higher with the weights.

The rule $(|k_i^2 - k_j^2| + 1)^\gamma$ uses the square of the degrees. We also tested the simpler alternative rule $(|k_i - k_j| + 1)^\gamma$ on a Barabasi-Albert network. We obtained the same behavior, except for a shift, see Fig. 3.5.

Until now we used the weights as representing a time of interaction, and thus payoffs were the product of the weight times the numerical payoffs as explained in Sect. 7.2.3. We can also consider them simply as an expression of trust. In this case the weights only influence the choice of a neighbor to imitate, but the payoffs are just the ordinary payoffs, Eq. 8.6, without weight multiplication. For the PD, the assortative weights ($\gamma < 0$) imply close to zero cooperation, and the disassortative weights tend to one half cooperation. We show the mean cooperation for all games in Fig. 3.6, and the entire game's space in the middle panel of Fig. 3.3, using the rule $(|k_i^2 - k_j^2| + 1)^\gamma$. We observe that all the games are positively influenced for $\gamma > 0$ which indicates that simply imitating the strategy of agents with which the link is stronger has a favorable effect on cooperation.

The Fermi dynamics (see Sect. 7.2.3) is a flexible imitation protocol. For $\beta \simeq 10$ it approaches the replicator dynamics results in unweighted networks [19]. However, when $\beta \ll 1.0$ the Fermi dynamics leads to the diffusion approximation [23]. Here, this approximation means that when a player selects a strategy, after having selected a neighbor, in the majority of cases he chooses the strategy at random and only rarely he selects it proportionally to difference of payoffs. For unweighted BA networks at steady state there is no cooperation increase and defection prevails in the PD (see left image of Fig. 3.7 and [19]). However, on the weighted network with $\gamma = 1.0$, cooperation remains high, although lower than the replicator dynamics case (Fig. 3.7, image on right). We performed 200 runs instead of 50 because the system is noisier, and each run lasted for 12000 instead of 4000 time steps, since approaching steady state is slower. In Fig. 3.8 we display the cooperation levels as a function of β for the weighted graph with $\gamma = 1$ after 4000 synchronous time steps and 50 repetitions. This seems to confirm the robustness of cooperation, on this kind of topology, against noise in the choice of a neighbor. For $\beta \leq 10^{-2}$ the dynamics is probably not at steady state. Steady state might be difficult to attain because the dynamic becomes very slow as β approaches 0. However, the difference from the BA is very interesting (See also [19]); it shows that the model is applicable to a broader range of real situations, where the behavior of players is subject to errors of various kinds.
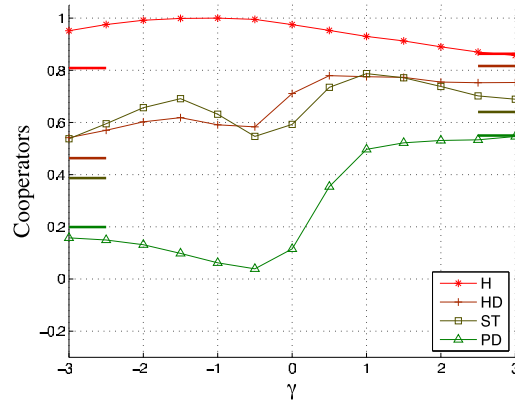
Fig. 3.10 (Color online) Average cooperation in random scale-free graphs obtained with the configuration model with an exponent $\alpha = -3$ of the power law degree distribution. Strategy update rule is replicator dynamics. Averages over 50 independent runs.

In order to see how cooperation is affected when degree heterogeneity is low, we use Erdös-Rényi random graphs and then set the weights according to our rule. The Barabasi-Albert graph gives drastically better results but there is an improvement in weighted random graphs compared to the unweighted case: see Fig. 3.9 and the bottom panel of Fig. 3.3. Indeed, while cooperation in the PD is almost absent on random graphs, with our weighting scheme, cooperation increases to levels similar to those found in unweighted BA networks, as seen by comparing Fig. 3.9 for $\gamma = 1$ with Fig. 3.2 for $\gamma = 0$.

It is worth noting that Barabási–Albert graphs are only a particular class of scale-free growing networks. Due to their construction, they possess historical correlations between early hub nodes [11]. In other words, hubs tend to be interconnected among themselves and it transpires that this feature is favorable for cooperation [19, 21]. Thus, we also tested scale-free networks that have no degree correlation, such as the "configuration model" [9, 11] which yields random scale-free graphs if built from the right degree sequence. We used the configuration model with an exponent $\alpha = -3$ of the power-law degree distribution. The results, shown in Fig. 4.3, are qualitatively similar to those obtained on BA networks (Fig. 3.2), except for a small drop in cooperation near $\gamma = 1$. The largest differences are observed for the ST game, but they are still small in absolute terms. The result on random scale-free weighted networks is interesting and confirms the role of weights in the establishment of asymptotic high levels of cooperation in our model networks, in spite of the fact that these networks are less conducive to cooperation than BA networks [17, 22].

3.5 Cooperative Unweighted Graphs from Weighted Ones
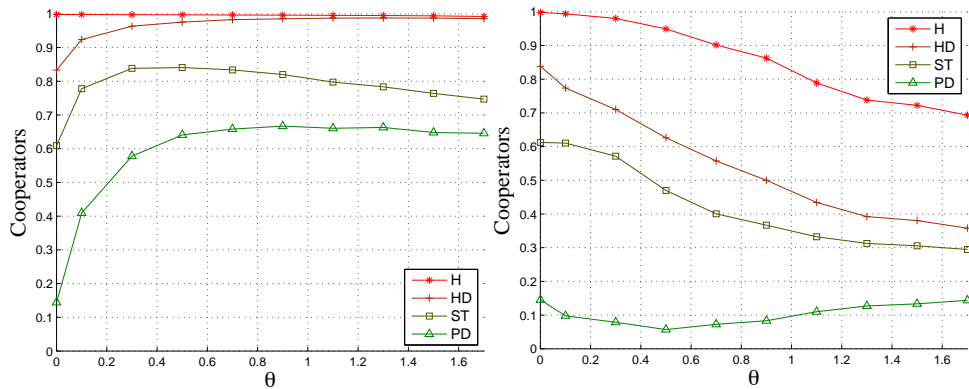
Fig. 3.11 (Color online) Average cooperation for the filtered unweighted graphs obtained from Barabási–Albert networks with $\gamma = 1.0$ (left) and $\gamma = -1.0$ (right), as a function of the parameter θ (see text). Values are averages over 50 runs, and strategy update is by replicator dynamics.

Understanding game dynamics may be simpler on unweighted graphs than on weighted graphs. In order to get an intuitive idea of the mechanism seen on weighted networks, we constructed two unweighted models from the weighted one as described below.

The first model is a rather raw but revealing way of extracting an unweighted structure from the weighted graph by filtering out edges with low enough weights. The resulting topology should be of help in understanding the origins of the large promotion of cooperation we found on our particular class of weighted correlated networks. Starting with a BA graph, we set the weights according to the form $(|k_i^2 - k_j^2| + 1)^\gamma$, discard the edges with a weight inferior to a threshold θ, and finally set all weights of the remaining links to one. Every edge with weight $w < \theta \langle w \rangle$, $\theta=\{0.0,0.1,0.3,...,1.9\}$, is discarded. During

the edge filtering process some vertices may become isolated. The problem is that their strategy cannot change after having been assigned randomly at the beginning. In the weighted network these nodes interact rarely since the frequency of interaction depends on the link weight. For the sake of simplicity, our choice has been to discard them in the simulations, otherwise the simulation results would be biased owing to the isolated nodes with unchanging strategy.
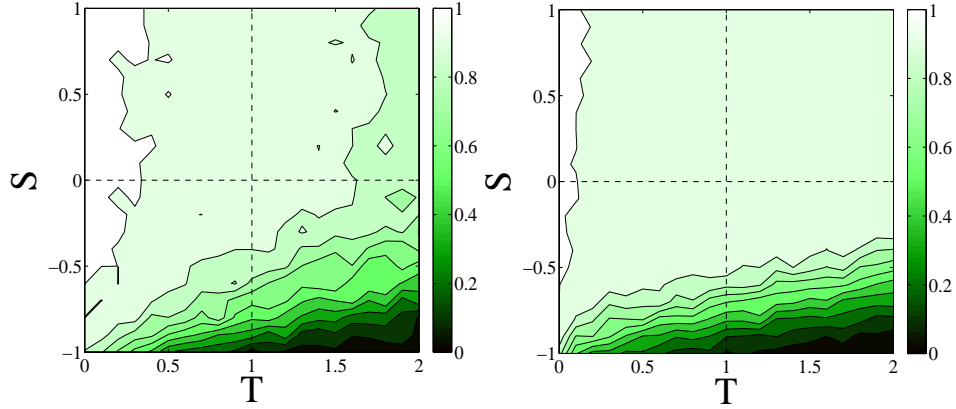
Fig. 3.12 (Color online) Left : Cooperation phase space on Barabási–Albert networks for the weighted case with $\gamma = 1$ and the correlation function $(|k_i^2 - k_j^2| + 1)^\gamma$. Right : Corresponding cooperation phase space for the filtered unweighted network with $\gamma = 1$ and $\theta = 0.7$. Averages over 50 runs using replicator dynamics.

The mean cooperation on the filtered graphs as a function of θ is shown in the left image of Fig. 3.11. The mean cooperation level in all the games increases with the threshold up to a certain point and then stays approximately constant. The cooperation increase is particularly notable for PD in which one goes from 0.15 up to about 0.65, i.e. a four-fold increase. The right image of Fig. 3.12 shows the average cooperation in the whole S-T plane for $\gamma = 1$ and $\theta = 0.7$. It is apparent that the high degree of cooperation that was present in the original weighted graph, which is reported in the left image of Fig. 3.12 is fully maintained apart from some small differences due to the details of the dynamics and slightly different network sizes. This means that the filtered unweighted graph provides at least as much cooperation as the original weighted one and, therefore, is in some non-rigorous sense, equivalent to it. For higher values of θ, not only in the average but also for the whole game space, the trend remains very similar for the PD; in the ST there is some small loss of cooperation, while the HD gains a little bit (the corresponding figures are not shown to save space).

In the right image of Fig. 3.11 we show the mean cooperation values that are reached when the links are filtered in the same way but with $\gamma = -1$. Since the weights are now the reciprocals of the original ones, this roughly amounts to cutting the strongest links with respect to the case $\gamma = 1$. The result is a generalized loss of cooperation in the average, a

fact that shows the importance of strong links. The fact that cooperation goes below 1 in the Harmony game is due to graph fragmentation.
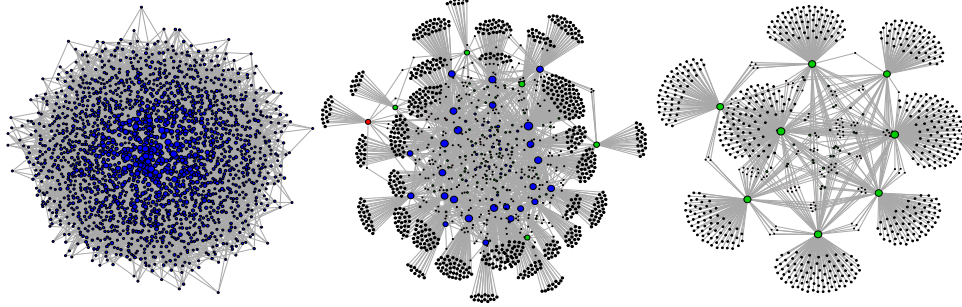
Fig. 3.13 (Color online) Typical filtered graph plots as a function of γ, with Fruchtermann-Reingold layout, coloration of cores, and the size of a vertex $\propto log(k_i)$. From left to right: $\gamma = 0.0, 1.0, 3.0$; $\theta = 0.7$ for all images. Only the giant connected components are shown.
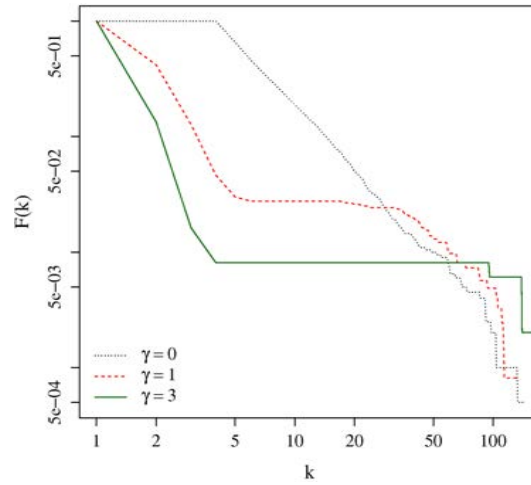
Fig. 3.14 (Color online) Cumulated degree distribution of the filtered and unfiltered networks in log-log scales. dotted gray line, dashed red line, green thick line stand, respectively, for $\gamma = 0.0, 1.0, 3.0$. The original unfiltered graph has been obtained through the Barabási–Albert construction.

We display some particular but representative graphs obtained through the filtering process in Fig. 3.13. The topologies show hubs connected to many low degree vertices and the hubs are possibly connected directly or through some intermediate vertices with low degree, while the low degree vertices are not connected between them. This effect increases with increasing γ and can be seen explicitly in Fig. 3.13. The empirical degree distribution curves of the BA graphs before and after transformation are shown in Fig. 3.14. We observe

that there are less nodes with degree between $\simeq 5$ and $\simeq 50$, thus separating vertices in two sets, large degree and low degree vertices, an almost bipartite network. In fact, the Newman's coefficient of assortativity [11] is of the order of ~ -0.6, for the filtered BA graph with $\theta = 0.7, \gamma = 1$, and of the order of ~ -0.9 for $\theta = 0.7, \gamma = 3$, while it is ~ -0.05 for the original graph, which indicates that the graph indeed becomes more bipartite as there are few links between nodes of similar degree and γ increases. Another class of networks in which one finds this almost bipartite degree distributions has been generated by Poncela et al. [18] in a completely unrelated way. They use a dynamical process in which new players attach to existing nodes at random, or preferentially to those that have been successful in the past. Their graphs are highly cooperative in the dynamical regime, but when used as static graphs cooperation is much lower. In another study, Rong et al. [20] find that when a network becomes assortative by degree, the large-degree vertices tend to interconnect to each other closely, which destroys the sustainability among cooperators and promotes the invasion of defectors, whereas in disassortative networks, the isolation among hubs protects the cooperative hubs in holding onto their initial strategies to avoid extinction. This study, although it is different from ours since it does not start from weighted networks, also shows the role of degree disassortativity in influencing cooperation.

The above model gave us some general ideas about the possible structure of highly cooperative unweighted networks. Now we shall try to better understand the microscopical foundations of the phenomena by studying a small graph containing the minimal features required to parallel the behavior on weighted networks.

In Roca et al. [19] the authors give an intuitive explanation for the cooperation induced by degree heterogeneity in unweighted BA networks. Gómez-Gardeñes et al. [6] provide a deeper analysis of the origins of cooperation in the PD case but here the simple argument of [19] will be sufficient. In their view, the hubs drive the population, fully or partially, to cooperation in HD games. The reason is the following: the hubs get more payoff, thus a defector hub triggers the change of his neighbors to defection, while a cooperator hub triggers it to cooperation, favoring cooperation since cooperative hubs surrounded by co-operators get a higher payoff. In our weighted case the topology of the network leads to cooperation not only in the HD game, but also in the PD game. In this case the idea of hubs driving the population to cooperation is very relevant, because the new topology amplifies this effect.

According to Eq. 3.2 for $\gamma > 0$, the smaller the difference between the degrees of two connected nodes, the smaller the weight of the corresponding link. Thus, two connected hubs will have a relatively low link weight, while a link between a hub and a low-degree vertex will be given a high weight. Also, links between two low-degree nodes will make the corresponding link weight almost negligible, a fact that we have exploited in the filtered graphs above. With these ideas in mind, let us consider the graph in the right part of Fig. 3.15 where two hubs are connected to 36 vertices having degree one or two, depending on whether they are connected to one hub or to both. We will consider two extreme cases: either the two hubs are connected, or they aren't. We obtain a bipartite graph when the hubs are not connected, and an almost bipartite one when there is a link between them. The number of common neighbors of A and B is 8 in the figure, so as to be in a region where cooperation is high, as shown in the left image of Fig. 3.15 when *A* and *B* are connected. These data have been obtained by numerically simulating the games' evolution

on the graph of Fig. 3.15 with replicator dynamics and varying the number of common neighbors from 0 to 24. The upper row of Fig. 3.16 shows the games' phase space with or without an edge between the two hubs for the graph of Fig. 3.15 starting from a random initial distribution, while the lower row of Fig. 3.16 shows the same plots with the following initial distribution: A is cooperator, B is defector, random strategies are assigned to the other vertices. The plots show that the model in which the hubs are connected induces more cooperation in all games. When hubs are not connected (the left images) results are very similar in the upper and lower images because propagation via the hubs is no longer possible. Now, we shall try to explain the mechanism at work referring to the graph in Fig. 3.15.
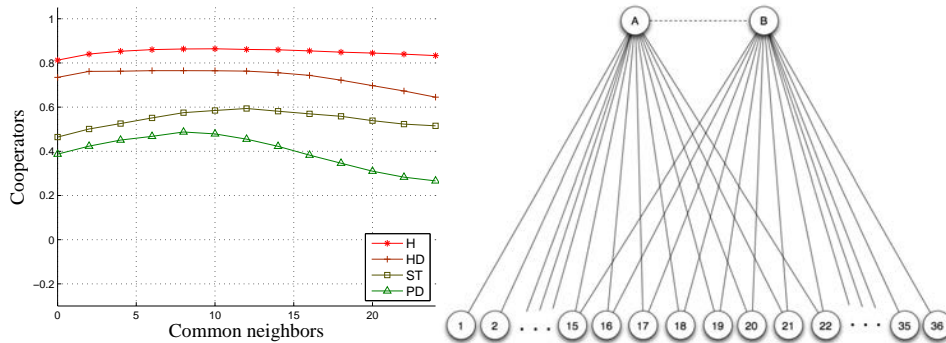
Fig. 3.15 (Color online) Average cooperation over 1000 repetitions of 500 time steps on the bipartite graph shown on the right as a function of the number of common neighbors to A and B. Replicator dynamics is used to update agents' strategy. The initial strategy distribution is random. The graph displayed has 8 common neighbors.

If node A is a cooperator and node B is a defector, by Roca's et al. arguments [19], A will have an advantage and could spread cooperation to B. However, if A and B are not directly connected, strategy migration will have to go through a low degree node and this will make further progress more difficult because B is a hub and is likely to collect a higher payoff. On the other hand, when there is a link between A and B, B could imitate cooperator A at some point. To spread cooperation further now cooperator B needs cooperator neighbors in order to get a sufficiently high payoff. B could obtain this from common neighbors with A, which are more likely to be cooperators than the neighbors that are only connected to it and not to A. Therefore, having a direct connection between A and B is crucial for the dynamics to lead to high degrees of cooperation. This can be seen in the numerical results shown in Fig. 3.16 for the case in which A has a link to B (right part) and to the opposite case (left part). A certain number of shared neighbors between A and B seems to play an important role. Without them, there would be segregation of strategies, reflected in the average cooperation level in Fig. 3.15 (left) for 0 or a low number of common neighbors for the HD and the PD. As this number increases, however, cooperation may propagate from hub to hub. When the number of common neighbors becomes too high, around 13,

a cooperator hub is no longer favored as now his cooperator and defector neighbors will be about the same number.
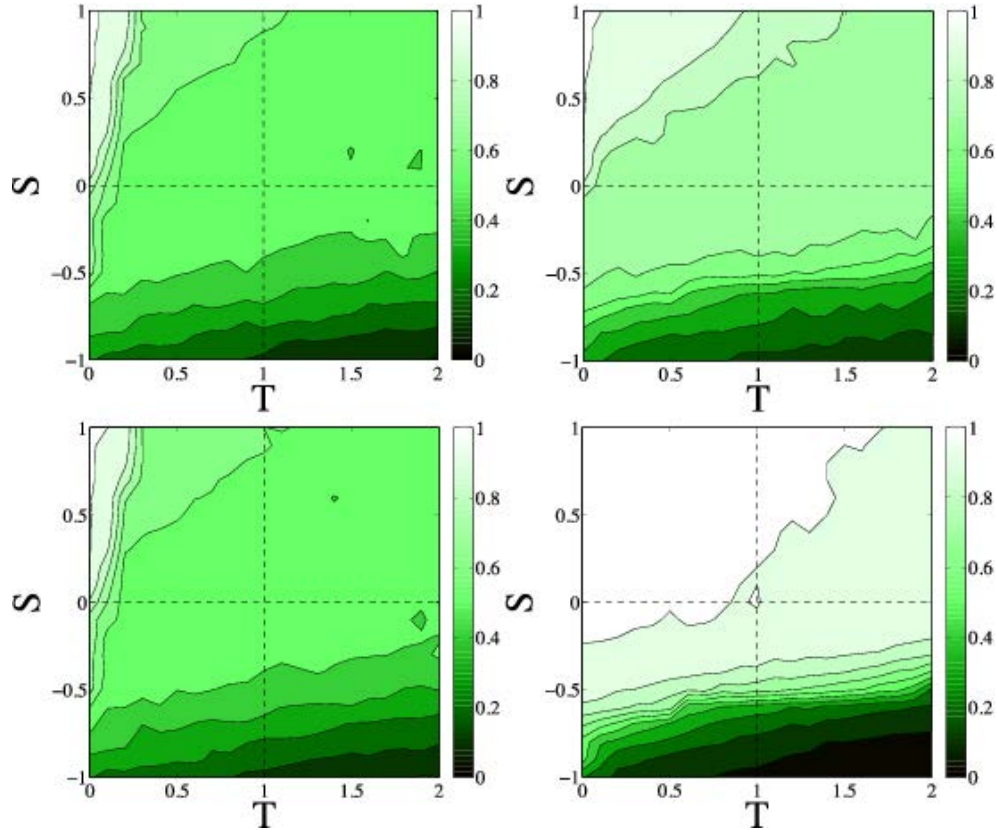
Fig. 3.16 (Color online) Average cooperation over 1000 repetitions of 500 time steps for 8 common neighbors without a link between A and B (left), and with a link between A and B (right) (see Fig. 3.15). Strategy update uses the replicator dynamics rule. Upper row: The initial strategy distribution is random; Lower row: The initial strategy distribution is random except for the hubs, one is set cooperator, the other defector.

It is worth noting that Perc et al. [16] with an apparently unrelated grid population model in which a fraction of players is more influential in the sense that they can transmit their strategy to others more easily, also obtain a high amount of cooperation in the weak PD game. For this to happen, it is also needed that, with a small probability a player can randomly link temporarily to distant sites in the lattice. When both features are present cooperation is boosted.

3.6 Discussion and Conclusions

Although weighted networks are closer to reality, evolutionary games on complex networks have been essentially studied on unweighted networks until now, both for simplicity as well as because weights in social networks are notoriously difficult to assess. In this article we introduced a new degree-weight correlation form in a model derived from three standard unweighted networks classes: BA graphs, the configuration model, and Erdös-Rényi random graphs. We studied the evolutionary game dynamics of standard two-person, two-strategies games on these classes of networks for which accurate results exist in the unweighted cases. A weight-degree correlation of the form $(k_i k_j)^\gamma$ had already been studied [4, 5], giving a small gain in cooperation for a restricted range of γ on BA networks. However, it has empirically been found that real social weights are not correlated to $k_i k_j$ [2, 14]. Thus in this work we used the perpendicular coordinate $|k_i^2 - k_j^2|$ in the weight-degree correlation $(|k_i^2 - k_j^2| + 1)^\gamma$ to study the proportion of cooperators at steady state on static weighted networks, and varying the weights from a more assortative case to a more disassortative case passing through the unweighted case. As γ increases toward disassortative weights, cooperation dramatically increases until a maximum of 0.6 averaged in the whole PD game phase space. And results are equally good for the HD and ST games, both for the replicator dynamics as well as for the Fermi rule. A small value of $\gamma > 0$ such as 0.5 or one is sufficient to induce unprecedented amounts of cooperation, and this remains true also for the linear correlation form $(|k_i - k_j| + 1)^\gamma$. The outcome at steady state depends on the initial conditions: starting from lower cooperation fractions induce less cooperation at steady state, which is also the case in the unweighted networks [19]. The best results were obtained for BA networks or random scale-free graphs, but even with Erdos-Rényi random graphs, which are known to induce little or no cooperation in the unweighted case [19], results are better, especially for the PD in which the amount of cooperation is comparable with the corresponding result for an unweighted BA graph. On the other hand, the assortative weights ($\gamma < 0$) are in general slightly detrimental to cooperation, except for the PD game where the increase is small anyway. Summing up, we can say that the main result in this part is that payoff-proportional imitation induces cooperation in a large part of the Prisoner's Dilemma with the given weights and $\gamma > 0$ on heterogeneous networks. The other games are positively affected as well.

In the second part of the present work we provided qualitative arguments for the emergence of large increases of cooperation in unweighted networks derived from the weighted ones. To this end, we proposed to filter out edges with low weight in the original network and to set all the remaining weights to 1. The cooperation level in those unweighted graphs, after removing isolated vertices, is similar or even higher than in the weighted networks. The features observed are: a bipolar distribution of degree (low degree and high degree vertices), degree disassortativity, low degree vertices are connected only to hubs while some connections between hubs may still exist for moderate γ, thus a nearly bipartite graph. Then, keeping only the necessary features, we constructed a small network which helps to intuitively understand the origins of the large increase in cooperation. We found that while low degree vertices surrounding hubs advantage cooperators, common

neighbors between hubs and direct links between hubs are important for the propagation of cooperation in the network.

A general consideration on the results we obtained is the following. We do not know whether the weighted networks, or the unweighted ones derived from them do really exist, at least in an approximate form. Ours is only an abstract model and weighted network data to perform empirical analyses are difficult to find. Nevertheless, in the future it would be interesting to study empirical degree-weight correlations in real-life network. If correlations of the type assumed in this work with $\gamma > 0$ could be found, then the corresponding networks would likely be favorable for cooperation in evolutionary games. Also, considering dynamical network evolution linked to a game [15], cooperative network similar to ours could emerge at steady state, because they maximize the number of satisfied players. Nevertheless, naturally occurring social networks do have a large amount of clustering, which is not the case in our filtered unweighted networks, but could be obtained on the weighted ones. Finally, the highly hierarchical cooperative unweighted structures found in this work could be created on purpose, if cooperation is the objective. This could be especially useful when the network nodes are not only persons but also organizations or institutions that happen to interact according to game rules similar to those used in the simulations.

Acknowledgments

References

[1] R. Albert and A.-L. Barabasi. Statistical mechanics of complex networks. *Reviews of Modern Physics*, 74:47–97, 2002.

[2] A. Barrat, M. Barthélemy, R. Pastor-Satorras, and A. Vespignani. The architecture of weighted complex networks. *Proc. Natl. Acad. Sci.*, 101(11):3747–3752, 2004.

[3] B. Bollobás. *Modern Graph Theory.* Springer,Berlin, Heidelberg, New York, 1998.

[4] P. Buesser, J. Peña, E. Pestelacci, and M. Tomassini. The influence of tie strength on evolutionary games on networks: An empirical investigation. *Physica A*, 2011. to appear.

[5] W.B. Du, H. R. Zheng, and M.B. Hu. Evolutionary prisoner's dilemma on weighted scale-free networks. *Physica A*, 387:3796–3800, 2008.

[6] J. Gómez-Gardeñes, M. Campillo, L. M. Floría, and Y. Moreno. Dynamical organization of cooperation in complex topologies. *Phys. Rev. Lett.*, 98:108103, 2007.

[7] C. Hauert and M. Doebeli. Spatial structure often inhibits the evolution of cooperation in the snowdrift game. *Nature*, 428:643–646, April 2004.

[8] J. Hofbauer and K. Sigmund. *Evolutionary Games and Population Dynamics*. Cambridge, N. Y., 1998.

[9] M. Molloy and B. Reed. A critical point for random graphs with a given degree sequence. *Random Structures and Algorithms*, 6:161, 1995.

[10] M. E. J. Newman. Scientific collaboration networks. II. shortest paths, weighted networks, and centrality. *Phys. Rev. E*, 64:016132, 2001.

[11] M. E. J. Newman. *Networks: An Introduction*. Oxford University Press, Oxford, UK, 2010.

[12] M. A. Nowak and R. M. May. Evolutionary games and spatial chaos. *Nature*, 359:826–829, October 1992.

[13] J.-P. Onnela, J. Saramäki, J. Hyvönen, G. Szabó, M. Argollo de Menezes, K. Kaski, A.-L. Barabási, and J. Kertész. Analysis of a large-scale weighted network of one-to-one human communication. *New Journal of Physics*, 9:179, 2007.

[14] J.-P. Onnela, J. Saramäki, J. Hyvönen, G. Szabó, D. Lazer, K. Kaski, J. Kertész, and A.-L. Barabási. The architecture of weighted complex networks. *Proc. Natl. Acad. Sci.*, 101(11):3747–3752, 2004.

[15] M. Perc and A. Szolnoki. Coevolutionary games - A mini review. *Biosystems*, 99:109–125, 2010.

[16] M. Perc, A. Szolnoki, and G. Szabó. Fluctuating epidemics on adaptive networks. *Phys. Rev. E*, 78:066101, 2008.

[17] J. Poncela, J. Gómez-Gardeñes, Y. Moreno, and L. M. Floría.

[18] J. Poncela, J. Gómez-Gardeñes, A. Traulsen, and Y. Moreno.

[19] C. P. Roca, J. A. Cuesta, and A. Sánchez. Evolutionary game theory: temporal and spatial effects beyond replicator dynamics. *Physics of Life Reviews*, 6:208–249, 2009.

[20] Z. Rong, X. Li, and X. Wang. Roles of mixing patterns in cooperation on a scale-free networked game. *Phys. Rev. E*, 76:027101, 2007.

[21] F. C. Santos and J. M. Pacheco. Scale-free networks provide a unifying framework for the emergence of cooperation. *Phys. Rev. Lett.*, 95:098104, 2005.

[22] F. C. Santos, J. M. Pacheco, and T. Lenaerts. Evolutionary dynamics of social dilemmas in structured heterogeneous populations. *Proc. Natl. Acad. Sci. USA*, 103:3490–3494, 2006.

[23] G. Szabó and G. Fáth. Evolutionary games on graphs. *Physics Reports*, 446:97–216, 2007.

[24] B. Voelkl and C. Kasper. Social structure of primate interaction networks facilitates the emergence of cooperation. *Biol. Lett.*, 5:462–464, 2009.

[25] J. W. Weibull. *Evolutionary Game Theory*. MIT Press, Boston, MA, 1995.

Chapter 4

Evolution of Cooperation on Spatially Embedded Networks

Abstract In this work we study the behavior of classical two-person, two-strategies evolutionary games on networks embedded in a Euclidean two-dimensional space with different kinds of degree distributions and topologies going from regular to random, and to scale-free ones. Using several imitative microscopic dynamics, we study the evolution of global cooperation on the above network classes and find that specific topologies having a hierarchical structure and an inhomogeneous degree distribution, such as Apollonian and grid-based networks, are very conducive to cooperation. Spatial scale-free networks are still good for cooperation but to a lesser degree. Both classes of networks enhance average cooperation in all games with respect to standard random geometric graphs and regular grids by shifting the boundaries between cooperative and defective regions. These findings might be useful in the design of interaction structures that maintain cooperation when the agents are constrained to live in physical two-dimensional space.

4.1 Introduction

In a strategic context, Game Theory is an "interactive decision theory" where an agent's optimal action for herself depends on expectations on the actions of other agents - including herself [18]. This approach has proved very useful in a number of settings in biology, economy, and social science. Evolutionary game theory in particular is well suited to the study of strategic interactions in animal and human populations that are large and well-mixed in the sense that any agent can interact with any other agent in the population (see e.g. [14, 32, 33]). However, lattice-structured populations were used starting with the works of Axelrod on the repeated Prisoner's Dilemma [6] and of Nowak and May on the one-shot case [21]. Especially in the last few years, population structures with local interactions have been brought to the focus of research as it is known that social interactions can be better represented by networks of contacts in which nodes represent agents and links stand for their relationships. This literature is already rather abundant and it is difficult to be exhaustive; good recent reviews can be found in [24, 25, 29] and important foundational work dealing with the microscopic agent dynamics appears, among others, in [2, 23, 31, 34]. Most of the recent work has dealt with populations of agents structured as non-spatial graphs (relational graphs), i.e. networks in which there is no underlying spatial structure

and distances are measured in terms of edge hops. Relational networks are adequate in many cases; for instance, when two people have a connection in Facebook, for the purposes of the electronic communication, their actual physical distance is irrelevant, although many links in the network will be related to closeness in space. However, often it is the case that actual distances matter; for example, networks such as the road or the railway networks are of this type. Thus, while the recent focus in complex network research has been mainly on relational graphs, spatial graphs are also very important and have attracted attention (see [7] for an excellent recent review).

In evolutionary games regular graphs such as one- and two-dimensional lattices have been used early on to provide a local structure to the population of interacting agents [6, 21]. These networks can be considered relational for certain purposes but can also be trivially embedded in some low-dimensional Euclidean space, with the associated distance metric. Practically the totality of the work on spatial evolutionary games has been done on this kind of structure and a large literature has been produced (for a summary with references to previous work see [22]). To the best of our knowledge, only few works have dealt with spatial networks other than grids in games e.g. [16, 35]. In [16] geometric random graphs, which are Euclidean graphs built by drawing links between nodes that are within a given distance, and spatially embedded Watts–Strogatz networks are used in connection with the Naming Game. Ref. [35] deals with games on Apollonian networks, which can be viewed as Euclidean networks that can be built by recursively joining a new node in the interior of a triangle with the nodes at its vertices. This kind of graphs will be referred to later in the present work. Clearly, grids are only an approximation to actual spatial graphs representing networks of contacts in the physical world [7].

In the present work we extend the ideas and methods of evolutionary game theory to fixed spatial networks that go beyond the much-studied discrete two-dimensional lattices. Previous results show that networks with heterogeneous degree distributions increase cooperation in the Hawks-Dowes games, while regular lattices increase cooperation in the Stag-Hunt games [25, 27, 28]. Therefore we study spatial network models with a scale-free degree distribution as a first step. In a second part, by extending a previous work [35], we show that Apollonian networks [3] are such that both the benefits of spatiality and scale-free degree distribution can be gathered. Some previous works use reduced game spaces. As these settings are not suitable for our discussion, we extend them to a larger game space. Mobility (see e.g. [13, 17]) is an important issue in these spatial networks but, as an obvious first step, here we shall deal only with static networks. Our exploratory approach is based on numerical Monte Carlo simulations since an exact analytical description is essentially only possible in the mean-field case.

4.2 Evolutionary Games on Networks

4.2.1 The Games Studied

We investigate three classical two-person, two-strategy, symmetric games classes, namely the Prisoner's Dilemma (PD), the Hawk-Dove Game (HD), and the Stag Hunt (SH).

These three games are simple metaphors for different kinds of dilemmas that arise when individual and social interests collide. The Harmony game (H) is included for completeness but it doesn't originate any conflict. The main features of these games are summarized here for completeness; more detailed accounts can be found elsewhere e.g. [14, 32, 33]. The games have the generic payoff matrix M (equation 8.1) which refers to the payoffs of the row player. The payoff matrix for the column player is simply the transpose $M^\top$ since the game is symmetric.

$$
\begin{array}{cc}
 & \begin{array}{cc} C & D \end{array} \\
\begin{array}{c} C \\ D \end{array} & \begin{pmatrix} R & S \\ T & P \end{pmatrix}
\end{array}
\tag{4.1}
$$

The set of strategies is $\Lambda = \{C, D\}$, where C stands for "cooperation" and D means "defection". In the payoff matrix R stands for the *reward* the two players receive if they both cooperate, P is the *punishment* if they both defect, and T is the *temptation*, i.e. the payoff that a player receives if he defects while the other cooperates getting the *sucker's payoff* S. In order to study the usual standard parameter space [25, 28], we restrict the payoff values in the following way: $R = 1$, $P = 0$, $-1 \leq S \leq 1$, and $0 \leq T \leq 2$.

For the PD, the payoff values are ordered such that $T > R > P > S$. Defection is always the best rational individual choice, so that (D, D) is the unique Nash Equilibrium (NE) and also the only fixed point of the replicator dynamics [14, 33]. Mutual cooperation would be socially preferable but C is strongly dominated by D.

In the HD game, the order of P and S is reversed, yielding $T > R > S > P$. Thus, when both players defect they each get the lowest payoff. Players have a strong incentive to play D, which is harmful for both parties if the outcome produced happens to be (D, D). (C, D) and (D, C) are NE of the game in pure strategies. There is a third equilibrium in mixed strategies which is the only dynamically stable equilibrium [14, 33].

In the SH game, the ordering is $R > T > P > S$, which means that mutual cooperation (C, C) is the best outcome, Pareto-superior, and a NE. Pareto-superior means that the equilibrium is a set of strategies, one for each player, such that there is no other strategy profile in which all players receive payoffs at least as high, and at least one player receives a strictly higher payoff. The second NE, where both players defect is less efficient but also less risky. The tension is represented by the fact that the socially preferable coordinated equilibrium (C, C) might be missed for "fear" that the other player will play D instead. The third mixed-strategy NE in the game is evolutionarily unstable [14, 33].

Finally, in the H game $R > S > T > P$ or $R > T > S > P$. In this case C strongly dominates D and the trivial unique NE is (C, C). The game is non-conflictual by definition and does not cause any dilemma, it is mentioned to complete the quadrants of the parameter space.

In the TS-plane each game class corresponds to a different quadrant depending on the above ordering of the payoffs as depicted in Fig 4.1, left image, and the figures that follow. We finally remark that a rigorous study of the evolutionary dynamics of 2×2 matrix games in finite mixing populations has been published by Antal and Scheuring [4].

4.2.2 Population Structure

The population of players is a connected undirected graph $G(V, E)$, where the set of vertices V represents the agents, while the set of edges E represents their symmetric interactions. The population size N is the cardinality of V. The set of neighbors V_i of an agent i are the agents that are directly connected to i; the cardinality $|V_i|$ is the degree k_i of vertex $i \in V$. The average degree of the network is called $\langle k \rangle$, and $p(k)$ is the network's degree distribution function.

4.2.3 Payoff Calculation and Strategy Update Rules

We need to specify how individual's payoffs are computed and how agents decide to revise their current strategy, taking into account that each agent only interacts locally with its first neighbors, not globally as in well mixed populations. Let $\sigma_i(t)$ be a vector giving the strategy profile at time t with $C = (1, 0)$ and $D = (0, 1)$ and let M be the payoff matrix of the game (equation 8.1). The quantity

$$\Pi_i(t) = \sum_{j \in V_i} \sigma_i(t) \ M \ \sigma_j^\top(t) \tag{4.2}$$

is the cumulated payoff collected by player i at time step t.

   We use an asynchronous scheme for strategy update, i.e. players are updated one by one by choosing a random player in each step. Several strategy update rules are customary in evolutionary game theory. Here we shall describe the four imitative update protocols that have been used in our simulations. The first three are well known; we thank an anonymous reviewer for suggesting a rule very similar to the fourth one presented here.
The *local fitness-proportional* rule is stochastic and gives rise to replicator dynamics (RD) [11, 12]. Player i's strategy σ_i is updated by randomly drawing another player j from the neighborhood V_i, and replacing σ_i by σ_j with probability:

$$p(\sigma_i \to \sigma_j) = \begin{cases} (\Pi_j - \Pi_i)/K & \text{if } \Pi_j > \Pi_i \\ 0 & \text{if } \Pi_j \leq \Pi_i \end{cases} \tag{4.3}$$

where $\Pi_j - \Pi_i$ is the difference of the payoffs earned by j and i respectively. $K = \max(k_i, k_j)[(\max(1, T) - \min(0, S)]$ ensures proper normalization of the probability $p(\sigma_i \to \sigma_j)$. This normalization increase the frequency of imitations between nodes with smaller degree. A more flexible update rule without the problem of normalization is the *Fermi* rule. Here the randomly chosen player i is given the opportunity to imitate a randomly chosen neighbor j with probability :

$$p(\sigma_i \to \sigma_j) = \frac{1}{1 + exp(-\beta(\Pi_j - \Pi_i))} \tag{4.4}$$

where β is a constant corresponding to the inverse temperature of the system, i.e. high temperature implies that imitation is random to a large extent and depends little on the payoffs. Thus when $\beta \to 0$ the probability of imitating j tends to a constant value 0.5

and when $\beta \to \infty$ the rule becomes deterministic: i imitates j if $(\Pi_j - \Pi_i) > 0$, otherwise it doesn't. For $\beta \subset [1.0, 10.0]$ the rule leads approximatively to similar results as the *local fitness-proportional* one. Another imitative strategy update protocol is to switch to the strategy of the neighbor that has scored best in the last time step. In contrast with the previous one, this rule is deterministic. This *imitation of the best* (IB) policy can be described in the following way: the strategy $s_i(t)$ of individual i at time step t will be

$$s_i(t) = s_j(t-1), \tag{4.5}$$

where

$$j \in \{V_i \cup i\} \ s.t. \ \Pi_j = \max\{\Pi_k(t-1)\}, \ \forall k \in \{V_i \cup i\}. \tag{4.6}$$

That is, individual i will adopt the strategy of the player with the highest payoff among its neighbors including itself. If there is a tie, the winner individual is chosen uniformly at random. The next update rule is a randomized version of the imitation of the best that we call IBR. Here player i imitates a neighbor j with probability given by formula 4.3. The constant K appearing in formula 4.3 is such that $\sum_{j \in V_i} p_{ij} = 1$.

A final remark is in order here. The above model rules are common and almost standard in numerical simulation work, which has the advantage that the mathematics is simpler and results can be compared with previous work such as, for instance, [25, 28]. However, it is far from clear whether these rules are representative of the ways in which human players actually take their strategic decisions, as has been shown by many laboratory experiments. In these experiments it seems that learning and heuristics play an important role. Moreover, players are inhomogeneous in their behavior while our stereotyped automata all behave in the same way and never change or adapt. Some less conventional work along these lines can be found in [9, 30]. In Cardillo et al. [9] standard strategy update rules are used but they are permitted to co-evolve with the agent's strategies. In Szolnoki et al. [30], rather than imitating strategies, agents imitate a proxy that stands for emotions among their neighbors.

4.2.4 Simulation Parameters

The TS-plane has been sampled with a grid step of 0.1 and each value in the phase space reported in the figures is the average of 50 independent runs using a fresh graph realization for each run, except for strictly regular or degree-invariant networks. The evolution proceeds by first initializing the players at the nodes of the network with one of the two strategies uniformly at random such that each strategy has a fraction of approximately 1/2 unless otherwise stated. For each grid point, agents in the population are chosen sequentially at random to revise their strategies (asynchronous updating). Payoffs are updated after each strategy change. We let the system evolve for a period of $2 * N$ time steps. At this point the system has reached a steady state in which the frequency of cooperators is stable except for small fluctuations. We then let the system evolve for 300 further steps and take the average cooperation value in this interval. We repeat the whole process 50 times for each grid point and, finally, we report the average cooperation values over those 50 repetitions.

4.3 Results

In the following sections we investigate how spatiality affects cooperation through its effect on network topology. In section 4.3.1 we study a class of spatial scale-free networks, and in section 4.3.2 we study Apollonian networks, a different model of spatial scale-free network leading to high levels of cooperation. Spatial scale-free networks and Apollonian networks combine spatiality and scale-free degree distribution. In section 4.3.3 we propose a class of hierarchical spatial networks derived from lattices and random geometric graphs which also improve cooperation.
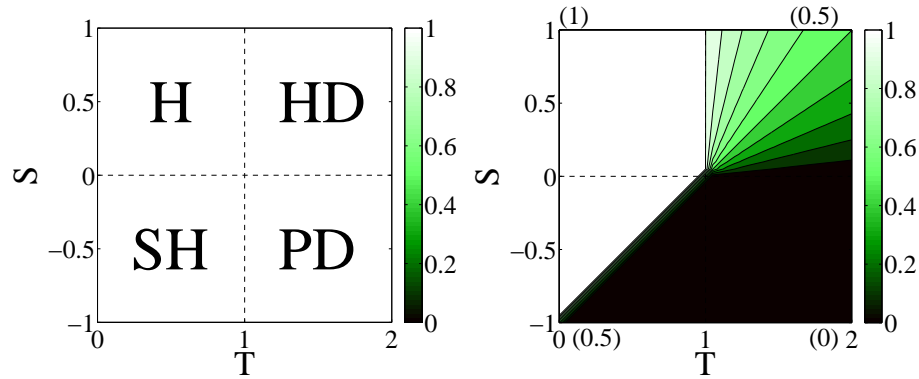
Fig. 4.1 (Color online) Left image: The games phase space (H= Harmony, HD = Hawk-Dove, PD = Prisoner's Dilemma, and SH = Stag Hunt). Right image: Average cooperation over 50 runs at steady state in a well mixed population (right image). The initial fraction of cooperators is 0.5 randomly distributed among the graph nodes and the update rule is imitation proportional to the payoff. Lighter tones stand for more cooperation. Figures in parentheses next to each quadrant indicate average cooperation in the corresponding game space.

Fig. 4.2 (Color online) Average cooperation over 50 runs at steady state in BA networks. Network size is $N = 10000$, $\langle k \rangle = 8$. The initial fraction of cooperators is 0.5 randomly distributed among the graph nodes. Lighter tones stand for more cooperation. The update rule is imitation proportional to the payoff (left image), imitation of the best (middle image), randomized imitation of the best (right image).
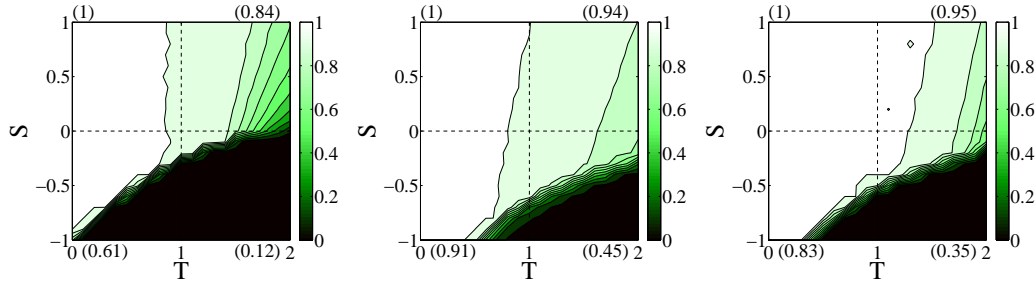
Fig. 4.3 (Color online) Average cooperation over 50 runs at steady state on the configuration model with exponent $\gamma = 3.0$, with $N = 10000$, and $\langle k \rangle = 8.0$. The initial fraction of cooperators is 0.5 randomly distributed among the graph nodes. The update rule is imitation proportional to the payoff (left image), imitation of the best (middle image), randomized imitation of the best (right image).

Fig. 4.4 (Color online) Average cooperation over 50 runs at steady state in a regular lattice, the size is $N = 10000$, $\langle k \rangle = 8$. The initial fraction of cooperators is 0.5 randomly distributed among the graph nodes. Figures in parentheses next to each quadrant indicate average cooperation in the corresponding game space. The update rule is imitation proportional to the payoff (left image), imitation of the best (middle image), randomized imitation of the best (right image).

4.3.1 Spatial Scale-Free Networks

The right image of Fig. 4.1 shows cooperation in the well-mixed population case as a baseline to which we refer when evaluating the amount of cooperation that evolves in network-structured populations. Scale-free networks, such as the Barabási–Albert (BA) [1] and the configuration model (CF) [19], are known to induce high levels of cooperation in HD games and also improve cooperation in the PD and the SH [25, 28]. Results on these topologies are shown for future reference in Figs. 4.2 and 4.3. On the other hand, spatial grids induce high levels of cooperation in SH games but not in PD games, and they reduce the levels of cooperation in the HD games as compared to the well-mixed case [25],

see Fig. 4.4. In order to understand how cooperation is affected by the combination of spatiality and heterogeneous degree distribution, we used a spatial network model with a given degree distribution. Our construction is inspired by the one given by Rozenfeld et al. [26] and only differs from the latter in the way in which a given node looks for its k neighbors. We start from a given sequence of target degrees $\{k_1, k_2, \ldots, k_N\}$ and we place the N nodes in a regular lattice as in [26]. However, instead of selecting the nearest neighbors of a given node, the neighbors of a node are chosen in the following way. For each of the k edges of a node we perform a random walk on the underlying lattice starting from this node until we find a free neighbor whose effective degree is less than its target degree and we create a link to that node. The process is halted when the effective degree of the considered node is equal to the target degree. Since it is possible that a node has already cumulated edges up to its target degree, we fix a maximum $m = N$ for the number of random walk steps for the construction of one edge. We used a scale-free distribution $p(k) \propto k^{-\gamma}$ with exponent $\gamma \in \{2.0, 3.0, 4.0\}$. In order to keep a constant mean degree $\langle k \rangle = 8$, the lower bound of the scale-free degree sequence was shifted. Thus, as γ increases the distribution becomes more peaked around $\langle k \rangle$. The network model just described, called SFSN, gives very similar results on cooperation as the one of Rozenfeld et al.; thus we show only those concerning our model.
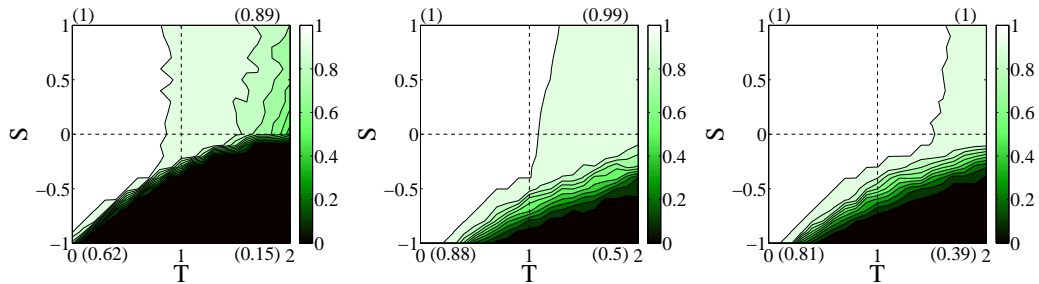

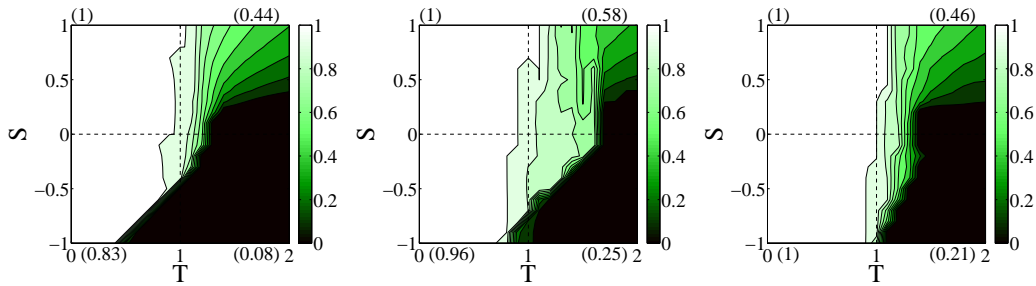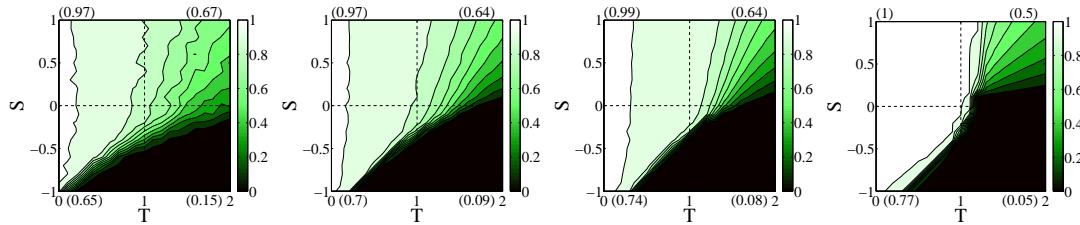**Fig. 4.5** (Color online) Average cooperation over 50 runs at steady state on SFSN networks (see text). Size is $N = 10000$, $\langle k \rangle = 8$ and $\gamma = 2.0$ (first image), 3.0 (second image), and 4.0 (third image). The fourth image corresponds to random geometric graphs with $\langle k \rangle = 20$. The initial fraction of cooperators is 0.5 randomly distributed among the graph nodes and the update rule is imitation proportional to the payoff.

For comparison purposes, and by analogy with Erdös-Rényi random graphs [20] in relational networks, we take as a spatial baseline case the random geometric graph (RGG). Random geometric graphs are constructed as follows [7, 10]. N nodes are placed randomly on a subset of $\mathbb{R}^n$; then two nodes are linked if their distance is less than a constant r. The resulting graph has a binomial degree distribution which tends to a Poisson degree distribution as $N \to \infty$ and $r \to 0$ [7, 10], with $\langle k \rangle = Nq(r)$ and $q(r) = \pi r^2/S$, for $n = 2$, is the probability that a node is in a disk of radius r. S is the total surface.

Average cooperation on SFSNs with RD and IB update rules for $\gamma = 2.0, 3.0, 4.0$ are shown in Figs. 4.5 and 4.6. The first remark is that spatial scale-free networks are slightly less conducive to cooperation than the corresponding BA and CF relational networks. This can be seen by comparing the first images of Fig. 4.2 and Fig. 4.3, which corresponds to the BA and CF cases, with the second image of Fig. 4.5 which refers to SFNSs with $\gamma = 3$.
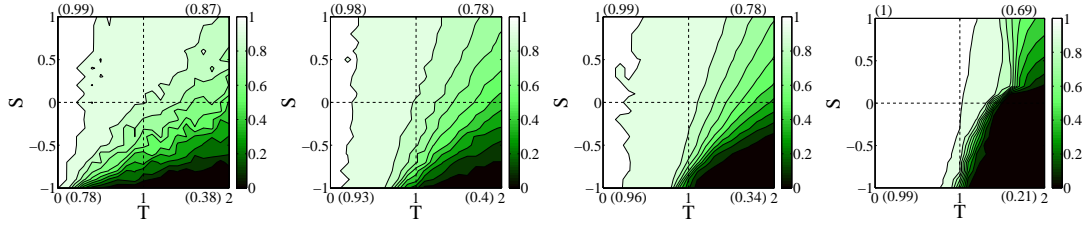
Fig. 4.6 (Color online) Average cooperation over 50 runs at steady state on SFSN networks with imitation of the best update rule. Size is $N = 10000$, $\langle k \rangle = 8$ and $\gamma = 2.0$ (first image), 3.0 (second image), 4.0 (third image). The fourth image corresponds to random geometric graphs with $\langle k \rangle = 20$. The initial fraction of cooperators is 0.5 randomly distributed among the graph nodes.

Nevertheless, it can be seen that SFNSs do favor cooperation especially in the HD and the PD space with respect to the RGG case depicted in Fig. 4.5, rightmost image. It can also be observed that the gains in the transition between cooperation and defection that is apparent in the SH games with increasing γ, are partially offset for low γ. The comparison with the RGG case (rightmost image) shows that cooperation levels tend to those of the random graph case with increasing γ, except for the HD quadrant where the RGG topology causes some cooperation loss. As in non-spatial networks [25], the imitation of the best neighbor strategy update rule is more noisy and gives rise, in general, to somewhat higher levels of cooperation. Results with IBR rule are similar to those with IB and are not presented.

4.3.2 Apollonian Networks: A Spatial Scale-Free Model with Higher Cooperation

An interesting case of scale-free spatial networks are the Apollonian networks (AN) [3] for which we show in this section that they lead to high levels of cooperation. Apollonian networks are constructed by linking adjacent circles in Apollonian packings. In the simplest case, an Apollonian packing is built by starting from three tangent circles, adding a smaller circle tangent to the three previous ones, and iterating the process for each new hole between three circles (see Fig. 4.7 and [3]). Our sample Apollonian networks have been obtained in this way after nine iterations and are of size $N = 9844$ nodes. AN belong to a class of networks that are scale-free, small-world, planar and embedded in Euclidean space. The degree-distribution exponent is $\gamma = 2.585$ and the clustering coefficient $C_{cl} = 0.83$ [3].

In a recent work, Yang et al. [35] have shown that Apollonian networks foster cooperation on the weak prisoner's dilemma ($R = 1, P = 0, S = 0, T \in [0,3]$) using update proportional to payoff. The space covered is thus just the segment at the frontier between HD and PD. Here, with the aim of extending the scope of the study, we sample the full ST-plane. Our results are summarized in Fig. 4.8. They show that the AN topology is more conducive to cooperation than SFNS and BA networks in the HD games, but also in the SH games, by shifting to the right the transition from cooperation to defection at
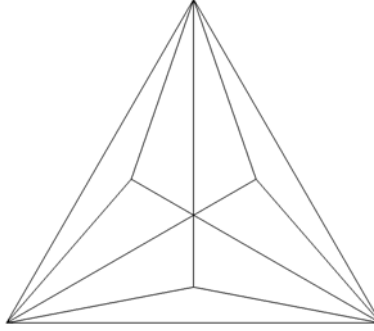
Fig. 4.7 (Color online)Apollonian network after two generations (see text).
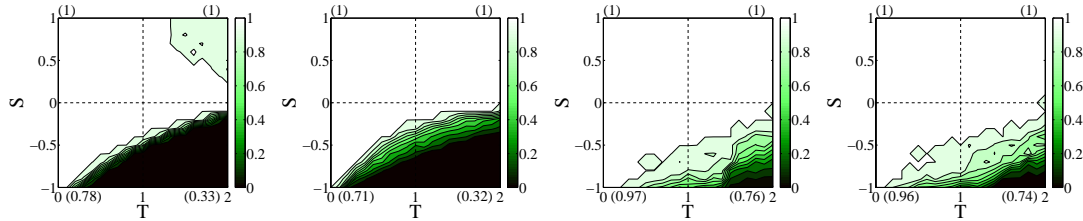
Fig. 4.8 (Color online) Average cooperation over 50 runs at steady state on the Apollonian network of size $N = 9844$, and $\langle k \rangle \simeq 6.0$. The initial fraction of cooperators is 0.5 randomly distributed among the graph nodes. From left to right the strategy update rules are: replicator dynamics, Fermi rule, imitation of the best, and probabilistic imitation of the best.

$S = -1$, as in other spatial networks. However, the amount of cooperation gain depends on the strategy update rule. Replicator dynamics and the Fermi rule (first and second image from the left respectively) have a similar behavior, and are also analytically close (if the exponent β of the Fermi rule is between 1 and 10). On the other hand, the rule that prescribes straight imitation of the best (third image), and the rule that imitates the best neighbor probabilistically (rightmost image) perform better. Intuitively, the first two rules choose a very good neighbor to imitate less often than the latter two, especially when compared with deterministic imitation of the best. This could favor the latter rules in an Apollonian network when some cooperators surrounded by a majority of cooperators have gained a foothold on several hubs.

In [35], the authors discuss the topology features that induce the high cooperation levels. They point out, beside other facts, the presence of connections between hubs and that there exist nodes with high g_i and U_i, g_i being the degree gradient between a node i and its neighbors $\{V_i\}$, $g_i = \sqrt{\frac{1}{k_i} \sum_{j \in V_i} (k_i - k_j)^2}$ and $U_i = k_i * g_i$. By transforming the network they show that these features are linked to high levels of cooperation. They point out the high clustering coefficient and explain that clustering increases cooperation on the reduced PD games as shown in [5].

4.3.3 High Levels of Cooperation on Lattice and Derived Structures

Simple hierarchical networks were shown to be favorable to cooperation by using a rigorous stochastic process of the Moran type by Lieberman et al. [15]. In [8] we showed how to construct relational hierarchical networks that induce high levels of cooperation. By analogy with the latter work, in this section we construct a lattice embedded in two-dimensional space with a similar local structure and obtain high levels of cooperation. This model shows that space along with some specific constraints creates such cooperative topologies. We first place the nodes on a regular square lattice and label them according to their integer coordinates (i, j). Each node with coordinates such that $i \bmod 4 = r$ and $j \bmod 4 = 2r$ is a "hub" of radius r which is connected to all "small nodes" in a square neighborhood of side $2 * r + 1$ and to the four closest hubs. This topology models a situation where there exist two kinds of nodes distributed in space. One kind (vertices with few connections) tries to make undirected connections to the other kind (hubs) while minimizing distances. Low-degree nodes have connections to hubs only. The hubs, in turn, form a lattice in which they are connected to the closest hubs. In Fig. 4.9 we show such a graph with $r = 2$. Cooperation levels are very good in all games and for all the strategy revision rules, as seen in Fig. 4.10. Indeed, the cooperation enhancement goes beyond the best levels found in relational networks as can be seen by comparing Fig. 4.10 with Fig. 4.2, which refers to BA networks.
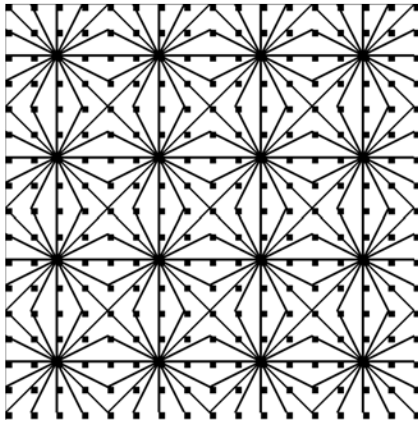
Fig. 4.9 (Color online) Lattice topology with two kind of nodes. Each hub is fully connected to a square neighborhood of side 5 and to the 4 nearest hubs.

Starting from random geometric graphs with arbitrary radius distribution, in the limiting case where there are two different kinds of nodes, we show how a network with similar properties to those of the above lattice can emerge by using the RGG model. We constructed random geometric graphs in the same way as explained in Sect. 4.3.1, except that two nodes are linked if the sum of their radii is larger than their mutual distance. In Fig. 4.11 (left) we used the following distribution of radius: 1/16 of the population has an arbitrary radius r and the other vertices have a null radius. The undirected resulting
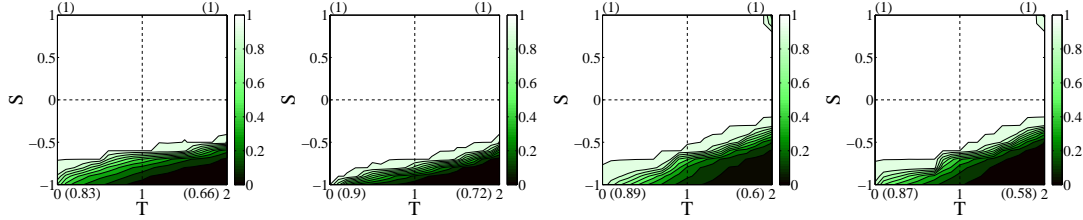
Fig. 4.10 (Color online) Average cooperation levels on the lattice. The size of the graph is 10000 nodes. From left to right the strategy update rules are: replicator dynamics, Fermi rule, imitation of the best, and probabilistic imitation of the best. In all cases the initial fraction of cooperators is 0.5 randomly distributed among the graph nodes.
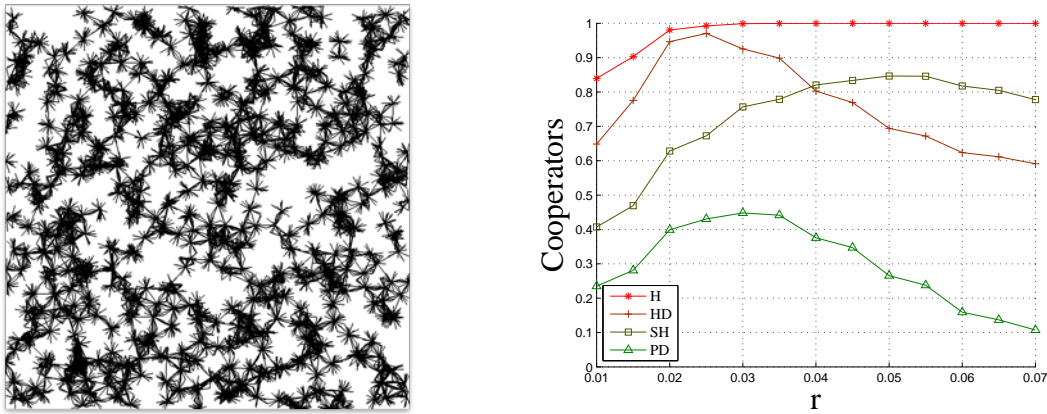
Fig. 4.11 (Color online) Left : an instance of a random geometric graph with two kinds of nodes and $r = 0.03$. Right: Average cooperation levels on an ensemble of these graphs as a function of the hubs radius; the frequency of hubs is 1/16, and the radius of small vertices is null. The update rule is imitation proportional to payoff and the initial fraction of cooperators is 0.5 randomly distributed among the graph nodes. In both images isolated vertices were discarded.

network is composed of hubs mainly connected to low-degree vertices, which in turn are not connected among themselves. The low-degree vertices which are not connected to any hubs are isolated. In order to focus on the interesting part of the network, we discarded them, taking into account that they cannot change their initially attributed strategies. Fig. 4.11 (right) shows that cooperation is greatly enhanced for a sizable range of radius r, although it doesn't reach the exceptional levels of the lattice. The shape of the curves can be qualitatively understood noting that, when r is small, say less than 0.015, the hubs have few connections between themselves and the network becomes fragmented into small clusters. On the other hand, when r is large, the mechanism leading to cooperation explained in detail in [8] doesn't work anymore. Now low-degree vertices may be connected to several hubs. This fact weakens the probability for defector hub to imitate the strategy of a high payoff cooperator hub, since cooperator hubs are no longer surrounded by low-degree cooperators.

4.3.4 Network Type and Assortativity of Strategies

A potentially interesting question concerns the way in which strategies are distributed at steady-state among the network nodes. At the beginning the distribution is uniform random but during the dynamics it typically evolves and its final state could be different in different network types, according to the game played. This effect can be evaluated by using several measures of "similarity" between vertices. Here we have chosen a measure that is inspired by Newman's work on assortativity in networks [20] [1]. A state will be called "assortative" if cooperators tend to be surrounded by coperators and defectors by defectors. It will be called "disassortative" in the opposite case, and there will be an absence of correlations between strategies if the distribution is random.
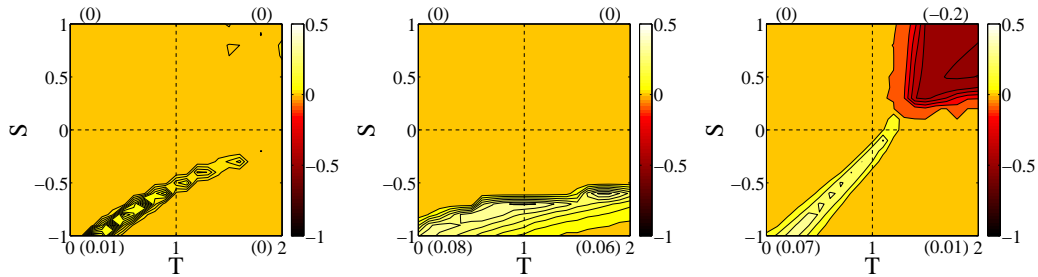
Fig. 4.12 (Color online) Average strategy assortativity levels with the replicator dynamics on the Apollonian network (left image), cooperative grid (middle image), and the regular geometric graph with $\langle k \rangle = 8$ (right image). In all cases the initial fraction of cooperators is 0.5 randomly distributed among the graph nodes.

In Figs. 4.12 we report the results of our assortativity analysis for Apollonian networks (left), the spatial cooperative grid defined at the beginning of sect. 4.3.3 (middle), and for RRGs (right). The first thing to notice is that strategy disassortativity is only present in the RGG for the HD quadrant, as the HD stable equilibrium in well-mixed populations, and also partly in random graphs, consists of a mix of Cs and Ds. Now, due to the HD payoff structure, locally a cooperator tends to be surrounded by defectors and the other way around for a defector. On the other hand, in the middle and left images, in the HD space assortativity disappears because now the corresponding game phase space becomes totally cooperative (compare with the leftmost images of Figs. 4.8 and 4.10). For the SH there is an increase in cooperation too going from the RGG to Apollonian, and especially the lattice. The SH game features two monomorphic stable equilibria in well-mixed populations which explains why assortativity is near zero in most of the quadrant. Nevertheless, in the unstable middle and low region C and D can coexist thanks to the local network structure that allows clusters to form. But here, contrary to the HD, the strategies show some positive assortativity since it is best for players to coordinate on

[1] To calculate the mean assortativity of a player at steady-state, we take the frequency of neighbors having the same strategy and we compute the mean over the whole network. Then we subtract the same quantity assuming that the strategies are randomly distributed in the same network

the same action. In Fig. 4.12 we observe that this assortative region bends downwards and extends to the right in the left and middle image with respect to the RGG case (right image). This region extends to the PD phase space in the two highly cooperative networks.

4.4 Discussion and Conclusions

Evolutionary games on static spatial networks have been intensively studied in the past but mainly on two-dimensional regular lattices, either taking into account Euclidean distances explicitly or implicitly, as they can be trivially embedded in a metric space. However, lattices are only an approximation of actual network of contacts in geographical space. Indeed, many economic, transportation, and communication systems rely on actual positions in space and agents usually have a variable number of neighbors. For this reason, here we have studied typical two-person, two-strategies evolutionary games on spatial networks having homogeneous degree distributions such as geometric random graphs, as well as heterogeneous ones with right-skewed degree distributions such as scale-free networks. We have studied evolutionary games on two spatial scale-free networks models: a first one based on a variant of Rozenfeld et al.'s construction [26] called SFSN, and the Apollonian networks [3]. Concerning the second model, we extended previous results to a much larger parameter's space, allowing to discuss our results more accurately. We find that cooperation is promoted on spatial scale-free networks with respect to the random geometric graphs, except in the Stag-Hunt games. Now if we compare SFSNs with BA relational networks, SFSNs show the same trend but the gains are lower with all dynamics. Still, this is an interesting results since SFSNs are important in practice, for example in ad hoc communication networks. On Apollonian networks cooperation is the highest ever observed on networks of the scale-free type in all the games studied here, although Apollonian networks would be difficult to reproduce in practice. We also point out that these results are robust with respect to the several standard strategy update rules used in our simulations.

Finally, we have introduced a two-dimensional hierarchical net whose structure has been inspired by a previous relational graph model which highly promotes cooperation [8]. On this particular spatial network cooperation reaches the highest values, with 66% of the population being cooperators in the average in the PD, the totality in the HD, and 83% in the SH with the local fitness-proportional rule and the Fermi rule. IB and IBR give similar figures. Of course, these unprecedented cooperation levels are theoretically interesting but can only be actually reached if the special network can be formed and kept fixed, since naturally formed networks could hardly take this shape. However, using similar ideas, we have shown that more realistic networks can be produced that can attain a rather high level of cooperation using a modified construction starting from random geometric graphs.

The general conclusion of this work is that promotion of cooperation in all the games' parameter space is possible on static networks of agents constrained to act in geographical space, provided that agents interact according to some special spatial network of contacts that creates a connection hierarchy among the agents.

Acknowledgments

We thank the anonymous reviewers for their detailed and insightful remarks that helped to improve the manuscript.

References

[1] R. Albert and A.-L. Barabási. Statistical mechanics of complex networks. *Reviews of Modern Physics*, 74:47–97, 2002.

[2] P.M. Altrock and A. Traulsen. Fixation times in evolutionary games under weak selection. *New Journal of Physics*, 11(1):013012, 2009.

[3] J. S. Andrade, H. J. Herrmann, R. F. S. Andrade, and L. R. da Silva. Apollonian networks: Simultaneously scale-free, small world, euclidean, space filling, and with matching graphs. *Phys. Rev. Lett.*, 94:018702, 2005.

[4] T. Antal and I. Scheuring. Fixation of strategies for an evolutionary game in finite populations. *Bull. Math. Biol.*, 68:1923–1944, 2006.

[5] S. Assenza, J. Gómez-Gardeñes, and Vito Latora. Enhancement of cooperation in highly clustered scale-free networks. *Phys. Rev. E*, 78:017101, 2008.

[6] R. Axelrod. *The Evolution of Cooperation*. Basic Books, Inc., New-York, 1984.

[7] M. Barthélemy. Spatial networks. *Physics Reports*, 499:1–101, 2011.

[8] P. Buesser and M. Tomassini. Supercooperation in evolutionary games on correlated weighted networks. *Phys. Rev. E*, 85:016107, 2012.

[9] A. Cardillo, J. Gómez-Gardeñes, D. Vilone, and A. Sánchez. Co-evolution of strategies and update rules in the prisoner's dilemma game on complex networks. *New Journal of Physics*, 12(10):103034, 2010.

[10] J. Dall and M. Christensen. Random geometric graphs. *Phys. Rev. E*, 66:016121, 2002.

[11] C. Hauert and M. Doebeli. Spatial structure often inhibits the evolution of cooperation in the snowdrift game. *Nature*, 428:643–646, April 2004.

[12] D. Helbing. Interrelations between stochastic equations for systems with pair interactions. *Physica A*, 181:29–52, 1992.

[13] D. Helbing and W. Yu. Migration as a mechanism to promote cooperation. *Advances in Complex Systems*, 11:641–652, 2008.

[14] J. Hofbauer and K. Sigmund. *Evolutionary Games and Population Dynamics*. Cambridge, N. Y., 1998.

[15] E. Lieberman, C. Hauert, and M. A. Nowak. Evolutionary dynamics on graphs. *Nature*, 433:312–316, 2005.

[16] Q. Lu, G. Kormiss, and B. K. Szymanski. Naming games in two-dimensional and small-world-connected random geometric networks. *Phys. Rev. E*, 77:016111, 2008.

[17] S. Meloni, A. Buscarino, L. Fortuna, M. Frasca, J. Gómez-Gardeñes, V. Latora, and Y. Moreno. Effects of mobility in a population of prisoner's dilemma players. *Phys. Rev. E*, 79:067101, 2009.

[18] R. B. Myerson. *Game Theory*. Harvard University Press, Cambridge, MA, 1991.

[19] M. Newman, S. Strogatz, and D. Watts. Random graphs with arbitrary degree distributions and their applications. *Phys. Rev. E*, 64:026118, 2001.

[20] M. E. J. Newman. *Networks: An Introduction*. Oxford University Press, Oxford, UK, 2010.

[21] M. A. Nowak and R. M. May. Evolutionary games and spatial chaos. *Nature*, 359:826–829, October 1992.

[22] M. A. Nowak and K. Sigmund. Games on grids. In U. Dieckmann, R. Law, and J. A. J. Metz, editors, *The Geometry of Ecological Interactions: Simplifying Spatial Complexity*, pages 135–150. Cambridge University Press, Cambridge, UK, 2000.

[23] H. Ohtsuki, C. Hauert, E. Lieberman, and M.A. Nowak. A simple rule for the evolution of cooperation on graphs and social networks. *Nature*, 441(7092):502–505, 2006.

[24] M. Perc and A. Szolnoki. Coevolutionary games - A mini review. *Biosystems*, 99:109–125, 2010.

[25] C. P. Roca, J. A. Cuesta, and A. Sánchez. Evolutionary game theory: temporal and spatial effects beyond replicator dynamics. *Physics of Life Reviews*, 6:208–249, 2009.

[26] A. F. Rozenfeld, R. Cohen, D. Ben-Avraham, and S. Havlin. Scale-free networks on lattices. *Phys. Rev. Lett.*, 89:218701, 2002.

[27] F. C. Santos and J. M. Pacheco. Scale-free networks provide a unifying framework for the emergence of cooperation. *Phys. Rev. Lett.*, 95:098104, 2005.

[28] F. C. Santos, J. M. Pacheco, and T. Lenaerts. Evolutionary dynamics of social dilemmas in structured heterogeneous populations. *Proc. Natl. Acad. Sci. USA*, 103:3490–3494, 2006.

[29] G. Szabó and G. Fáth. Evolutionary games on graphs. *Physics Reports*, 446:97–216, 2007.

[30] A. Szolnoki, N.G. Xie, C. Wang, and M. Perc. Imitating emotions instead of strategies in spatial games elevates social welfare. *EPL (Europhysics Letters)*, 96(3):38002, 2011.

[31] A. Traulsen, J.M. Pacheco, and M.A. Nowak. Pairwise comparison and selection temperature in evolutionary game dynamics. *Journal of theoretical biology*, 246(3):522, 2007.

[32] F. Vega-Redondo. *Economics and the Theory of Games*. Cambridge University Press, Cambridge, UK, 2003.

[33] J. W. Weibull. *Evolutionary Game Theory*. MIT Press, Boston, MA, 1995.

[34] B. Wu, P.M. Altrock, L. Wang, and A. Traulsen. Universality of weak selection. *Physical Review E*, 82(4):046106, 2010.

[35] D-P. Yang, H. Lin, C.-X. Wu, and J. Shuai. Topological conditions of scale-free networks for cooperation to evolve. *arXiv*, 98:1106.5386, 2011.

Part II
Cooperation and Opportunistic Migration

Chapter 5

Random Diffusion and Cooperation in Continuous Two-Dimensional Space

Abstract This work presents a systematic study of population games of the Prisoner's Dilemma, Hawk-Dove, and Stag Hunt types in two-dimensional Euclidean space under two-person, one-shot game-theoretic interactions, and in the presence of agent random mobility. The goal is to investigate whether cooperation can evolve and be stable when agents can move randomly in continuous space. When the agents all have the same constant velocity cooperation may evolve if the agents update their strategies imitating the most successful neighbor. If a fitness difference proportional is used instead, cooperation does not improve with respect to the static random geometric graph case. When viscosity effects set-in and agent velocity becomes a quickly decreasing function of the number of neighbors they have, one observes the formation of monomorphic stable clusters of cooperators or defectors in the Prisoner's Dilemma. However, cooperation does not spread in the population as in the constant velocity case.

5.1 Introduction and Previous Work

Cooperative behavior is socially beneficial but difficult to obtain among selfish individuals. In this context, the Prisoner's Dilemma game is a widely used paradigm for the investigation of how cooperation might evolve in a population of self-regarding agents. In fact, game-theoretical results predict defection as a Nash equilibrium or as a stable state of the population dynamics [15, 33]. In spite of this, non-negligible amounts of cooperative behavior can be observed daily in the animal kingdom, in the human society, and also in the laboratory, where controlled experiments can be carried out. Many mechanisms have been suggested to explain these behaviors, such as direct and indirect reciprocity, kin reciprocity, group reciprocity, and population structure among others (see e.g. [18] and references therein for a summary of this vast amount of work).

Among the various reasons that have been advocated, the structure of the interacting population is one of the simplest factors that can change the generalized defection outcome with respect to the well-mixed population case. The population structure of the interacting agents can be generically represented by a relational graph in which two directly linked vertices stand for two interacting agents. This locality of contacts means that only pairs or groups of individuals that are direct neighbors play the game among themselves. By

using theoretical models and simulations, it has been found that some network structures appear to be more conducive to cooperation than others, albeit this result is contingent upon the evolutionary dynamics of the model [22, 25, 28, 31]. However, an earlier way of considering the effect of population structures makes use of the concept of geographical space. Indeed, physical space may be more adequate than generic relational structures in many cases in which territoriality plays an important role. A simple first approximation of physical space is given by a regular discrete lattice in two dimensions. Building on previous work by Axelrod [3], Nowak et al. [20] and Nowak et al. [19] were able to show by extensive simulations that, even when the game is one-shot, i.e. pairs of players interact anonymously, cooperation can evolve and can persist for a non-negligible region of the game phase space thanks to positive assortment among cooperators. Of course, anonymity of neighbors is difficult to maintain in a real unchanging social network environment, but this is the context that has been adopted in previous modeling work. A summary of this and other early work is provided in [21]. Actually, the gains in the PD are relatively limited and depend on the players' strategy update rule used [25]. Meanwhile, the improvements are large in the related game called Stag Hunt (SH) [25, 30] when played on a grid. Evolutionary games on arbitrary static spatially embedded networks have been recently studied in [4].

All the above refers to static environments. However, it is easy to see that fixed environments are the exception rather than the rule. Evolutionary games on dynamic networks have been investigated in recent years, see e.g. [10, 24, 27, 35] and the review article [23]. Although the models differ in their assumptions and the details of the dynamics, there is a consensus emerging on the fact that purposeful, or strategic link update is a further factor allowing cooperating individuals to escape exploiting defectors by cutting links to them and forming new links with fellow cooperators, which facilitates clustering and positive assortment of cooperators, ultimately leading to sustained global cooperation. In a way analogous to the dynamic network case, in the case of spatially embedded agents it is easy to think of mobile rather than fixed individuals. Many examples can be found in biological and ecological sciences, in human populations, and in engineered systems such as ad hoc networks of mobile communicating devices or mobile robot teams. Mobility may have positive or negative effects on cooperation, depending on several factors. An early brief investigation of random grids and spatial drift is to be found in Nowak et al. [19]. Another study was carried out by Enquist and Leimar [11] whose main conclusion of [11] was that mobility may seriously restrict the evolution of cooperation. In the last decade there have been several new studies of the influence of mobility on the behavior of various games in spatial environments covering essentially two strands of research: one in which the movement of agents is seen as a random walk, and a second one in which movement may contain random elements but it is purposeful, or strategy-driven. Examples of the latter kind of work are to be found in [1, 6, 8, 14, 16, 26]. In spite of the difference among the proposed models, the general message of this work is that purposeful contingent movement may lead to highly cooperating stable or quasi-stable population states depending on the individuals' density and the degree of mobility.

As said above, the other line of investigation is centered on random diffusion of the mobile agents through space, either in continuous space [17] or, more commonly, on diluted grids [29, 32]. Random diffusion, with its tendency to mix-up the population has been

thought to hinder cooperation by weakening the possibility of cooperator cluster formation. In spite of this, the work of [29, 32] shows that cooperation can be maintained with respect to the static case and even enhanced for some parameters' ranges. In the continuous space case of [17] cooperation can be maintained only for low velocities and low temptation to defect. Within this framework, there has also been work on n-person Prisoner's Dilemma and public goods games, either in the one-shot case [5], as well as in the iterated, short memory case [7]. The effect of diffusion in a spatial ecological public goods game has been studied by Wakano et al. [34] using a partial differential equation formalism.

The present investigation belongs to the random diffusion category and deals with memoryless agents performing random movements and interacting in pairs with other agents in continuous space. Indeed, we believe that while grids are interesting because of their simplicity, a continuous space approach is more natural and less restricted. Our approach follows Meloni et al. [17] but it largely extends and completes it in various ways. Indeed, Meloni et al. studied the weak Prisoner's Dilemma, which is the segment at the frontier between the genuine Prisoner's Dilemma game space and the Hawk-Dove game [15]. Here we explore the full conventional Prisoner's Dilemma space and also the regions belonging to the Stag Hunt and Hawk-Dove games. Furthermore, we use a second strategy update rule besides their fitness-proportional one. Finally, while the velocity of the agents was held constant and the same for all individuals in the population in [17], we explore the effects of having players diffusing with different velocities. Some relationships with the results found in the grid-based diffusion systems proposed in [29, 32] will also be discussed.

5.2 Model Description

In this section we describe our model and the numerical simulations parameters. We also describe what is new with respect to the previous work.

5.2.1 The Spatial Environment

The environment in which the set of agents N interact and move is a square in the Euclidean plane of side $L = 1$ thus having unit area. For the purposes of the dynamics the square is wrapped around into a torus. Agents are initially distributed uniformly at random over the space. Every agent j has an interaction neighborhood which has the same extension for all agents and is given by a circle of radius r around the given agent. All the agents that fall into this circle at a given time t are considered to be neighbors $\mathcal{N}(j, t)$ of the agent, i.e. $\mathcal{N}(j, t) = \{\forall k \in N \mid dist(j, k) < r\}$, where $dist(j, k)$ is the Euclidean distance between agents (points) j and k. Agents are simply material points, they do not have an area. Since the spatial region area has unit value, the density ρ of the agents is $\rho = |N|$.

Given the above setting, at any point in time the current implicit network of contacts between the agents turns out to be a Random Geometric Graph (RGG) [9] as illustrated

in Fig. 5.1. The average degree $\bar{k}$ of a RGG is $\bar{k} = \pi\rho r^2$. Thus it is possible to consider $\bar{k}$ as a parameter of RGGs, instead of the radius r. Therefore, in order to construct an RGG with an average degree that tends to $\bar{k}$, it is sufficient to use the radius $r = \sqrt{\bar{k}/(\pi\rho)}$. This class of networks has an high average clustering coefficient [9] and positive degree-degree correlations [2].

5.2.2 Games Studied

Agents in our system, when they interact in pairs, play one of three common two-person, two-strategy, symmetric game classes, namely the Prisoner's Dilemma (PD), the Hawk-Dove Game (HD), and the Stag Hunt (SH). These three games are simple metaphors for different kinds of dilemmas that arise when individual and social interests collide. The games have the generic payoff matrix M (eq. 8.1) which refers to the payoffs of the row player. The payoff matrix for the column player is simply the transpose $M^\top$ since the games are symmetric.

$$
\begin{array}{cc}
 & \begin{array}{cc} C & D \end{array} \\
\begin{array}{c} C \\ D \end{array} & \begin{pmatrix} R & S \\ T & P \end{pmatrix}
\end{array}
\tag{5.1}
$$

The set of strategies is $\Lambda = \{C, D\}$, where C stands for "cooperation" and D means "defection". In the payoff matrix R stands for the *reward* the two players receive if they both cooperate, P is the *punishment* if they both defect, and T is the *temptation*, i.e. the payoff that a player receives if he defects while the other cooperates getting the *sucker's payoff* S.

For the PD, the payoff values are ordered such that $T > R > P > S$. Defection is always the best rational individual choice, so that (D, D) is the unique Nash Equilibrium (NE) and also the only fixed point of the replicator dynamics [15].

In the HD game, the order of P and S is reversed, yielding $T > R > S > P$. Players have a strong incentive to play D, which is harmful for both parties if the outcome produced happens to be (D, D). The only dynamically stable equilibrium is in mixed strategies [15, 33].

In the SH game, the ordering is $R > T > P > S$, which implies that mutual cooperation (C, C) is the payoff superior outcome and a NE. The second NE, where both players defect is less efficient but also less risky. The third mixed-strategy NE in the game is evolutionarily unstable [15].

Finally, in the Harmony game, which is included to complete the square, $R > S > T > P$ or $R > T > S > P$. In this case C dominates D and the trivial unique NE is (C, C).

In order to study the usual standard parameter space [25, 28], we restrict the payoff values in the following way: $R = 1$, $P = 0$, $-1 \leq S \leq 1$, and $0 \leq T \leq 2$. In the resulting TS-plane each game class corresponds to a different quadrant depending on the above ordering of the payoffs: PD is the lower right quadrant, HD corresponds to the upper left region, and SH belongs to the lower left quadrant.
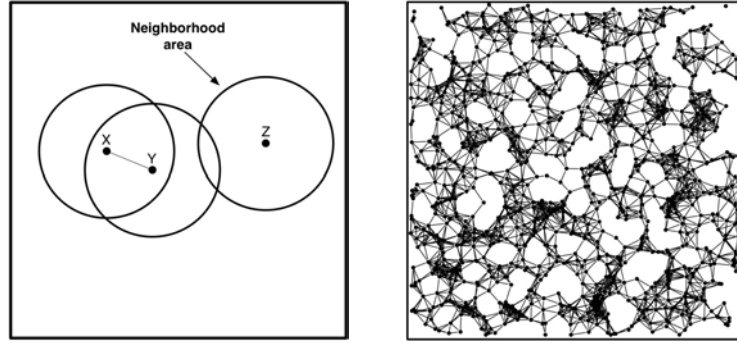
Fig. 5.1 Neighborhood area (left image) and an example of a RGG with $|N| = 1000$ and $\bar{k} = 10$ (right image).

5.2.3 Agent and Population Dynamics

The population dynamic is simulated by the following stochastic process at each time step t:

1. An agent is chosen uniformly at random among the population
2. The agent plays the game with each of his neighbors in turn and accumulates his payoff
3. The chosen agent undergoes a strategy revision phase based on his current payoff and the payoff of his neighbors
4. The agent moves randomly to another position in space

Step 1 means that the population evolution is asynchronous in time, which amounts to a Monte Carlo process simulation. At the end of step 2 the player computes his total payoff accumulated through the two-person games played with his neighbors $\mathcal{N}_i$. Let $\sigma_i(t)$ be a vector giving the strategy profile at time t with $C = (1,0)$ and $D = (0,1)$ and let M be the payoff matrix of the game (eq. 8.1). The quantity

$$\Pi_i(t) = \sum_{j \in \mathcal{N}_i} \sigma_i(t) \ M \ \sigma_j^\top(t) \tag{5.2}$$

is the cumulated payoff collected by player i at time step t.

In step 3 the chosen agent adopts a strategy in $\Lambda = \{C, D\}$ according to a microscopic revision rule. Several update rules are customary in evolutionary game theory [31]. Two imitative protocols have been used in our simulations: *fitness difference proportional* and *imitation of the best.* The fitness difference proportional rule (FDP) is linear and stochastic [12, 13]. Player i's strategy σ_i is updated by randomly drawing another player j from the neighborhood $\mathcal{N}_i$, and replacing σ_i by σ_j with probability:

$$p(\sigma_i \to \sigma_j) = \begin{cases} (\Pi_j - \Pi_i)/K & \text{if } \Pi_j > \Pi_i \\ 0 & \text{if } \Pi_j \leq \Pi_i \end{cases} \tag{5.3}$$

where $\Pi_j - \Pi_i$ is the difference of the payoffs earned by j and i respectively. $K = \max(k_i, k_j)[\max(1, T) - \min(0, S)]$ ensures proper normalization of the probability $p(\sigma_i \to \sigma_j)$.

Another imitative strategy update protocol is to deterministically switch to the strategy of the neighbor that has scored best in the last time step [20]. This imitation of the best (IB) policy can be described in the following way: the strategy $\sigma_i(t)$ of individual i at time step t will be

$$\sigma_i(t) = \sigma_j(t-1), \tag{5.4}$$

where

$$j \in \{\mathcal{N}_i \cup i \mid \Pi_j = \max\{\Pi_k(t-1)\}\}, \ \forall k \in \{\mathcal{N}_i \cup i\}. \tag{5.5}$$

That is, individual i will adopt the strategy of the player with the highest payoff among its neighbors including itself. If there is a tie, the winner individual is chosen uniformly at random.

Finally, in Step 4 the individual moves to another position in the plane in the following way. First, the magnitude of the displacement v is constant and the same for all agents for a given simulation run. Next, a direction is chosen by randomly drawing an angle in the range $[0, 2\pi]$.

The iteration of steps 1, 2, 3, and 4 gives rise to a sequence of RGGs $\{G(t)\}_t$, and a sequence of population strategy profiles $\{\sigma_1(t), \ldots, \sigma_{|N|}(t)\}_t$, with $t \in \mathbb{N}$. Given our assumptions, both sequences are Markov chains.

In another set of simulations the velocity v is not constant for all individuals but will instead depend on a given individual's neighborhood, see Sect. 5.4.

5.3 Constant Velocity Results and Discussion

The parameters used in the simulations were the following. The number of players was $|N| = 1000$; the mean degrees of the RGGs constituting the populations were either $\bar{k} = 4$ or $\bar{k} = 8$. The maximum number of simulation steps was 2000. Here one step means the update of all the $|N|$ players in the average, since updating is asynchronous. Simulations end either when a monomorphic population has been obtained, or when the maximum number of steps has been reached. Cooperation frequencies in the population are computed when the run stops. As for the game space, the TS-plane has been sampled in steps of 0.05 in the T and S directions thus forming a 41×41 grid. As stated above, at the beginning of each run agents are randomly distributed over the space with an agent being a cooperator with probability 0.5. Cooperation frequencies for each game space grid point are computed as the average value of 100 runs. The last parameter is the individual's velocity v. As stated, in each given simulation run, all the agents are assigned the same constant velocity v. We have studied the cases $v = 0$ (the static case), $v = 0.01$, and $v = 0.001$.

Figures 5.2 and 5.3 show the results for the entire games' phase space when players update their strategy using the FDP rule (see Sect. 5.2.3) with $\bar{k} = 4$ and $\bar{k} = 8$ respectively. In the figures, velocity decreases from left to right and the $v = 0$ case refers to a static RGG. Since Meloni et al. [17] used the same update rule, we first compare their results with ours. The game space sampled in [17] corresponds to the segment at the frontier between the PD and HD game spaces with $R = 1$, $P = 0$, $S = 0$, and $1 \leq T \leq 2$ (weak PD game). When our velocities are suitably normalized in order to be comparable

with the corresponding values in [17], our results do qualitatively agree with theirs for the weak PD, i.e. cooperation can only evolve for low T values, small velocity, and small mean degrees, or radii used in the simulations shown in the figures. However, when one looks at the entire PD game space, one can see that the gains in cooperation are indeed very small or non-existent when the agents can move. Only in the case of $v = 0.001$ cooperative outcomes are found in the small area in the upper left corner of the PD quadrant with S slightly less than 0, and T between 1.0 and about 1.1. It is likely that the separation between defection and cooperation in this small region would become crisper if we could perform extremely long runs and use larger population, both of which contribute to dramatically increase the computing time. However, these considerations do not change the global result, i.e. defection prevails almost completely in the PD.

For the other games, the HD behavior is practically not influenced by the agents' movement except for the case $\bar{k} = 4$ and $v = 0.01$ where there is more defection than what one observes in the static case, i.e. $v = 0$. This is due to the particular status of the HD in which the only stable state is the mixed one. When small cooperator or defectors clusters form, they are subsequently invaded by the other strategy and their composition remain close to the proportions of the mixed NE. The situation is different and more interesting in the SH case which features bistability. Here cooperation benefits from the agents' diffusion with low velocity $v = 0.001$ because slow movement favors the spreading of the efficient strategy. Instead, when $v = 0.01$ the populations are less cooperative than in the static case.

Fig. 5.2 Average cooperation values using FDP as an update rule. The mean degree is $\bar{k} = 4$. From left to right: $v = 0.01$, $v = 0.001$, and $v = 0$. The bold-face numbers next to each quadrant are average cooperation values for the corresponding game. The results are averages over 100 runs.

While Meloni et al. [17] did not use the IB rule, Vainstein et al. [32] and Sicardi et al. [29] performed an extensive study of random migration in diluted grids employing this rule. They investigated the influence of the density of players and of their mobility on cooperation when the agents have the possibility of migrating to an empty neighboring site in the grid, if any, with a certain probability. It must be said that our continuous space system is not directly comparable to the setting of [29, 32]. Indeed, in their case the mobility parameter, a quantity that is related to the players' displacements, and thus to their implicit velocity, depends on the density of players in the grid, while in our continuous collisionless model velocity is a well-defined independent quantity. Keeping in mind the
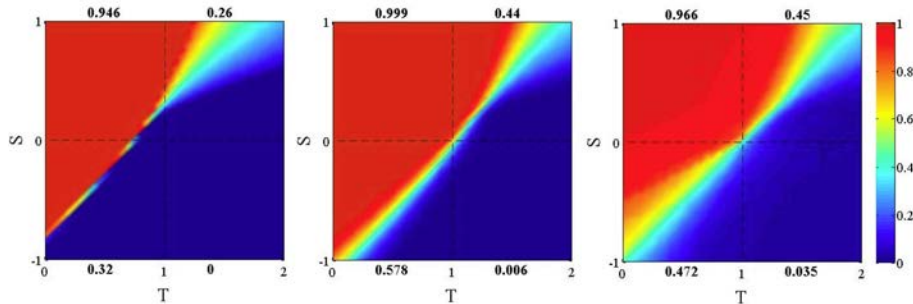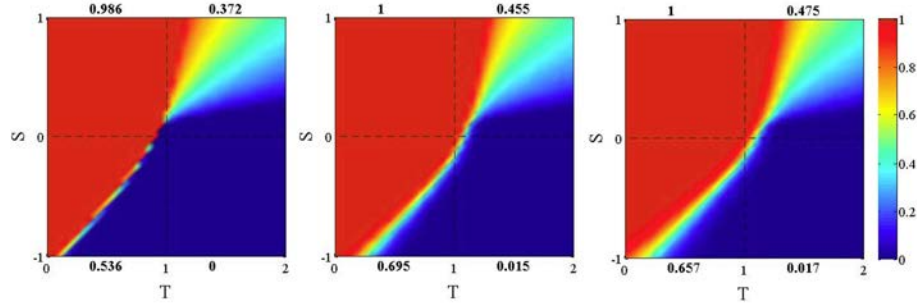
Fig. 5.3 Average cooperation values using FDP as an update rule. The mean degree is $\bar{k} = 8$. From left to right: $v = 0.01$, $v = 0.001$, and $v = 0$. The bold-face numbers next to each quadrant are average cooperation values for the corresponding game. The results are averages over 100 runs.
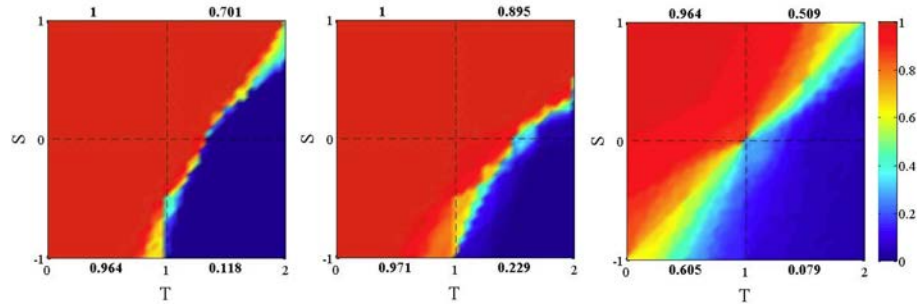
Fig. 5.4 Average cooperation values using imitation of the best as an update rule. The mean degree is $\bar{k} = 4$. From left to right: $v = 0.01$, $v = 0.001$, and $v = 0$. The bold-face numbers next to each quadrant are average cooperation values for the corresponding game. The results are averages over 100 runs.
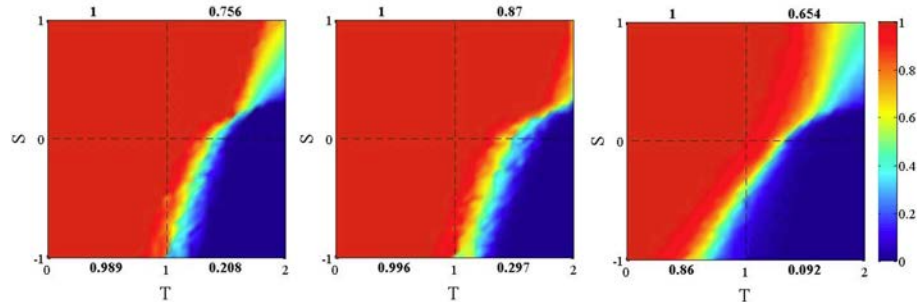
Fig. 5.5 Average cooperation values using imitation of the best as an update rule. The mean degree is $\bar{k} = 8$. From left to right: $v = 0.01$, $v = 0.001$, and $v = 0$. The bold-face numbers next to each quadrant are average cooperation values for the corresponding game. The results are averages over 100 runs.

differences, it is nevertheless interesting to compare the results of [29, 32] with ours. In Figs. 5.4 and 5.5 we show average cooperation levels in the whole T-S space when the

update rule is imitation of the best. In [29, 32] equilibrium cooperation values for only some points in the PD, HD, and SH spaces were reported, albeit using a much larger population size. In [29, 32] each player has at most four neighbors which means that the mean degree is less than four, since there are empty sites when their density $\rho < 1$; we should thus compare their results with those of Fig. 5.4. Sicardi et al. found that for intermediate densities ρ and for the games sampled in the T-S plane, cooperation states are reached in the three games PD, HD, and SH. This result is qualitatively confirmed and generalized by looking at the two leftmost images of Fig. 5.4. Indeed, when agents can move the SH quadrant becomes fully cooperative, the HD results are improved with respect to the static case, and a larger cooperative region appears in the PD space too. Results are better in terms of cooperation for lower velocities. Fig. 5.5 confirms all the trends when the mean connectivity of the agents doubles; indeed, more connections seem to further favor cooperation because cooperator cluster formation becomes easier.

For the sake of illustration, Fig. 5.6 shows spatial snapshots of a particular but typical run at successive time steps. The particular game shown here, which converges to full cooperation, has $R = 1$, $P = 0$, $S = 0$, and $T = 1.3$, $v = 0.001$, $\bar{k} = 4$, and thus it belongs to the weak PD along the segment between the PD and HD games (see Fig. 5.4 middle image). The sequence of figures represent evolving RGGs. Starting from a $50 - 50$ initial configuration, there is first a fall in cooperation followed by a steady increase caused
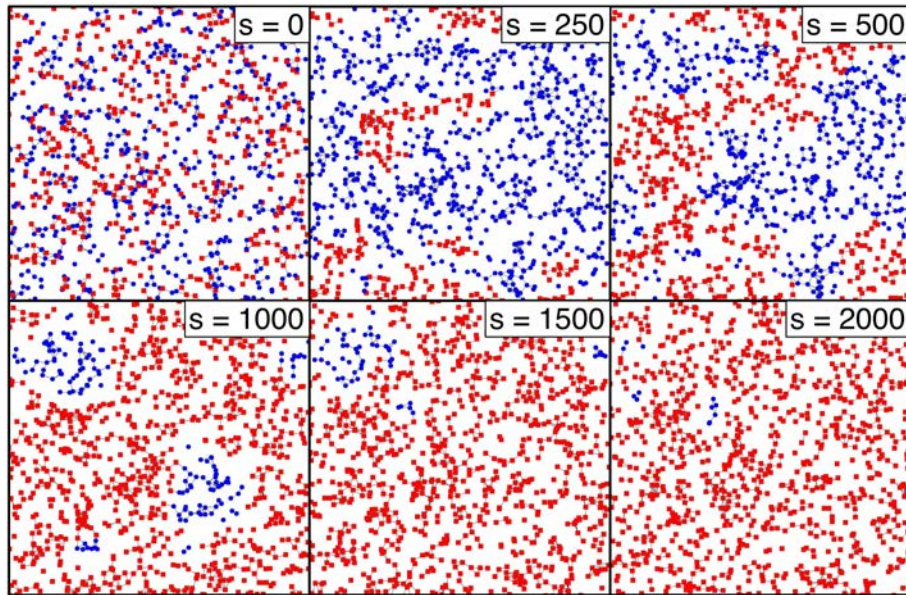
Fig. 5.6 Time evolution of a particular run with $R = 1$, $P = 0$, $S = 0$, $T = 1.3$, $v = 0.001$, and $\bar{k} = 4$. Red squares represent cooperators; blue circles stand for defectors; The initial proportion of cooperators is 0.5. s gives the time step at which the corresponding snapshot has been taken.

by cooperation spreading around small cooperative subgraphs. Although the last image still contains a few defectors, those are likely to disappear if the simulation would last longer. This mechanism is common to the SH game too, which converges to cooperation

everywhere in the parameters space, and also in the cooperative HD and PD regions. The graph and strategy evolution found with FDP instead of IB when the final state is full cooperation are similar but take longer times.

In conclusion, it appears that cooperation tends to be enhanced for a sizable part of the parameters space when agents update their strategies using the IB rule, and are able to move around. In addition, since our results and the partial ones of [29, 32] are coherent between themselves starting from two rather different models, the phenomenon can be considered robust. Some caveats are in order however. In the first place, the IB strategy update rule requires knowing the payoffs of the neighbors, which is likely to be cognitively unfeasible in many biological situations of interest. Perhaps it is conceivable, at least in a stylized manner, in human societies. As we saw above, the results are not as good with FDP update, which is also based on payoff differences but has a stochastic component that could be thought to roughly represent some uncertainty in the decision process.

5.4 Viscosity and Non-Constant Velocity

In the basic model agents move with a constant pre-defined velocity v which is the same for all of them. However, this does not seem very realistic. If one looks at a crowd moving in space, for instance, one sees that the magnitude of the displacements of an agent strongly depends on the density of people around him. We have tried to model this effect in a very simple but general way, although it might not be suitable for any particular given real situation. Now the velocity becomes a function of the instantaneous degree k of the agent such that the more neighbors she has, the more her movement is hindered. For simplicity, we have chosen a negative exponential function form. Thus an agent of degree k will have an instantaneous velocity $v(k)$ given by:

$$v(k) = v_0 \, e^{-\beta k} \qquad (5.6)$$

Here v_0 is the agent velocity when there are no neighbors, and β is a scaling factor to be chosen empirically which influences the speed of the decay and thus the mobility. For $\beta = 0$ we recover the constant velocity model, while for $\beta \to \infty$ viscosity is maximal and we recover the static case for $k \neq 0$. After some numerical experimentation, we have chosen to study the effect of two different values of β: 1 and 0.1.

The following discussion is for an initial contact radius that corresponds to $\bar{k} = 4$, the strategy update rule is IB, and $v_0 = 0.01$. However, as time goes by, owing to the non-uniform random diffusion caused by viscosity effects, the average degree is not maintained and will tend to increase. Let us first examine the case $\beta = 0.1$. In this case the displacements are less hindered and thus viscosity is comparatively low. Before presenting average results for the whole $T - S$ plane which are globally interesting but could hide some important dynamical phenomena, we will show a particular, suitably chosen game. Figure 5.7 shows the time evolution for a game in the weak PD segment with $R = 1$, $P = 0$, $S = 0$, and $T = 1.3$. The phenomena observed are very different from those that appeared in the same game with constant velocity shown in Fig. 5.6. With constant velocity, this game region led to full cooperation. Instead, with velocity damping, although

average cooperation is still of the order of the initial $50 - 50$ proportion, the spatial distribution of cooperators and defectors is no longer random: there is cluster formation of each strategy which is essentially caused by progressive velocity reduction due to viscosity. Once the dense clusters are formed, agents cannot move away easily just because viscosity is too high.

It is thus clear that cooperation cannot spread past the clusters as in the case with constant velocity, and the clusters are just connected components which are disconnected from the other parts. In fact, in the limit of very long simulation times, the clusters become more and more dense because of the lack of a minimal repulsion distance in the model.

Now we describe the case of $\beta = 1$. Taking the same game as before, we obtained the dynamics depicted in the snapshots of Fig. 5.8. With a larger β value one would expect that viscosity plays a more important role in hindering the agents' movements. This is indeed the case. At the very beginning agents do not diffuse much already but are still able to move enough to join other agents and form more elongated spread-out clusters in which nodes have few connections, as opposed to the dense clusters observed with $\beta = 0.1$. Indeed, for the higher β value a small number of neighbors is already sufficient to severely hinder the agents' motion. Now, because viscosity is high, these configurations do not change their shapes much as time goes by. After an initial loss, non-negligible levels of cooperation are recovered at steady state and, again, strategies cluster together but with a definite difference in cluster shape with respect to the previous case.

Fig. 5.7 Time evolution of a particular run with $R = 1$, $P = 0$, $S = 0$, $T = 1.3$, initial $\bar{k} = 4$, $\beta = 0.1$ and $v_0 = 0.01$. Red squares represent cooperators; blue circles stand for defectors; The initial proportion of cooperators is 0.5. s gives the time step at which the corresponding snapshot has been taken. The final cooperation frequency at $s = 2000$ is 0.57.

Figure 5.9 illustrates the behavior of the average velocity and the mean degree in the system as a function of time for a single typical run with the same $v_0 = 0.01$. We remark that this behavior is general and does not depend on the particular game parameters or agent strategy. For the sake of studying long-term system behavior, we have performed 20000 steps to draw these figures. Clearly, as velocity and degree are related in Eq. 5.6, one would expect that the lower β the higher the mean speed in the system, and the same should be true for the mean degree. In fact, Fig. 5.9 left image shows that velocity indeed decreases exponentially for $\beta = 0.1$. The mean velocity can never go to zero as the lowest possible velocity for such a finite system is $v_0\, e^{-\beta(N-1)}$. Actually, towards the end
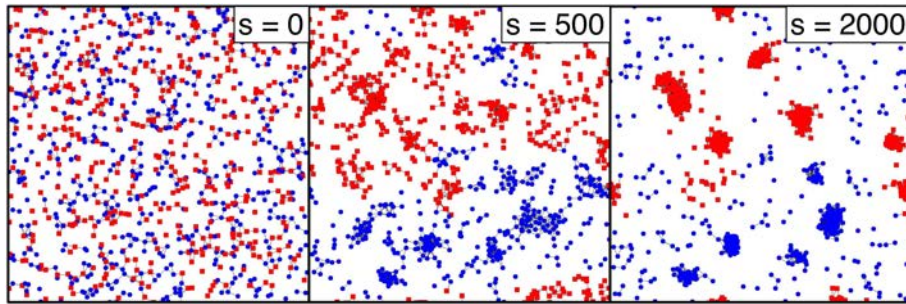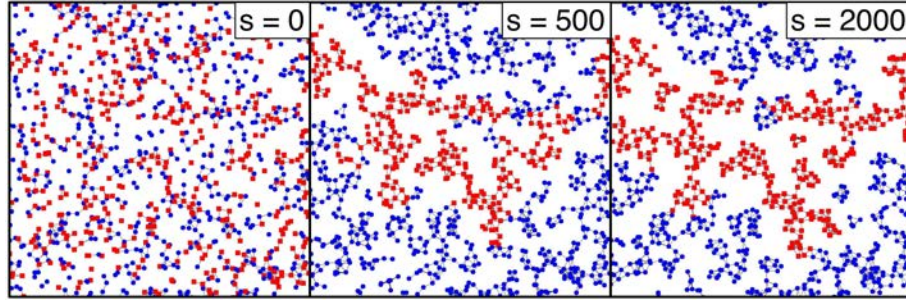
Fig. 5.8 Time evolution of a particular run with $R = 1$, $P = 0$, $S = 0$, $T = 1.3$, initial $\bar{k} = 4$, $\beta = 1$ and $v_0 = 0.01$. Red squares represent cooperators; blue circles stand for defectors; The initial proportion of cooperators is 0.5. s gives the time step at which the corresponding snapshot has been taken. The final cooperation frequency at $s = 2000$ is 0.38.

of the simulation, the mean velocity is the average of individuals that have not yet joined a densely connected cluster (see Fig. 5.7 rightmost image) and move around in space more freely, and those within a cluster which are almost at rest. The network counterpart of this velocity damping is the large increase of mean degree $\bar{k}$ (Fig. 5.9, right image) which is due to the fact that individuals are densely packed into clusters. In the case $\beta = 1$ mobility is more restricted from the start but, since the clusters that form are less dense, the velocity decreases more slowly.

To conclude this section, we show the global cooperation results in Fig. 5.10. Although these average results do not provide information on the fine system dynamics, as we said above, we still observe that, even in the more realistic simulation of a viscous system, there are non-negligible gains of cooperation compared to the RGG static case (rightmost image of Fig. 5.4). On the other hand, it doesn't make much sense to compare the present results with those at constant velocity (left and middle images of Fig. 5.4) since there are variable scale factors between the two cases; nevertheless, the global cooperation pattern is similar to the one found with constant velocity $v = 0.01$.

5.5 Conclusions

We have presented a systematic study of some population games by extensive numerical simulations in two-dimensional Euclidean space under two-person, one-shot game-theoretic interactions, and in the presence of agent random mobility. The goal was to investigate whether cooperation can evolve and be stable when agents can move randomly in space. Individuals in the population only interact with other agents that are contained in a circle of radius r around the given agent, where r is much smaller than the spatial dimension occupied by the whole population. For the game-theoretic interactions we have used two common microscopic payoff-based strategy update rules: fitness difference proportional and imitation of the best neighbor. We have studied a large game parameter space which
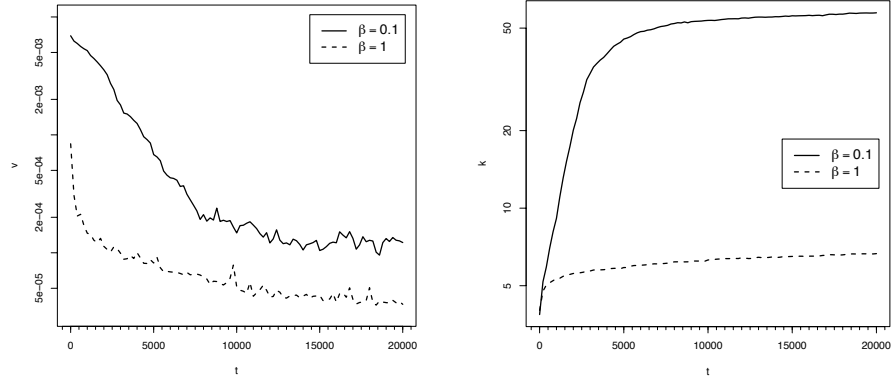
Fig. 5.9 Average system velocity for $\beta = 0.1$ and $\beta = 1$ (left image) and evolution of the mean degree $\bar{k}$ for the same values of β (right image); $v_0 = 0.01$.
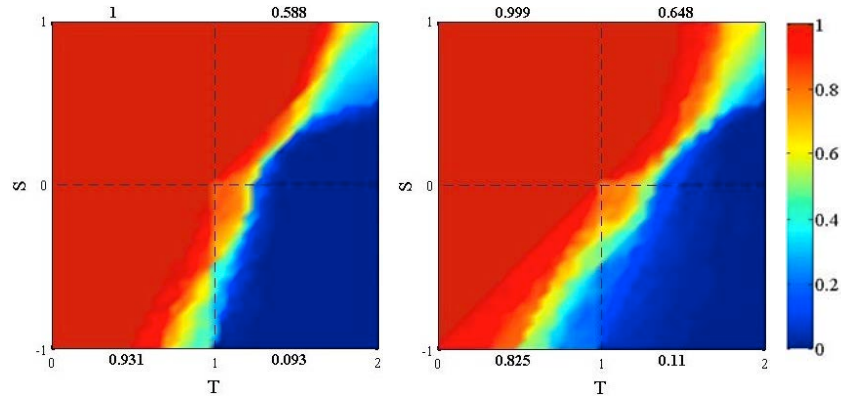
Fig. 5.10 Average cooperation values using imitation of the best as an update rule in the viscous model. The initial mean degree is $\bar{k} = 4$ but it evolves during the run. Left: $\beta = 0.1$; Right: $\beta = 1$. The results are averages over 100 runs.

comprises the Prisoner's Dilemma, the Stag Hunt, and the Hawk-Dove class of games. We have investigated two models which differ only in their mobility aspects.

In the first model, the velocity is the same for all agents in the population and it remains constant throughout the dynamics. Our main results with this model are the following. Under fitness difference proportional update, the effect of mobility on cooperation is very small and there is little difference with the case in which the agents sit at the nodes of a random geometric graph and don't move. These results extend previous ones obtained by Meloni et al. [17] which were limited to the weak Prisoner's Dilemma region, the segment with $S = 0$ and $1 \le T \le 2$ in the game's phase space.

However, when the imitation of the best neighbor rule is used instead, random mobility promotes cooperation in all the games' parameter space. Indeed, in the steady state we observe full cooperation in the Stag Hunt games while cooperation is also boosted in the Hawk-Dove. The Prisoner's Dilemma class of games is the most critical one but random

mobility seems to significantly improve the situation opening up to cooperation a large region of the PD space. The results are qualitatively the same with two different radii r that lead to network mean degrees 4 and 8 respectively. The main mechanism leading to the evolution of cooperation is the random initial formation of small clusters of cooperators followed by other cooperators joining the initial clusters thanks to their mobility, together with defectors slowly becoming cooperators because of the latter higher payoff.

In the second model agents do not move with constant scalar velocity; rather, velocity is assumed to be a negative exponential function of the agent's connectivity degree. This introduces a damping factor which can be seen as a kind of viscosity due to the accumulation of individuals around a given agent, leading to a more hindered random movement. The numerical simulation study of the average cooperation levels in the TS-plane in this case leads to results that are qualitatively similar to those obtained in the constant velocity case, although the gains in cooperation with respect to a static population represented by a RGG are slightly less. However, average values do not reveal the particular dynamics that are at work. To study this aspect, we have simulated a particular Prisoner's Dilemma game with two different velocity damping factors β, one giving rise to low viscosity and the second to a higher viscosity. With low viscosity, starting with a uniform distribution of the agents in the plane, the system evolves toward the formation of dense monomorphic clusters of cooperators or defectors. In these clusters agents are almost at rest in the steady state and only individuals that have not joined a cluster still move. Under these conditions, contrary to the case with constant velocity, cooperation cannot spread past the cluster boundaries because of the lack of individual dispersion. With high viscosity the agents' movements are more hindered from the beginning but they are still able to join clusters of their kind. The situation is similar to the previous case, i.e. clusters of C's and D's do form and remain stable, with the important difference that now they are much less dense and, consequently, the mean degree of the population is smaller. Again, viscosity and progressive velocity loss do not allow cooperation to spread to the whole population. One can thus conclude that random agent movements in physical space that take into account the natural fact that crowding effects have an effect on the agents' mobility may still lead to cooperative outcomes in many cases. However, the dynamics lead to cluster formation and condensation which hinders further spreading of cooperators especially in the harder Prisoner's Dilemma case. In future work we would like to address the detailed study of cluster dynamics and the effect of strategy noise on the system evolution.

References

[1] C. A. Aktipis. Know when to walk away: contingent movement and the evolution of cooperation. *Journal of Theoretical Biology*, 231:249–2160, 2004.

[2] A. Antonioni and M. Tomassini. Degree correlations in random geometric graphs. *Physical Review E*, 86(3):037101, 2012.

[3] R. Axelrod. *The Evolution of Cooperation*. Basic Books, Inc., New-York, 1984.

[4] P. Buesser and M. Tomassini. Evolution of cooperation on spatially embedded networks. *Physical Review E*, 86:066107, 2012.

[5] A. Cardillo, S. Meloni, J. Gómez-Gardeñes, and Y. Moreno. Velocity-enhanced cooperation of moving agents playing public goods games. *Physical Review E*, 85:067101, 2012.

[6] Z. Chen, J. Gao, Y. Kai, and X. Xu. Evolution of cooperation among mobile agents. *Physica A*, 390:1615–1622, 2011.

[7] R. Chiong and M. Kirley. Random mobility and the evolution of cooperation in spatial N-player iterated Prisoner's Dilemma games. *Physica A*, 391:3915–3923, 2012.

[8] R. Cong, B. Wu, Y. Qiu, and L. Wang. Evolution of cooperation driven by reputation-based migration. *PLoS ONE*, 7(5):35776, 2012.

[9] J. Dall and M. Christensen. Random geometric graphs. *Physical Review E*, 66:016121, 2002.

[10] V. M. Eguíluz, M. G. Zimmermann, C. J. Cela-Conde, and M. San Miguel. Cooperation and the emergence of role differentiation in the dynamics of social networks. *American Journal of Sociology*, 110(4):977–1008, 2005.

[11] M. Enquist and O. Leimar. The evolution of cooperation in mobile organisms. *Animal Behaviour*, 45:747–757, 1993.

[12] C. Hauert and M. Doebeli. Spatial structure often inhibits the evolution of cooperation in the snowdrift game. *Nature*, 428:643–646, April 2004.

[13] D. Helbing. Interrelations between stochastic equations for systems with pair interactions. *Physica A*, 181:29–52, 1992.

[14] D. Helbing and W. Yu. The outbreak of cooperation among success-driven individuals under noisy conditions. *Proc. Natl. Acad. Sci. USA*, 106:3680–3685, 2009.

[15] J. Hofbauer and K. Sigmund. *Evolutionary Games and Population Dynamics*. Cambridge, N. Y., 1998.

[16] L.-L. Jiang, W.-X. Wang, Y.-C. Lai, and B.-H. Wang. Role of adaptive migration in promoting cooperation in spatial games. *Physical Review E*, 81:036108, 2010.

[17] S. Meloni, A. Buscarino, L. Fortuna, M. Frasca, J. Gómez-Gardeñes, V. Latora, and Y. Moreno. Effects of mobility in a population of Prisoner's Dilemma players. *Physical Review E*, 79:067101, 2009.

[18] M. A. Nowak. Five Rules for the Evolution of Cooperation. *Science*, 314(5805):1560–1563, 2006.

[19] M. A. Nowak, S. Bonhoeffer, and R. May. More spatial games. *International Journal of Bifurcation and Chaos*, 4(1):33–56, 1994.

[20] M. A. Nowak and R. M. May. Evolutionary games and spatial chaos. *Nature*, 359:826–829, October 1992.

[21] M. A. Nowak and K. Sigmund. Games on grids. In U. Dieckmann, R. Law, and J. A. J. Metz, editors, *The Geometry of Ecological Interactions: Simplifying Spatial Complexity*, pages 135–150. Cambridge University Press, Cambridge, UK, 2000.

[22] H. Ohtsuki, C. Hauert, E. Lieberman, and M.A. Nowak. A simple rule for the evolution of cooperation on graphs and social networks. *Nature*, 441(7092):502–505, 2006.

[23] M. Perc and A. Szolnoki. Coevolutionary games - A mini review. *Biosystems*, 99:109–125, 2010.

[24] E. Pestelacci, M. Tomassini, and L. Luthi. Evolution of cooperation and coordination in a dynamically networked society. *Journal of Biological Theory*, 3(2):139–153, 2008.

[25] C. P. Roca, J. A. Cuesta, and A. Sánchez. Evolutionary game theory: temporal and spatial effects beyond replicator dynamics. *Physics of Life Reviews*, 6:208–249, 2009.

[26] C. P. Roca and D. Helbing. Emergence of social cohesion in a model society of greedy, mobile individuals. *Proc. Natl. Acad. Sci. USA*, 108:11370–11374, 2011.

[27] F. C. Santos, J. M. Pacheco, and T. Lenaerts. Cooperation prevails when individuals adjust their social ties. *PLoS Computational Biology*, 2:1284–1291, 2006.

[28] F. C. Santos, J. M. Pacheco, and T. Lenaerts. Evolutionary dynamics of social dilemmas in structured heterogeneous populations. *Proc. Natl. Acad. Sci. USA*, 103:3490–3494, 2006.

[29] E. A. Sicardi, H. Fort, M. H. Vainstein, and J. J. Arenzon. Random mobility and spatial structure often enhance cooperation. *Journal of Theoretical Biology*, 256:240–246, 2009.

[30] B. Skyrms. *The Stag Hunt and the Evolution of Social Structure*. Cambridge University Press, Cambridge, UK, 2004.

[31] G. Szabó and G. Fáth. Evolutionary games on graphs. *Physics Reports*, 446:97–216, 2007.

[32] M. H. Vainstein, A. T. C. Silva, and J. J. Arenzon. Does mobility decrease cooperation? *Journal of Theoretical Biology*, 244:722–728, 2007.

[33] F. Vega-Redondo. *Economics and the Theory of Games*. Cambridge University Press, Cambridge, UK, 2003.

[34] J. Y. Wakano, M. A. Nowak, and C. Hauert. Spatial dynamics of ecological public goods. *Proc. Natl. Acad. Sci. USA*, 106:7910–7914, 2009.

[35] B. Wu, D. Zhou, F. Fu, Q. Luo, L. Wand, and A. Traulsen. Evolution of cooperation on stochastic dynamical networks. *PLoS ONE*, 5(6):e11187, 2010.

Chapter 6

Spatial Organisation of Cooperation with Contingent Agent Migration

Abstract In the framework of game theory and cooperation, we study standard two-person population games when agents in the population are allowed to move to better positions in a two-dimensional diluted grid. We show that cooperation may thrive for small interaction radius and when mobility is low. Furthermore, we show that, even when the agents cannot change their game strategy, interesting spatial patterns do emerge as players explore their neighborhood in order to find a better place to migrate to. In the Prisoner's Dilemma and Stag-Hunt games, when the losses experienced by cooperators against defectors as well as the game and migration radius are large enough, players move in a coherent way because clusters of cooperators followed by defectors form. On the other hand, in the Hawk-Dove game or when the migration radius is small, players end up blocked into stationary clusters.

6.1 Introduction

Systems whose parts are contained in physical space are very important in biological and social sciences since most interactions among living beings or artificial actors take place in such a space. Thus game-theoretical interactions among spatially embedded agents distributed according to a fixed structure in the plane have been studied in detail since the pioneering works of Axelrod [2] and Nowak and May [10]. The related literature is very large; see, for instance, the review article by Nowak and Sigmund [11] and references therein for a synthesis. Most of this work was based on populations of agents arranged according to planar regular grids for mathematical simplicity and ease of numerical simulation. Recently, some extensions to more general spatial networks have been discussed in [3]. Strategic behavior on fixed spatial structures is important but, in the majority of real situations both in biology and in human societies, actors have the possibility to move around in space. Many examples can be found in biological and ecological sciences, in human populations, and in engineered systems such as ad hoc networks of mobile communicating devices or robot teams. Mobility may have positive or negative effects on cooperation, depending on several factors. For instance, early on Enquist and Leimar [5] studied a model in which space is not explicitly represented but assortment of strategies is made non-uniform by introducing the possibility of abandoning a non-profitable rela-

tionship and searching for another partner, thus modifying the homogeneous well-mixed original population structure. Their main conclusion was that mobility may seriously restrict the evolution of cooperation. In the last decade there have been several new studies of the influence of mobility on the behavior of various games in spatial environments representing essentially two strands of research: one in which the movement of agents is seen as a random walk, and a second one in which movement may contain random elements but it is purposeful, or strategy-driven. In the present study we focus on situations where, instead of randomly diffusing, agents possess some basic cognitive abilities and they actively seek to improve their situation by moving in space represented as a discrete grid in which part of the available sites are empty and can thus be the target of the displacement. This approach has been followed, for example, in [1, 4, 6, 7, 9]. The mechanisms invoked range from success-driven migration [7], adaptive migration [9], flocking behavior [4], and cooperators walking away from defectors [1]. The general qualitative message of this work is that purposeful contingent movement may lead to highly cooperating stable or quasi-stable population states if some conditions are satisfied. Despite all the above work, the quantitative results strongly depend on the assumptions made and on the details of the models.

Our approach here is inspired by the work of [6, 7] which they call "success-driven migration" and which has been shown to be able to produce highly cooperative states. In this model, locally interacting agents playing either defection or cooperation in a two-person Prisoner's Dilemma are initially randomly distributed on a grid in equal proportions with a certain density such that there are empty grid points. Agents are updated one at a time. When chosen for updating, the agent evaluates the current payoff she would accumulate by playing two-person games with all her current neighbors but she can also "explore" an extended square neighborhood by testing all the empty positions up to a given distance. If the player finds that it would be more profitable to move to one of these positions then she does it, choosing the best one among those tested, otherwise she stays at her current place. Helbing and Yu find that robust cooperation states may be reached by this single mechanism, even in the presence of random noise in the form of random strategy mutations and random agent relocation. Our study builds upon this work in several ways. In the first place, whilst Helbing and Yu had a single game neighborhood, we systematically investigate game neighborhood and migration neighborhood, showing that only some values of this pair of parameters allow the evolution of cooperation using success-driven migration. Second, we present systematical results for a whole game phase space including the Hawk-Dove class of games, the Stag Hunt coordination class, and the Prisoner's Dilemma class, while only the Hawk-Dove and the Prisoner's Dilemma are studied in [6]. We find that fully cooperative states can be reached for the standard neighborhoods and for several migration distances in the Stag Hunt case, while cooperation can also be achieved in the Prisoner's Dilemma for a non-negligible part of its game space. Mobility is less beneficial in the hawk-dove game where cooperation levels are on the average only slightly better than in the static, motionless case . Finally, we also study the extreme case of system evolution when agents cannot change their initially attributed strategy and are only allowed to test free cells within their migration radius in order to possibly move to more profitable regions. Here cooperation cannot evolve by definition but we are interested in the dynamical patterns that may form, i.e. whether or not the

agent distribution remains uniform during the dynamics. In this case, in the Prisoner's dilemma and Stag Hunt games we find that players move in a coherent way because clusters of cooperators followed by defectors are formed. On the other hand, in the Hawk-Dove game or when the radius within which players move is small, players end up blocked into stationary clusters.

6.2 Evolutionary Games and Migration in Two-Dimensional Space

6.2.1 The Games Studied

We investigate three classical two-person, two-strategy, symmetric games classes, namely the Prisoner's Dilemma (PD), the Hawk-Dove Game (HD), and the Stag Hunt (SH). These three games are simple metaphors for different kinds of dilemmas that arise when individual and social interests collide. The Harmony game (H) is included for completeness but it is not a dilemma since cooperation is trivially the NE. The main features of these games are summarized here for completeness; more detailed accounts can be found elsewhere e.g. [8, 16, 17]. The games have the generic payoff matrix M (equation 6.1) which refers to the payoffs of the row player. The payoff matrix for the column player is simply the transpose $M^\top$ since the game is symmetric.

$$
\begin{array}{cc}
 & \begin{array}{cc} C & D \end{array} \\
\begin{array}{c} C \\ D \end{array} & \begin{pmatrix} R & S \\ T & P \end{pmatrix}
\end{array}
\tag{6.1}
$$

The set of strategies is $\Lambda = \{C, D\}$, where C stands for "cooperation" and D means "defection". In the payoff matrix R stands for the *reward* the two players receive if they both cooperate, P is the *punishment* if they both defect, and T is the *temptation*, i.e. the payoff that a player receives if he defects while the other cooperates getting the *sucker's payoff* S.

In order to study the usual standard parameter space [12, 13], we restrict the payoff values in the following way: $R = 1$, $P = 0$, $-1 \le S \le 1$, and $0 \le T \le 2$.

For the PD, the payoff values are ordered such that $T > R > P > S$. Defection is always the best rational individual choice, so that (D, D) is the unique Nash Equilibrium (NE) and also the only fixed point of the replicator dynamics [8, 17]. Mutual cooperation would be socially preferable but C is strongly dominated by D.

In the HD game, the order of P and S is reversed, yielding $T > R > S > P$. Thus, when both players defect they each get the lowest payoff. Players have a strong incentive to play D, which is harmful for both parties if the outcome produced happens to be (D, D). (C, D) and (D, C) are NE of the game in pure strategies. There is a third equilibrium in mixed strategies which is the only dynamically stable equilibrium [8, 17].

In the SH game, the ordering is $R > T > P > S$, which means that mutual cooperation (C, C) is the best outcome and a NE. The second NE, where both players defect is less efficient but also less risky. The difficulty is represented by the fact that the socially preferable coordinated equilibrium (C, C) might be missed for "fear" that the other player

will play D instead. The third mixed-strategy NE in the game is evolutionarily unstable [8, 17].

Finally, in the H game $R > S > T > P$ or $R > T > S > P$. In this case C strongly dominates D and the trivial unique NE is (C, C). The game is non-conflictual by definition and does not cause any dilemma, it is mentioned to complete the quadrants of the parameter space.

There is an infinite number of games of each type since any positive affine transformation of the payoff matrix leaves the NE set invariant [17]. Here we study the customary standard parameter space [12, 13], by fixing the payoff values in the following way: $R = 1$, $P = 0$, $-1 \leq S \leq 1$, and $0 \leq T \leq 2$.

In the TS-plane each game class corresponds to a different quadrant depending on the above ordering of the payoffs as depicted in Fig 6.1, left image, and the figures that follow. The right part of Fig 6.1 shows the standard replicator dynamics results for a well mixed population [17].
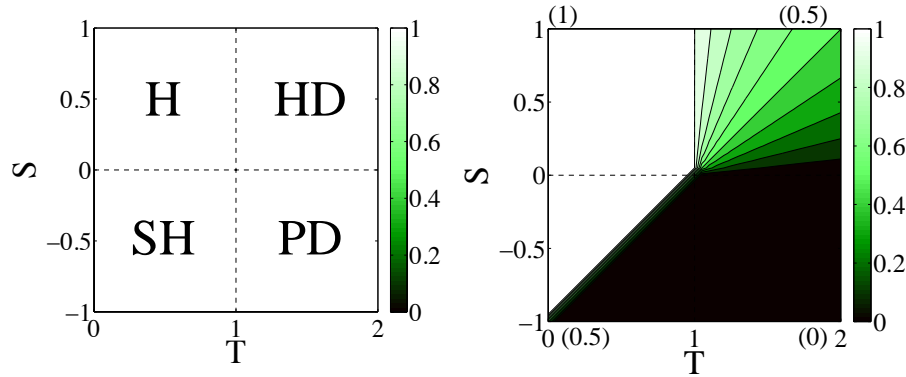
Fig. 6.1 (Color online) Left image: The games phase space (H= Harmony, HD = Hawk-Dove, PD = Prisoner's Dilemma, and SH = Stag Hunt) as a function of S, T ($R = 1$, $P = 0$). Right image: cooperation at steady state in a well mixed population for comparison purposes. Lighter tones stand for more cooperation. Figures in parentheses next to each quadrant indicate average cooperation in the corresponding game space.

6.2.2 Population Structure

The euclidean two-dimensional space is modeled by a discrete square lattice of side L with toroidal borders. Each vertex of the lattice can be occupied by one player or be empty. The *density* is $\rho = N/L^2$, where $N \leq L^2$ is the number of players. Players can interact with k neighbors which lie at a distance smaller or equal than a given constant R_g. Players can also migrate to empty grid points at a distance smaller than R_m. The relationships between the neighborhoods defined as above and the customary square Moore neighborhoods of increasing order are illustrated in Fig. 6.2.
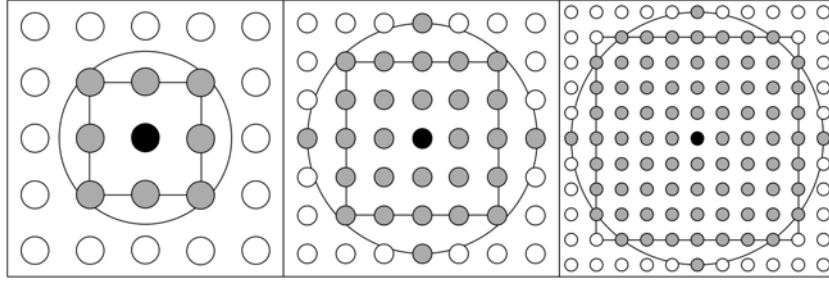
Fig. 6.2 Relationships between the neighborhoods defined by the radii R_g and R_m and the Moore square neighborhoods. Left: with the 1.5 radius the neighborhood is identical with the standard Moore neighborhood at distance one. Middle: radius 3 is almost equivalent to a Moore neighborhood at distance two marked as a square. Right: with radius 5 the closer Moore neighborhood has distance four.

6.2.3 Payoff Calculation and Strategy Update Rules

Here it is specified how individual's payoffs are computed and how agents decide to revise their current strategy. We take into account that each agent i interacts locally with a set of neighbors V_i lying closer than R_g. Let $\sigma_i(t)$ be a vector giving the strategy profile at time t with $C = (1,0)$ and $D = (0,1)$ and let M be the payoff matrix of the game (equation 6.1). The quantity

$$\Pi_i(t) = \sum_{j \in V_i} \sigma_i(t) \, M \, \sigma_j^\top(t) \tag{6.2}$$

is the cumulated payoff collected by player i at time step t.

We use an asynchronous scheme for strategy update and migration, i.e. players are updated one by one by choosing a random player in each step with uniform probability and with replacement. Then the player migrates with probability p or updates its strategy with probability $1-p$. Several update rules are customary in evolutionary game theory [12]. Here we shall use imitative strategy update protocol which consists in switching to the strategy of the neighbor that has scored best in the last time step. This *imitation of the best* (IB) policy can be described in the following way: the strategy $\sigma_i(t)$ of individual i at time step t will be

$$\sigma_i(t) = \sigma_j(t-1), \tag{6.3}$$

where

$$j \in \{V_i \cup i\} \; s.t. \; \Pi_j = \max_{k \in \{V_i \cup i\}} \{\Pi_k(t-1)\}. \tag{6.4}$$

That is, individual i will adopt the strategy of the player with the highest payoff among its neighbors including itself. If there is a tie, the winner individual is chosen uniformly at random.

A final remark is in order here. The above model rules are common in numerical simulation work, which has the advantage that the mathematics is simpler and results can be compared with previous work. However, they are homogeneous among the agents and

there is no learning. It is far from clear whether they are able to model real situations in biological systems and especially human societies. However, we feel that these considerations are outside the scope of the present numerical investigation.

6.2.4 Strategy Imitation and Migration rules

When player i is chosen for update, she changes her strategy with probability $1 - p$ or migrates with probability p. If the pseudo-random number drawn dictates that i should migrate, then she considers N_{test} randomly chosen positions in the disc of radius R_m around itself in order to take into account her bounded rationality. $N_{test} = 20$ has been used in all the simulations. For each trial position the player computes the payoff that she would obtain in that place with her current strategy. The positions already occupied are just discarded from the possible choices. Then player i stays at her current position if she obtains there the highest payoff, or migrates to the most profitable position among those explored during the test phase. If several positions, including her current one, share the highest payoff she chooses one at random. The protocol described in Helbing and Yu [7] is slightly different: the chosen player chooses the strategy of the best neighbor including himself with probability $1 - r$, and with probability r his strategy is randomly reset. Before this imitation step i deterministically chooses the highest payoff free position in a square neighborhood surrounding the current player and including himself. If several positions provide the same expected payoff, the one that is closer to the old position of i is selected.

Algorithm 1: migration of player i

---

  for $j \in [1, N_{test}]$ **do**
      choose random position x_j in V_i
      if x_j *is free* **then**
         compute the expected payoff $\Pi(x_j)$ of player i at x_j

  choose the best $\Pi(x_j)$; if several x_j share the same $\Pi(x_j)$ choose one at random and migrate to this position

---

6.2.5 Mobility Measure

In order to assess if a player has a definite direction of motion with respect to time we will use the following mobility measure. Mobility is defined as $M = max_{t \in [0,\tau]}(D_t)/L$ where τ is the time interval for a player to travel a total distance L if she moves the maximal distance R_m at each time step in the same direction. D_t is the Euclidean distance from the initial position to the position at time t. The interval τ is not taken from the beginning of the simulation but rather after a time sufficient for the mobile patterns to form. Thus M measures the ratio between the maximal distance over time reached by a player from her

initial position and the maximal distance that it is possible to reach in the best case. We multiplied this measure by four in order to increase the contrast in the images. However, this measure is not a strict indicator of coherent motion as moving clusters can collide and change direction.

6.2.6 Simulation Parameters
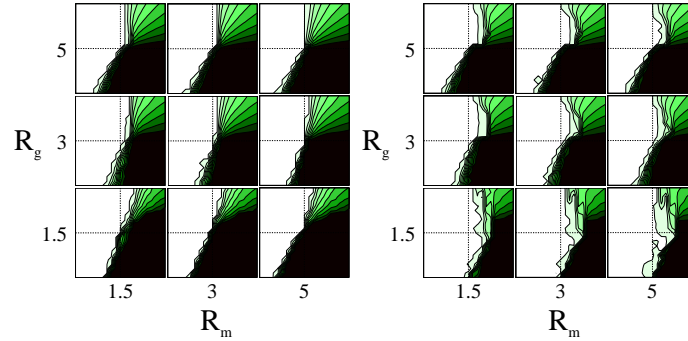
Fig. 6.3 (Color online) Average cooperation levels with IB strategy revision rule as a function of R_g and R_m with $p = 0.5$ and $\rho = 0.5$. Left image: Random migration. Right image: best fitness migration rule. The size of the population is 1000 players. In all cases the initial fraction of cooperators is 0.5 randomly distributed among the occupied grid points.
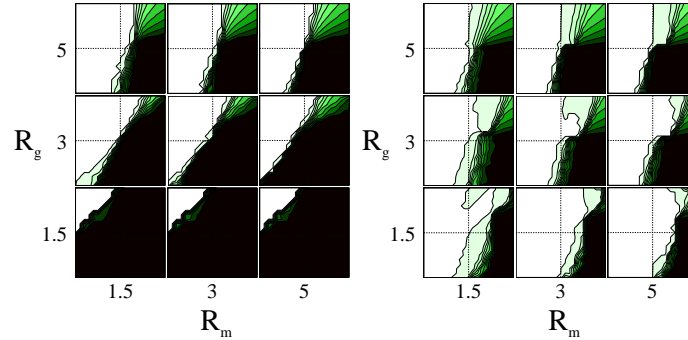
Fig. 6.4 (Color online) Average cooperation levels with IB strategy revision rule as a function of R_g and R_m with $p = 0.5$ and $\rho = 0.1$. Left image: Random migration. Right image: best fitness migration rule. The size of the population is 1000 players. In all cases the initial fraction of cooperators is 0.5 randomly distributed among the occupied grid points.

The TS-plane has been sampled with a grid step of 0.1 and each value in the phase space reported in the figures is the average of 50 independent runs. The evolution proceeds

by first initializing the population by creating a player in each cell of the underlying lattice with probability ρ. Then the players' strategies are initialized uniformly at random such that each strategy has a fraction of approximately 1/2 unless otherwise stated. For each grid point, agents in the population are chosen sequentially at random with replacement to revise their strategies or positions. Payoffs are constantly updated. To avoid transient states, we let the system evolve for a period of $\tau = 1000$ time steps, for each time step $N = 1000$ players are chosen for update. At this point almost always the system reaches a steady state in which the frequency of cooperators is stable except for small statistical fluctuations. We then let the system evolve for 50 further steps and take the average cooperation value, or the mobility, in this interval. We repeat the whole process 50 times for each grid point and, finally, we report the average cooperation values over those 50 repetitions.

6.3 Results

6.3.1 Strategy Evolution and Mobility

In this section we discuss cooperation results with the IB rule and adaptive migration and explore the influence of different radii R_m and R_g and the density ρ. Fig. 6.3 left image displays the cooperation level in the ST-planes with the IB rule and a density $\rho = 0.5$ for several combinations of R_g and R_m. For the sake of comparison, and in order to have a baseline case, Fig. 6.3 left image shows the case in which migration is not dictated by success but, rather, it is simply random, i.e. the target of migration will be a free cell randomly drawn among those contained in the R_m disk. The right image depicts cooperation levels when migration is success-driven. We see that, for $R_g = 1.5$, full cooperation is achieved in the SH quadrant for all R_m in the case of contingent migration while cooperation is notably lower in the random migration case for all R_m. For the PD cooperation remains nearly constant through R_m for $R_g = 1.5$, or slightly improves with smaller R_m in the contingent migration case with average values in the quadrant of about 0.3. In contrast, it is almost zero in the random diffusion case. Increasing the game radius R_g doesn't help and all average values tend to fall independent of R_m. This is because enlarging the neighborhood of a player is a step towards the mixed population in which cooperation results are worse, as can be seen in Fig. 6.1. We have observed that the increase in cooperation for $R_g = 1.5$ with "intelligent" migration is essentially due to the formation of cooperator clusters that remain relatively stable throughout evolution thanks to the possibility for cooperators to join one of those clusters. With larger R_g values, small cooperator clusters are easier to break and large C clusters, which would help cooperation to establish itself in the cluster, cannot form and defection prevails at least in the PD case. The Hawk-Dove game, due to its mixed-strategy equilibrium benefits less from success-driven migration as the two other games.

Density is a parameter that heavily influences the evolution of cooperation [14, 15], also in the presence of intelligent migration [7, 9]. Too high densities are detrimental because they tend to limit the mobility of agents to a point that only cooperator clusters
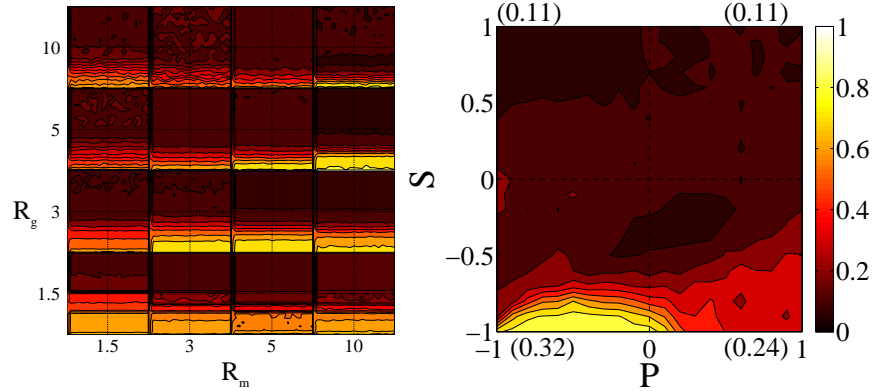
Fig. 6.5 (Color online) Left: average mobility levels in the ST-plane as a function of R_g and R_m. Right: mobility in the SP-plane for $T = 1$, $R_m = 10$ and $R_g = 10$. The best fitness migration rule is used. The size of the population is 1000 players and $\rho = 0.1$. Cooperators fraction is 0.5 randomly distributed among the population. Lighter tones stand for more mobility.

that appear owing to statistical fluctuations in the initial population compositions can eventually remain stable. It appears that low and intermediate densities give more freedom to the population for moving around and to search for better positions. Figure 6.4 right image shows average cooperation results for the IB strategy revision rule and the same combinations of radii but for $\rho = 0.1$ instead of 0.5. With $\rho = 0.1$ cooperation generally increases. In this case defectors attack clusters with a smaller rate since they are more diffused in space and move randomly until they find a cluster of cooperators. The advantage of intelligent migration with respect to random motion is even more marked here by comparing with the left image. In the latter defection appears to be even stronger than in the mixed population, but this is rather special and is due to the fact that the system is very diluted which causes most encounters to be between just two players.

6.3.2 Mobility Only: Emergence of Dynamic Clusters

In this section we study the emergence of dynamic clusters. These clusters are formed by a cohesive group of cooperators followed by defectors. The left image of Fig. 6.5 displays the mobility of nodes (see Sect. 6.5) for several ST-planes as a function of the game and migration radius. Lighter tones stand for higher mobility and indicate that such dynamic clusters may form. It can be observed that the dynamic clusters tend to appear with low S. The horizontal stripes of constant M can be explained by the fact that, as long as $P = 0$, all positive values of T are identical since the best target position for migration remains the same. On the other hand, when P is comparable to T or larger, defectors form clusters among themselves and stop following cooperators, which causes M to decrease. In contrast, when P is negative enough, defectors repel each other and they can not gather behind cooperators. These effects are reflected in the averages shown in the right image of Fig. 6.5.

S=0.5   S=-0.5   S=-1.0
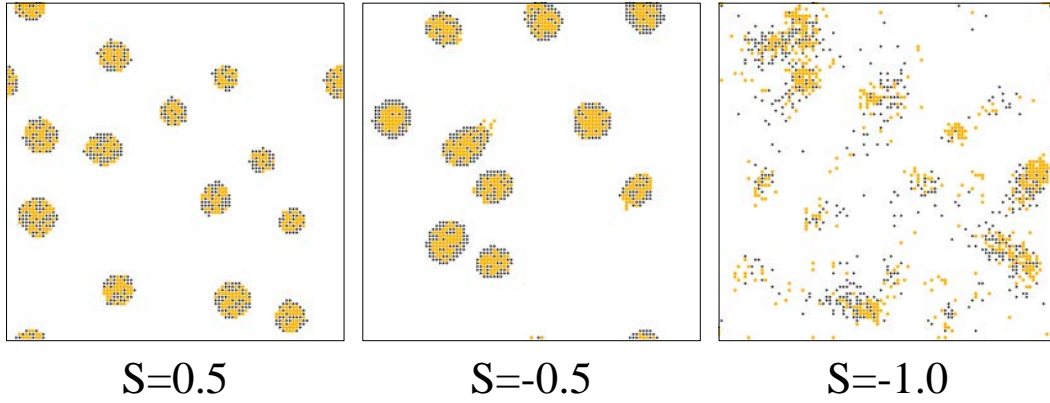
Fig. 6.6 (Color online) Cluster for $R_g = 5$ and $R_m = 10$, $T = 1.5$. Cooperators are represented as orange circles and defectors as black triangles.

$R_g=1.5$ $R_g=3$ $R_g=5$ $R_g=10$ $R_g=20$
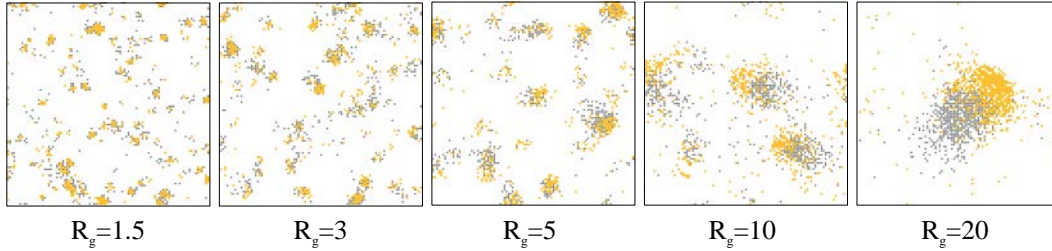
Fig. 6.7 (Color online) Cluster for $R_m = 10$, $T = 1.5$, $S = -1.0$ for different R_g values. Cooperators are represented in orange and defectors in black.

We display dynamic clusters for some particular runs in Figs. 6.6 and 6.7. Figure 6.6 shows clusters that have formed after a number of time steps and that are already stable as a function of S with $R_g = 5$ and $R_m = 10$. The corresponding game can be inferred from Fig. 6.5 left image. From left to right the images show situations with increasing cluster mobility. There is a sort of mobility transition such that, while the first two images show clusters that do not move, the rightmost one corresponds to a situation in which the clusters are much more dynamical.

Figure 6.7 shows the clusters appearance when mobility is high (compare with Fig. 6.5 left image) as a function of the radius of play R_g for the same game as above, which is in the PD region. One can see that there is a direct relationship between increasing R_g and the cluster size. With a given R_m, which is here 10, when R_g is comparatively small, clusters do form but they are continuously destroyed and reformed in an other places without a definite motion.

6.3.2.1 The Effect of Strategy Update

In the limiting case $p \to 1$, i.e. very little strategy update with respect to migration, dynamical patterns form before any significant strategy update. Fig. 6.8 displays the ST-plane in that case. It can be observed that cooperation is lost for the lower values of S. This loss of cooperation can be related to an increase in mobility by comparing Fig. 6.4 (right) with Fig. 6.8 and by remarking that the loss of cooperation between these two cases correspond to the relatively high levels of mobility seen in Fig. 6.5 for this area of the game space. In the case $p = 0.5$ the dynamical patterns cannot fully form since the strategy evolution is too fast. In fact as clusters of cooperators form defectors are attracted towards them. Considering only the case in which cooperation thrives, if p is small enough the incoming defectors are transformed into cooperators directly while approaching the cluster. Thus the cluster remains static and grows. On the other hand, when p tends to one, the migrating defectors cumulated around the cluster will eventually cause it to move.
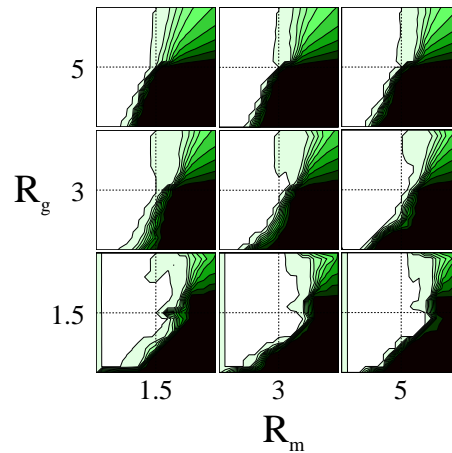
Fig. 6.8 (Color online) Average cooperation levels with best fitness migration rule and IB strategy update rule as a function of R_g and R_m, $\rho = 0.1$, and $p = 0.99$. The size of the population is 1000 players. The initial fraction of cooperators is 0.5 randomly distributed among the occupied grid points.

6.4 Conclusion

In the framework of game theory we have studied the evolution of cooperation in spatially structured populations when a given focal player can only interact with players contained in a radius R_g centered on the focal player that is small with respect to the space available. This locality of interactions is a realistic feature of actual populations and markedly differs from the customary well mixed population. Besides being able to adapt their strategy with probability $1 - p$, in our model players can also move around to unoccupied places in the

underlying two-dimensional grid also with probability p. The amount of displacement is determined by the migration radius R_m. Migration depends on the payoff, i.e. a player that has decided to migrate can examine a number of free positions around it within the radius R_m, earn a potential payoff by fictitious play with the neighbors at that position, and finally choose to migrate to the position that provides the best payoff among those tested. We show that an equal amount of migration and of strategy mutation in the original position gives rise to full cooperation in the SH game space and, to comparatively high values in the more difficult PD game space. This is particularly striking when compared with the baseline case in which strategy revision is identical but migration is to a randomly chosen free cell in the disk of radius R_m.

We have also investigated pattern formation in the population under the effects of intelligent migration only. In this case too we start from a $50 - 50$ random distribution of cooperators and defectors. However, now cooperation cannot evolve since strategy changes are not allowed. What we do observe is a very interesting and intricate phenomenon of dynamical or almost static pattern formation that is related to the underlying game played and that also depends on the R_g and R_m radii. We have analyzed the nature and dynamics of these clusters and we have shown that mobility of agents can be high when the sucker payoffs S reaches negative enough values compared to the reward payoff R. The temptation T has only to be positive as the punishment P is null in our settings. For high interaction radius R_g and migration radius R_m the motion is coherent and the cooperators tend to gather and move in the same direction with swarms of defectors following them. When R_m is small players can be blocked into clusters. On the other hand, when R_g is low and R_m high the clusters are constantly destroyed and reformed in different places. For both R_g and R_m low small clusters are formed and the motion is not definite. Future work should include the study of the effect of strategy update and mobility noise in the dynamics, as well as the use of different strategy update and, possibly, migration rules.

6.5 Acknowledgments

References

[1] C. A. Aktipis. Know when to walk away: contingent movement and the evolution of cooperation. *J. Theor. Biol.*, 231:249–2160, 2004.

[2] R. Axelrod. *The Evolution of Cooperation.* Basic Books, Inc., New-York, 1984.

[3] P. Buesser and M. Tomassini. Evolution of cooperation on spatially embedded networks. *Phys. Rev. E*, 86:066107, 2012.

[4] Z. Chen, J. Gao, Y. Kai, and X. Xu. Evolution of cooperation among mobile agents. *Physica A*, 390:1615–1622, 2011.

[5] M. Enquist and O. Leimar. The evolution of cooperation in mobile organisms. *Anim. Behav.*, 45:747–757, 1993.

[6] D. Helbing and W. Yu. Migration as a mechanism to promote cooperation. *Advances in Complex Systems*, 11:641–652, 2008.

[7] D. Helbing and W. Yu. The outbreak of cooperation among success-driven individuals under noisy conditions. *Proc. Natl. Acad. Sci. USA*, 106:3680–3685, 2009.

[8] J. Hofbauer and K. Sigmund. *Evolutionary Games and Population Dynamics.* Cambridge, N. Y., 1998.

[9] L.-L. Jiang, W.-X. Wang, Y.-C. Lai, and B.-H. Wang. Role of adaptive migration in promoting cooperation in spatial games. *Physical Review E*, 81:036108, 2010.

[10] M. A. Nowak and R. M. May. Evolutionary games and spatial chaos. *Nature*, 359:826–829, October 1992.

[11] M. A. Nowak and K. Sigmund. Games on grids. In U. Dieckmann, R. Law, and J. A. J. Metz, editors, *The Geometry of Ecological Interactions: Simplifying Spatial Complexity*, pages 135–150. Cambridge University Press, Cambridge, UK, 2000.

[12] C. P. Roca, J. A. Cuesta, and A. Sánchez. Evolutionary game theory: temporal and spatial effects beyond replicator dynamics. *Physics of Life Reviews*, 6:208–249, 2009.

[13] F. C. Santos, J. M. Pacheco, and T. Lenaerts. Evolutionary dynamics of social dilemmas in structured heterogeneous populations. *Proc. Natl. Acad. Sci. USA*, 103:3490–3494, 2006.

[14] E. A. Sicardi, H. Fort, M. H. Vainstein, and J. J. Arenzon. Random mobility and spatial structure often enhance cooperation. *J. Theor. Biol.*, 256:240–246, 2009.

[15] M. H. Vainstein, A. T. C. Silva, and J. J. Arenzon. Does mobility decrease cooperation? *J. Theor. Biol.*, 244:722–728, 2007.

[16] F. Vega-Redondo. *Economics and the Theory of Games.* Cambridge University Press, Cambridge, UK, 2003.

[17] J. W. Weibull. *Evolutionary Game Theory.* MIT Press, Boston, MA, 1995.

Chapter 7

Opportunistic Migration in Spatial Evolutionary Games

Abstract We study evolutionary games in a spatial diluted grid environment in which agents strategically interact locally but can also opportunistically move to other positions within a given migration radius. Using the imitation of the best rule for strategy revision, it is shown that cooperation may evolve and be stable in the Prisoner's Dilemma game space for several migration distances but only for small game interaction radius while the Stag Hunt class of games become fully cooperative. We also show that only a few trials are needed for cooperation to evolve, i.e. searching costs are not an issue. When the stochastic Fermi strategy update protocol is used cooperation cannot evolve in the Prisoner's Dilemma if the selection intensity is high in spite of opportunistic migration. However, when imitation becomes more random, fully or partially cooperative states are reached in all games for all migration distances tested and for short to intermediate interaction radii.

7.1 Introduction

Spatially embedded systems are very important in biological and social sciences since most interactions among living beings or artificial actors take place in physical two- or three-dimensional space [7]. Along these lines, game-theoretical interactions among spatially embedded agents distributed according to a fixed structure in the plane have been studied in detail, starting from the pioneering works of Axelrod [2] and Nowak and May [15]. The related literature is very large; see, for instance, the review article by Nowak and Sigmund [16] and references therein for a synthesis. Most of this work was based on populations of agents arranged according to planar regular grids for mathematical simplicity and ease of numerical simulation. Recently, some extensions to more general spatial networks have been discussed in [3]. The study of strategic behavior on fixed spatial structures is necessary in order to understand the basic mechanisms that may lead to socially efficient global outcomes such as cooperation and coordination. However, in the majority of real situations both in biology and in human societies, actors have the possibility to move around in space. Many examples can be found in biological and ecological sciences, in human populations, and in engineered systems such as ad hoc networks of mobile communicating devices or robot teams. Mobility may have positive or negative effects on cooperation, depending on several factors. An early investigation was carried out by En-

quist and Leimar [9] who concluded that mobility may seriously restrict the evolution of cooperation. In the last decade there have been several new studies of the influence of mobility on the behavior of various games in spatial environments representing essentially two strands of research: one in which the movement of agents is seen as a random walk, and a second one in which movement may contain random elements but it is purposeful, or strategy-driven.

Random diffusion of mobile agents through space, either in continuous space or, more commonly, on diluted grids has been investigated in [14, 19, 20]. In the present study we focus on situations where, instead of randomly diffusing, agents possess some basic cognitive abilities and they actively seek to improve their situation by moving in space represented as a discrete grid in which part of the available sites are empty and can thus be the target of the displacement. This approach has been followed, for example, in [1, 4, 5, 6, 8, 10, 11, 13]. The mechanisms invoked range from success-driven migration [11], adaptive migration [13], reputation-based migration [6], risk-based migration [4], flocking behavior [5], and cooperators walking away from defectors [1]. In spite of the difference among the proposed models, the general qualitative message of this work is that purposeful contingent movement may lead to highly cooperating stable or quasi-stable population states if some conditions are satisfied. Another related line of research has dealt with the case in which the grid is diluted but there is no migration. Recent work has shown that in this case cooperation is optimally promoted when the population density is close to the percolation threshold of the lattice [22, 23]. This interesting result could be somehow seen as a base case in the study of cooperation in diluted lattices with migration.

Our approach is based on numerical simulation and is inspired by the work of Helbing and Yu [10, 11] which they call "success-driven migration" and which has been shown to be able to produce highly cooperative states. In this model, locally interacting agents playing either defection or cooperation in a two-person Prisoner's Dilemma are initially randomly distributed on a grid such that there are empty grid points. Agents update their strategies according to their own payoff and the payoff earned by their first neighbours but they can also "explore" an extended square neighborhood by testing all the empty positions up to a given distance. If the player finds that it would be more profitable to move to one of these positions then she does it, choosing the best one among those tested, otherwise she stays at her current place. Helbing and Yu find that robust cooperation states may be reached by this mechanism, even in the presence of random noise in the form of random strategy mutations and random agent relocation. Our study builds upon this work in several ways. In the first place, whilst Helbing and Yu had a single game neighborhood and migration neighborhood, we systematically investigate these two parameters showing that only some combination do foster cooperation using success-driven migration. Secondly, cost issues are not taken into account in [11]. However, it is clear that moving around to test the ground is a costly activity. In a biological setting, this could mean using up energy coming from metabolic activity, and this energy could be in short supply. In a human society setting, it is the search time that could be limited in a way or another. Additionally to physical energy, cognitive abilities could also limit the search. We present results for a whole game phase space including the Hawk-Dove class of games, and the Stag Hunt coordination class. Helbing's and Yu's agents based their strategy change on the imitation of the most successful neighbour in terms of accumulated payoff. We kept this rule but also added the

Fermi strategy-updating rule, a choice that allows us to introduce a parametrized amount of imitation noise. With the imitiation of the best policy we find that cooperation prevails in the Stag Hunt and may evolve in the Prisoner's Dilemma for small interaction radius. With the Fermi rule fully cooperative states are reached for the standard neighborhoods independently of the migration distances when the rate of random strategy imitation is high enough.

7.2 Methods

7.2.1 The Games Studied

We investigate three classical two-person, two-strategy, symmetric games classes, namely the Prisoner's Dilemma (PD), the Hawk-Dove Game (HD), and the Stag Hunt (SH). These three games are simple metaphors for different kinds of dilemmas that arise when individual and social interests collide. The Harmony game (H) is included for completeness but it doesn't originate any conflict. The main features of these games are well known; more detailed accounts can be found elsewhere e.g. [12, 21, 24]. The games have the generic payoff matrix M (equation 8.1) which refers to the payoffs of the row player. The payoff matrix for the column player is simply the transpose $M^\top$ since the game is symmetric.

$$
\begin{array}{c}
\quad C \quad\ D \\
\begin{array}{c} C \\ D \end{array}
\begin{pmatrix} R & S \\ T & P \end{pmatrix}
\end{array}
\tag{7.1}
$$

The set of strategies is $\Lambda = \{C, D\}$, where C stands for "cooperation" and D means "defection". In the payoff matrix R stands for the *reward* the two players receive if they both cooperate, P is the *punishment* if they both defect, and T is the *temptation*, i.e. the payoff that a player receives if he defects while the other cooperates getting the *sucker's payoff* S. For the PD, the payoff values are ordered such that $T > R > P > S$. Defection is always the best rational individual choice, so that (D, D) is the unique Nash Equilibrium (NE). In the HD game the payoff ordering is $T > R > S > P$. Thus, when both players defect they each get the lowest payoff. (C, D) and (D, C) are NE of the game in pure strategies. There is a third equilibrium in mixed strategies which is the only dynamically stable equilibrium [12, 24]. In the SH game, the ordering is $R > T > P > S$, which means that mutual cooperation (C, C) is the best outcome and a NE. The second NE, where both players defect is less efficient but also less risky. The third NE is in mixed strategies but it is evolutionarily unstable [12, 24]. Finally, in the H game $R > S > T > P$ or $R > T > S > P$. In this case C strongly dominates D and the trivial unique NE is (C, C). The game is non-conflictual by definition; it is mentioned to complete the quadrants of the parameter space.

There is an infinite number of games of each type since any positive affine transformation of the payoff matrix leaves the NE set invariant [24]. Here we study the customary standard parameter space [17, 18], by fixing the payoff values in the following way: $R = 1$, $P = 0$, $-1 \leq S \leq 1$, and $0 \leq T \leq 2$. Therefore, in the TS plane each game class corresponds to a different quadrant depending on the above ordering of the payoffs as depicted in Fig. 7.1,

left image. The right image depicts the well mixed replicator dynamics stable states for future comparison.
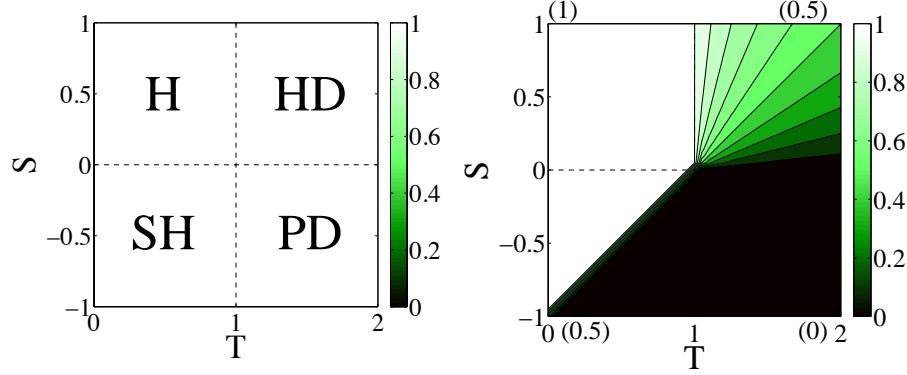
Fig. 7.1 (Color online) Left image: The games phase space (H= Harmony, HD = Hawk-Dove, PD = Prisoner's Dilemma, and SH = Stag Hunt) as a function of S, T ($R = 1$, $P = 0$). Right image: replicator dynamics stable states [12, 24] with 50% cooperators and defectors initially in a well mixed population for comparison purposes. Lighter tones stand for more cooperation. Values in parentheses next to each quadrant indicate average cooperation in the corresponding game space.

7.2.2 Population Structure

The Euclidean two-dimensional space is modeled by a discrete square lattice of side L with toroidal borders. Each vertex of the lattice can be occupied by one player or be empty. The *density* is $\rho = N/L^2$, where $N \leq L^2$ is the number of players. Players can interact with k neighbours which lie at an Euclidean distance smaller or equal than a given constant R_g. Players can also migrate to empty grid points at a distance smaller than R_m. We use three neighborhood sizes with radius 1.5, 3, and 5; they contain, respectively, 8, 28, and 80 neighbours around the central player.

7.2.3 Payoff Calculation and Strategy Update Rules

Each agent i interacts locally with a set of neighbours V_i lying closer than R_g. Let $\sigma_i(t)$ be a vector giving the strategy profile at time t with $C = (1, 0)$ and $D = (0, 1)$ and let M be the payoff matrix of the game (equation 8.1). The quantity

$$\Pi_i(t) = \sum_{j \in V_i} \sigma_i(t) \ M \ \sigma_j^\top(t) \tag{7.2}$$

is the cumulated payoff collected by player i at time step t.

We use two imitative strategy update protocols. The first is the Fermi rule in which the focal player i is given the opportunity to imitate a randomly chosen neighbour j with probability:

$$p(\sigma_i \to \sigma_j) = \frac{1}{1 + exp(-\beta(\Pi_j - \Pi_i))} \tag{7.3}$$

where $\Pi_j - \Pi_i$ is the difference of the payoffs earned by j and i respectively and β is a constant corresponding to the inverse temperature of the system. When $\beta \to 0$ the probability of imitating j tends to a constant value 0.5 and when $\beta \to \infty$ the rule becomes deterministic: i imitates j if $(\Pi_j - \Pi_i) > 0$, otherwise it doesn't. In between these two extreme cases the probability of imitating neighbour j is an increasing function of $\Pi_j - \Pi_i$. The second imitative strategy update protocol is to switch to the strategy of the neighbour that has scored best in the last time step. In contrast with the previous one, this rule is deterministic. This *imitation of the best* (IB) policy can be described in the following way: the strategy $\sigma_i(t)$ of individual i at time step t will be

$$\sigma_i(t) = \sigma_j(t-1), \tag{7.4}$$

where

$$j \in \{V_i \cup i\} \; s.t. \; \Pi_j = \max\{\Pi_k(t-1)\}, \; \forall k \in \{V_i \cup i\}. \tag{7.5}$$

That is, individual i will adopt the strategy of the player with the highest payoff among its neighbours including itself. If there is a tie, the winner individual is chosen uniformly at random.

7.2.4 Population Dynamics and Opportunistic Migration

We use an asynchronous scheme for strategy update and migration, i.e. players are updated one by one by choosing a random player in each step with uniform probability and with replacement. Then the player migrates with probability 1/2, otherwise it updates its strategy. If the pseudo-random number drawn dictates that i should migrate, then it considers N_{test} randomly chosen positions in the disc of radius R_m around itself. The quantity N_{test} could be seen as a kind of "energy" available to a player for moving around and doing its search. N_{test} being fixed for a given run, it follows that an agent will be able to make a more complete exploration of its local environment the smaller the R_m. For each trial position the player computes the payoff that it would obtain in that place with its current strategy. The positions already occupied are just discarded from the possible choices. Then player i stays at its current position if it obtains there the highest payoff, or migrates to the most profitable position among those explored during the test phase. If several positions, including its current one, share the highest payoff then it chooses one at random. We call this migration *opportunistic* or *fitness-based*. The protocol described in Helbing and Yu [11] is slightly different: the chosen player chooses the strategy of the best neighbour including itself with probability $1 - r$, and with probability r, with $r \ll 1 - r$, its strategy is randomly reset. Before this imitation step i deterministically chooses the highest payoff free position in a square neighborhood of size $(2M + 1) \times (2M + 1)$ cells

surrounding the current player and including itself, where M can take the values $0, 1, 2, 5$. If several positions provide the same payoff, the one that is closer is selected.

7.2.5 Simulation Parameters

The TS plane has been sampled with a grid step of 0.1 and each value in the phase space reported in the figures is the average of 50 independent runs. The evolution proceeds by first initializing the population by distributing $N = 1000$ players with uniform probability among the available cells. Then the players' strategies are initialized uniformly at random such that each strategy has a fraction of approximately $1/2$. To avoid transient states, we let the system evolve for a period of $\tau = 1000$ time steps and, in each time step, N players are chosen for update. At this point almost always the system reaches a steady state in which the frequency of cooperators is stable except for small statistical fluctuations. We then let the system evolve for 50 further steps and take the average cooperation value in this interval. We repeat the whole process 50 times for each grid point and, finally, we report the average cooperation values over those 50 repetitions.

7.3 Results

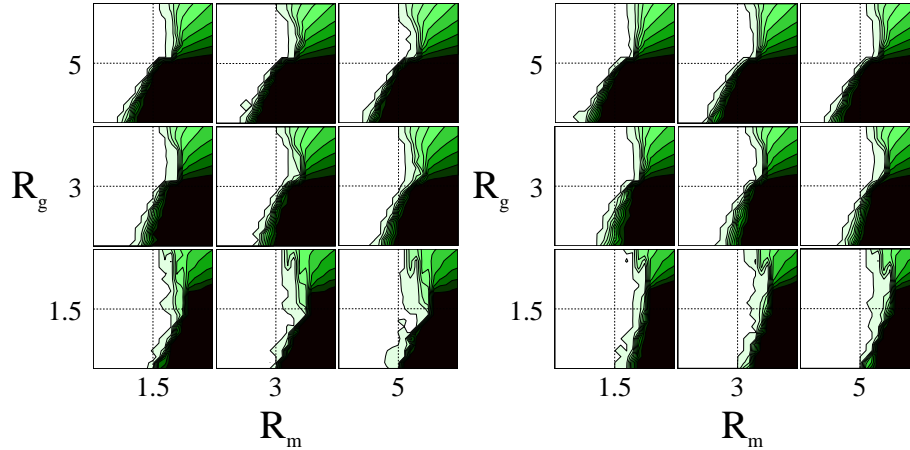### 7.3.1 Imitation of the Best and Opportunistic Migration

Fig. 7.2 (Color online) Average cooperation levels with opportunistic migration and IB rule as a function of R_g and R_m. Left: $N_{test} = 20$; Right: $N_{test} = 1$. The size of the population is 1000 players and the density ρ is 0.5. In all cases the initial fraction of cooperators is 0.5 randomly distributed among the occupied grid points.

In this section we study cooperation with the IB rule and fitness-based opportunistic migration, and we explore the influence of different radii R_m and R_g and other parameters such as the density ρ and the number of trials N_{test}. The left image of Fig. 7.2 displays the TS plane with the IB rule, a density $\rho = 0.5$, and $N_{test} = 20$. For small $R_g = 1.5$ full cooperation is achieved in the SH quadrant for all R_m. The average levels of cooperation in the PD games are $0.33, 0.31, 0.30$ for $R_m = 1.5, 3, 5$ and $R_g = 1.5$ respectively. It is remarkable that cooperation emerges in contrast to the well mixed population case (Fig. 7.1, right image), and also that better results are obtained with respect to a fully populated grid in which agents cannot move [17]. The HD doesn't benefit in the same way and the cooperation levels are almost the same in the average. Cooperation remains nearly constant as a function of R_m for a given R_g value but increasing R_g has a negative effect. For higher game radius, $R_g \in \{3, 5\}$ cooperation is progressively lost in the PD games while there is little variation in the HD quadrant among the different cases due to the dimorphic structure of these populations. In the SH quadrant there is a large improvement compared to the well mixed case but the gain tends to decrease with increasing R_g. In the PD with high R_g, cooperators cannot increase their payoff by clustering, since the neighborhood of defectors covers adjacent small clusters of cooperators, the payoff of defectors becomes higher and they can invade cooperators clusters. Figure 7.3 illustrates in an idealized manner what happens to a small cooperators cluster when the game radius R_g increases using a full grid for simplicity. For $R_g = 1.5$ (left image) the cooperator cluster is stable
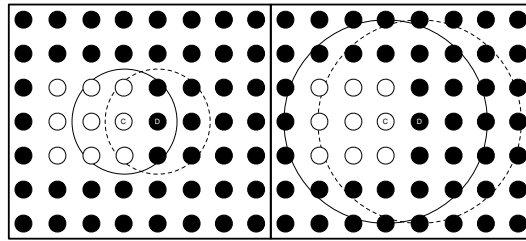
Fig. 7.3 Illustration of the effect of the playing radius R_g on the payoff of individuals. Left image: $R_g = 1.5$, righ image: $R_g = 3$. The drawings refer to a locally full grid and are intended for illustrative purposes only (see text).

as long as $8R > 3T$ since the central cooperator gets a payoff of $8R$, while the best payoff among the defectors is obtained by the individual marked D (and by the symmetrically placed defectors) and is equal to $3T$ since $P = 0$. Under this condition all the cooperators will thus imitate the central one. On the other hand, the defector will turn into a C as long as $5R + 3S > 3T$, thus provoking cooperator cluster expansion for parameter values in this range. On the contrary, for $R_g = 3$ (right image) the central cooperator gets $8R + 20S$ whilst the central defector at the border has a payoff of $7T$. Thus the cooperator imitates the defector if $7T > 8R + 20S$, i.e. $7T > 8 + 20S$ since $R = 1$. This qualitative argument helps to explain the observed cooperation losses for increasing R_g.

This inequality is satisfied almost everywhere in the PD quadrant except in a very small area in its upper left corner.

Helbing and Yu [11] found very encouraging cooperation results in their analysis but they only had a small game radius corresponding to the Von Neumann neighborhood which is constituted, in a full lattice, by the central individual and the four neighbours at distance one situated north, east, south, and west. We also find similar results for our smallest neighborhood having $R_g = 1.5$, which corresponds to the eight-points Moore neighborhood but, as R_g gets larger, we have just seen that a sizable portion of the cooperation gains are lost. We think that this is an important point since there are certainly situations in which those more extended neighborhoods are the natural choice in a spatially extended population.
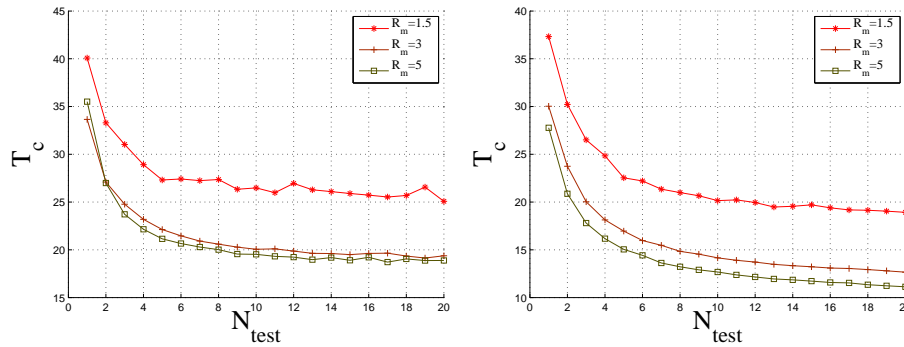

Fig. 7.4 (Color online) Average convergence time T_c with IB rule as a function of N_{test} for $R_g = 1.5$ and $R_m = 1.5, 3, 5$. Left image: $S = -0.5$, $T = 0.5$. Right image: $S = -0.1$, $T = 1.1$. The time to convergence is defined as the number of simulation steps needed for the number of cooperators N_c or defectors N_d to be smaller than $0.1N$. Times of convergence are averaged over 500 independent runs.

The number of trials N_{test} could also be a critical parameter in the model. The right image of Fig. 7.2 refers to the same case as the left one, i.e. the IB update rule with opportunistic migration and $\rho = 0.5$, except for the number of trials which is one instead of 20. We observe that practically the same cooperation levels are reached at steady state in both cases for $R_m = 5$ and $R_m = 3$, while there is a small increase of the average cooperation in the PD games for $R_g = 1.5$ which goes from 0.33, 0.31, and 0.30 for $N_{test} = 20$ to 0.41, 0.36, and 0.33 for $N_{test} = 1$, for $R_m = 1.5, 3, 5$ respectively. On the whole, it is apparent that N_{test} does not seem to have a strong influence. However, one might ask whether the times to convergence are shorter when more tests are used, a fact that could compensate for the extra work spent in searching. But Figs. 7.4 show that convergence times are not very different and decrease very quickly with the number of essays N_{test}. This is shown for two particular games, one in the middle of the SH quadrant (left image), and the other near the upper left corner of the PD space (right image). Thus, a shorter time does not compensate for the wasted trials. Since moving around to find a better place is a costly activity in any real situation, this result is encouraging because it says that searching more intensively doesn't change the time to convergence for more than four tests. Thus, quite high levels of cooperation can be achieved by opportunistic

migration at low search cost, a conclusion that interestingly extends the results presented in [11].

In diluted grids, density is another parameter that influences the evolution of cooperation [19, 20], also in the presence of intelligent migration [11, 13]. Too high densities should be detrimental because clusters of cooperators are surrounded by a dense population of defectors, while low densities allow cooperator clusters to have less defectors in their neighborhood once they are formed. We have performed numerical simulations for two other values of the density besides 0.5, $\rho = 0.2$ and $\rho = 0.8$. We do not show the figures to save space but the main remark is that there is a monotone decrease of cooperation going from low to higher densities in the low S region that influences mainly the PD and, to a smaller extent, the SH games.

7.3.2 Opportunistic Migration and Noisy Imitation

In this section we use the more flexible strategy update protocol called the Fermi rule which was described in Sect. 7.2.3 and in which the probability to imitate a random neighbour's strategy depends on the parameter β. We have seen that using the IB rule with adaptive migration leads to full cooperation in the SH quadrant and improves cooperation in a part of the PD quadrant (Fig. 7.2). This result does not hold with the Fermi rule with $\beta \geq 1$, and we are back to full defection in the PD and almost 50% cooperation as in the well mixed case in the SH; this behavior can be appreciated in the leftmost image of Fig. 7.5.
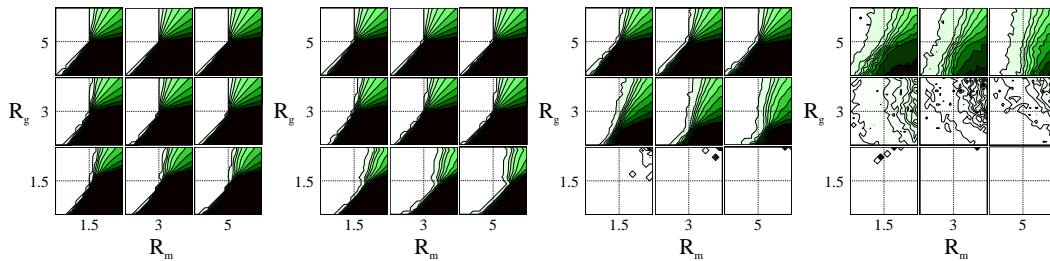
Fig. 7.5 (Color online) Average cooperation levels with opportunistic migration and the Fermi rule as a function of R_g and R_m. From left to right $\beta = 1.0, 0.1, 0.01, 0.001$. The density ρ is 0.5 and $N_{test} = 20$. The size of the population is 1000 players. In all cases the initial fraction of cooperators is 0.5 randomly distributed among the population.

An interesting new phenomenon appears when β becomes small, of the order of 10^{-2}. In this case, the levels of cooperation increase in all games for R_g values up to 3 and cooperation raises to almost 100% in all game phase space for $R_g = 1.5$, for all migration radii, see the third image of Fig. 7.5. The positive trend continues with decreasing β (see rightmost image) and cooperation prevails almost everywhere. As we said above, the Fermi rule with $\beta = 0.01$ or less implies that the decision to imitate a random neighbour becomes almost random itself. Thus, the spectacular gains in cooperation must depend

in some way from opportunistic migration for the most part. Figure 7.6 illustrates the dynamical behavior of a particular case in the PD space. Here $T = 1.5$, $S = -0.5$, $R = 1$, $P = 0$; that is, the game is in the middle of the PD quadrant. The other parameters are: $\beta = 0.01$, $R_g = 1.5$, and $R_m = 3$. This particular game would lead to full defection in almost all cases but here we can see that it leads to full cooperation instead.

t=0   t=1   t=20   t=150

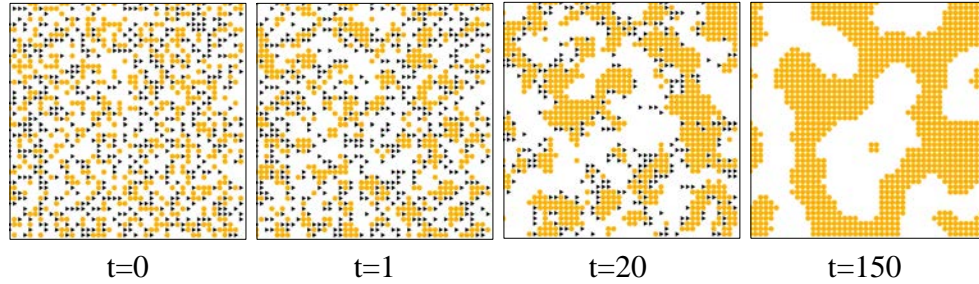**Fig. 7.6** (Color online). Time evolution for the case of a PD with $T = 1.5$, $S = -0.5$, $R = 1$, $P = 0$. Here $\beta = 0.01$, $R_g = 1.5$, $R_m = 3$. The density $\rho = 0.5$ and $N_{test} = 20$. There are 1000 players and the strategies are initially attributed uniformly at random in a $50 - 50$ proportion.

This is a surprising phenomenon that needs an explanation. At the beginning, due to opportunistic migration, cooperators will be likely to form small clusters between themselves more than defectors, as the latter tend to follow cooperators instead of clustering between themselves since the (D, D) payoff is equal to 0. The low β value will make strategy change close to random and thus strategy update will have a neutral effect. Indeed, as soon as cooperator clusters form due to migration, defectors that enter a cooperator cluster thanks to random imitation cannot invade them. The situation there is akin to a full grid and the number of defectors inside the cluster will fluctuate. Meanwhile, defectors at the border of a cooperator cluster will steadily turn into cooperators thus extending the cluster. This is due to the fact that lone defectors at the border will tend to imitate cooperators since defectors are less connected, and strategy imitation is almost random. Finally, the defectors inside the clusters will reach the border and turn into cooperators as well. The phenomenon is robust with respect to the migration radius R_m, as can be seen in the lower part of the third and fourth images of Fig. 7.5. Cooperation prevails even when P becomes positive which increases the payoff for defectors to aggregate. We have simulated the whole phase space for $P = 0.2$ and $P = -0.2$. The results are similar to those with $P = 0$ except that cooperation decreases slightly with increasing P. On the same images it can be seen that the game radius R_g has a large influence and cooperation tends to be lost for radii larger than 1.5. The reasons for this are very similar to those advocated in Sect. 7.3.1 where Fig. 7.3 schematically illustrates the fact that increasing R_g makes the situation more similar to a well mixed population. In these conditions, the payoff-driven strategy imitation process becomes more important and may counter the benefits of opportunistic migration. However, since we believe that system possessing locality are important in practice, the findings of this section seem very encouraging for

mobile agents that are better at finding more profitable positions and moving to them rather than at strategic reasoning.

7.4 Discussion and Conclusions

In this work we have explored some possibilities that arise when agents playing simple two-person, two-strategy evolutionary games may also move around in a certain region seeking better positions for themselves. The games examined are the standard ones, like the Prisoner's Dilemma, the Hawk-Dove, or the Stag Hunt. In this context, the ability to move around in space is extremely common in animal as well as human societies and therefore its effect on global population behavior is an interesting research question. As already pointed out by other researchers [1, 5, 6, 10, 11, 13], adding a form of contingent mobility may result in better capabilities for the population to reach socially valuable results. Among the existing models, we have started from a slightly modified form of the interesting Helbing's and Yu's model [11] and have explored some further avenues that were left untouched in the latter work. In the model agents live and move in a discrete two-dimensional grid space in which part of the cells are unoccupied. Using a strategy update rule that leads an agent to imitate her most successful neighbour as in [11], and having the possibility to explore a certain number of free positions around oneself to find a better one, the gains in cooperative behavior are appreciable in the Prisoner's Dilemma, in qualitative agreement with [11]. In the Hawk-Dove games the gains in cooperation are small but, in addition, we find that cooperation is fully promoted in the class of Stag Hunt games which were not considered in [11]. In Helbing and Yu the exploration of the available cells in search of a better one was fixed and deterministic. The question of the amount of effort needed to improve the agent's situation was left therefore open, although this is clearly an important point, given that in the real world more exploration usually entails an increasing cost be it in terms of energy, time, or money. By using a similar search strategy but to random positions within a given radius, and by varying the number of searches available to the agent, we have seen that the convergence times to reach a given average level of cooperation do not degrade significantly by using fewer trials. This is a reassuring finding, given the above remarks related to the search cost.

Helbing and Yu explored migration effects under a number of sizes of the square neighborhood around a given agent. However, they only had a single neighborhood for the game interactions, the standard five-cells Von Neumann neighborhood. We have explored this aspect more deeply and presented results for several combinations of game radius R_g and migration radius R_m. In fact, it turns out that increasing the interaction radius has an adverse effect on cooperation to the point that, at $R_g = 5$, cooperation levels are similar to those of a well mixed population, in spite of fitness-based migration. Thus, positive results are only obtained when agents interact locally in a relatively small neighborhood which, fortunately, seems to be a quite common condition in actual spatial systems.

Most importantly, we have explored another important commonly used strategy update rule, the Fermi rule. This rule is also imitative but allows to control the intensity of selection by varying a single parameter β. When β is high, i.e. larger than one, almost all

the cooperation gains observed with the imitation of the best rule are lost and we are back to a scenario of defection in the Prisoner's Dilemma space and the Stag Hunt games are also influenced negatively. Migration does not help in this case. However, when β is low, of the order of 0.01, a very interesting phenomenon emerges: cooperation prevails everywhere in the game space for small game radius and for all migration radii, including in the PD space, which is notoriously the most problematic class of games. With $\beta = 0.01$ or lower the strategy update is close to random; however, fitness-based migration is active and thus we see that migration, and not strategy update, is the main force driving the population towards cooperation and we have hypothesized a qualitative mechanism that could explain this striking result. Cooperation is robust with respect to the migration radius R_m but increasing R_g affects the results negatively for $R_g \geq 3$. The effect is mitigated the more random the strategy update, i.e. by further decreasing β.

7.4.1 Acknowledgments

References

[1] C. A. Aktipis. Know when to walk away: contingent movement and the evolution of cooperation. *J. Theor. Biol.*, 231:249–2160, 2004.
[2] R. Axelrod. *The Evolution of Cooperation.* Basic Books, Inc., New-York, 1984.
[3] P. Buesser and M. Tomassini. Evolution of cooperation on spatially embedded networks. *Phys. Rev. E*, 86:066107, 2012.
[4] X. Chen, A. Szolnoki, and M. Perc. Risk-driven migration and the collective-risk social dilemma. *Phys. Rev. E*, 86:036101, 2012.
[5] Z. Chen, J. Gao, Y. Kai, and X. Xu. Evolution of cooperation among mobile agents. *Physica A*, 390:1615–1622, 2011.
[6] R. Cong, B. Wu, Y. Qiu, and L. Wang. Evolution of cooperation driven by reputation-based migration. *PLOS ONE*, 7(5):35776, 2012.
[7] U. Dieckmann, R. Law, and J.A.J. Metz (Eds). *The Geometry of Ecological Interactions: Simplifying Spatial Complexity.* Cambridge University Press, Cambridge, 2000.
[8] M. Droz, J. Szwabiński, and G. Szabó. Motion of influential players can support cooperation in prisoner's dilemma. *Eur. Phys. J. B*, 71:579–585, 2012.
[9] M. Enquist and O. Leimar. The evolution of cooperation in mobile organisms. *Anim. Behav.*, 45:747–757, 1993.
[10] D. Helbing and W. Yu. Migration as a mechanism to promote cooperation. *Advances in Complex Systems*, 11:641–652, 2008.
[11] D. Helbing and W. Yu. The outbreak of cooperation among success-driven individuals under noisy conditions. *Proc. Natl. Acad. Sci. USA*, 106:3680–3685, 2009.

[12] J. Hofbauer and K. Sigmund. *Evolutionary Games and Population Dynamics*. Cambridge, N. Y., 1998.

[13] L.-L. Jiang, W.-X. Wang, Y.-C. Lai, and B.-H. Wang. Role of adaptive migration in promoting cooperation in spatial games. *Physical Review E*, 81:036108, 2010.

[14] S. Meloni, A. Buscarino, L. Fortuna, M. Frasca, J. Gómez-Gardeñes, V. Latora, and Y. Moreno. Effects of mobility in a population of Prisoner's Dilemma players. *Phys. Rev. E*, 79:067101, 2009.

[15] M. A. Nowak and R. M. May. Evolutionary games and spatial chaos. *Nature*, 359:826–829, October 1992.

[16] M. A. Nowak and K. Sigmund. Games on grids. In U. Dieckmann, R. Law, and J. A. J. Metz, editors, *The Geometry of Ecological Interactions: Simplifying Spatial Complexity*, pages 135–150. Cambridge University Press, Cambridge, UK, 2000.

[17] C. P. Roca, J. A. Cuesta, and A. Sánchez. Evolutionary game theory: temporal and spatial effects beyond replicator dynamics. *Physics of Life Reviews*, 6:208–249, 2009.

[18] F. C. Santos, J. M. Pacheco, and T. Lenaerts. Evolutionary dynamics of social dilemmas in structured heterogeneous populations. *Proc. Natl. Acad. Sci. USA*, 103:3490–3494, 2006.

[19] E. A. Sicardi, H. Fort, M. H. Vainstein, and J. J. Arenzon. Random mobility and spatial structure often enhance cooperation. *J. Theor. Biol.*, 256:240–246, 2009.

[20] M. H. Vainstein, A. T. C. Silva, and J. J. Arenzon. Does mobility decrease cooperation? *J. Theor. Biol.*, 244:722–728, 2007.

[21] F. Vega-Redondo. *Economics and the Theory of Games*. Cambridge University Press, Cambridge, UK, 2003.

[22] Z. Wang, A. Szolnoki, and M. Perc. If players are sparse social dilemmas are too: Importance of percolation for evolution of cooperation. *Scientific Reports*, 2:369, 2009.

[23] Z. Wang, A. Szolnoki, and M. Perc. Percolation threshold determines the optimal population density for public cooperation. *Phys. Rev. E*, 85:037101, 2012.

[24] J. W. Weibull. *Evolutionary Game Theory*. MIT Press, Boston, MA, 1995.

Part III
Cyclic Games and Opportunistic Migration

Chapter 8

The Role of Opportunistic Migration in Cyclic Games

Abstract We study cyclic evolutionary games in a spatial diluted grid environment in which agents strategically interact locally but can also opportunistically move to other positions within a given migration radius. We find that opportunistic migration can inverse the cyclic prevalence between the strategies when the frequency of random imitation is large enough compared to the payoff-driven imitation. At the transition the average size of the patterns diverges and this threatens diversity of strategies.

8.1 Introduction

Cyclic behavior can be observed in evolutionary games when there are more than two strategies available to the players, a well-known case being the *Rock-Scissors-Paper* (RSP) class of games [8]. This behavior is not only of theoretical interest since it is partly responsible for the biodiversity on Earth, and has been actually observed in several biological situations such as the dynamic behavior of side-blotched lizards populations [18], coral reef invertebrates [10], and competition among different bacteria strands [13] among others. These games have been studied extensively both theoretically and by computer simulations. Rigorous results are available for well mixed populations in the infinite population size limit pointing to the fact that the system may converge toward a stable or Lyapunov stable interior rest point, or to an unstable rest point leading to an heteroclinic cycle, depending on the relative values of the payoffs (see, for example, [8, 16, 19]). Cyclic behavior has also been found in studies of the public goods game type when players, besides being able to choose between cooperating or defecting behavior, also have the choice of not taking part in the game (so-called "loner" strategy) [6]. Interestingly, a little later this oscillating behavior was actually observed in an experiment with human subjects by D. Semman et al. [17]. Likewise, in a spatial setting such as two-dimensional grids or, more generally, on relational networks, several results have been obtained. Szabó and Hauert [20] and Szabó and Vukov [22] studied the Prisoner's Dilemma on two-dimensional grids with three strategies: cooperate, defect, and loners and observed that the three strategies survive in a cyclic dominance way akin to the RSP game. A similar phenomenon manifests itself on random graphs but with different characteristics. In [21] Szabó et al. investigated the behavior of the RSP game on regular small-world networks. In more recent work A.

Szolnoki and coworkers have further studied the evolutionary Prisoner's Dilemma on spatial grids and random graphs showing that with a third tit-for-tat strategy the system can show a variety of interesting behaviors including stationary and oscillatory states [23]. When agents can only cooperate or defect but have time-dependent learning capabilities Szolnoki et al. [24] showed that cooperator and defectors can coexist and propagating waves appear in the spatially extended system.

In another strand of research players also have the possibility of moving around in space, a feature that is central in ecosystems. Spatial travelling waves and cyclic dominance are typical features of these more biologically realistic settings which are often based on stochastic partial differential equations discretized on a grid to model random diffusion [14, 15]. Another recent paper employs a continuous time space/time formalism in the RSP game with a non-diffusive spatial component [5]. The spatial flux is based on local gradients of relative fitness. In this respect, this study is closer to our approach described below but if focuses on pattern formation and dynamics. Indeed, the strategies are distributed at the start and remain fixed. While the system shows the formation of spirals in space for some initial conditions, and of strategy domains for others, since strategy proportions do not change extinction phenomena are absent. Other important recent works dealing with migration in diluted grid systems are [25, 26].

In this paper we present a new model based on RSP games in which agents enjoy mobility but their displacements are not random; rather, they change place in a purposeful manner. Contingent mobility has previously been used under various forms in two-strategies evolutionary games of the Prisoner's Dilemma, Hawk-Dove, or Stag Hunt types [1, 2, 3, 4, 7, 11]. The idea here is that the agents possess some basic reactive or elementary reasoning capability that allow them to sense the situation in their local spatial environment and to employ some simple heuristic to move accordingly. Heuristics range from very simple ones such as cooperators moving away from surrounding defectors when the latter are in the majority [1, 11], to more elaborate ones such as "success-driven migration" where agents may try many destinations in space and choose to jump to the most favorable one in terms of expected payoff [2, 7]. Here agents use a simplified form of an heuristic introduced in [2] which consists in randomly trying one single free position in space within a given migration radius and to move there if it is empty and more profitable than the starting one. Our setting requires minimal rational capabilities on the part of the players but it is clearly not adequate for low-level biological organisms such as bacteria where it is likely that movements are almost random. On the other hand, the heuristics used are within the reach of many superior animal populations and certainly of humans. We show in the paper that the addition of opportunistic migration notably changes the dynamical behavior of species. In particular conditions, spatial traveling waves become much longer and tend to diverge with respect to the finite system size causing strategy extinction and thus threatening diversity. On the other hand, in different contexts this result could be seen as a positive one as it tends to stabilize an oscillating system.

8.2 Methods

We investigate a class of two-person, three-strategy, symmetric rock-scissors-paper game as a metaphor for cyclic behavior. These games have the generic payoff matrix M (equation 8.1) which refers to the payoffs of the row player. The payoff matrix for the column player is simply the transpose $M^\top$ since the game is symmetric.

$$
\begin{array}{c}
\begin{array}{ccc} S1 & S2 & S3 \end{array} \\
\begin{array}{c} S1 \\ S2 \\ S3 \end{array}
\left(
\begin{array}{ccc}
0 & b_2 & -b_1 \\
-b_1 & 0 & b_2 \\
b_2 & -b_1 & 0
\end{array}
\right)
\end{array}
\tag{8.1}
$$

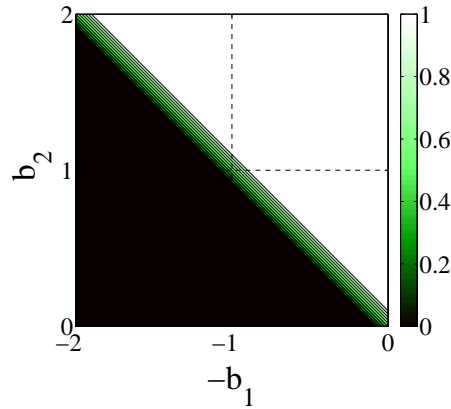Where b_1 and b_2 are positive. The set of strategies is $\Lambda = \{S1, S2, S3\}$.

Fig. 8.1 Diversity phase space in a well-mixed population as a function of the game's payoffs b_1 and b_2 with $a = 0$. Diversity is maximal for light tones and disappears for black tones.

The Euclidean two-dimensional space is modeled by a discrete square lattice of side L with toroidal borders. Each vertex of the lattice can be occupied by one player or be empty. The *density* is ρ and N is the number of players. Players can interact with k neighbours which lie at an Euclidean distance smaller or equal than a given constant R_g. Players can also migrate to empty grid points at a distance smaller than R_m. We use three neighborhood sizes with radius 1.5, 3, and 5; they contain, respectively, 8, 28, and 80 neighbours around the central player.

Each agent i interacts locally with a set of neighbours V_i lying closer than R_g. Let $\sigma_i(t)$ be a vector giving the strategy profile at time t with $S_1 = (1, 0, 0)$, $S_2 = (0, 1, 0)$, and $S_3 = (0, 0, 1)$, and let M be the payoff matrix of the game (equation 8.1). The quantity

$$
\Pi_i(t) = \sum_{j \in V_i} \sigma_i(t) \, M \, \sigma_j^\top(t)
\tag{8.2}
$$

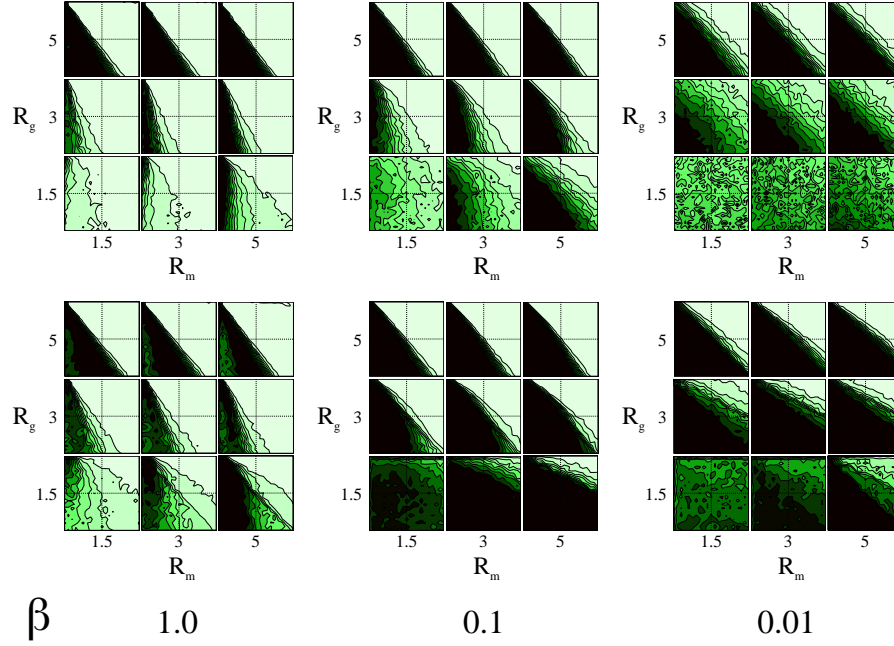is the cumulated payoff collected by player i at time step t.

Fig. 8.2 Average diversity levels with random migration (first row) and opportunistic migration (second row) as a function of the game radius R_g and the migration radius R_m. The size of the grid is $L = 50$ and the density ρ is 0.5. In all cases the initial strategies of the players are attributed uniformly at random. Diversity is maximal for light tones and disappears for black tones as can be seen in the color code bar of Fig. 8.1.

We use the imitative strategy update called the Fermi rule [19] in which the focal player i is given the opportunity to imitate a randomly chosen neighbour j with probability:

$$p(\sigma_i \rightarrow \sigma_j) = \frac{1}{1 + exp(-\beta(\Pi_j - \Pi_i))} \tag{8.3}$$

where $\Pi_j - \Pi_i$ is the difference of the payoffs earned by j and i respectively and β is a constant corresponding to the inverse temperature for the imitation update. When $\beta \rightarrow 0$ (high temperature) the probability of imitating j tends to a constant value 0.5 and when $\beta \rightarrow \infty$ (low temperature) the rule becomes deterministic: i imitates j if $(\Pi_j - \Pi_i) > 0$, otherwise it doesn't. In between these two extreme cases the probability of imitating neighbour j is an increasing function of $\Pi_j - \Pi_i$.

We use an asynchronous Monte Carlo [19] scheme for strategy update and migration, i.e. players are updated one by one by choosing a random player in each step with uniform probability and with replacement. Then the player migrates with probability 1/2, otherwise it updates its strategy.

If the pseudo-random number drawn dictates that i should migrate, then the player considers a randomly chosen position in the disc of radius R_m around itself. If the position is already occupied the player does not migrate, otherwise the player computes the payoff that it would obtain in that place with its current strategy. Then player i stays at its
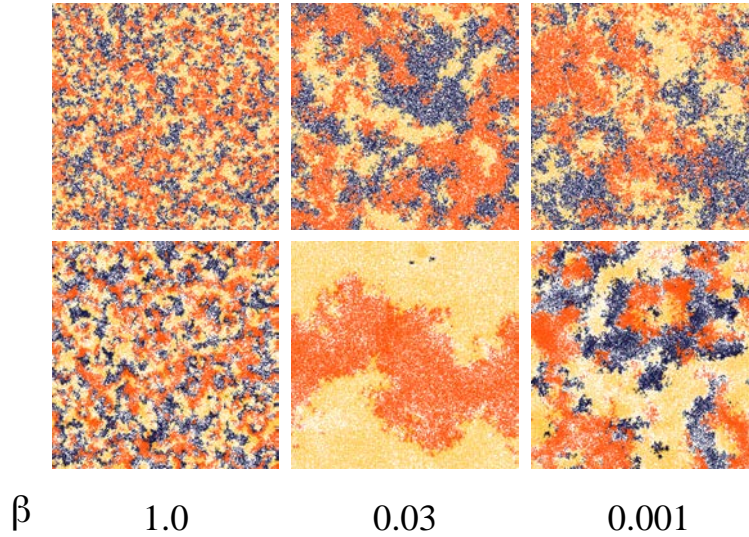
$$\beta \qquad 1.0 \qquad\qquad 0.03 \qquad\qquad 0.001$$

Fig. 8.3 Screenshots with random migration (upper images) compared with opportunistic migration (lower images) as a function of β, $R_g = 1.5$, $R_m = 1.5$, $b_1 = 1.5$, and $b_2 = 0.5$ (*game* 1). The size of the grid is $L = 400$ and the density ρ is 0.5. In all cases the initial strategies of the players are randomly attributed. Each color is associated with a different strategy: S_1 is yellow, S_2 corresponds to blue, and S_3 is depicted in orange.

current position if it obtains higher payoff there, or migrates to the trial position in the opposite case. In order to introduce noise in the migration player i can decide to migrate with probability :

$$p(\mathbf{x}_k \to \mathbf{x}_l) = \frac{1}{1 + exp(-\beta_m(\Pi_i^l - \Pi_i^k))} \tag{8.4}$$

where $\Pi_i^l - \Pi_i^k$ is the difference of the payoffs earned by player i in the positions $\mathbf{x}_l$ and $\mathbf{x}_k$, where $\mathbf{x}_k$ is the original position of player i and β_m is a constant corresponding to the inverse temperature for the migration. We call these migrations *opportunistic* or *fitness-based*.

We use two measures in order to assess diversity. The first one is called diversity and is simply the normalized product of the strategy frequencies : $(n_1 n_2 n_3)/(1/3)^3$. It is proportional to the probability that three randomly chosen players adopt different strategies. Here the highest value of the product is reached when the distribution of the strategies is homogeneous, and if one or more strategy has vanished diversity becomes zero. Indeed, when there are only two strategies remaining, dominance will cause one of the two to disappear afterwards.

The second measure is called the wavelength. It is a rough empirical approximation for the wavelength of a traveling wave or simply for the size of a domain where more than half of the players adopt locally the same strategy. We compute the width of a domain surrounding a player along the x axis d_x and y axis d_y and then choose the shortest width among d_x and d_y and take the average over all players p. Note that we could obtain similar results by taking the average over d_x and d_y. In order to obtain the wavelength around a
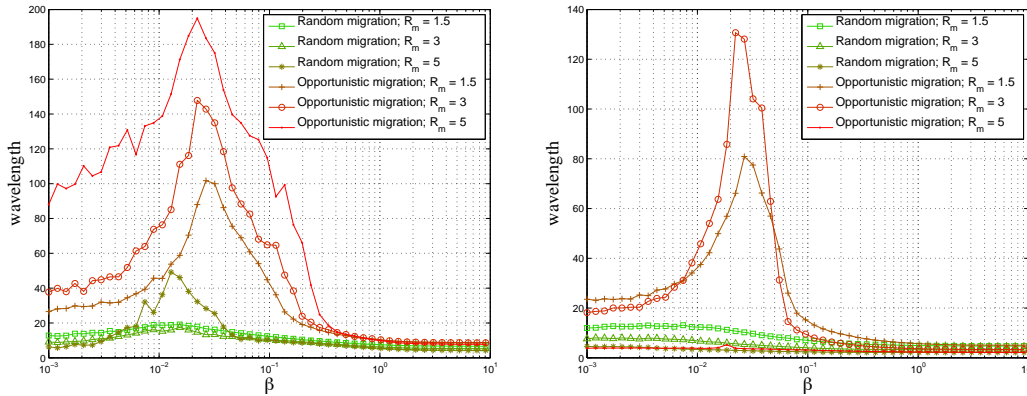
Fig. 8.4 Average wavelength after time $T = 5000$ as a function of β with random migration and opportunistic migration. $R_g = 1.5$, $R_m = 1.5, 3, 5$. Left image : $b_1 = 1.5$, $b_2 = 0.5$ (*game* 1). Right image : $b_1 = 0.5$, $b_2 = 1.5$ (*game* 2). The size of the grid is $L = 200$ and the density ρ is 0.5. In all cases the initial strategies of the players are randomly attributed.

player p with strategy s we compute the distance to the border of the s domain along the x and y axis in the positive and negative direction around the player p. In order to detect if a site i is inside a domain of players adopting strategy s, we compute the frequency of players with that strategy inside the Moore neighborhood ($R_g = 1.5$) of i, including i. If the frequency is smaller than 0.5, i is considered to be out of the domain. Practically we move gradually on the axis until we reach the end of the domain. The next steps take into account the case where the spatial distribution of the population contains empty regions, i.e the frequencies of strategies cannot be computed. In that case, if there are no players in the neighborhood of i, the position of i is incremented. Then, if the new place is in a domain with the same strategy we consider that it is still the same domain and continue to increment the test position. Otherwise, the position is considered to be out of the domain and the width of the region without players is subtracted from the total width.

Next, we present here the measure for the invasion speed. We call this measure cyclicity and it takes values $\in [-1, 1]$. The cyclicity measure for a player at a given time step t is 1 if the strategy has changed according to the natural cycling order ($S1 \rightarrow S2 \rightarrow S3 \rightarrow S1$) between $t - 1$ and t, 0 if the strategy has not changed and -1 if the strategy changed in the opposite way. The global cyclicity is the average of this quantity over the players during a time interval τ after the system has evolved for t time steps.

For the numerical simulations, the diversity phase-space generated by b_1 and b_2 has been sampled with a step of 0.1 and each value in the phase space reported in the figures is the average of $n = 50$ independent runs. For the wavelength plots the number of independent runs is $n = 200$. The evolution proceeds by first initializing the population by adding players on grid cells with probability ρ. Then the players' strategies are initialized uniformly at random such that each strategy has a fraction of approximately $1/3$. We let the system evolve for a period of $t = 1000$ time steps for phase-space diagrams and $t = 5000$ for wavelength plots. In each time step N players are chosen for update. We then let the system
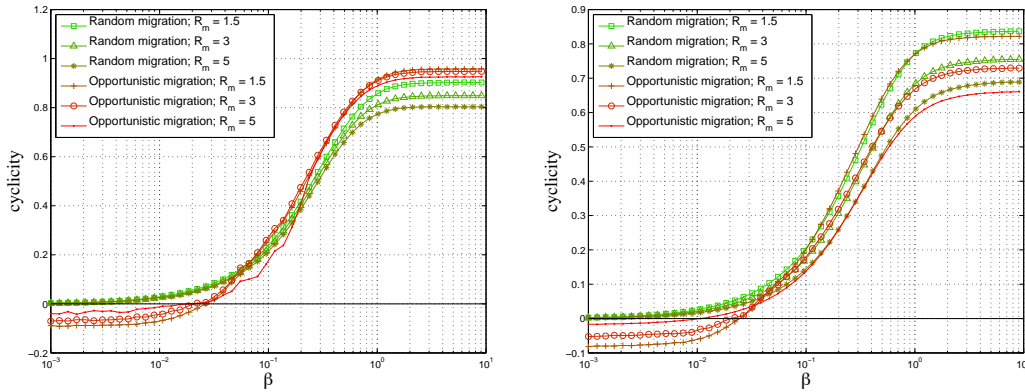
Fig. 8.5 Average cyclicity after time $T = 5000$ as a function of β with random and opportunistic migration. $R_g = 1.5$, $R_m = 1.5, 3, 5$. Left image : $b_1 = 1.5$, $b_2 = 0.5$ (*game* 1). Right image : $b_1 = 0.5$, $b_2 = 1.5$ (*game* 2). The size of the grid is $L = 200$ and the density ρ is 0.5. In all cases the initial strategies of the players are randomly attributed.

evolve for τ further steps and take the average measure value in this interval. Finally we report the average diversity or wavelength values over the n repetitions.

8.3 Results

In order to obtain an overview of the effect of opportunistic migration, the diversity measure is displayed as a function of the game parameters b_1 and b_2 for several values of β. Fig. 8.2 depicts the diversity phase-space for a lattice of size $L = 50$ after time $T = 1000$ as a function of β, R_g and R_m. The upper images refer to the random migration case, used here as a benchmark case, and the lower images refer to the opportunistic migration case. By comparing with the well-mixed case shown in Fig. 8.1, it can be observed that diversity can thrive in adverse games (lower left quadrant) when the interactions radius R_m and R_g are short $(R_g, R_m < 5)$. However this does not hold in the opportunistic migration case for all values of β as can be seen in Fig. 8.2. For $\beta = 0.1$ and 0.01 a small game radius R_g creates the opposite effect for $R_m = 1.5, 3, 5$: extinction extend in the upper right quadrant where diversity thrives in the ideal well-mixed case such that nearly all the games of the phase-space lose diversity. For higher game radius $R_g = 5$ the game space where full diversity thrives is similar to the one found in the random migration case. However this does not imply that the wavelength is similar in the extinction region. Although the small system size used for this exploratory analysis may cause finite-size effects i.e., extinction due to fluctuations, the results show that there is perhaps an interesting phenomenon occurring when β is tuned and thus we try to elucidate it further in the following.

We study the wavelength on larger lattices as a function of β since too small lattices do not let us appreciate large wavelengths due to finite size effects. Since the systematic study of the full game phase space would be computationally too heavy, we report the
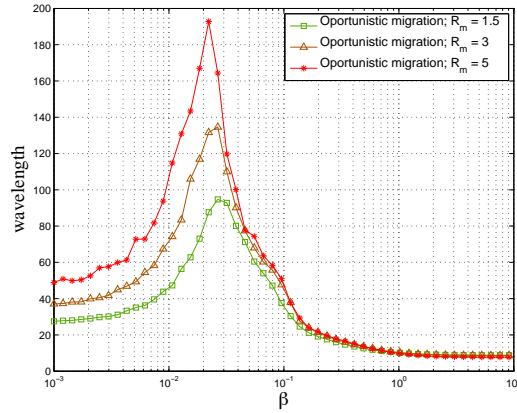
Fig. 8.6 Average wavelength for opportunistic migration after $T = 5000$ as a function of β for *game* 1: $b_1 = 1.5$, $b_2 = 0.5$. $L = 400$ and $R_m = 1.5, 3, 5$. In all cases the density ρ is 0.5 and the initial strategies of the players are randomly attributed.

wavelength for two representative games in the plane. The first game (*game* 1) is in the middle of the left lower quadrant of the phase space, $b_1 = 1.5; b_2 = 0.5$, and the second game (*game* 2) is in the middle of the right upper quadrant, $b_1 = 0.5; b_2 = 1.5$. Fig. 8.4 depicts the wavelength as a function of R_m and β for *game* 1 and *game* 2, and $R_g = 1.5$, and a frequency of migration of $1/2$. In the opportunistic migration case a marked peak appears for values of β between 0.01 and 0.1. Results for a frequency of migration of $1/4$ and of $3/4$ respectively are reported in the Suppl. Mat. Fig. 8.3 displays some typical snapshots around the phase transition for random and opportunistic migration. In the central image of the lower row it is clearly visible how domains become larger and extinction sets in for $\beta = 0.03$ with opportunistic migration. In Fig. 8.5 the average cyclicity is plotted as a function of β for the opportunistic and random migration cases. It can be seen in the opportunistic migration case that the cyclicity vanishes at the peak and is slightly reversed on the left of the transition so that the position of the peak corresponds to the inversion of the cycling order. This effect can be explained in the extreme case $\beta \to 0$ where the imitation tends to be random but the migration is opportunistic. In that case, the players adopting a strategy s_i which is payoff-dominated by a strategy s_{i-1} form clusters at the border between the two strategy regions since they try to minimize the number of s_{i-1} players in their neighborhood. Meanwhile the players adopting the strategy s_{i-1} are attracted toward the s_i clusters and surround them with a smaller density. Since the strategy update rule is almost random imitation for very small β the more clustered players spread their strategy faster than the surrounding players. In fact this effect can be understood in a bipartite population with two degree homogeneous sub-populations p_1 and p_2 where players imitate randomly their neighbors. A quick calculation shows that the size of the sub-population which has the largest average degree spreads its strategy faster (see Suppl. Mat.). Also in the Suppl. Mat. it is explained how the effect works using the example of a specific spatial configuration consisting of two neighboring infinite regions with different strategies. In the random migration case it is more difficult to find an

explanation since there is no clustering, but the phenomenon is weaker and the peak is less marked. The increase of the wavelength when the cyclicity vanishes is not new and has been studied in [12] in a cyclic voter model with three strategies and a probability to imitate the dominant (dominated) strategy P respectively $(1 - P)$ but the phenomenon is not caused by migration, as in our case, since agents don't move and only the P parameter varies. In [9] authors study a spatial five-species predator-prey model with site exchange and invasions between neighbors according to the Rock-Paper-Scissors-Lizard-Spock game. They study the invasion velocities and species density fluctuations as a function of the invasion rates. It is reported that the fluctuations of species frequency diverge and invasion velocities between associations of strategies vanish when tuning the invasion rates. Coming back to the opportunistic migration case, we have checked that the inversion is stable with growing system size. Using short simulation times, such that the system has not reached extinction which means that this data is about the (initial) transient period of the system and not yet at the stationary state, cyclicity can be measured we show that the inversion is similar for all system sizes studied (see figures in Suppl. Mat.). In Fig. 8.8 we display the average wavelength for $L = 400$, $R_m = 1.5, 3, 5$ and for *game* 1: $b_1 = 1.5$, $b_2 = 0.5$. By comparing with the corresponding curve in fig. 8.4 where $L = 200$ we remark that the peak becomes sharper for $L = 400$ thanks to the larger system size. This is due to the fact that the system can reach extinction before the end of the simulation due to fluctuations of the wavelength even if the mean wavelength is smaller than the system size.

Finally, we study the effect of noise on the migration process using the Fermi rule with parameter β_m (see Methods section). We observe that, as β_m is decreased, the system undergoes a transition inside an interval where the phenomenon gradually disappears. (See Fig. 3 in Suppl. Mat.). Thus, the global effect of migration noise is to prevent extinction provided that it is high enough, i.e. β_m less than 0.2. Of course, as migration noise increases, the situation resembles more and more to random walk migration, as it should.

8.4 Discussion

We studied the diversity of strategies in a RSP game in a spatial layout where players migrate opportunistically to more favorable places in their neighborhood. Differently from the many RSP-like systems that have been studied previously in which diffusion is either absent or is random, we found that the diversity is not maintained for large areas of the games' phase space, leading to strategy extinction, when the exponent of the strategy update rule is such that the imitative update is sufficiently noisy. Furthermore, studying the size of the patterns for two representative games as a function of β we found that a transition occurs where the size of the patterns diverges and the prevalence of the strategies is reversed. Finally, we also introduced a migration noise and we found that if this noise is larger than a threshold the divergence of the wavelength disappears.

8.5 Supplementary Material

8.5.1 Well-mixed population

Suppose that we have two populations (species) p_1 and p_2. All the players from one population have the same type of neighborhood, but the degree of a player is given by the mean number of links to p_1 and p_2. For example players of population p_1 have a degree given by $k_1 = k_{11} + k_{12}$. Where the k_{ij} represent the mean number of link connecting one player of population p_i to players of population p_j. Let N_i be the number of players in p_i, then the variation of N_i corresponding to a particular set of k_{ij} is given by :

$$\dot{N}_i = N_j \frac{k_{ji}}{k_j} - N_i \frac{k_{ij}}{k_i} \tag{8.5}$$

Now since $N_i k_{ij} = N_j k_{ji}$ is the total number of links between p_1 and p_2 the equation becomes:

$$\dot{N}_i = N_i k_{ij} \left(\frac{1}{k_j} - \frac{1}{k_i} \right) \tag{8.6}$$

Therefore $\dot{N}_i < \dot{N}_j \iff k_i < k_j$. Which means that the population with the highest degree (the players inside the cluster) grows faster in this particular configuration.

8.5.2 Configuration Analysis

Suppose that the lattice is composed of two infinite regions of infinite size containing two populations p_1 and p_2 with different densities of players ρ_1 and ρ_2 where the players adopt different strategies, see Fig. 8.7 where player A belong to the region 1 and player B to region 2 and both have a Moore neighborhood of eight players. We compute the probability that population i grows by one player. In time step t one player is chosen for strategy update. Taking the Moore neighborhood into account we see that only players at the border of the two region can imitate a player from the other region. Since we will compare the probability that p_1 grows with the probability that p_2 grows we can use

$$\frac{\rho_1}{\rho_1 + \rho_2}$$

as the probability that a player of population p_1 at the border is chosen. Since the player chooses a neighbor randomly and imitates it, the probability that population p_1 grows by one is given by

$$\frac{\rho_1 \rho_2}{(\rho_1 + \rho_2)(\rho_2 + \rho_1 5/3)}$$

The same formula is valid for region 2 by exchanging the indexes. Therefore the number of players of type 1 increases faster if and only if $\rho_1 > \rho_2$.
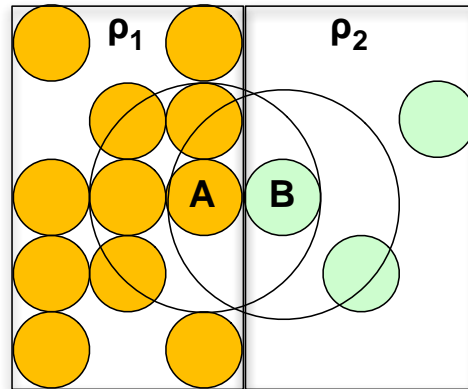
Fig. 8.7
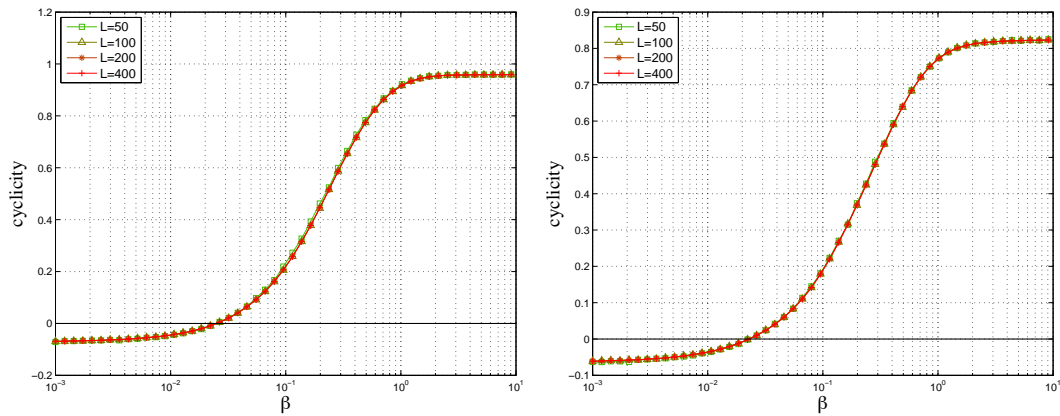
Fig. 8.8

8.5.3 Cyclicity scaling

In Fig. 8.8 we show the average cyclicity (see main text for the definition) after time $T = 500$ as a function of β for $L = 50, 100, 200, 400$, $R_g = 1.5$, $R_m = 1.5$. Left image : $b1 = -1.5$, $b2 = 0.5$ (*game* 1). Right image : $b1 = -0.5$, $b2 = 1.5$ (*game* 2). In all cases the density ρ is 0.5 and the initial strategies of the players are randomly attributed The inversion of cyclicity is similar in all cases.

8.5.4 Migration Noise

Figure 8.9 shows the dependence of the wavelength on the migration noise parameter β_m for *game* 1 and *game* 2 (see main text).

Fig. 8.9 Average wavelength after time $T = 5000$ as a function of β (the exponent of the strategy update rule) for several β_m (the exponent of the noisy migration rule) with opportunistic migration for $R_g = R_m = 1.5$. Left image : $b1 = -1.5$, $b2 = 0.5$ (*game* 1). Ri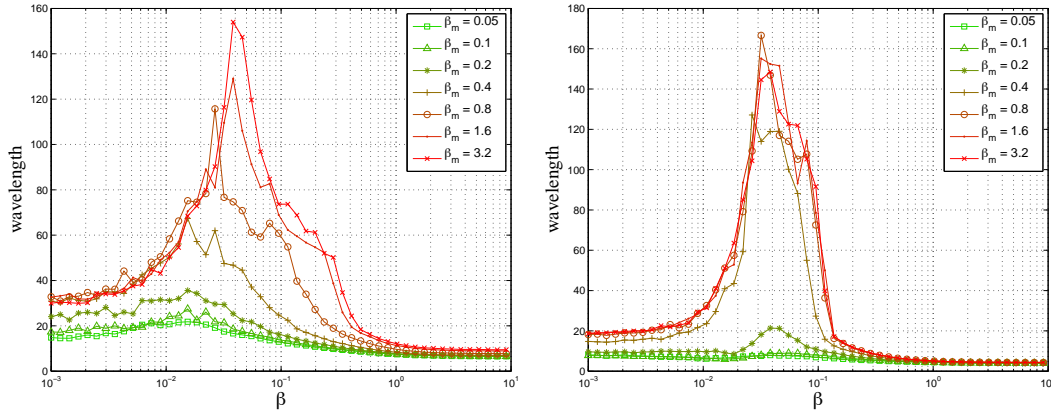ght image : $b1 = -0.5$, $b2 = 1.5$ (*game* 2). The size of the grid is $L = 200$ and the density ρ is 0.5. In all cases the initial strategies of the players are randomly attributed.

8.5.5 Migration Frequency Dependence

The following figures 8.10 show the wavelength as a function of β for migration probability 1/4 (left image) and 3/4 (right image). The number of simulation time steps is 10000 for the system represented in the right image and it is 3333, in order to keep the strategy update number constant to 2500 as in the 1/2 case. In the case of $R_m = 5$ in the right image, the wavelength saturates due to the $L = 200$ system size. To observe the peak, a larger L should be used but this would take an extremely long simulation time.

8.6 Acknowledgments

References

[1] C. A. Aktipis. Know when to walk away: contingent movement and the evolution of cooperation. *Journal of Theoretical Biology*, 231:249–2160, 2004.
[2] P. Buesser and M. Tomassini. Opportunistic migration in spatial evolutionary games. *Phys. Rev. E*, 88:042806, 2013.
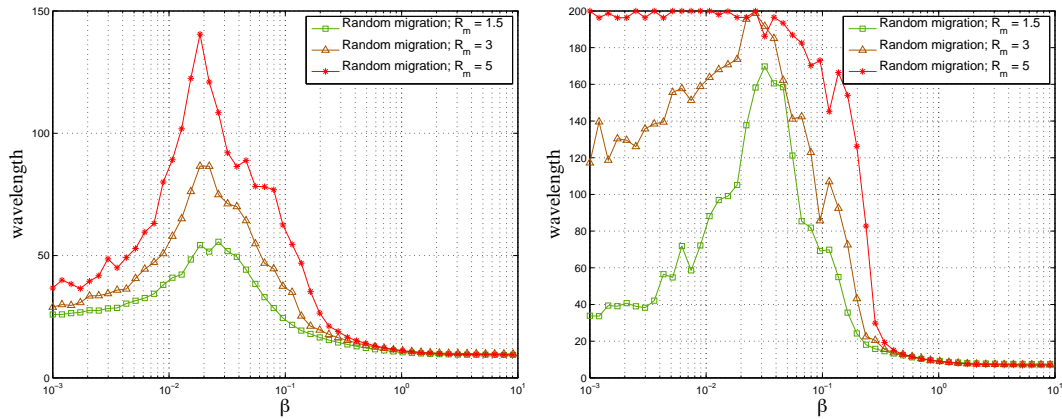
Fig. 8.10 Average wavelength as a function of β (the exponent of the strategy update rule) for several β_m (the exponent of the noisy migration rule) with opportunistic migration for $R_g = R_m = 1.5$, $b1 = -1.5$, $b2 = 0.5$ (*game* 1). The frequency of migration is 3/4 in the right image and it is 1/4 in the left image. The size of the grid is $L = 200$ and the density ρ is 0.5. In all cases the initial strategies of the players are randomly attributed. The saturation of the red curve is due to the wavelength reaching and then overtaking the system size.

[3] Z. Chen, J. Gao, Y. Kai, and X. Xu. Evolution of cooperation among mobile agents. *Physica A*, 390:1615–1622, 2011.

[4] R. Cong, B. Wu, Y. Qiu, and L. Wang. Evolution of cooperation driven by reputation-based migration. *PLOS ONE*, 7(5):35776, 2012.

[5] R. deForest and A. Belmonte. Spatial pattern dynamics due to the fitness gradient flux in evolutionary games. *Phys. Rev. E*, 87:062138, 2013.

[6] C. Hauert, S. DeMonte, J. Hofbauer, and K. Sigmund. Volunteering as Red Queen mechanism for cooperation in public goods games. *Science*, 296:1129–1132, 2002.

[7] D. Helbing and W. Yu. The outbreak of cooperation among success-driven individuals under noisy conditions. *Proc. Natl. Acad. Sci. USA*, 106:3680–3685, 2009.

[8] J. Hofbauer and K. Sigmund. *Evolutionary Games and Population Dynamics*. Cambridge, N. Y., 1998.

[9] G. Szabó J. Vukov, A. Szolnoki. Diverging fluctuations in a spatial five-species cyclic dominance game. *Phys. Rev. Lett.*, 88:022123, 2013.

[10] J. B. C. Jackson and L. Buss. Allelopathy and spatial competition among coral reef invertebrates. *Proc. Natl. Acad. Sci.*, 72:5160–5163, 1975.

[11] L.-L. Jiang, W.-X. Wang, Y.-C. Lai, and B.-H. Wang. Role of adaptive migration in promoting cooperation in spatial games. *Physical Review E*, 81:036108, 2010.

[12] Y. Itoh K. Tainaka. Topological phase transition in biological ecosystems. *Europhys. Lett.*, 15:399, 1991.

[13] B. Kerr, M. A. Riley, M. W. Feldman, and B. J. M. Bohannan. Local dispersal promotes biodiversity in a real-life game of rock-paper-scissors. *Nature*, 418:171–174, 2002.

[14] X. Ni, W.-X. Wang, Y.-C. Lai, and C. Grebogi. Cyclic competition of mobile species on continuous space: pattern formation and coexistence. *Phys. Rev. E*, 82:066211, 2010.

[15] T. Reichenbach, M. Mobilia, and E. Frey. Mobility promotes and jeopardizes biodiversity in rock-paper-scissors games. *Nature*, 448:1046–1049, 2007.

[16] W. H. Sandholm. *Population Games and Evolutionary Dynamics*. MIT Press, Cambridge, MA, 2010.

[17] D. Semman, H-J. Krambeck, and M. Milinski. Volunteering leads to rock-paper-scissors dynamics in a public goods game. *Nature*, 425:390–393, 2003.

[18] B. Sinervo and C. M. Lively. The rock-scissors-paper game and the evolution of alternative male strategies. *Nature*, 380:240–243, 1996.

[19] G. Szabó and G. Fáth. Evolutionary games on graphs. *Physics Reports*, 446:97–216, 2007.

[20] G. Szabó and C. Hauert. Evolutionary prisoners's dilemma game with voluntary participation. *Phys. Rev. E*, 66:062903, 2002.

[21] G. Szabó, A. Szolnoki, and R. Izsák. Rock-scissors-paper game on regular small-world networks. *J. Phys. A: Math. Gen.*, 37:2599–2609, 2004.

[22] G. Szabó and J. Vukov. Cooperation for volunteering and partially random partnership. *Phys. Rev. E*, 69:036107, 2004.

[23] A. Szolnoki, M. Perc, and G. Szabó. Phase diagrams for three-strategy evolutionary prisoner's dilemma games on regular graphs. *Phys. Rev. E*, 80:056104, 2010.

[24] Attila Szolnoki, Zhen Wang, Jinlong Wang, and Xiaodan Zhu. Dynamically generated cyclic dominance in spatial prisoner's dilemma games. *Phys. Rev. E*, 82:036110, 2010.

[25] Z. Wang, A. Szolnoki, and M. Perc. If players are sparse social dilemmas are too: Importance of percolation for evolution of cooperation. *Scientific Reports*, 2:369, 2012.

[26] Z. Wang, A. Szolnoki, and M. Perc. Percolation threshold determines the optimal population density for public cooperation. *Phys. Rev. E*, 85:037101, 2012.

Chapter 9
Conclusion

In this final chapter, we will try to assess what the contributions of the thesis are, what problems remain open, and what are the possibilities for further research. We divide the discussion in five parts. The first part investigate weighted networks and cooperative unweighted topologies, the second deals with spatial networks, the third with random and opportunistic migration for two-strategy games, the fourth part is concerned with opportunistic migration and three-strategy cyclic games, and in the last section we list open problems and future research.

9.1 Weighted Networks

Although weighted networks are closer to reality, evolutionary games on complex networks have been essentially studied on unweighted networks, both for simplicity as well as because weights in social networks are notoriously difficult to assess, and also owing to the lack of generally accepted theoretical models of the formation and structure of weighted social networks. We tried to answer the question by using numerical simulations and several methods for assigning weights to links.

The first method for assigning weights was to start from a bipartite graph where the two sets of nodes represent affiliations and players, and then generate a weighted graph by discarding affiliations nodes and creating edges between two players with a weight corresponding to the number of affiliations of which both players are members. The starting graph were a real collaboration graph and a bipartite theoretical network model. In the real bipartite network case we report that the transition between cooperation and defection in the ST-plane is smoother than in the unweighted case. This effect indicates that cooperation and defection coexist. However the main features remain similar with respect to the unweighted case. This investigation was performed to illustrate the study with a real-life case but the results cannot be generalized in the absence of a sufficient amount of statistics on several social networks. In the bipartite formation model, cooperation was almost identical in the weighted case compared to the same unweighted network.

Then, using random and Barabási-Albert networks, we assigned to each edges a randomly chosen weight drawn from a random or scale-free distribution. In that case the weights are assigned to edges independently of the underlying network topology. Again, the results

are that cooperation levels are similar to those found on the unweighted networks.

The last method for assigning weights was to correlate the weight of an edge with the degrees of its end points. Unlike in the previous models, the levels of cooperation where very sensitive to the particular weight-degree correlation used. We used to types of correlations, the first one is given by $w_{ij} = (k_i k_j)^\gamma$ and is typical from transportation networks but not from the available social networks, this rule takes as parameter the cumulated amplitude of the degrees. The second correlation is given by $w_{ij} = (|k_i^2 - k_j^2| + 1)^\gamma$ and is complementary to the first, this rule takes as parameter the difference between degrees and can be tuned in order to obtain either assortative or disassortative weights. We found that for the first rule cooperation was increased between $\gamma = 0.5$ and $\gamma = 1$. However the most interesting rule is the second one since high levels of cooperation are observed for $\gamma > 0$. In other words, disassortative weights increase cooperation compared to assortative weights or to the unweighted network. Furthermore this effect is robust against imitation noise, since levels of cooperation remained high even with low β, i.e. the inverse noise in the Fermi rule. This is contrasting with the unweighted Barabási-Albert case where levels of cooperation decrease with increasing β.

It is interesting to note that the weighted networks can be transformed into new unweighted topologies which have the same effect on cooperation than the weighted network. Indeed, in order to find such a topology we discarded the edges having a weight smaller than a threshold and took the other edges as unweighted. The levels of cooperation obtained on such a network are as high and even higher than in the weighted case. We investigated the unweighted topology obtained for the networks with the highest levels of cooperation in order to understand better how cooperation spreads. We found that the degree distribution is bipartite and the set of hubs is mainly connected to small degree vertices. There are connections between hubs which are necessary for cooperation to spread and the proportion of low degree nodes connected to several hubs has also an influence on cooperation levels. We summarized these results by constructing a small network model with two hubs and a number of small degree vertices. On the other hand, for assortative weights which lead to less cooperation, the unweighted topology of the networks tends to be divided into several components. Each small component consists of nodes with similar degrees and therefore levels of cooperation should be as on a regular random network. However we observe a smooth transition between cooperation and defection in the ST-plane. The reason is probably that the component are small and therefore extinction of one strategy, independently of the game, due to fluctuations or initial conditions is possible.

Finally, since we do not know if this type of degree-weight correlations exists in real networks, it might be interesting to perform further investigations provided that more data are available.

9.2 Spatial Networks

In the second part of the thesis we have studied cooperation on several type of spatial networks. The initial question was to understand if cooperation could benefit at the same

time from spatial clustering and the positive effect of scale-free degree distribution. We have shown that just imposing a scale-free distribution on a spatial network does not lead to particularly high levels of cooperation. In fact the phase space is between the one obtained for a spatial lattice and for a scale-free distribution depending on the scale-free exponent of degree distribution. However we showed that Apollonian lattice, a scale-free spatial topology, displays very high levels of cooperation. This topology is very hierarchical, and is constructed by adding recursively a vertex inside each connected triple of vertices, starting from a triangle. This type of networks has a high clustering coefficient and a large average degree gradient between neighbors.

Then we remarked that highly cooperative networks as those found in the previous part of this thesis, can be naturally embedded in space. The topology that we created might be interpreted as follows. Hubs and small degree vertices are displayed regularly in space, each small degree vertex is connected to the closest hub, if several hubs lay at the same distance or about the same distance the vertex is connected to all of them. On the other hand neighboring hubs are interconnected. In this way we obtain a topology very similar to the supercooperative network. We extended also the geometric random graph model in order to create networks which tend to be similar to the supercooperative ones. Indeed we display vertices randomly in space and draw, for each vertex, a radius from a distribution consisting of two different values, one small and one large. Then each vertex i is connected to a vertex j if j lays at a distance smaller than the sum of their radii. The networks obtained in such a way display high levels of cooperation for some radius distribution, although not as high as in the previous one.

Additionally, we modified the imitate the best protocol such that a vertex does not imitate only the best neighbor, but rather choose a neighbor with probability proportional to the difference of payoffs. With this update rule, the levels of cooperation tend to be similar to the imitation of the best case rather than to the replicator rule case or Fermi case. The difference between these types of rules is that in one case the player chooses a neighbor randomly before comparing the payoffs of the neighbor with his own payoff, while in the other cases the player compares all the payoffs in its neighborhood. This led us to the conclusion that the higher levels of cooperation obtained with the imitation of the best is not only due to the fact that this rule is purely deterministic but is also a consequence of the capacity for a player to compare the payoffs of all the neighbors.

We studied also the assortativity of strategies at steady state. Since HD and SH games are in the anti-coordination and coordination class, they tend to be respectively assortative and disassortative. In fact, in the SH case the population tends to adopt fully one strategy, at the transition in the ST plane, both strategies can persist but the configuration is assortative. We have shown that the effect of the different network topologies is to change the phase space regions where the games are in the coordination and anti-coordination class. In fact, on the lattice with high levels of cooperations discussed above, the PD games are transformed into coordination games.

9.3 Migration and Cooperation

In chapter 5 we study the coevolution of the strategies with a random migration where agents move in a continuous space with a fixed velocity magnitude while the direction of displacement is randomly chosen. Later in the same chapter, we study the case where the magnitude of the agents speed depends on the degree as a negative exponential. In this study we use $0.01, 0.001$ and 0 as velocity magnitude, or equivalently the distance crossed by a player at each time step, for a total space size $L = 1$. Since we use $\bar{k} = 4, 8$, the corresponding interaction radii are $RG = 0.0357, 0.0504$. Thus the migration ranges, $0.01, 0.001$, are small compared to the the interaction radii. In this chapter we remark that the random migration and the small migration ranges, in particular 0.001 which is 30 times smaller than RG leads to high levels of cooperation. When the speed magnitude increases up to 0.01 the cooperation levels decrease slightly. Furthermore these high levels of cooperation are observed with the imitation of the best update rule but not with the Fermi rule. It is difficult to explain exactly why cooperation spreads in those conditions, however it can be observed that the some initial clusters of cooperators are formed which are also somehow isolated subgraphs. Then these cooperative regions extends and cooperation seems to be advantaged with the low speed magnitudes. In the case where speeds depends inversely on the density, i.e. with damping, it appears that more isolated clusters forms, and cooperative clusters do not extend.

   In chapters 6 and 7 we study the evolution of cooperation on diluted grids when the agents are able to change their strategies and at the same time to test some places around and move to the most profitable one. We used the values $1.5, 3, 5$ for the game and migration radii which are respectively the radius defining the size of the neighborhood where the payoffs are computed R_g, and the migration radius R_m. Concerning the strategy updates we used two rules. The first one is the imitation of the best. Results show that the cooperation levels are higher in the payoff dependent migration case compared to the random migration case, and cooperation extends to a part of the prisoner's dilemma quadrant in the former case. We obtain also full cooperation in the stag-hunt quadrant. In the random migration case, when the density is low and the game radius are still relatively small, agents interact only with few neighbors, which is detrimental for cooperation. On the other hand, with same setting but a higher game radius, the system tends to the case where the migration range is small compared to the interaction radius as in chapter 5. Indeed we have $R_g = 5$, $R_m = 1.5$ and $\rho = 0.1$, and the average degree is therefore $\bar{k} = \rho \pi R_g^2 = 0.1 * \pi * 25 = 7.854$. Thus we approach the cases studied in chapter 5, particularly for speed magnitude $v = 0.01$, and the cooperation levels in the ST-plane are indeed somehow similar in that specific case.

In the opportunistic migration case the results are generally independent of R_m, but R_g has an strong influence on cooperation. In fact, as R_g increases above 3 all cooperation is lost in the prisoner's dilemma, and it is progressively lost in the stag hunt also. Therefore the high levels of cooperation obtained with the imitation of the best update rule are only valid for short interaction radii.

The parameter N_{test} is the number of places that a player tests in order to find the best

one in the neighborhood, it represents the effort that a player spends for searching. We computed the convergence times as a function of N_{test} and found that above $N_{test} = 4$ the convergence times are almost constant as a function of N_{test} for $R_m = 1.5, 3, 5$. Furthermore we displayed the phase space for $N_{test} = 1, 20$ and cooperation was even slightly higher for $N_{test} = 1$. We concluded that it is not necessary to test systematically all the places in the neighborhood in order to obtain more cooperation or to shorten the convergence time, but by testing only 4 randomly chosen places we obtained the same results.

When the rate of strategy update tends to be small compared to the rate of migration update, we observe that for low values of S, gains of cooperation are mostly lost. This can be explained by the fact that the mobility of the agents is decreased, thus preventing cooperator clusters to be stable. In the same line of research we studied the case where the strategies of the agents are fixed, and only the position can change. We observe a increase of mobility for low S values. However, with the same game settings but for R_g large, we report that mobility is very high since dynamical clusters with a definite direction of motion form.

The second update rule was the Fermi one. For $\beta = 1.0$ there is only a small shift in the ST games in favor of cooperation compared to the well-mixed case, and no cooperation in the prisoner's dilemma games. In fact results with random migration and Fermi update, which are not included in this work, show that cooperation is only slightly higher in the payoff dependent migration case than in the random migration case. On the other hand something unexpected happened for smaller β. Indeed, as β decreases, the levels of cooperation increase, and finally cooperation takes the whole phase-space for $\beta < 0.01$ and $R_g = 1.5, 3$. This is contrasting for example with the random migration case, which is not displayed in this work, where decreasing β do not lead to higher levels of cooperation.

These high levels of cooperation hold for all R_m, however for high values of R_g the cooperation levels tend to those observed in the well-mixed case. Additionally, the payoffs are also increased for high R_g, since the number of neighbors is higher and this has the same effect as increasing β.

We explained these high levels of cooperation in the extreme case where imitation is purely random as follows. Cooperators tend to migrate towards other cooperators and form clusters, while defectors are attracted toward these clusters. When a cluster of cooperator is formed, cooperation spreads. In fact when a defector arrive at the border of a cooperator cluster the number of cooperators in its neighborhood is higher than the number of defectors. Then, because of the random imitation, the defector tends to switch to cooperation. Thus cooperation can spread in all games if the agents migrate opportunistically but simply imitate a randomly chosen neighbor.

Finally this phenomenon is not restricted to spatial layout. Indeed random imitation could also improve cooperation when the network is adaptive, i.e. the agents can rewire edges to other players when they are not satisfied with a neighbor.

9.4 Migration and Diversity

In chapter 8 we study the effect of opportunistic migration on cyclic games. We use the same migration update rule as in chapter 7, but with $N_{test} = 1$. We display our results in the phase space defined by the parameters b_1, b_2, two positive constants representing the payoff that a player earns against a player adopting respectively a dominant strategy or a dominated strategy. As showed in the introduction, in section 1.4.2 for the well-mixed case, the region where $b_2 > b_1$ has a mixed strategy attractor $x^* = (1/3, 1/3, 1/3)$, while for $b_2 < b_1$ the orbits are repelled from x^* and are attracted by the borders, which leads to extinction if the number of players is finite. On a spatial lattice the two types of game lead to the formation of dynamic spatial regions where players adopt the same strategy. In this part of the thesis we study diversity and the size of these regions as a function of the migration type and β, the inverse noise of the Fermi rule. First we study diversity on small lattices with the game phase space defined by $b_1, b_2 \in [-1, 1]$. Secondly we study the size of the patterns and restrict to two games in order to take larger system sizes and keep reasonable computing durations. For the basic case where agents lie on the site of regular lattice, the transition between the two types of games is smooth for small game radii. When the game radius becomes larger the phase space is more similar to the well-mixed case. Our results in the random migration case show that the size of the patterns is smaller for small R_m and R_g. In the opportunistic migration case with small R_g the diversity phase space shows that there are some intermediate values of β where the size of the patterns grows. Thus we studied the size of the patterns as a function of β for two representative games of the phase space, one with a mixed-strategy attractor and the other without. The results show that the size of the patterns is peaked for values of β between 0.1 and 0.01 and for the two game tested. Then we plotted a measure of the cyclicity and showed that the peak corresponds to a reversal of the cyclicity. In other words, the dominated strategies spread faster than their respective dominant strategies at the border between two regions.

In fact the phenomenon is similar to the one observed in our previous study on two-strategy games and migration. At the borders between two strategy regions, the players adopting the dominated strategy form clusters since they earn a larger payoff in this configuration than in a configuration where they are more diluted and can be surrounded by players adopting the dominant strategy. Therefore in the extreme case where imitation is random the dominated strategy spreads faster because of this clustered configuration. As β decreases from higher values, there is a point where this phenomenon cancels cyclicity. For cyclic games in general, without migration, the size of the patterns tends to diverge when the game is tuned to the point where the cyclic prevalence is cancelled. In our case the cyclicity is tuned by the payoff dependent migration and β .

9.5 Open Problems and Further Research

A thesis work cannot pretend to study the subjects presented here extensively. Many threads remain necessarily open. In this section, we discuss some interesting questions that would deserve further study. Concerning weighted networks, we found high levels of cooperation with some types of degree-weight correlations. However these degree-weight correlations are only hypothesized, therefore the next step could be to search if such correlations exist in real weighted networks, and to find if these real degree-weight correlations are assortative or disassortative.

Concerning unweighted networks, we found highly cooperative topologies that were derived from the weighted ones. It would be interesting to systematically optimize the topology of the networks with respect to cooperation and compare the resulting graphs with these cooperative topologies. Small network sizes could be used in order to reduce the computation times.

In general we studied the case where agents have either strategy C or D. However it would be interesting to investigate the effect of topology when the strategy space is continuous or approximately continuous, i.e. different levels of cooperation exist. A different but close case is when each vertex of the network represents a well-mixed population.

Concerning migration, we studied migration on discrete grids where one cell can be occupied by only one player. If several players could live in the same cell the dynamic would be affected. When only one player can be in a cell, we observe "traffic jams", i.e. players can not move because there is no more empty places in the neighborhood.

Another alternative migration update is that each agent has a speed vector which is the sum of the forces exerted by the neighbors. Each force is a vector in the direction of the neighbor whose amplitude and direction depends on the payoff earned with that neighbor. In chapter 1.2 we highlighted the importance of feelings and reciprocity in human relationships following [1], where authors also give a payoff functional which takes into account both social emotions and monetary payoffs in a public goods game. If the game is a two-player prisoner's dilemma, the feelings of a cooperator could be anger against defectors, and self-esteem, gratitude and other positive feelings when the other cooperates. A defector could feel guilty when playing with a cooperator. Taking this into account the temptation to defect should be lowered because of guilt. The anger feeling could decrease also the sucker payoff, and the reward payoff should be increased in order to take into account the positive emotions. Thus the sucker and temptation payoff tends to be decreased compared to punishment, and particularly the reward payoff, and the game could be transformed into a coordination game. In the case where migration is still possible, it seems plausible that the defectors and cooperators will still try to have cooperators in their neighborhoods and that cooperators will try to minimize the number defectors in their neighborhood. Thus the situation could be such that agents migrate according to a prisoner's dilemma while the imitation tends to be a coordination game. This might lead to high levels of cooperation as in the case where the agents imitates their neighbors randomly and could be worth studying, by conveniently adapting the standard update rules.

References

[1] S. Bowles and H. Gintis. *A Cooperative Species.* Princeton University Press, Princeton and Oxford, 2011.

Chapter 10
List of Publications

10.1 Publications Appearing in this Work

Chapter 2: P. Buesser, J. Peña, E. Pestelacci, M. Tomassini, The Influence of Tie Strength on Evolutionary Games on Networks: An Empirical Investigation, Physica A: Statistical Mechanics and its Applications 390 (2011) 4502–4513

Chapter 3: P. Buesser, M. Tomassini, Supercooperation in Evolutionary Games on Correlated Weighted Networks, Physical Review E 85 (2012) 016107

Chapter 4: P. Buesser, M. Tomassini, Evolution of Cooperation on Spatially Embedded Networks, Physical Review E 86 (2012) 066107

Chapter 5: A. Antonioni, M. Tomassini, P. Buesser, Random Diffusion and Cooperation in Continuous Two-Dimensional Space, Journal of Theoretical Biology 344 (2013) 40-48

Chapter 6: P. Buesser, M. Tomassini, Spatial Organisation of Cooperation with Contingent Agent Migration, ECAL 2013, Advances in Artificial Life (2013) 192-199

Chapter 7: P. Buesser, M. Tomassini, Opportunistic Migration in Spatial Evolutionary Games, Physical Review E 88 (2013) 042806

Chapter 8: P. Buesser, M. Tomassini, The Role of Opportunistic Migration in Cyclic Games, PLOS ONE 9 (2014) e98190

10.2 Other Publications

P. Buesser, F. Daolio, M. Tomassini, Optimizing the robustness of scale-free networks with simulated annealing, ICANNGA'11 Proceedings of the 10th international conference on

Adaptive and natural computing algorithms Part II (2011) 167-176

R. Bonazzi, P. Buesser , A. Holzer. Cooperation Support Systems for Open Innovation. Proceedings of the 13th WOA conference. (2012, Mai)